REAL-TIME CHANGE OF NITRIC OXIDE IN RAT HIPPOCAMPAL SLICES AND ASTROCYTIC GLUTATHIONE RELEASE VIA GLUTAMATE-DEPENDENT PATHWAYS

_____

JOÃO GONÇALO LEAL DE OLIVEIRA E SILVA FRADE

UNIVERSIDADE DE COIMBRA

2007

Dissertação apresentada à Faculdade de Ciências e Tecnologia da Universidade de Coimbra para obtenção do grau de Doutor em Bioquímica, especialidade de Toxicologia Bioquímica.

A quem muito foi dado, muito será pedido;

a quem muito foi confiado, muito mais será exigido.

(Lc, 12:48b)

Ao meu Pai e à minha Mãe

Aos meus Imãos, Cunhado e Sobrinhas

Agradecimentos

São muitas as pessoas que, de uma forma ou de outra, contribuíram para o trabalho agora apresentado, a quem gostaria de expressar a minha gratidão.

À minha Família, primeiros nesta lista porque primeiros para mim. Sempre foi nela que encontrei o meu refúgio, o meu maior apoio, o meu lugar no Mundo. É a todos que dedico este esforço, em especial ao meu Pai e à minha Mãe: as metas que alcanço são também vossas, por tudo o que me deram (dão) e por estarem sempre presentes ao meu lado...

Ao meu Orientador Científico, o Professor Doutor João Laranjinha, do Laboratório de Bioquímica da Faculdade de Farmácia, pelo entusiasmo com os estudos aqui apresentados e pelo que aprendi com a sua postura científica, espírito crítico e disponibilidade, o meu muito obrigado.

Ao Professor Doutor Rui Barbosa, do Laboratório de Métodos Instrumentais de Análise da Faculadade de Farmácia, por contribuir decisivamente para o trabalho desenvolvido, e pelo rigor e orientação sempre presentes que tanto me ensinaram, o meu muito obrigado.

Aos Docentes do Laboratório de Bioquímica da Faculdade de Farmácia, os Professores Doutores Leonor Almeida, João Sardinha Alface, José Custódio, Teresa Dinis e Armanda Santos, pela amabilidade com que sempre me trataram e pela disponibilidade científica permanente, deixo o meu agradecimento.

To those at the Institute of Neurology, London (UK), particularly Doctors Simon Heales and Simon Pope, thank you so much for all your support and friendship, and for making my stay abroad such a memorable and fruitful experience.

Aos Amigos e Colegas de Laboratório, mais novos e mais velhos, que partilharam tantas alegrias e experiências, e com quem sempre pude contar ao longo destes anos. A todos, em especial à Irmandade da Bioquímica, obrigado pela vossa amizade, incentivo e carinho.

Aos Funcionários dos Laboratórios de Bioquímica e Métodos Instrumentais de Análise, nomeadamente o Sr. Pedro, D. Celeste, D. Isaura e Maria João, estou grato pelo profissionalismo e pela atenção que sempre me dispensaram.

A todos os meus Amigos, de Curso, da Típica, da Secção de Fado, do CUMN e da CVX, e a todos aqueles que a (falta de) memória me faz esquecer de nomear: talvez nunca saibam o quanto são importantes para mim, mas sem vocês não tinha chegado lá. Obrigado por poder contar sempre convosco.

INDEX

Abbreviations

$^{\bullet}$NO	Nitric oxide
$^{\bullet}$NO$_2$	Nitrogen dioxide
5-HT	Serotonin
aCSF	artificial CerebroSpinal Fluid
AMPA	α-amino-3-hydroxy-5-methylisoxazole-4-propionate
AMPAR	AMPA receptor
ApN	Aminopeptidase
BH4	Tetrahydrobiopterin
BSO	Buthionine Sulphoxime
CaM	Calmodulin
CcO	Cytochrome c Oxidase
cGMP	Cyclic guanosine monophosphate
CP-AMPAR	Ca^{2+}-permeable AMPA receptor
Cont	Control
CysGly	Cysteinylglycine
D-AP5	D($-$)-2-amino-5-phosphonopentanoic acid
DETA/NO	Diethylenetriamine/NO
DMEM	Dulbecco's modified Eagle's medium
DPA	Differential Pulse Amperometry
DTPA	Diethylenetriaminepentacetic acid
EBSS	Earle's Balanced Salt Solution
EC50	Half maximal (50) Effective Concentration
ECD	Electrochemical detection
EDRF	Endothelial-Derived Relaxing Factor
eNOS	Endothelial isoform of NOS
FAD	Flavin Adenine Dinucleotide
FBS	Fetal Bovine Serum
FMN	Flavin mononucleotide
GAPDH	Glyceraldehyde 3-phosphate dehydrogenase
GCS	γ-glutamylcysteine synthetase
GLAST	Glutamate aspartate transporter
GLT1	Glutamate transporter 1
Glu	Glutamate
GRIP	Glutamate Receptor Interacting Protein
GS	GSH synthethase
GSH	Glutathione
GSNO	S-nitrosoglutathione
GSSG	Glutathione disulphide
GSx	amount of GSH plus twice the amount of GSSG
H$_2$O$_2$	Hydrogen peroxide

HBSS	Hank's Balanced Salt Solution
HPLC	High Performance Liquid Chromatography
iNOS	Inducible isoform of NOS
L.O.D.	Limit of detection
L-arg	L-arginine
LDH	Lactate dehydrogenase
L-NAME	NG-Nitro-L-arginine methyl ester
MB	Methylene blue
MEM	Minimum Essential Medium
MM	Minimal medium
Mrp1	Multidrug resistance protein 1
N_2O_3	Dinitrogen trioxide
NADPH	Nicotinamide Adenine Dinucleotide Phosphate
NBQX	2,3-Dioxo-6-nitro-1,2,3,4-tetrahydrobenzo[f]quinoxaline-7-sulfonamide
NiTMHPP	Nickel(II) tetrakis(3-methoxy-4-hydroxyphenyl) porphyrin
NMDA	N-methyl-D-aspartate
NMDAR	NMDA receptor
nNOS	Neuronal isoform of NOS
NO^-	Nitroxyl anion
NO^+	Nitrosonium ion
NOS	Nitric Oxide Synthase
NSF	N-ethylmaleimide sensitive factor
O_2	Molecular oxygen
$O_2^{\cdot -}$	Superoxide anion
$ONOO^-$	Peroxynitrite
PBS	Phosphate Buffer Saline
PDZ domain	PSD-95 discs large/ZO-1 homology domain
pGC	particulate Guanylate Cyclase
PhTx-4,3,3	Philantotoxin-4,3,3
PhTx-7,4	Philantotoxin-7,4
PSD-95	Post Synaptic Density protein 95
RNOS	Reactive Nitrogen / Oxygen Species
RNS	Reactive Nitrogen Species
ROS	Reactive Oxygen Species
SEM	Standard Error of the Mean
sGC	soluble Guanylate Cyclase
SOD	Superoxide Dismutase
γGCL	γ-glutamyl-cysteine ligase
γGT	γ-glutamyltranspeptidase
VGCC	Voltage-gated calcium channels

Abstract

Nitric oxide ($^\bullet$NO) is a multi-faceted radicalar messenger involved in the modulation of numerous biological processes. It is implicated in the regulation of physiological events such as neuronal plasticity, host defense and blood flow, but may also trigger cell toxic pathways, notably cell death associated with neurodegenerative processes.

The bioactivity of $^\bullet$NO is afforded by its unusual chemical properties. $^\bullet$NO is a highly diffusible molecule that permeates membranes after being produced, thus conveying information by its local concentration, rather than by its chemical structural features, as happens with other classical modulators. A critical insight towards its role *in vivo* depends on the assessment of its concentration dynamics, both in time and space. The same properties that determine its unique biological effects also make its measurement a challenging task, particularly because of its gaseous nature and reactivity, which limit its half-life. Given this scenario, it has been a challenging task determining the rate and pattern of $^\bullet$NO changes in hippocampus following stimulation of ionotropic glutamate receptors, because of the involvement of glutamate receptor-dependent $^\bullet$NO production in both the mechanisms of synaptic plasticity and those of neurodegeneration via excitotoxic phenomena.

In this work, the use of microsensors endowed with appropriate analytical properties allowed the real-time measurement of endogenous $^\bullet$NO production in rat hippocampal slices with minimal tissue damage, via activation of glutamate ionotropic receptors. Stimulation of slices with glutamate, NMDA and AMPA clearly uncovered the transitory nature of $^\bullet$NO signals, pointing to operating regulatory mechanisms not only for the production but also for the decay. When using the physiological agonist glutamate, a much higher concentration was required (up to 100 fold) to induce the production of $^\bullet$NO, as compared with NMDA, in what was

considered to be the result of active glutamate regulatory mechanisms in synapses. In this regard, the use of NMDA overcame these mechanisms and the concentration-dependent relationship between the agonist and $^{\bullet}$NO signals highlighted a close physiological interaction between NMDAR and nNOS. Still, when using NMDA, signals were shown to decrease upon consecutive stimulations, regardless of agonist concentration and signal amplitude, suggesting the activation of pathways that critically shape $^{\bullet}$NO signals. This was further supported by continuously stimulating slices with NMDA (as a model for excitotoxic conditions where glutamate receptors and NOS are overactivated), where a higher and transitory $^{\bullet}$NO production was observed. These distinct features were also apparent when using KCl and the NOS substrate L-arginine as stimuli.

When addressing the role of AMPAR receptors in $^{\bullet}$NO production it was found that, as compared with NMDAR, AMPA stimulation resulted in a marked and distinct $^{\bullet}$NO transitory production, which was dependent on extracellular Ca^{2+} and independent of NMDAR activation. A slower rate of production and lower $^{\bullet}$NO levels, despite similar recovery periods to baseline, point to a less effective coupling with nNOS, and agree with the notion of a fine tuning of $^{\bullet}$NO production via AMPAR activation.

Excitotoxic conditions like the one mimicked by stimulating slices continuously with NMDA presumably lead to the activation of protective mechanisms. Amongst these is glutathione (GSH), a major endogenous antioxidant released by astrocytes to support and protect neurons in harmful conditions. When investigating the response of astrocytes in the presence of high glutamate it was observed an increase in extracellular GSH. Results suggest intracellular GSH release to be the mechanism responsible for the observed increase, and this is proposed to be a possible protective mechanism against glutamate toxicity.

Resumo

O óxido nítrico ($^\bullet$NO) é um mensageiro celular multifacetado e tem sido objecto de intensa investigação científica em sistemas biológicos. Está implicado na regulação de eventos fisiológicos, onde se destacam a plasticidade neuronal, a resposta imunitária e a circulação sanguínea, mas também em vias de toxicidade celular, em particular a morte celular associada a processos neurodegenerativos.

A bioactividade do $^\bullet$NO resulta das suas invulgares propriedades químicas. O $^\bullet$NO é uma molécula radicalar altamente difusível composta por apenas dois átomos que, uma vez produzido, permeia membranas, actuando como mensageiro intercelular. A informação associada ao $^\bullet$NO, estará, pois, contida no gradiente da sua concentração, independentemente de características estruturais que suportam interacções selectivas e complementares com alvos moleculares, como acontece com outros moduladores celulares. Dado este cenário, a determinação da dinâmica de concentração de $^\bullet$NO em tecidos, tanto no tempo como no espaço, é determinante para a clarificação da sua função *in vivo*. Contudo, as mesmas características químicas que conferem ao $^\bullet$NO efeitos biológicos singulares tornam também particularmente difícil a sua detecção em tempo real, em especial devido à sua natureza gasosa e ao seu reduzido tempo de meia-vida. A medição da velocidade de formação e o perfil de variação do $^\bullet$NO no hipocampo, em resultado da activação de receptores ionotrópicos do glutamato, assumem particular relevância, uma vez que estes se encontram envolvidos em mecanismos de plasticidade sináptica e em neurodegenerescência desencadeada por eventos excitotóxicos.

Neste trabalho, o fabrico de microsensores com propriedades analíticas adequadas para a detecção de $^\bullet$NO permitiu a medição em tempo real deste mensageiro, quando produzido endogenamente em fatias de

hipocampo de rato, na sequência de activação de receptores ionotrópicos de glutamato. Quando comparada com outras estratégias experimentais, a utilização desta ferramenta de análise permitiu estudar a dinâmica de produção e decaimento do ˙NO produzido endogenamente, suprindo assim um aspecto frequentemente negligenciado na área. Neste âmbito, a utilização de glutamato, NMDA e AMPA revelou claramente a natureza transitória dos sinais de ˙NO, apontando para a ocorrência de mecanismos regulatórios importantes não apenas na sua produção mas também no seu decaimento. A estimulação de fatias com o agonista fisiológico glutamato implicou um aumento significativo da sua concentração (até 100 vezes) para induzir a produção de ˙NO, quando comparada com estimulações usando NMDA ou AMPA, observação explicada pela existência de mecanismos regulatórios da concentração de glutamato em sinapses. Nesta perspectiva, a utilização do agonista não fisiológico NMDA permitiu ultrapassar estes mecanismos e destacar a interacção física e funcional entre receptores NMDA e nNOS, patente na clara dependência dos sinais de ˙NO obtidos face à concentração de agonista utilizada. Contudo, e apesar desta relação, os sinais de ˙NO obtidos após estimulações consecutivas com NMDA decaíram em intensidade de forma independente da concentração do agonista ou da intensidade de ˙NO inicialmente obtida. Este último aspecto é de destacar, pois implica que a perda de intensidade observada não depende da concentração de ˙NO *per se* (e consequentemente de um efeito tóxico tantas vezes atribuído ao ˙NO), mas antes sugere a activação de mecanismos de regulação que determinam a sua produção endógena. Esta observação foi confirmada por estimulação contínua de fatias com NMDA (considerada um modelo de excitotoxicidade, em virtude da sobreactivação de receptores de glutamato e nNOS), onde uma maior mas ainda assim transitória produção de ˙NO foi observada e, particularmente, em condições onde os receptores NMDA demonstraram estar activados (pelo menos parcialmente). Nesta linha, padrões distintos

foram também obtidos aquando da utilização de KCl e o substrato de nNOS L-arginina.

A investigação respeitante ao papel dos receptores AMPA na produção de ˙NO, quando comparada com a actividade dos receptores NMDA, revelou que a estimulação com AMPA induziu uma pronunciada mas distinta produção transitória de ˙NO. Esta revelou ser dependente de Ca^{2+} extracelular e independente da activação de receptores NMDA, tendo sido registados sinais onde a concentração de pico do ˙NO foi observada mais tardiamente. A observação de uma menor velocidade de produção e concentrações mais baixos de ˙NO, apesar de ocorrer para periodos de recuperação semelhantes quando comparados com os obtidos com NMDA, sugerem um acoplamento menos eficiente entre receptores AMPA com a nNOS, o que está de acordo com a noção de um controlo fino da produção de ˙NO via activação de receptores AMPA. A participação de receptores AMPA na produção endógena de ˙NO foi ainda verificada por inibição selectiva dos receptores ionotrópicos de glutamato na presença de glutamato, demonstrando o mesmo efeito mediado pelo agonista fisiológico. Na tentativa de determinar a origem de Ca^{2+} essencial à actividade da nNOS ficou patente uma contribuição, ainda que parcial, de receptores AMPA permeáveis a Ca^{2+}, o que constituiu uma observação surpreendente face à baixa expressão destes receptores no hipocampo descrita na literatura.

Condições de excitotoxicidade onde se reproduz uma activação continuada de receptores NMDA levam, presumivelmente, à activação de mecanismos celulares protectores. Entre estes encontra-se o glutatião (GSH), um antioxidante endógeno libertado por astrócitos para protecção e suporte de neurónios em condições fisiológicas e de elevada toxicidade celular. Ao investigar-se a resposta dos astrócitos na presença de uma elevada concentração de glutamato observou-se o aumento de GSH extracelular ao longo do tempo. As experiências realizadas excluiram, como mecanismos

responsável por este aumento, a ruptura da membrana plasmática e consequente libertação de conteúdos membranares, síntese *de novo* de GSH, inibição dos mecanismos extracelulares de degradação de GSH por glutamato e activação de receptores membranares de glutamato. Os resultados sugerem, portanto, que a libertação de GSH intracelular é o mecanismo responsável pelo aumento observado, sendo proposto como um mecanismo de protecção contra a toxicidade do glutamato.

CHAPTER 1

INTRODUCTION

1.1 - Historical Perspective

Since its early description in 1987 as the endothelial-derived relaxing factor (EDRF) nitric oxide ($^\bullet$NO) has emerged as both a fundamental signaling molecule in the regulation of a great number of cellular functions (Bredt *et al.* 1994), and as a potent mediator of cellular damage in a wide range of pathological conditions (Dawson *et al.* 1998). $^\bullet$NO-related molecules were long used clinically without knowledge of their mechanism of action. A prominent example is William Murrell's first use of nitroglycerin to treat *angina pectoris* in 1876 (Marsh *et al.* 2000), a nitrovasodilator still in use nowadays for the same purpose. Ferid Murad's group found in the late 70's that several compounds, including nitroglycerin and a variety of oxidants, were able to activate guanylate cyclase (Arnold *et al.* 1977; Braughler *et al.* 1979), an enzyme at time known to increase the production of cyclic guanosine monophosphate (cGMP) and mediate relaxation of blood vessels, by an unknown mediator. Amongst the candidate molecules was $^\bullet$NO, but the notion that it could be produced by mammals was considered unlikely for a long time. Robert Furchgott and John Zawadski published in 1980 a milestone paper where they recognized the importance of the endothelium in acetylcholine-induced vasorelaxation (Furchgott *et al.* 1980). Acetylcholine was a well-known vasodilating agent when injected *in vivo*, but generally caused isolated blood vessels to constrict *in vitro*. These scientists concluded that, when preserving endothelium during preparation of transverse vascular rings, acetylcholine was able to induce the release of a diffusible factor that would relax endothelium-denuded blood vessels by activating guanylate cyclase. Although the nature of this diffusible factor (termed EDRF) remained elusive for long time, it was shown to be quickly inactivated by oxyhemoglobin and agents known to generate superoxide anion ($O_2^{\bullet-}$), but rescued by superoxide dismutase (SOD) (Gryglewski *et al.* 1986; Moncada *et al.* 1986). It was finally in 1987 that Louis

Ignarro and Salvador Moncada independently identified EDRF to be $^\bullet$NO by chemiluminescence (Ignarro *et al.* 1987; Palmer *et al.* 1987). A novel research area was definitely opened, and Robert Furchgott, Louis Ignarro and Ferid Murad were awarded with the Nobel Prize in Physiology or Medicine in 1998 for their discoveries concerning "the nitric oxide as a signaling molecule in the cardiovascular system". Two decades after the identification of $^\bullet$NO as the EDRF an enormous research effort is still driven towards unveiling its role in physiological ad pathological pathways.

1.2 - Nitric Oxide

1.2.1 - Nitric Oxide Synthases

1.2.1.1 - Biosynthesis

$^\bullet$NO is produced *in vivo* by nitric oxide synthase (NOS, EC 1.14.13.39), a highly regulated enzyme that uses L-arginine (L-arg) and molecular oxygen (O_2) as substrates (Palmer *et al.* 1988; Palmer *et al.* 1988). The three main isoforms identified to date are products of different genes and have different cellular localization, regulation and catalytic properties. This has afforded several distinct nomenclatures, the first being based on their localization. Garthwaite and collaborators demonstrated that activation of glutamatergic receptors, particularly the N-methyl-D-aspartate (NMDA) subtype, induces $^\bullet$NO synthesis from L-arg in rat brain slices (Garthwaite *et al.* 1988; Garthwaite *et al.* 1989). This observation led to NOS cloning and isolation in the brain, where it was shown to occur in a number of different cells and regions (Bredt *et al.* 1990; Bredt *et al.* 1990; Schmidt *et al.* 1991). As this was the first $^\bullet$NO synthase to be identified it was named NOS1 or neuronal NOS (nNOS), but

soon after a second isoform was isolated from macrophages and termed NOS2 or inducible NOS (iNOS) (Hevel *et al.* 1991; Stuehr *et al.* 1991) because it could be readily induced by proinflammatory cytokines (Busse *et al.* 1990; Radomski *et al.* 1990). The first source of ˙NO identified, the endothelial ˙NO synthase, was the last to be cloned and is known as eNOS or NOS3 (Pollock *et al.* 1991). These isoforms can also be divided according to their expression, being termed constitutive (nNOS and eNOS) because they are present in large cellular populations at all times, or inducible (iNOS), as its expression depends largely on immunologic or inflammatory stimulus. Another major difference is that the latter is largely Ca^{2+}-independent (Busse *et al.* 1990), whereas the former are not (Stuehr *et al.* 1991). Although still a matter on controversy a fourth isoform, related to nNOS but (as opposed to it) shown to be myristoylated (Elfering *et al.* 2002), was demonstrated to occur in rat liver mitochondrial preparations and therefore named mtNOS (Bates *et al.* 1995; Ghafourifar *et al.* 1997; Giulivi *et al.* 1998). Although no gene was found for the mtNOS and its occurrence has been disputed, the mitochondria is a critical target for ˙NO actions and the role of ˙NO on mitochondria and its impact on cell physiology has recently been reviewed (Brown 2007).

In NOS, electrons from nicotinamide adenine dinucleotide phosphate (NADPH) flow between subunits to activate O_2 at the heme group, where L-arg is used to generate ˙NO, L-citrulline and H_2O (Figure 1.1, B). The enzyme converts the guanidino nitrogen of L-arg to ˙NO and L-citrulline in a process that consumes five electrons (Bredt *et al.* 1994) and requires it to cycle twice (Figure 1.1, A). In the first step, NOS consumes one mol of NADPH to hydroxylate L-arginine to N^{ω}-hydroxyl-L-arginine, which is an enzyme-bound intermediate (Stuehr *et al.* 1991). In an unusual second step one electron from NADPH and another from N^{ω}-hydroxyl-L-arginine lead to oxygen incorporation and scission of the C-N bond, yielding citrulline and ˙NO (Figure 1.1, B)

(Stuehr *et al.* 1991). The fact that NOS binds and activates O_2 twice to generate ˙NO from L-arg explains its role in some pathological pathways, particularly in the generation of $O_2^{˙-}$.

A

Arginine   N^ω-hydroxyarginine   Citrulline   Nitric Oxide

B

L-arg + O_2 + NADPH + H^+ ⟶ NOH-L-Arg + H_2O + $NADP^+$ **1st step**

OH-L-Arg + O_2 + $^1/_2$ (NADPH + H^+) ⟶ L-citrulline + NO + H_2O + $^1/_2$ $NADP^+$ **2nd step**
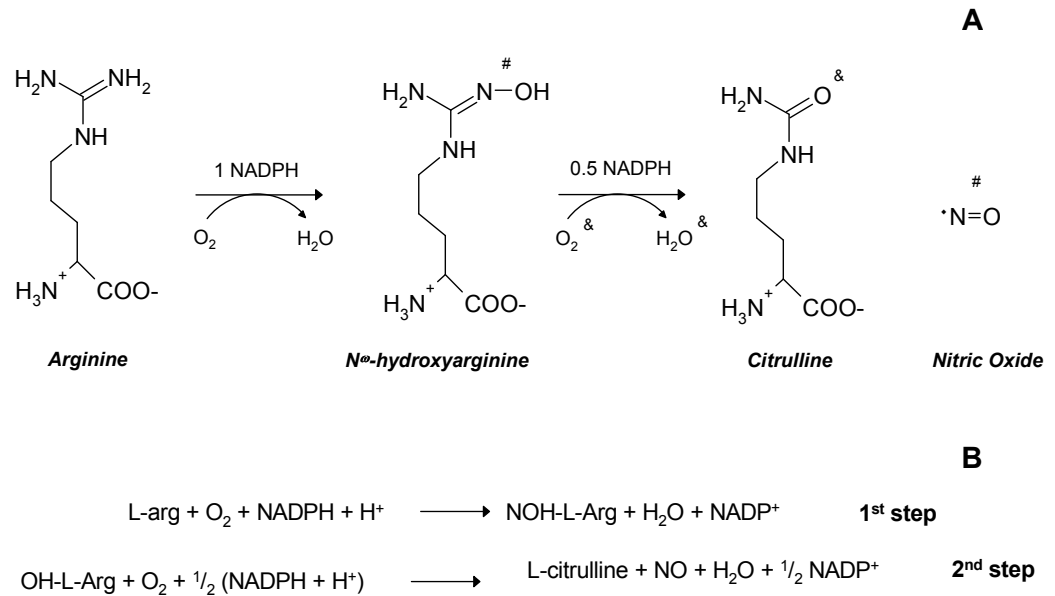
Figure 1.1: Synthesis of ˙NO by NOS. A) The guanidino nitrogen of L-arg is converted to ˙NO in a two-step reaction at the heme group of NOS dimer. B) Partial reactions result in a stoichiometry of 1 L-.arg, 1.5 NADPH and 2 O_2 to form 1 L-citrulline, 1.5 $NADP^+$, 1 H_2O and 1 ˙NO molecules. Adapted from (Stuehr *et al.* 2001) and (Alderton *et al.* 2001).

1.2.1.2 - Reductase and Oxygenase Domains

NOS isoforms are dimeric and each subunit is composed by two domains, one oxygenase and one reductase, connected to each other by a central Ca^{2+}/calmodulin-binding region (Figure 1.2, A) (Marletta 1993). Dimerization increases NOS activity by creating high-affinity binding sites for L-arg and BH4, removing heme from the solvent phase, and facilitating electron flow between domains (Crane *et al.* 1999; Li *et al.* 1999). The electron

transport pathway mentioned above involves both domains in the heterodimer, as illustrated in Figure 1.2 B (Siddhanta *et al.* 1998).

The C-terminal reductase domain of NOS (Figure 1.2 B, rectangular shape) catalyzes three electron transfer reactions, starting with 1) NADPH reduction of bound flavin adenine dinucleotide (FAD), 2) distribution of single electrons between FAD and flavin mononucleotide (FMN) and 3) electron transfer from reduced FMN to NOS heme. These reactions are initiated by
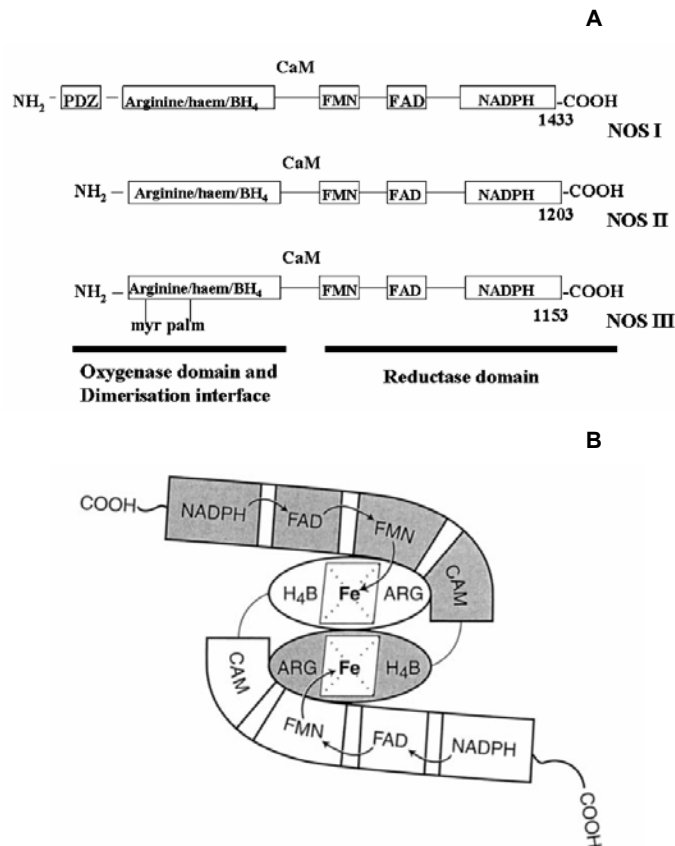
Figure 1.2: Subunit structure and proposed model for NOS. A) All NOS isoforms are composed of two subunits, each comprising a reductase and oxygenase domains with binding sites for several cofactors, connected by a central calmodulin-binding motif (CaM). B) Domain swapping occurs between subunits (grey and white) to properly align reductase (rectangular) and oxygenase (oval) domains for $^{\bullet}$NO synthesis. Binding sites: ARG, L-arg; haem or Fe, heme group; BH_4 or H_4B, tetrahydrobiopterin; CaM or CAM, calmodulin; FMN, flavin mononucleotide; FAD, flavin adenine dinucleotide; NADPH, nicotinamide adenine dinucleotide phosphate. Adapted from (Bruckdorfer 2005) and (Siddhanta *et al.* 1998).

Ca^{2+}-activated CaM binding to NOS reductase domain. Electrons transferred into the reductase domain then pass to the catalytic N-terminal oxygenase domain (Figure 1.2 B, oval shape) (Siddhanta *et al.* 1998). This contains binding sites for the substrate L-arg, tetrahydrobiopterin (BH4) and particularly iron protoporphyrin IX (heme), where O$_2$ is activated for $^{\bullet}$NO synthesis (Masters *et al.* 1996; Stuehr 1997). A close structural similarity is observed between isoforms, suggested to arise from a common ancestral NOS gene, as the distinct NOS genes have a similar genomic structure (Xu *et al.* 1994).

Several differences in these domains account for distinct features of NOS isoforms, as summarized briefly in Table 1.1. Myristoylation (Myr) and palmitoylation (Palm) sites are present in eNOS oxygenase domain, allowing it to be targeted to the cellular membrane (Garcia-Cardena *et al.* 1996). nNOS is to eNOS, but its N-terminal 220 amino-acids exhibit a special region called PDZ domain, which allows it to be directed to synapses and interact with membrane receptors and other proteins (PDZ stands for PSD-95 discs large/ZO-1 homology domain, and PSD-95 for post synaptic density protein 95) (Brenman *et al.* 1996; Christopherson *et al.* 1999). Both enzymes constitutively produce $^{\bullet}$NO after a conformational change (Matsuda *et al.* 1999; Abu-Soud *et al.* 2000) induced by Ca^{2+}/CaM binding, in turn controlled by amino acid inserts that serve as autoinhibitory loops (Salerno *et al.* 1997; Roman *et al.* 2000). The same is not true for iNOS. This isoform was also shown to be dependent on Ca^{2+} (Iida *et al.* 1992), but because these inserts are absent and CaM binding is strong (Cho *et al.* 1992), low physiological Ca^{2+} levels are sufficient to activate it (Roman *et al.* 2000). This isoform is therefore regulated by transcription (Cho *et al.* 1992; Vodovotz *et al.* 1993). iNOS is often called a high-output source of $^{\bullet}$NO but this is a consequence of high levels of transcription, as it does not produce $^{\bullet}$NO at a substantially greater rate than nNOS or eNOS (Nathan *et al.* 1994).

Table 1.1: Structural and physiological **c**haracteristics of NOS isoforms.

	nNOS (NOS1)	eNOS (NOS3)	iNOS (NOS2)
Main localization	brain	endothelial cells	macrophages
Main physiological function	neurotransmission	regulation of blood flow	non-specific immunity
Cellular Localization	cytosol	membrane	cytosol
Expression	constitutive	constitutive	inducible
Ca^{2+} changes	dependent	dependent	independent
Size (Human)	160 kDa	131 kDa	130 kDa
Number of amino acids (Human)	1434	1153	1153
Genes (Human)	160 kb, chromosome 12	37 kb, chromosome 17	21 kb, chromosome 7
Protein-protein interactions	CaM/Ca^{2+}, PSD-95, PSD-93, PDZ domains, PIN, caveolin-1, Hsp90, CAPON, COOH-terminal-binding protein	CaM/Ca^{2+}, caveolin-1 and -3, Hsp90	CaM/Ca^{2+}, kalirin
Covalent modifications	Phosphorylation	Myristoylation, palmitoylation, phosphorylation	-

Adapted from (Marletta et al. 1998; Alderton et al. 2001; Kone et al. 2003; Bruckdorfer 2005). PIN, Protein inhibitor of NOS; Hsp90, heat-shock protein 90; PSD-93 and -95, Post synaptic density protein-93 and -95; PDZ, PSD discs large/ZO-1 homology; CAPON, COOH-terminal PDZ ligand of nNOS

1.2.2 - Chemical Biology

1.2.2.1 - Physical and Chemical Properties of Nitric Oxide

˙NO mediates a number of physiological pathways quite differently from other neurotransmitters. Contrary to what is conventionally found in the literature, ˙NO *per se* is not very reactive when compared with other O or N-centered radicals. Being an intermediate between O_2 and nitrogen (N_2) its

reactivity relates with that of O_2. In the ${}^{\bullet}NO$ molecule, the nitrogen atom has five valence electrons and oxygen has six. This results in one unpaired electron that makes 1) an effective bond of 2.5 between N and O and 2) gives the molecule its free radical properties. Like molecular oxygen, ${}^{\bullet}NO$ undergoes fast reactions with heme groups and free radicals. This supports its binding to heme proteins like soluble guanylate cyclase (detailed latter) (Beckman *et al.* 1996; Pacher *et al.* 2007) and its antioxidant properties (Kanner *et al.* 1991). In fact, by acting as a chain terminating agent and originating stable intermediate products, ${}^{\bullet}NO$ breaks propagating oxidation chains (*e.g.* lipid peroxidation) and may facilitate subsequent repair by antioxidants such as ascorbic acid, tocopherol, or (Pacher *et al.* 2007).

${}^{\bullet}NO$ is a small free radical but is also hydrophobic, reaching only 1.93 mM (25°C) or 1.63 mM (37°C) concentrations in aqueous solutions (at a pressure of 1 atm) (Wilhelm *et al.* 1977). At physiological ionic strength and temperature its solubility is 1.55 mM. Malinski *et al.* reported it to be six- to sevenfold higher in membranes when compared to the aqueous phase, and suggested that membranes could act as "reservoirs" for ${}^{\bullet}NO$ (Malinski *et al.* 1993). Due to its physical and chemical properties ${}^{\bullet}NO$ is therefore capable of permeating cellular membranes with a diffusion coefficient similar to that of O_2 (Wise *et al.* 1969), calculated at 37°C to be 3.3 X 10^{-5} cm^2s^{-1} in endothelial cells (Malinski *et al.* 1993) and 3.8 ± 0.3 X 10^{-5} cm^2s^{-1} in brain tissue (Koppenol 1998). Jack Lancaster suggested in 1994 that ${}^{\bullet}NO$ could diffuse to considerable high distances (hundreds of μm), relying his arguments in kinetic modeling of ${}^{\bullet}NO$ diffusibility based on published data (Lancaster 1994). As eukaryotic cells are 10-100 μm in size, and the half-life of ${}^{\bullet}NO$ was reported to be around 4 s (Lancaster 1994; Koppenol 1998), this free radical has the potential to diffuse to organelles and cells adjacent to its production site and mediate their function, as reported initially in studies concerning EDRF (Furchgott *et al.* 1980; Garthwaite *et al.* 1988). In this regard, Ledo *et al.*

reported recently that ˙NO can diffuse at least 400 μm in the CA1 region of hippocampal slices (Ledo *et al.* 2005). Signaling molecules generally rely on structural characteristics to convey information, but this does not apply to ˙NO. With only two atoms it cannot be readily distinguished by its shape, and must therefore convey information by changes in its local concentration. Consequently, decay mechanisms are of the outmost importance when it comes to ˙NO-mediated pathways in a particular system, as its physiological actions only terminate once its elimination is complete (Pacher *et al.* 2007).

From what was previously mentioned ˙NO can mediate a number of reaction by itself or following interaction with other molecules. As depicted at the end of this section in Figure 1.3, this affords a distinction between direct and indirect reactions.

1.2.2.2 - Direct Reactions

Direct effects are those in which ˙NO interacts directly with biological molecules, generally at low concentrations. These include reactions with 1) metal complexes and 2) radical species (Wink *et al.* 1998).

1) Metal Complexes

There are three major types of ˙NO reactions with metals: (I) the binding to the metal center, (II) a redox reaction with O_2-bound metal complexes, and (III) high valent oxo-complexes. In the first set, ˙NO reacts with some transition metals to form stable metal nitrosyl complexes, and key examples are the formation of Fe-NO complexes that occur in guanylate cyclase and NOS itself (Wink *et al.* 1998). These reactions do not involve changes in the metal center charge and are therefore termed nitrosylation. From the chemical point of view it corresponds to the addition of a nitrosyl

group, NO, stressing the concept of the addition of a chemical group that, if it were free, it would be a radical (Martinez-Ruiz *et al.* 2004) (reaction 1):

$$Fe(II) + \cdot NO \leftrightarrow Fe(II)\text{-}NO \qquad\qquad (1)$$
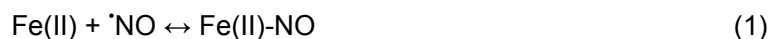
Although $\cdot NO$ can bind to similar heme structures its effects are dependent on the physiological role and activity of the target molecule. Guanylate cyclase is the major efector enzyme of $\cdot NO$ signaling (Ignarro 1990) and its activation occurs upon binding of $\cdot NO$, leading to the formation of a Fe-nitrosyl complex that induces the production of the secondary messenger cGMP (Ignarro 1990; Murad 1994). On the other hand, $\cdot NO$ binding to the NOS oxygenase domain causes the enzyme to inactivate, in what is considered to be feedback regulatory mechanism of NOS activity (Assreuy *et al.* 1993; Marletta 1993).

The second and third type of reactions involving metal centers and $\cdot NO$ concerns those with metal-oxygen complexes and metallo-oxo complexes (reaction 2 and 4, respectively). Reaction 2 is a major example of the first, also serving to highlight one long-known major biological effect of $\cdot NO$: its reaction with oxyhemoglobin to form methemoglobin and nitrate (Doyle *et al.* 1981).

$$Hb\ (Fe\text{-}O_2) + \cdot NO \rightarrow met\ Hb\ Fe(III) + NO_3^- \qquad\qquad (2)$$
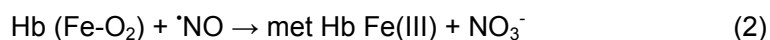
Due to the high concentration of oxyhemoglobin and its relatively fast ($k = 10^7\ M^{-1}s^{-1}$) reaction with $\cdot NO$, reaction 2 is a primary metabolic fate and control mechanism for $\cdot NO$ levels *in vivo* (Lancaster 1994).

The third type of reactions concerns high valent metal complexes that are formed from oxidation by agents such as hydrogen peroxide. The hypervalent metal complexes (reaction 3) are powerful oxidants that can lead to cellular damage by lipid peroxidation (Puppo *et al.* 1988), but reaction with

$^{•}$NO prevents these deleterious oxidative effects (Kanner *et al.* 1991; Wink *et al.* 1994).

$$Fe^{(2,3)+} + H_2O_2 \rightarrow Fe^{(4,5)+}=O + H_2O \quad\quad\quad (3)$$

$$Fe^{4+}=O + {}^{•}NO \rightarrow Fe^{3+} + NO_2^{-} \quad\quad\quad (4)$$
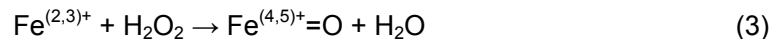
2) Radical species

Amongst the direct reactions of $^{•}$NO are those with alkoxyl or peroxyl radicals formed during lipid peroxidation (reaction 5). Padmaja and Huie found that their rate of reaction with $^{•}$NO in aqueous solution to be elevated, with k = 1-3 x 10^9 $Lmol^{-1}s^{-1}$ (Padmaja *et al.* 1993).

$$LOO^{•} + {}^{•}NO \rightarrow LOONO \quad\quad\quad (5)$$

This reaction has led researchers to propose a role for $^{•}$NO in terminating lipid peroxidation chain reactions (Wink *et al.* 1994), particularly after reports indicating that $^{•}$NO partitions more in membranes (Malinski *et al.* 1993). $^{•}$NO can also react with tyrosyl radicals, an essential intermediate species found, for instance, in the catalytic turnover of ribonucleotide reductase expressed in tumor cells (Lepoivre *et al.* 1992), or stabilize carbon-centered radicals formed in DNA by ionizing radiation (Mitchell *et al.* 1996).

1.2.2.3 - Indirect Reactions

Unlike direct effects, indirect effects are mediated by reactive nitrogen/oxygen species (RNOS) derived from $^{•}$NO reactions with 1) O_2 and 2) $O_2^{•-}$. In this regard, direct reactions with thiols or other molecules too slow to

be significant in biological systems proceed only through an activation step of $^{\bullet}$NO by oxygen or superoxide anion and metal ions (Wink *et al.* 1994).

1) Reaction with O_2 and autoxidation

$^{\bullet}$NO is unstable and reactive in the presence of oxygen, leading to the formation of several RNOS. One example is nitrogen dioxide ($^{\bullet}$NO$_2$), a brown coloured pollutant produced in the atmosphere of major cities (reaction 6, -d[NO]/dt = $2k_g$[NO]^2[O$_2$]) (Bruckdorfer 2005). Another is dinitrogen trioxide (N$_2$O$_3$) (reaction 7), that further hydrolyses to nitrite and nitrous acid (HNO$_2$). Both are known to be injurious to biological tissues when present in the atmosphere (Schwartz *et al.* 1983):

$$2\ ^{\bullet}\text{NO} + \text{O}_2 \rightarrow 2\ ^{\bullet}\text{NO}_2 \qquad\qquad (6)$$

$$^{\bullet}\text{NO}_2 + {^{\bullet}}\text{NO} \rightarrow\ \text{N}_2\text{O}_3 + 2\ \text{H}_2\text{O} \rightarrow 2\ \text{HNO}_2 \qquad (7)$$
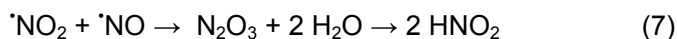
In aqueous solutions $^{\bullet}$NO also undergoes autoxidation by a third order rate reaction similar to gas phase, but in this case only N$_2$O$_3$ can be detected as an intermediate, as no free $^{\bullet}$NO$_2$ is formed because of its instability in the aqueous medium (Ford *et al.* 1993; Wink *et al.* 1995). The reaction proceeds at a different overall stoichiometry when compared to the gaseous phase (reaction 8), but with a similar rate law of -d[NO]/dt = $4k_{aq}$[NO]^2[O$_2$], where k_{aq} = 2 x 10^6 M^{-1}s^{-1} at 25°C (Ford *et al.* 1993).

$$4\ ^{\bullet}\text{NO} + \text{O}_2 + 2\ \text{H}_2\text{O} \rightarrow 4\ \text{NO}_2^- + 4\ \text{H}^+ \qquad (8)$$

This rate constant for the autoxidation reaction of $^{\bullet}$NO is pH-independent and similar between 25 ºC and 37 ºC (Ford *et al.* 1993; Wink *et al.* 1995) either in aqueous or hydrophobic solvents (Nottingham *et al.* 1989).

These kinetic parameters enhance the understanding of how $^\bullet$NO can serve as a double-edged sword in physiological processes. As these reactions are second order for $^\bullet$NO, low concentrations afford a longer life-time in tissues, where it mediates regulatory processes by reacting with heme proteins (as mentioned before). In contrast, high levels of $^\bullet$NO (*e.g.* produced by activated macrophages) would facilitate the reaction with O_2 and the onset of oxidative and nitrosative stress, with known cytotoxic consequences (Wink *et al.* 1998). The same rationale can be used to determine where $^\bullet$NO autoxidation is higher in cells. The reaction between $^\bullet$NO and O_2 progresses at similar rates in membranes or cytoplasm (Nottingham *et al.* 1989), but because both are 20 times more abundant in membranes reactive intermediates are expected to occur in the lipid bilayer, causing membrane-associated protein damage (Wink *et al.* 1998). N_2O_3 is expected to be the predominant product, and because membranes have low amounts of H_2O its hydrolysis to nitrite is reduced (reaction 7). In these circumstances nitrosation of amines and thiols becomes favored, and result in the formation of bioactive S-nitrosothiols (Stamler 1994).

2) Reaction with $O_2^{\bullet-}$

The reaction between $O_2^{\bullet-}$ and $^\bullet$NO occurs at diffusion controlled rates with a rate constant of 1×10^{10} $M^{-1}s^{-1}$ (Huie *et al.* 1993), yielding peroxynitrite (ONOO-, reaction 9).

$$^\bullet NO + O_2^{\bullet-} \rightarrow ONOO^- \quad\quad\quad\quad (9)$$

ONOO$^-$ is a powerful oxidant *in vivo*, endowed with a reduction potential of E°(ONOO$^-$, $2H^+$/ $NO_2^\bullet$, H_2O) of 1.6 V at pH 7 (Koppenol *et al.* 1992). It can directly oxidize protein and nonprotein thiols and sulfhydryls (Radi *et al.* 1991) and induce lipid peroxidation (Hogg *et al.* 1993), being the

major player in $^{\bullet}$NO-attributed cytotoxicity (Pacher *et al.* 2007). The major determinant of ONOO$^-$ formation is the abundance of both radicals, as the rate of formation of peroxynitrite is first order for both (reaction 9, -d[ONOO$^-$]/dt = k[$^{\bullet}$NO][O$_2$$^{\bullet-}$]) (Huie *et al.* 1993). Hence, production rates and/or reactions of O$_2$$^{\bullet-}$ and $^{\bullet}$NO with biological components determine ONOO$^-$ formation. $^{\bullet}$NO production greatly follows NOS activity, as mentioned before, and levels of O$_2$$^{\bullet-}$ are generally low *in vivo* due to superoxide dismutase (SOD) activity, which dismutates O$_2$$^{\bullet-}$ to hydrogen peroxide (H$_2$O$_2$) at a rate of 2.4 x 10^9 M^{-1}s^{-1} (Fielden *et al.* 1974). On basis of the higher rate constant of reaction 9, $^{\bullet}$NO competes with SOD for O$_2$$^{\bullet-}$. However, under normal conditions, and depending on compartmentalization issues, micromolar amounts of SOD (Nakano *et al.* 1990) overcomes $^{\bullet}$NO, preventing the formation of ONOO$^-$ (Koppenol 1998). Also worth noting are $^{\bullet}$NO diffusion across membranes and its reaction with hemoglobin, because both afford a further decrease in its concentration (Lancaster 1994). Hence, ONOO$^-$ formation is limited to regions close to the location of the $^{\bullet}$NO source and, more importantly, of O$_2$$^{\bullet-}$ source, as this free radical is unable to permeate membranes (Fridovich 1995). Candidate places are mitochondria and the vicinity of NADPH oxidase or xanthine oxidase, as all are places where O$_2$$^{\bullet-}$ can build up simultaneously with $^{\bullet}$NO (Rubbo *et al.* 1994; Brown 2007).

Indirect effects of $^{\bullet}$NO can be subdivided into nitrosation, oxidation and nitration as follows, depending on the final outcome:

I) Nitrosation: a reaction that involves the addition of a nitroso group (NO) (Martinez-Ruiz *et al.* 2004), that occurs when an equivalent of NO$^+$ is added to an amine, thiol, or hydroxy aromatic group (*e.g.* conversion of thiol peptides to S-nitrosothiol peptides). A major nitrosative species is N$_2$O$_3$ (Jourd'heuil *et al.* 1999). Conversely to N$_2$O$_3$, $^{\bullet}$NO$_2$ radical may promote S-nitrosation via a radical pathway.

II) Oxidation: Oxidation chemistry includes one or two electron removal from substrate, as well as hydroxylation reactions. Conversely to peroxynitrite, N_2O_3 is a relatively mild oxidant (Wink *et al.* 1998).

III) Nitration: a reaction corresponding to the incorporation of a nitro triatomic group (- NO_2) (Martinez-Ruiz *et al.* 2004). The formation of nitrotyrosine from different RNOS such as $ONOO^-$ is a good example, encompassing $^\bullet NO_2$ radical (upon interaction with metals) and CO_3^- radical anion (upon reaction with CO_2) as radical intermediates.
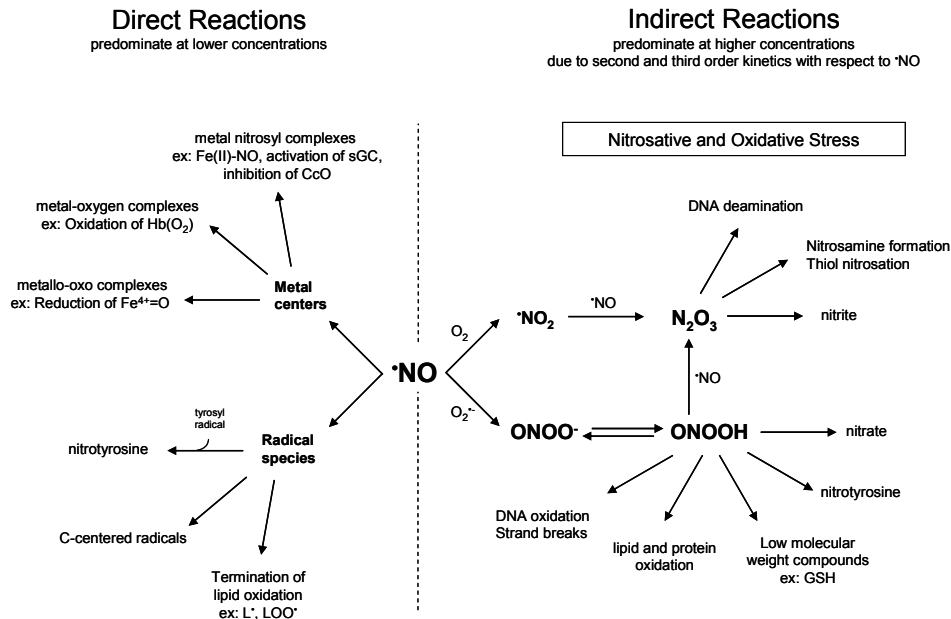
Figure 1.3: $^\bullet$NO-mediated reactions in biological systems. From a simply standpoint $^\bullet$NO participates in direct and indirect reaction, targeting different biologic components *per se* or yielding distinct end metabolites depending on which intermediate is formed (respectively). Adapted from (Davis *et al.* 2001) and (Wink *et al.* 1998).

1.2.3 - Regulation of nNOS

Given its impact in brain physiology, $^{\bullet}$NO production by nNOS is regulated at a number of different levels, as detailed briefly.

1.2.3.1 - Substrate and Cofactor Availability

$^{\bullet}$NO production is unlikely to be limited by its substrate as the concentration of L-arg in cells is considered to be far in excess of the saturation point of the enzyme, but the occurrence of inhibitory L-arg analogues like L-monomethlyl arginine (L-NMMA) could lead to NOS inhibition (Bruckdorfer 2005). Changes in nNOS cofactor pools (particularly NADPH) largely impact on $^{\bullet}$NO production (Vallance *et al.* 2001; Bruckdorfer 2005). In this regard, BH$_4$ plays a major role in electron transfer and dimer stabilization in nNOS (Panda *et al.* 2002) and in reducing its inhibition, by decreasing its susceptibility to protein kinase C-dependent phosphorylation (Okada 1998). Finally, nNOS is expressed as inactive monomers and is only activated by CaM binding, which promotes interaction between oxigenase and reductase domains and NOS dimer formation (Panda *et al.* 2001). Apparently, CaM not only enhances dimer stabilization but also increases nNO reductase activity and electron transfer, controlling $^{\bullet}$NO synthesis by governing heme iron reduction (Gachhui *et al.* 1998).

1.2.3.2 - Feedback Inhibition by Nitric Oxide

Due to the stability of Fe^{2+}-NO complexes, any enzyme that relies on a reduced ferrous heme group in its activity has the potential to be inhibited by $^{\bullet}$NO. nNOS is no exception, and this has been suggested as a self-regulatory mechanism that would allow the enzyme to be controlled by its product (Adak

et al. 1999). During steady-state ˙NO synthesis 70 to 90 % of nNOS was shown to be present as its ferrous-nitrosyl complex, formed only in the presence of NADPH, L-arg, and O_2 (Abu-Soud *et al.* 1995). As Fe^{3+}-NO complex is an intermediate during catalysis, a competition between ˙NO dissociation (normal catalysis) versus reduction to a Fe^{2+}-NO species (auto-inhibition) as been proposed to occur and raise the Km for oxygen, thus determining nNOS activity (Santolini *et al.* 2001). The rate of complex breakdown was shown to be directly proportional to O_2 concentration and is therefore one of the steps that limits nNOS turnover in the steady state, making nNOS-dependent ˙NO synthesis oxygen-dependent throughout the physiological range (Abu-Soud *et al.* 1996). Interestingly, ˙NO synthesis by eNOS was shown to depend more on slow electron transfer from its reductase domain to the heme rather than Fe^{2+}-NO complex formation, suggesting isoform-dependent regulatory pathways that can explain their different biological activities (Abu-Soud *et al.* 2000).

1.2.3.3 - Phosphorylation

Protein kinase C (PKC) and A (PKA) have been found to regulate nNOS activity through phosphorylation, together with Ca^{2+}/ CaM-dependent protein kinases I and II (CaMKI and CaMKII) (Okada 1998; Hayashi *et al.* 1999). The latter phosphorylate nNOS at Ser-741 and Ser-847 residues, respectively, to inhibit or suppress the enzyme activity (Hayashi *et al.* 1999; Komeima *et al.* 2000). In this regard, CaMKII is associated with NR2A and NR2B subunits of NMDA receptors in hippocampus and cortex (Gardoni *et al.* 1998) and can contribute to the constitutive nNOS phosphorylation seen by others (Rameau *et al.* 2003). However, activation of NMDA receptors (NMDAR) decreases the level of nNOS phosphorylation and consequently increases nNOS enzymatic activity, in a mechanism involving Ca^{2+}-regulated

phosphatases (Rameau *et al.* 2003). This was suggested to be a novel bidirectional regulatory pathway for nNOS activity, mediated by NMDAR and dependent on glutamate stimulation: physiological concentrations would result in nNOS phosphorylation and limited ˙NO production, whereas cytotoxic stimulations would promote dephosphorylation and toxic levels of ˙NO (Rameau *et al.* 2004).

1.2.3.4 - Protein Regulators

Protein-protein interactions are a major theme in the regulation of nNOS. This isoform exhibits a special motif at the N-terminal region called PDZ domain, which targets nNOS to synaptic sites where it interacts with membrane receptors (particularly the NMDAR) (Brenman *et al.* 1996). This interaction can be modulated because the adaptor protein CAPON (carboxy-terminal PDZ ligand of nNOS) competes for the same PDZ domain and separates nNOS from the NMDA receptor (Jaffrey *et al.* 1998). CAPON does not directly inhibit nNOS activity but rather reduces its ability to be stimulated by Ca^{2+} influx through NMDAR. CAPON also binds to synapsins I, II, and III and promotes a ternary complex with nNOS, inducing changes in the subcellular localization of nNOS (Jaffrey *et al.* 2002). nNOS also contains a binding site for the 10 kDa highly-conserved protein PIN (Jaffrey *et al.* 1996), which inhibits nNOS oxidase activity in a time-dependent manner (Hemmens *et al.* 1998). The molecular chaperone heat shock protein-90 (Hsp90) is a known regulator of eNOS activity (Garcia-Cardena *et al.* 1998) but has also been implicated in nNOS regulation (Bender *et al.* 1999) by enhancing calmodulin binding.

1.3 - Modulation of Cellular Pathways by Nitric Oxide

The mechanisms that support ˙NO wide range of effects in the central nervous system are still elusive, particularly in which concerns to the impact of rate and pattern of ˙NO changes in biological events. All NOS isoforms have been identified in the brain and this in suggested to impact on physiological and pathological pathways (Duncan *et al.* 2005). The next section frames a global picture of ˙NO activity in terms of target proteins and cellular pathways, with impact on brain physiology and pathology.

1.3.1 - Soluble Guanylate Cyclase

The activation of guanylate cyclase (or guanyly cyclase, EC 4.6.1.2), an enzyme that produces cGMP from GTP, is considered the major signal transduction pathway of ˙NO, supporting some of its best described activities such as vasorelaxation and neuromodulation (Figure 1.4). This activation occurs for low ˙NO concentration, with an EC50 value calculated in vitro of 100 nM (Forstermann *et al.* 1996). cGMP is synthesized by a family of enzymes expressed in nearly all cell types and composed of two classes, particulate and soluble (Krumenacker *et al.* 2004). The particulate guanylate cyclases (pGC) are membrane-bound receptor molecules that are activated following ligand binding to their extracellular domain (Lucas *et al.* 2000). The soluble guanylate cyclase (sGC) is a cytosolic heme-containing ˙NO-binding protein, composed of α and β subunits that make up the active enzyme. Activation of sGC occurs when ˙NO binds to the Fe^{2+}-containing heme prosthetic group located at the N-terminal region, increasing the Vmax of sGC by 100-200-fold (Stone *et al.* 1994). Produced cGMP modulates numerous signaling cascades mediated by cGMP-dependent protein kinases, cGMP-regulated

phosphodiesterases and cyclic nucleotide-gated ion channels in cardiovasculature, platelet function, neurotransmission, and other cellular pathways (Lucas *et al.* 2000).

1.3.2 - Energy Metabolism

Mitochondria play a central role in the modulation of cell life and death pathways, and several targets have been identified for ˙NO, encompassing direct and indirect reactions. The protein complexes I to IV that make up for the electron transport chain are susceptible to modifications by ˙NO, with mild or severe consequences depending on a number of factors. ˙NO inhibits mitochondrial respiration by two different means: 1) rapid, selective, potent and reversible inhibition of cytochrome oxidase by ˙NO (Brown 2001) and 2) slow, nonselective, weak and irreversible inhibition of complexes and mitochondrial components by reactive nitrogen species (RNS) (Radi *et al.* 2002).

Cytochrome c oxidase (CcO) is a complex of 13 subunits, containing 2
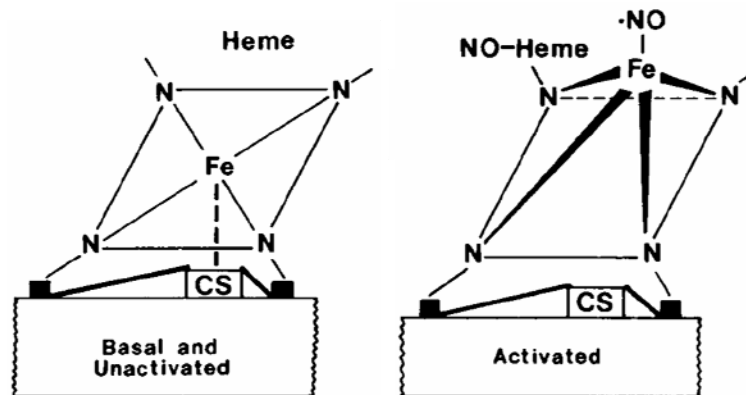
Figure 1.4: Guanylate cyclase activation by ˙NO. Left) In the basal and unactivated state, catalytical activity of GC is minimal due to steric hindrance, limiting the access of substrate to the catalytic site (CS). Right) ˙NO binding to heme iron to form the nitrosyl-heme adduct results in catalytic site exposure to GTP. Adapted from (Ignarro 1998).

heme groups (cyt *a* and cyt a_3) and 2 copper centers (CuA and CuB). $\cdot$NO can interact with the reduced cytochrome a_3^{2+} to yield the complex a_3^{2+}-NO in a competitive reaction with O_2 or bind to oxidized CuB^{2+}, reducing it to form the CuB^+-NO^+ complex that rapidly gives NO_2^- (Torres *et al.* 1995; Giuffre *et al.* 1996; Torres *et al.* 2000). This latter inhibitory reaction is not competitive with O_2 and is a catalytic degradation pathway for $\cdot$NO (Torres *et al.* 2000). Low concentrations of $\cdot$NO cause immediate inhibition of O_2 consumption with a half-inhibitory concentration of 60 to 270 nM, depending on O_2 concentration (Brown *et al.* 1994). $\cdot$NO binding to cytochrome a_3^{2+} is fast and comparable to that of O_2, with a rate of 0.4-1.0 x 10^8 $M^{-1}s^{-1}$ (Blackmore *et al.* 1991). Researchers hypothesize this to be a modulatory pathway of CcO activity and mitochondria respiratory rate to regulate O_2 distribution in tissues (Forfia *et al.* 1999; Giulivi 2003). When $\cdot$NO exposure is prolonged an irreversible inhibition of respiration develops (Clementi *et al.* 1998). This was attributed to the conversion of $\cdot$NO to $ONOO^-$ and other RNS, which inhibit respiration at multiple sites, including complexes I and II (Cassina *et al.* 1996; Clementi *et al.* 1998). Finally, $\cdot$NO can induce mitochondrial permeability transition and oxidative/nitrosative stress, with marked influence on cellular death and survival pathways (Brown 2007).

Aconitases are iron-sulfur cluster-containing proteins found in mitochondria and cytosol of cells that catalyze the reversible isomerization of citrate and isocitrate via cis-aconitate (Gruer *et al.* 1997). These enzymes contain unique [4Fe-4S] clusters in which one of the irons is not bound to an aminoacid residue, but rather to a hydroxide from solvent (Davis *et al.* 2001). Low levels of $ONOO^-$ cause the conversion of the Fe-S cluster from the $[4Fe-4S]^{2+}$ form to the inactive $[3Fe-4S]^{1+}$ with the loss of labile iron (Han *et al.* 2005). The activity of aconitase can be altered by $\cdot$NO, $ONNO^-$ and particularly

nitrosoglutathione (GSNO), in what can be regarded as a modulatory mechanism of aconitase activity under stress (Tortora *et al.* 2007).

Glyceraldehyde 3-phosphate dehydrogenase (GAPDH, EC 1.2.1.12) is a glycolytic enzyme that catalyses the conversion of D-glyceraldehyde-3-phospate (G-3-P) to 1,3-diphosphoglycerate (1,3-DPG). Alterations on glycolysis might alter cellular function, and ˙NO was shown to inhibit GAPDH by S- nitrosylation, an effect reversed by low-molecular-weight thiols like glutathione (GSH) (Padgett *et al.* 1997). S- nitrosylation of GAPDH facilitates further covalent modification of the enzyme by NADH, an irreversible event likely to be involved in pathological events (Mohr *et al.* 1996). GAPDH has also been proposed to play a role in less obvious cellular pathways, including modulation of protein kinases (Sirover 1999), apoptosis signaling (Carlile *et al.* 2000), and maintenance of blood–brain barrier integrity (Hurst *et al.* 2001). Modifications elicited by ˙NO on GAPDH can thus impact on a number of pathways.

1.3.3 - Glutamate Ionotropic Receptors

A regulatory role of ˙NO on ionotropic glutamate receptors is clearly established. The NMDAR is one subtype of glutamate ionotropic receptors critical for development, learning, and memory (McBain *et al.* 1994). Activation of NMDAR increases intracellular Ca^{2+} concentration, causing nNOS activation and subsequent ˙NO production (Garthwaite *et al.* 1988; Bredt *et al.* 1990). However, ˙NO can inhibit the NMDAR, decreasing the rise in intracellular Ca^{2+} elicited by NMDA (Manzoni *et al.* 1993). After site directed mutagenesis this downregulation was shown to arise after specific nitrosylation of cysteine 399 in the NR2A subunit of the NMDAR (Choi *et al.* 2000), in what was considered to be a negative feedback mechanism to

prevent excessive activation of the NMDA receptor and associated neurotoxicity (Lipton *et al.* 1994). Nevertheless, the efficacy of such inhibition on $^{\bullet}$NO production has been recently disputed (Ledo *et al.* 2005).

The α-amino-3-hydroxy-5-methyl-4-isoxazolepropionic acid (AMPA) receptor (AMPAR) is a K^+- and Na^+-permeable glutamate-activated receptor that, contrary to NMDAR, is not directly associated to nNOS activation. Nevertheless, it might be modulated by $^{\bullet}$NO, since this free radical was able to increase the affinity of AMPA binding sites by 15 to 30 % in different brain areas (Dev *et al.* 1994). More recently it was shown that nNOS inhibition decreased the amplitude of AMPA- and glutamate-induced intracellular Ca^{2+} rises in rat hypothalamic paraventricular nucleus, suggesting a role of endogenous $^{\bullet}$NO in the modulation of glutamate signaling (Roychowdhury *et al.* 2006). In this regard, postsynaptic AMPAR trafficking mediates some forms of synaptic plasticity, and the N-ethylmaleimide sensitive factor (NSF) is required for the surface expression of GluR2-containing AMPAR (Noel *et al.* 1999). The NSF is physiologically S- nitrosylated by endogenous nNOS-derived $^{\bullet}$NO, and this modification augments its binding to the AMPAR GluR2 subunit, resulting in increased surface insertion of AMPAR (Huang *et al.* 2005). The observation that AMPAR express PDZ-binding domains with impact on plasticity events (Kim *et al.* 2001) affords speculation on a close interaction with NOS, as observed for NMDAR, but evidences on this lack in the literature.

1.3.4 - Regulation of Neurotransmitter Release

$^{\bullet}$NO can mediate synaptic plasticity by potentiating or inhibiting neurotransmitter release. The release of norepinephrine, acetylcholine, glutamate and GABA has been shown to be stimulated by a $^{\bullet}$NO generator in rat hippocampal slices and inhibited by hemoglobin and Ca^{2+}-free buffer

(Lonart *et al.* 1992). NOS inhibitors were shown to increase extracellular levels of serotonine and dopamine in the rat ventral hippocampus, with L-arg exhibiting the opposite effect, suggesting that ˙NO could limit their release in hippocampus (Wegener *et al.* 2000). Meffert an co-workers demonstrated that ˙NO was able to promote vesicle exocytosis from hippocampal synaptosomes without raising Ca^{2+} (Meffert *et al.* 1994) and latter implicated post-translational modification of sulfhydryl groups by ˙NO in the alteration of synaptic protein interactions that govern neurotransmitter release (Meffert *et al.* 1996).

Of relevance to relate ˙NO and neurotransmitter regulation is the interaction between nNOS and CAPON, detailed in section 1.2.3.4. CAPON can bind to synapsin (Jaffrey *et al.* 2002), a synaptic vesicle-interacting protein located in presynaptic densities (Sudhof *et al.* 1989; Kristensen *et al.* 2001). Immunocytochemical studies have demonstrated nNOS expression in cytoplasmic and synaptic vesicles located in presynaptic densities (Loesch *et al.* 1994). Coupling of nNOS to synapsin may thus promote selective exposure of various synapsin-associated proteins to ˙NO and regulate neurotransmitter release (Meffert *et al.* 1996; Czapski *et al.* 2007). In this regard, the activation of NMDAR and production of ˙NO were implicated in reduced vesicular release at Schaffer collateral-CA1 excitatory synapses in hippocampal slices (Stanton *et al.* 2003), in an event requiring the activation of cGMP-dependent protein kinases. ˙NO can impact on other aspects of vesicle physiology in hippocampal neurons, namely vesicle endocytosis, in cGMP-dependent pathways (Micheva *et al.* 2003).

1.3.5 - Protein S-nitrosylation / S-nitrosation

The S-nitrosation of proteins with regulatory functions is receiving great attention as a major signal transduction pathway because of its occurrence in

physiological conditions and its influence on many protein functions (Stamler *et al.* 2001; Martinez-Ruiz *et al.* 2004). S-nitrosation affects a great number of cellular components and pathways such as Na^+/K^+ ATPase, ryanodine receptors, DNA expression and apoptosis (Davis *et al.* 2001; Jaffrey *et al.* 2001; Stamler *et al.* 2001). This ˙NO-mediated event can thus significantly alter cellular physiology and has been described as a novel enzyme-regulated (Liu *et al.* 2001) transduction mechanism similar to phosphorylation (Stamler *et al.* 2001; Mannick *et al.* 2002; Martinez-Ruiz *et al.* 2004).

1.4 - Hippocampus

The hippocampus is part of the limbic system, being located in both hemispheres in the medial portion of the temporal lobe. The hippocampus has been extensively used in the research of memory formation, learning and behavior, but also in the study of neurotransmission and cell death. This is one of the most vulnerable regions in the brain, and notably both loss and severe cellular degeneration have been observed in conjugation with memory impairment, particularly in Alzheimer's disease (Van Hoesen *et al.* 1990).

1.4.1 - Structure

The hippocampal formation is made up of the hippocampus and the neighboring temporal regions, namely the dentate gyrus and the subiculum. The hippocampus (Figure 1.5) consists of different regions termed CA1, CA2 and CA3 (CA is derived from the Latin *cornu ammonus*), where the main neuronal cell type is the pyramidal neuron. These cells are organized in a layer, termed the pyramidal layer, and communicate with cells located above and bellow by means of extensive axonal and dendritic processes. The

dentate gyrus is composed mainly of smaller neurons called granule cells, organized in a C-shape structure, that synapse with dendrites of the pyramidal cells (Amaral *et al.* 1989). The main inputs (afferents) to the hippocampus come from the entorhinal cortex to granule cells in the dentate gyrus via the perforant path. The axons of the granule cells are termed mossy fibers and terminate mainly on the apical dendrites of the pyramidal cells located in the CA3 region. The efferents from CA3 cells project as Schaffer collaterals to apical dendrites of CA1 pyramidal cells. The synapses of this so called "trysinaptic loop" (DG, CA3 and CA1 subregions) are excitatory and use glutamate as a neurotransmitter (Giap *et al.* 2000). From CA1 region there is a major efferent input to the subiculum, and from here to neighboring brain areas. The axons of all major neuronal types in hippocampus are arranged in bands parallel to each other, so that a transverse slice contains a complete
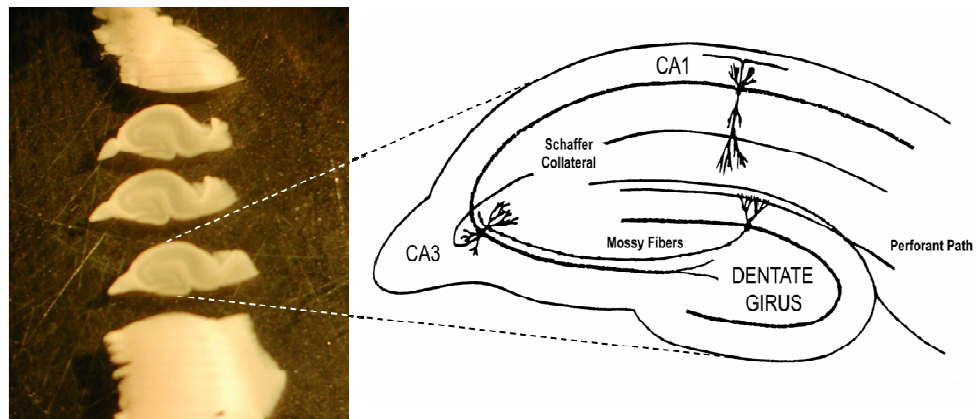
Figure 1.5: Hippocampal transverse slices. Transverse slices (left) are a suitable model to study neuronal activity because they retain the directional connectivity between cells of different subregions (right). Left image was obtained during hippocampal slice preparation, using a magnification lens. Right drawing depicts cellular pathways and hippocampal subregions.

loop, from perforant path to subiculum (Freund *et al.* 1996; Greenstein *et al.* 2000) (Figure 1.5). This lamellar organization, as it was initially described (Andersen *et al.* 1969), remains adequate to study hippocampal connectivity (Andersen *et al.* 2000).

Pyramidal and granule cells represent 90% of hippocampal neurons, and the remaining 10% of hippocampal cells are GABAergic interneurons. Other neurotransmitters are contained in varicosities and released in the hippocampus, where they largely participate in non-synaptic interactions. In this regard, fibers from the medial septum and the diagonal band of Broca to the hippocampus are cholinergic (Umbriaco *et al.* 1995), while serotonergic innervation of the hippocampus originates from the dorsal and median raphe nuclei (Conrad *et al.* 1974). Noradrenergic afferents originate exclusively from the locus coeruleus (Loy *et al.* 1980).

1.4.2 - Function

The hippocampus is involved in learning and memory formation (Squire *et al.* 1991). Experimentally, memory has been studied on basis of a model termed long term potentiation (LTP). LTP encompasses an increase in synaptic strength that lasts for hours or days as a result of a brief high-frequency period of electrical activity (called a tetanus), and is considered to be a key event in memory formation and learning (Squire *et al.* 1999). Although LTP can be induced in several synapses in the hippocampus mechanisms diverge (Nicoll *et al.* 1995), and two distinctions can be made. In mossy fibers, LTP is nonassociative. This means that it does not depend on postsynaptic activity, but only on a burst of brief, high frequency neural activity in the presynaptic neurons. This causes NMDAR-independent Ca^{2+} influx, activation of adenylyl cyclase and subsequent activation of cAMP-dependent protein kinase (PKA) (Huang *et al.* 1994; Weisskopf *et al.* 1994). Mossy fiber

pathway LTP is not essential for spatial memory formation (Huang *et al.* 1995), but might be crucial for other kinds of declarative memory. A second form of LTP is observed in the Schaffer collateral pathway, where LTP is dependent on postsynaptic NMDAR activation. This form of LTP is associative (Milner *et al.* 1998), *i.e.* it depends on concomitant activity of both pre-and postsynaptic cells, which consists in glutamate release and activation of NMDA and AMPA receptors (Bliss *et al.* 1993; Nicoll *et al.* 1995). LTP requires not only the firing of presynaptic neurons but also that they fire repetitively, so as to substantially depolarize the postsynaptic neuron and remove Mg^{2+} blockage, thus allowing sufficient Ca^{2+} entry to initiate the sequence of steps that lead to persistent enhancement of synaptic transmission. The opposite of LTP is long term depression (LTD), which corresponds to a prolonged decrease in synaptic strength after reduced electrical activity in neurons, was also reported in hippocampus (Manabe 1997). This can occur at the same neuronal connections involved in LTP, namely Schaffer collateral-CA1 synapses (Santschi *et al.* 1999) and mossy fibers-CA3 synapses (Tzounopoulos *et al.* 1998).

1.4.3 - Glutamate

Glutamate is the most abundant amino acid in the brain, where it is considered to be the major mediator of excitatory signals (Collingridge *et al.* 1989), and only a tiny fraction is normally present extracellularly (outside or between the cells). The highest concentrations are found inside nerve terminals (Storm-Mathisen *et al.* 1992) with neurons displaying a cytosolic concentration of 5 mM glutamate (Osen *et al.* 1995). Glutamate-mediated events terminate with its removal from synaptic clefts, predominantly via glial uptake (Anderson *et al.* 2000; Danbolt 2001). Astrocytes accumulate glutamate at concentrations lower than neurons, about 2 or 3 mM, because of

glutamate transformation to glutamine by the enzyme glutamine synthetase (Hertz *et al.* 1999).

An absolute requirement for glutamate to act as a neurotransmitter is that its extracellular concentration be kept low. The concentrations in extracellular fluid (about 13 to 22 % of brain tissue volume) (McBain *et al.* 1990; Nicholson *et al.* 1998) and in the cerebrospinal fluid (CSF) were reported to be around 3 to 4 µM and 10 µM, respectively (Lehmann *et al.* 1983; Hamberger *et al.* 1984), but numbers are probably lower, as microdialysis analysis revealed extracellular concentrations between 1 to 2 µM (Benveniste *et al.* 1984; Anderson *et al.* 2000). This is controlled mainly by astrocytic glutamate transporters that have the capacity to reduce extracellular glutamate concentrations (Auger *et al.* 2000). Cytosolic glutamate will leak out from neurons and astrocytes if they run out of energy and mediate excitotoxic oxidative stress and damage (Coyle *et al.* 1993), as observed after stroke or trauma (Anderson *et al.* 2000). Glutamate can activate a number of receptors in the hippocampus, as detailed below.

1.4.3.1 - Ionotropic Glutamate Receptors - NMDA Receptors

Ionotropic glutamate receptors are ligand-gated ion channels which pass electric current in response to glutamate binding. Their distinction is based on the differential actions of glutamate analogs on receptor activation.

The NMDAR is activated by the glutamate analogue NMDA and is permeable to Ca^{2+} (and, to a lower extent, Na^{+}). Under resting conditions the channel is blocked by Mg^{2+}, relieved whenever membrane depolarization occurs. These receptors are highly implicated in synaptic plasticity, especially LTP, but are also key players in neurotoxic insults, where disruption of energy metabolism causes neuronal depolarization, loss of Mg^{2+} blockage and excessive Ca^{2+} entry with the onset of oxidative and/or nitrosative stress

(Coyle *et al.* 1993; Pacher *et al.* 2007). NMDA receptors typically comprise four subunits. Heteromers always contain both NR1 (Moriyoshi *et al.* 1991) and NR2 (NR2A-NR2D) (Kutsuwada *et al.* 1992; Meguro *et al.* 1992; Ishii *et al.* 1993) subunits, and in some cases NR3 subunits (NR3A and NR3B) (Ciabarra *et al.* 1995; Sucher *et al.* 1995; Nishi *et al.* 2001). Glutamate binds to the NR2 subunits, whereas co-agonists glycine or D-serine bind to the NR1 subunits (Ivanovic *et al.* 1998; Mothet *et al.* 2000). Subunit composition determines several features of NMDAR. The NR2B predominates in extrasynaptic areas, whereas NR2A tends to be confined to synapses. Excitotoxicity is thought to involve extrasynaptic receptors (Hardingham *et al.* 2002) and NR2B-containing NMDA receptors have been implicated in the pathophysiology of neurodegenerative disorders such as Alzheimer's and Huntington's diseases (Gogas 2006), prompting . This prompted research on the therapeutic potential of selective NR2B antagonists such as ifenprodil in a number of disorders (Kemp *et al.* 2002).

1.4.3.2 - Ionotropic Glutamate Receptors - AMPA Receptors

A second class of ionotropic glutamate receptors was pharmacologically identified that respond selectively to the glutamate derivatives AMPA and Kainate. Molecular cloning revealed distinct AMPA and Kainate receptors: AMPA receptors (AMPAR) are homo- or hetero-tetramers composed of four subunits, GluR1-4 (or GluRA-GluRD), (Hollmann *et al.* 1989; Keinanen *et al.* 1990), and Kainate receptors (KR) are homo- or hetero-oligomers of the subunits GluR5-GluR7, KA1 and KA2 (Egebjerg *et al.* 1991; Werner *et al.* 1991; Bettler *et al.* 1992). The latter are involved in modulation of neurotransmitter release and are potential therapeutic targets in pathological processes (Lerma *et al.* 2001), but both are implicated in synaptic plasticity

and are responsible for most fast excitatory synaptic signaling (Collingridge *et al.* 2004).

Contrary to NMDAR, AMPAR are mainly permeable to Na^+ and K^+. Ca^{2+}-impermeability is regulated by post-transcriptional editing of the GluR2 subunit mRNA, leading to an amino acid change (from uncharged glutamine to positively-charged arginine) at a critical residue in the pore-lining region (Hume *et al.* 1991). Thus, AMPAR that lack GluR2 subunit or are composed of a defective GluR2 are Ca^{2+}-permeable (Hollmann *et al.* 1991; Sommer *et al.* 1991) and can both mediate excitotoxicity (Kim *et al.* 2001; Noh *et al.* 2005) and participate in excitatory synaptic transmission (Isa *et al.* 1996).

1.4.3.3 - Metabotropic Glutamate Receptors

Metabotropic glutamate receptors are G-protein-coupled receptors whose activation involves three steps: 1) glutamate binding to extracellular receptor proteins in the postsynaptic membrane, 2) activation of small intracellular proteins called G-proteins, and 3) activation of "effector" proteins located intracellularly by G-proteins. (Mark F. Bear *et al.* 1996). This causes slower, longer-lasting and diverse postsynaptic actions that depend on which G-protein is activated, which along with based on their sequence homologies serves to categorize them (Swanson *et al.* 2005). These receptors have been described in hippocampus, where they mediate LTP (Grover *et al.* 1999), modify synaptic transmission (Giocomo *et al.* 2006), modulate the activity of other membrane receptors (Sohn *et al.* 2007) and regulate transcription factors (O'Riordan *et al.* 2006).

1.4.4 - Nitric Oxide in Hippocampus

1.4.4.1 - Nitric Oxide Synthase Isoforms

The first report of ˙NO as an intercellular messenger in the brain was by Garthwaite and coworkers (Garthwaite *et al.* 1988), and led to nNOS isolation in a number of different brain regions (Bredt *et al.* 1990; Bredt *et al.* 1990; Schmidt *et al.* 1991). In hippocampus, nNOS was first identified in interneurons (Bredt *et al.* 1991; Valtschanoff *et al.* 1993). Wendland and collaborators demonstrated that this isoform was expressed in both dendrites and cell bodies of CA1 pyramidal cells (Wendland *et al.* 1994), an observation confirmed latter by results showing that that nNOS concentrates inside the postsynaptic plasma membrane of CA1 synapses (Burette *et al.* 2002). Moreover, nNOS is developmentally regulated (Northington *et al.* 1996; Liu *et al.* 2003) and is expressed constitutively throughout the hippocampus, with higher levels found in CA1 region as revealed by Western blot analysis (Liu *et al.* 2003). The nNOS-related mitochondrial isoform of nitric oxide synthase has also been found in hippocampus (Lores-Arnaiz *et al.* 2005).

The location of eNOS in the hippocampus has been controversial. It was originally reported to be in CA1 pyramidal cells (Dinerman *et al.* 1994; O'Dell *et al.* 1994), but was latter found exclusively associated with blood vessels and endothelial cells (Demas *et al.* 1999; Blackshaw *et al.* 2003). Its role in hippocampus seems to go further than vascular regulation. ˙NO-dependent LTP was found to be preserved in nNOS-deficient mice (O'Dell *et al.* 1994) but lost when eNOS was knocked out (Wilson *et al.* 1999). A combined deficit in eNOS and nNOS is required to eliminate ˙NO-dependent LTP, suggesting that both isoforms could compensate for each other in mice with a single mutation (Son *et al.* 1996). This was clarified recently by Garthwaite and collaborators, who concluded that both tonic and phasic ˙NO

signals are required for hippocampal LTP and that the two are generated by eNOS and nNOS, respectively (Hopper *et al.* 2006) , as previously suggested (Son *et al.* 1996).

iNOS is expressed in response to a wide range of stimuli, including endotoxins like lipopolysaccharide (LPS) and endogenous proinflammatory mediators such as tumor necrosis factor-α (TNF-α), interleukin 1-b (IL1b) and interferon-γ (IFNγ) (Rothwell *et al.* 2000; Lucas *et al.* 2006). In cultured hippocampal slices iNOS expression was only present in activated microglia (Duport *et al.* 2005), the immune-competent cells in central nervous system (Streit *et al.* 1988). The hippocampus is particularly vulnerable to inflammatory events when compared to other brain regions, as observed during severe sepsis (Semmler *et al.* 2005).

1.4.4.2 - Coupling to NMDA Receptors

The well established ˙NO production following NMDAR activation is a major route in ˙NO-mediated signaling pathways in brain (Garthwaite *et al.* 1995) (Figure 1.6). Many of the actions of nNOS are mediated by specific protein-protein interactions involving its N-terminus PDZ domain, that has been shown to influence the activity and/or the distribution of the enzyme in brain and muscle (Kone 2000). NMDAR are present at post-synaptic densities in macromolecular complexes comprising several proteins physically and functionally associated. Amongst them is PSD-95, a scaffold protein with several PDZ domains that allows a simultaneous interaction between NMDAR NR2 subunits (Kornau *et al.* 1995) and cytoplasmatic proteins. The PDZ domain in nNOS mediates its binding to PSD-95 (Brenman *et al.* 1996) and both interact with NMDAR to form a large ternary synaptic complex (Niethammer *et al.* 1996; Christopherson *et al.* 1999). By placing
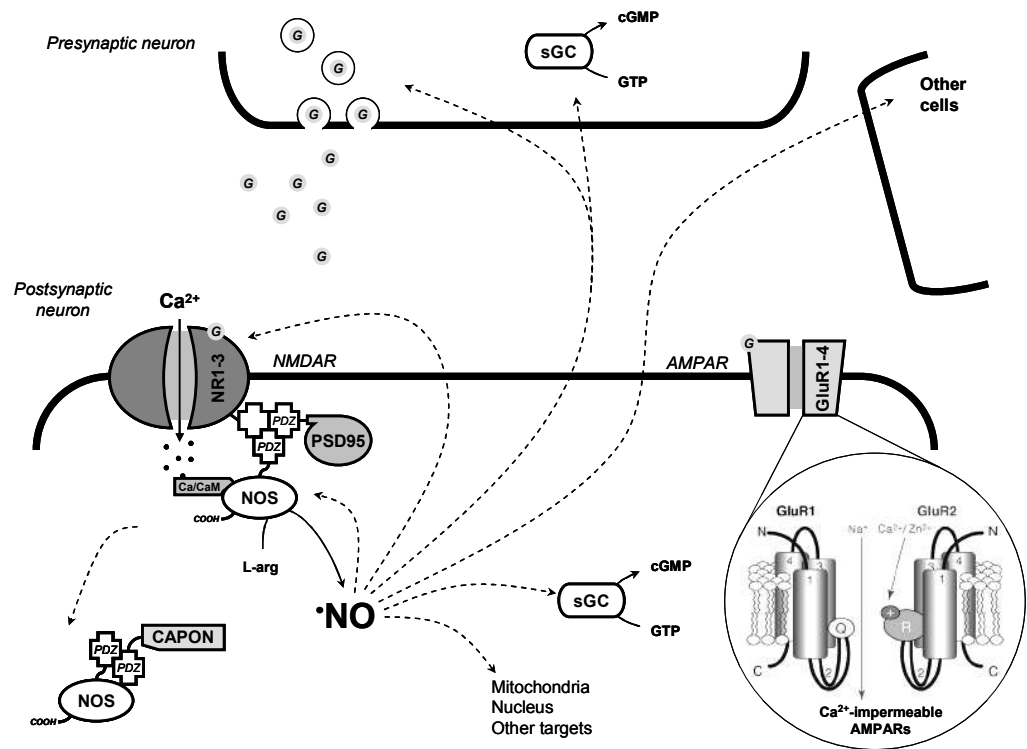
Figure 1.6: Coupling of nNOS to NMDAR. Intracellular Ca^{2+} rise following NMDAR activation leads to nNOS activation and ˙NO production, which in turn activates a number of cellular events in pre- and postsynaptic cells, as well in adjacent ones. nNOS is physically coupled to NMDAR by means of protein-protein interactions involving PDZ domains. AMPAR are virtually Ca^{2+}-impermeable when expressing the GluR2 subunit, as depicted (adapted from (Liu *et al*, 2007)).

nNOS near the NMDA receptor PSD-95 exposes the enzyme to the Ca^{2+} influx that occurs following receptor activation (Christopherson *et al.* 1999; Sattler *et al.* 2001; Tomita *et al.* 2001). Very recently ˙NO production was shown to increase by the recruitment of nNOS to the post-synaptic density via PSD-95, revealing the importance of this interaction in regulating ˙NO production (Ishii *et al.* 2006). Co-localization of nNOS, PSD-95 and the NMDA receptor has been shown immunohistochemically in the CA1 pyramidal cells of the rat hippocampal slice (Burette *et al.* 2002).

Although glutamate is responsible for the greater part of excitatory transmission in the brain, excessive exposure to this amino acid may trigger toxic pathways associated to neurological disorders (Coyle *et al.* 1993; Obrenovitch *et al.* 1997). Research on the role played by ˙NO might impact on both sides of such glutamate paradox, neurotransmission and excitotoxic insult (Dawson *et al.* 1991; Bliss *et al.* 1993; Dawson *et al.* 1998; Sattler *et al.* 2001; Calabrese *et al.* 2007; Pacher *et al.* 2007).

1.4.4.3 - Nitric Oxide and Hippocampal Synaptic Plasticity

Maintenance of LTP in hippocampus requires not only changes in postsynaptic neurons but also modifications on presynaptic cells (Lynch *et al.* 1985; Malinow *et al.* 1990), and this is thought to be mediated by a retrograde messenger generated by the postsynaptic neuron. Several molecules have been proposed to play this role in CA1 pyramidal neurons (Bazan *et al.* 1997; Schuman 1997) and ˙NO is the major candidate to promote synaptic plasticity (Holscher 1997; Haley 1998; Prast *et al.* 2001). This conclusion was supported by results showing ˙NO diffusion to the presynaptic terminal (O'Dell *et al.* 1991; Schuman *et al.* 1991) where it acts directly in the presynaptic neuron to induce hippocampal LTP (Arancio *et al.* 1996). This effect is mediated by enhanced neurotransmitter release (Meffert *et al.* 1994; Prast *et al.* 2001) and regulation of synaptic vesicles endocytosis (Micheva *et al.* 2003) (detailed in section 1.3.4). A principal mediator of signal transduction by ˙NO is sGC (Zabel *et al.* 1998; Denninger *et al.* 1999), also implicated in some forms of LTP (Son *et al.* 1998; Arancio *et al.* 2001). The role of ˙NO as a retrograde messenger to mediate synaptic plasticity was further supported by Burette *et al.*, which provided a link between nNOS and sGC by demonstrating their close association in synaptic spines in the CA1 region of hippocampal slices (Burette *et al.* 2002).

LTD can also be a consequence of ˙NO modulation. It requires the activation of a number glutamate receptors, including NMDAR (Bear *et al.* 1994), that may determine the direction of CA1 synaptic plasticity towards LTP or LTD (Liu *et al.* 2004). In this regard, decreased neurotransmitter release observed in LTD is dependent on ˙NO production and diffusion at Schaffer collateral-CA1 synapses (Stanton *et al.* 2003), in agreement with reports where NOS inhibitors blocked NMDAR-dependent LTD in hippocampus (Izumi *et al.* 1993). The activation of common pathways in LTP and LTD suggest that plasticity in hippocampus is regulated at the level of signal transduction by phosphoproteins (Bliss *et al.* 1993; Bear *et al.* 1994; MacDonald *et al.* 2006).

1.4.4.4 - NMDA Receptor-Independent Plasticity

Glutamate release into the synaptic cleft activates membrane receptors other than NMDAR, that have also been implicated in ˙NO production in brain. AMPA and KA injection induces an elevation in nitrite levels in hippocampus (Radenovic *et al.* 2005), and AMPAR were shown to increased cGMP content in cerebellar slices prepared from adult rats in a pathway involving nNOS activation (Okada 1992). In rat cerebellar slices AMPAR activation led to a lower production of ˙NO when compared to NMDAR, as observed by means of the fluorescent indicator diaminofluorescein-2 (Okada *et al.* 2004).

The link between ˙NO and non-NMDAR is also apparent when considering synaptic plasticity. AMPAR have been implicated in NMDA-mediated neuronal plasticity, as several reports indicate a rapid postsynaptic delivery of these receptors into dendritic spines that contributes to the enhanced AMPAR-mediated transmission observed during LTP (Shi *et al.* 1999). However, they also mediate NMDA-independent events, where Ca^{2+}-dependent synaptic plasticity is critically dependent on the entrance mechanism of Ca^{2+} in the postsynaptic cell (*e.g.* VGCC) and/or on AMPAR

subunit composition (Chen *et al.* 1998; Chittajallu *et al.* 1998; Zamanillo *et al.* 1999). AMPAR-mediated plasticity involves both native and modified receptors (Liu *et al.* 2007). GluR2-lacking Ca^{2+}-permeable AMPAR (CP-AMPAR) have long been described in hippocampus, where they participate in excitatory synaptic transmission (Isa *et al.* 1996) with impact on plasticity (Gardner *et al.* 2005). As observed on rat hippocampal slices, neuron-glia synapses in the CA1 region undergo activity-related modifications analogous to LTP that depend on CP-AMPAR (Ge *et al.* 2006). A rapid incorporation of CP-AMPAR and their subsequent replacement by GluR2-containing Ca^{2+}-impermeable AMPARs occurs in principal neurons during hippocampal NMDAR-dependent LTP (Plant *et al.* 2006), presumably following the recruitment of receptors existing in intracellular reserve pools (Ju *et al.* 2004; Terashima *et al.* 2004). Non-pyramidal neurons expressing CP-AMPAR have long been demonstrated to occur in different cell layers of both CA1 and CA3 regions (Isa *et al.* 1996).

The expression of CP-AMPAR can also change dramatically in pathological circumstances (Kwak *et al.* 2006; Liu *et al.* 2007). Damage can arise via excessive Ca^{2+} loading through CP-AMPAR. This can lead to ˙NO production, generation of ROS by mitochondria and release of apoptotic mediators such as cytochrome C, amongst others (Hong *et al.* 2004). Blockade of CP-AMPAR was shown to be protective against ischemia-induced neuronal cell death at Schaffer collateral-CA1 synapses (Noh *et al.* 2005). Pronounced and cell-specific reduction in GluR2 in CA1 vulnerable neurons was shown to occur only after global ischemia, strikingly with no significant changes in AMPA receptor subunit GluR1 at CA1, CA3 or dentate gyrus (Opitz *et al.* 2000). GluR2 mRNA levels are also decreased in motor neurons (Kawahara *et al.* 2003; Sun *et al.* 2005), the neuronal cells lost in amyotrophic lateral sclerosis (ALS).

From the previous, and taking into account the possible role for ˙NO in events mediated by AMPAR and CP-AMPAR, knowledge of NOS activity following AMPA simulation is of considerable relevance.

1.5 - Astrocytes

Without astrocytic involvement, normal function of glutamatergic neurons would not be possible. The most obvious neuronal function of glutamate - its release as a transmitter - is regulated by astrocytes. In normal synaptic transmission, glutamate released into the synaptic cleft by neurones is accumulated in astrocytes (Hertz *et al.* 1978) by means of glutamate transporters such as GLT1 and GLAST (Gadea *et al.* 2001). Afterwards, glutamate is returned to neurones in the form of glutamine. However, many other neuronal activities are influenced by these cells. Astrocytes have been implicated in physiological and pathological mechanisms, including sequestration and/or redistribution of K^+ during neural activity, providing energy substrates to neurons (*e.g.* lactate), maintenance of blood-brain barrier integrity, modulation of stroke outcome by free-radical scavenging and glutamate homeostasis, glioma formation and cytotoxic brain edema. New roles are also emerging and these include modulation of excitatory and inhibitory synapses, regulation of neurogenesis in adult brain (*e.g.* hippocampus) and mediators of neuroinflammation (Hertz *et al.* 1999; Dringen 2000; Araque *et al.* 2001; Ransom *et al.* 2003; Pellerin 2005). Astrocytes also protect neurones in other ways, providing metabolic and antioxidant support. One of the most important molecules in this respect is the antioxidant GSH (Schulz *et al.* 2000).

1.5.1 - Glutathione

1.5.1.1 - Function and Localization

GSH is a tripeptide composed of glutamate, cysteine and glycine (γ-glutamylcysteinylglycine), and is the most abundant intracellular thiol on plants and animals (Meister *et al.* 1983). The unusual peptidic γ-linkage between the glutamate and cysteine residues, via the carboxyl group attached to the γ-carbon of glutamate and not the orthodox α-carbon carboxyl group, is suggested to prevent degradation by aminopeptidases (Sies 1999). Glutathione disulphide (GSSG) is formed upon oxidation of GSH, and although dependent on several factors (including oxidative stress), the ration of GSH to GSSG is approximately 10:1 in the cytoplasm (Meister *et al.* 1983; Kirlin *et al.* 1999). A major function of GSH relates with the protection of cells from oxidizing species and maintenance of an appropriate cellular redox environment (Bolanos *et al.* 1996; Dringen *et al.* 1997; Ehrhart *et al.* 2001). Although it can also act as a cysteine carrier (Meister *et al.* 1983), GSH plays a major role in detoxification mechanisms involving xenobiotics (Borst *et al.* 1999), and participates in the post-translational modification of proteins (Klatt *et al.* 2000; Pineda-Molina *et al.* 2001). GSH is predominantly located in the cytoplasm (Wullner *et al.* 1999) and varies between brain regions, with lower levels in hippocampus when compared to cortex (Kang *et al.* 1999). In connection with observed differences in GSH content between cell types (Sagara *et al.* 1993), this later observation might determine a sub-regional vulnerability to oxidative stress in hippocampus (Van Hoesen *et al.* 1990).

1.5.5.2 - Metabolism

GSH is synthesized from glutamate, cysteine and glycine in two consecutive steps, catalyzed by ATP-dependent enzymes γ-glutamylcysteine synthetase (GCS, EC 6.3.2.2, reaction 10) and GSH synthethase (GS, EC 6.3.2.3, reaction 11) (Meister *et al.* 1983; Griffith 1999). Degradation into the constituent amino acids occurs via γ-glutamyltranspeptidase (γGT, EC 2.3.2.2), which is predominantly located in the outer leaflet of plasma membranes (Meister *et al.* 1983; Dringen *et al.* 1997) of endothelial (Hemmings *et al.* 1999) and glial (Dringen *et al.* 1997; Hemmings *et al.* 1999) cells, and bv cysteinyl-glycine dipeptidase (EC 3.4.13.6) (Meister *et al.* 1983; Josch *et al.* 1998), as depicted in Figure 1.7 at the end of this section.

glutamate + cysteine + Mg-ATP
$$\rightarrow \text{γ-glutamyl-cysteine + Mg-ADP + Pi} \qquad (11)$$

γ-glutamyl-cysteine + glycine + Mg-ATP
$$\rightarrow \text{glutathione + Mg-ADP + Pi} \qquad (12)$$
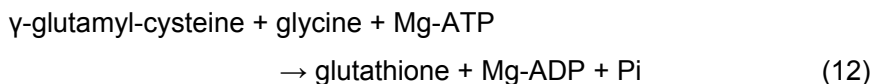
of GCS is similar to the intracellular concentration of cysteine (Griffith 1999), which limits the rate of GCS activity (Meister *et al.* 1983; Kranich *et al.* 1998). GSH binding was found to be competitive with glutamate (K_i GSH~2.3 mM) and dependent on the cysteinyl thiol group (Huang *et al.* 1993). The level of GCS present in the cell determines *de novo* synthesis of GSH and several agents have been shown to induce the expression of GCS light or heavy subunits. Amongst them are H_2O_2, $O_2^{\cdot-}$, $^{\cdot}NO$, lipid peroxidation products and insulin. Phosphorylation of GCS heavy subunits also modulates enzyme activity, leading to decreased Vmax without affecting Km for both glutamate and cysteine or causing subunit dissociation (Sun *et al.* 1996). Inhibiting GCS, and allowing the ongoing reactions involving the use GSH to proceed, depletes GSH cellular stores at different rates, as observed with the commonly

used inhibitor buthionine sulfoximine (BSO) (Griffith *et al.* 1979). Mammalian GSH synthetase is a homodimer and, unlike GCS, is not inhibited by GSH (Oppenheimer *et al.* 1979). Of note is the reaction catalyzed by γGT, which degrades GSH into a γ-glutamyl moiety and cysteinylglycine (CysGly) (Meister *et al.* 1983; Dringen *et al.* 1997). This dipeptide serves as a GSH precursor in neurons and causes a concentration-dependent increase in neuronal GSH content (Figure 1.7) (Dringen *et al.* 1999). The γ-glutamyl moiety is transferred to an acceptor that can be either an amino acid, a dipeptide, H_2O, GSSG or GSH (Meister *et al.* 1983; Stole *et al.* 1994). This enzyme is inhibited by acivicin, in a mechanism involving acivicin transformation to an inhibitory species that releases from γGT very slowly (Stole *et al.* 1994).

1.5.2 - Antioxidant Properties of Glutathione

The thiol group of GSH makes it an important scavenger of oxidizing species. GSH reacts rapidly and non-enzymatically with hydroxyl radical, the cytotoxic Fenton reaction product, and with N_2O_3 and $ONOO^-$, two cytotoxic products formed by the $^\cdot NO$ with O_2 and $O_2^{\cdot -}$, respectively (Kalyanaraman *et al.* 1996; Luperchio *et al.* 1996; Briviba *et al.* 1999). GSH is the substrate for the GSH peroxidase which reduces H_2O_2 and lipid peroxides to H_2O and alcohols, respectively. Of note this is a relevant defense mechanism in brain, where catalase activity is reduced (Meister *et al.* 1983; Dringen *et al.* 1997; Brigelius-Flohe 1999; Brigelius-Flohe *et al.* 1999).

GSH plays an important role against $^\cdot NO$-derived reactive species. Although $^\cdot NO$ reacts too slowly with GSH to be considered biologically relevant, the oxidation to NO^+ increases its reactivity to form S-nitrosoglutathione (GSNO) (Gaston 1999; Hughes 1999). The subsequent chemistry of GSNO is complex, as GSNO may react further with GSH to form GSSG, NO_2^- and ammonia (NH_3) (Singh *et al.* 1996).

The formation of GSNO is of relevance in brain, where it has been shown to react with NR2A subunits to downregulate the activity of NMDAR (Kim *et al.* 1999; Choi *et al.* 2000; Hermann *et al.* 2000; Chen *et al.* 2006). $^{\bullet}$NO reduction yields NO^{-}, which forms GSSG and hydroxylamine (NH_2OH) after reacting with GSH (Hughes 1999). At physiological conditions more than 90 % of ONOO^{-} reacts with GSH to form the unstable sulphenic acid (GSOH), which rapidly generates GSSG by reacting with another GSH molecule (Quijano *et al.* 1997) and can irreversibly oxidize proteins (Klatt *et al.* 2000). In this regard, the reversible covalent binding of GSH to cysteine residues also plays a protective role in preventing irreversible oxidation or nitration of proteins (Klatt *et al.* 2000). The fact that neurons exhibit lower amounts of GSH when compared to astrocytes was suggested as the reason why they are more susceptible to oxidative stress (Bolanos *et al.* 1995; Bolanos *et al.* 1996), and why the same oxidative insult results in a greater amount of cell death in neurons (Bolanos *et al.* 1995).

1.5.3 - Astrocytes, Neurons and Nitric Oxide

The trafficking of GSH between astrocytes and neurons is particularly important in conditions of oxidative stress (Dringen 2000). As illustrated in Figure 1.7, astrocytes are able to increase neuronal GSH levels by secreting GSH into the extracellular environment (Sagara *et al.* 1996; Dringen *et al.* 1999; Stewart *et al.* 2002), where it has been reported in the micromolar range (Han *et al.* 1999). Neurons are unable to take up GSH directly but can make use of CysGly and cysteine, which are produced from GSH by the consecutive action of γGT and aminopeptidase N (ApN), the latter expressed on the surface of neurones (Dringen *et al.* 1997; Dringen *et al.* 2001). Since cysteine is the rate limiting substrate for GSH synthesis the supply of this substrate by

astrocytes is essential for the maintenance of GSH levels in neurones (Dringen *et al.* 1999).

Previous studies have shown that, when exposed to H_2O_2, $^\cdot$NO and other reactive nitrogen species, astrocytes react by increasing GSH release (Sagara *et al.* 1996; Gegg *et al.* 2003). Astrocytes are more resistant than neurons to the effects of RNS acting upon the electron transport chain in mitochondria (Bolanos *et al.* 1995). Inhibition of respiration following $^\cdot$NO exposure leads to the rapid upregulation of phosphofructo-1-kinase (PFK1), a key regulatory enzyme for glycolysis, only in astrocytes (Almeida *et al.* 2004).
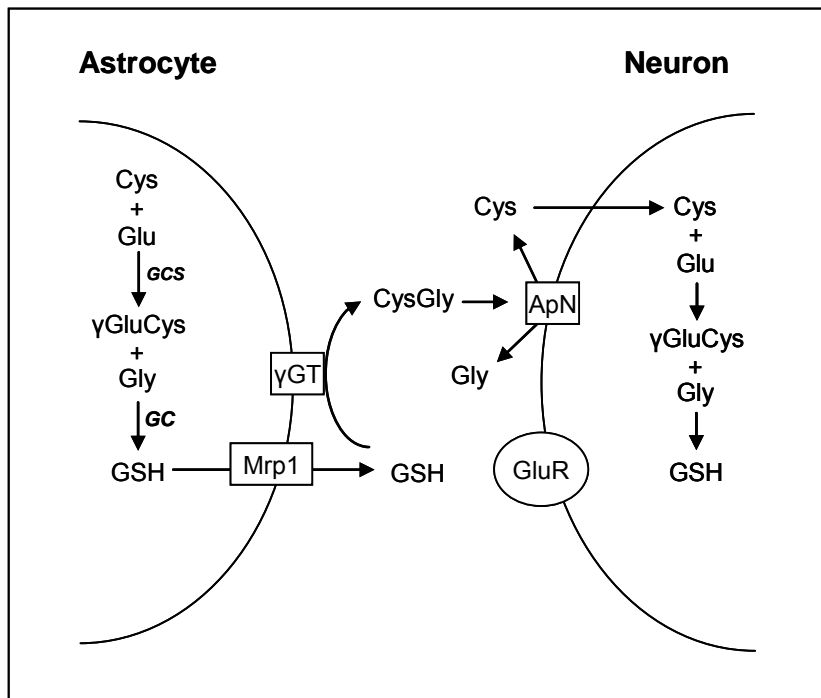
Figure 1.7: Astrocytes protect other neural cell types against the toxicity of various compounds by releasing GSH, thus supplying glutathione precursors to neighboring cells (Dringen 2000). GCS, γ-glutamylcysteine synthetase; GS, GSH synthethase; γGT, γ-glutamyltranspeptidase; ApN, Aminopeptidase.

Astrocytic GSH levels are approximately two times higher that those of neurons (Bolanos *et al.* 1995), and its levels increase in response to exposure to ˙NO (Gegg *et al.* 2003; Heales *et al.* 2004). The same study revealed that, following exposure of astrocytes to ˙NO, GCS levels were elevated, GSH efflux was doubled and γGT activity was increased by 42 % (Gegg *et al.* 2003). This increase in GSH release is hypothesized to be a neuroprotective mechanism which maintains and/or increases neuronal GSH levels to counteract the damaging effects of RNOS.

Extracellular levels of glutamate have been measured in various *in vivo* disease models by microdialysis and have been shown to reach concentrations of >500 µM (McAdoo *et al.* 1999). High levels of glutamate can also be maintained at concentrations of >50 µM for 1-2 hours during and following ischaemic insult (Orwar *et al.* 1994; Ritz *et al.* 2004). Since extracellular glutamate derives from intracellular vesicles (whose glutamate concentrations are between 0.24-11 mM (Harris *et al.* 1995), the local concentration of glutamate in these conditions is likely to be even higher. Prolonged exposure to such concentrations of glutamate is likely to result in significant neurotoxicity (Liu *et al.* 1999). Given this scenario, it is of considerable interest to investigate the mechanisms by which astrocytes protect neurones from glutamate toxicity (Hertz and Zielke, 2004).

1.6 - Detection of Nitric Oxide

The physiological actions of ˙NO are determined by its concentration dynamics in tissues, but some of its properties make ˙NO detection in biological samples a challenging task. Stable isotopes of L-citrulline or L-arg can be used to investigate NOS activity (van Eijk *et al.* 2007), and ˙NO effects are also inferred by monitoring cGMP production (Hopper *et al.* 2006). The steady-state concentration of this gaseous free radical is difficult to determine

because of its labile nature, a consequence of its short half-life and diffusion rate in tissues. Its free radical nature favors the reaction with free radicals, oxidant and antioxidant molecules, metal centers and a large number of proteins. Moreover, a number of molecules are reported to determine its production *in vivo*, by modulating NOS activity or activating regulatory pathways. These and other issues have to be address when selecting one the following methodologies.

1.6.1 - Chemiluminescence

The use of chemiluminescence to follow $^\bullet$NO production involves mainly gas phase measurements, as very few reports address its use in liquid phase experiments. This technique is based on the reaction of $^\bullet$NO with ozone (O_3) to produce nitrogen dioxide in the excited state (NO_2^*) (reaction 12):

$$^\bullet NO + O_3 \rightarrow NO_2^* + O_2 \tag{12}$$
$$NO_2^* \rightarrow NO_2 + light\ (600\ nm) \tag{13}$$

Photons are detected by a red-sensitive photomultiplier with a cutoff filter below 600 nm (reaction 13). This reaction is very specific to $^\bullet$NO and is insensitive to NO_2, a major interferent in the measurements of $^\bullet$NO in the gas phase (Lancaster Jr. 1996). This technique has been used to measure $^\bullet$NO in exhaled breath (Hadjikoumi *et al.* 2002) but detection of dissolved $^\bullet$NO is more complicated. The sample solution has to be purged with helium or nitrogen to transfer dissolved $^\bullet$NO to the reaction chamber (Maurer *et al.* 2000), which limits the usefulness of chemiluminescence in real-time measurements of $^\bullet$NO. Other strategy is based on the reaction of $^\bullet$NO with alkaline luminol in the presence of hydrogen peroxide (H_2O_2) (Kojima *et al.* 1997). Detection can be performed either by mixing the sample with luminol/H_2O_2 peroxide mixture

(Wiklund *et al.* 1999) or by placing a dialysis or gas permeable membrane between the sample and luminol/ H_2O_2 mixture (Kojima *et al.* 1997). This procedure offered better selectivity (since luminol could not react with species other than ˙NO) but had poor sensitivity and slow response time. In general chemiluminescence detection offers very good sensitivity and selectivity but it has few drawbacks, such as bulky instrumentation, time consuming procedures, and expensive reagents and equipment.

1.6.2 - Colorimetry

These techniques are based on the reaction of ˙NO with a target molecule that changes its spectral characteristics. Binding of ˙NO to the iron center of oxyhemoglobin (HbO_2) results in shifting the Soret band, which can be used as a qualitative and quantitative indicator of ˙NO. This reaction yields HbNO that latter decomposes to methemoglobin and nitrate (reaction 2) (Nims *et al.* 1996).

The nitrosation of Hb (or myoglobin, Mb) is useful in direct measurements of ˙NO (Kelm *et al.* 1997) and dosing experiments in the laboratory. Major drawbacks of this method are the difficulty to obtain pure HbO_2 or Mb, the time required to complete the analysis, and the reaction with interfering agents like nitrite (Nims *et al.* 1996). Other reagents that form colored compounds in the presence of ˙NO include ferrocyanide and 2,2'-azinobis(3-ethylbenzthiazoline-6-sulfonic acid (ABTS) (Nims *et al.* 1996).

The biological metabolites of ˙NO can be used to measure it indirectly, particularly nitrite and nitrate. The most common procedure is based on the Griess reagent, which consists of sulfanilamide and N-(1-naphthyl)ethylenediamine dihydrochloride (SULF/NEDD). The acidic mixture forms an azo dye with maximum absorption wavelength at 543 nm. To measure nitrate with this reagent it should be first reduced to nitrite (Sen *et al.*

1978), which can then be measured at the micromolar level. The main advantage of spectrophotometric measurement of ˙NO is that it requires common instrumentation with well-established procedures, but a poor detection limit (from 0.1 to 1 mM ˙NO) decreases its usefulness in experiments where ˙NO production ranges nanomolar concentrations. Care should also be taken to avoid reaction with sample components such as nitrosating compounds and reducing molecules like ascorbic acid, glutathione and dithiothreitol, as they can yield misleading results by interfering with sulfanilamide (Yao *et al.* 2004).

1.6.3 - Fluorimetric Assays

The ability of ˙NO to produce N-nitrosating agents has led to the development of several fluorimetric probes that have proven useful in bioimaging of ˙NO (Kojima *et al.* 2001). The aromatic diamino compound 2,3-diaminonaphthalene (DAN) acts as an indicator of ˙NO formation. DAN offers very week fluorescence signal but when it reacts with ˙NO to produce 2,3-naphthotriazole (NAT) the fluorescence intensity increases by more than a 100-fold (Miles *et al.* 1996). ˙NO metabolites in brain microdialysates can be monitored using liquid chromatography coupled with fluorescence detection, with DAN as sensitive reagent (Woitzik *et al.* 2001; Wada *et al.* 2002). This allows a sensitivity of less than 1 nM, but the extensive sample processing required to exclude numerous sources of contamination is a major disadvantage (Woitzik *et al.* 2001). 4,5-diaminofluoresceine (DAF-2) can also be used in real-time detection of ˙NO (Qiu *et al.* 2001). The reaction yields the highly fluorescent DAF-2 triazole (DAF-2T), but was shown to suffer serious interferences from endogenous molecules (*e.g.* ascorbic acid) and to be pH dependent (Zhang *et al.* 2002). Other probes based on the rhodamine chromophore were found to be pH insensitive above pH 4 (Kojima *et al.* 2001).

Sensitivity for measuring ˙NO is a considerable advantage when using fluorescence-based methods, but major problems are reagent preparation, time consumption experiments and lack of selectivity to ˙NO resulting from contamination from sample components (Wardman 2007).

1.6.4 - Electron Spin Resonance Spectroscopy

Electron Spin Resonance (ESR) spectroscopy allows the detection of free radical species because an unpaired electron can be oriented in a magnetic field and absorb incident microwave radiation to change its spin. Absorbed energy depends on the local electronic environment and determines the final spectrum, which can be used as a fingerprint for a particular radical. However, the labile nature of ˙NO prevents its direct detection, and a number of strategies are used to increase its half-life and stability to allow ESR detection (Berliner *et al.* 2001). Spin-traps are molecules that can react with free radicals, yielding ESR-stable adducts. Some ˙NO spin-traps take advantage of his strong binding to iron to form iron-nitrosyl complexes, and these include iron complex spin-traps such as N,N-diethyl dithiocarbamate-Fe(II) ([Fe(II)(DETC)$_2$]) (Tsuchiya *et al.* 1996) and N-methyl D-glucamine dithiocarbamate-Fe(II) ([Fe(II)(MGD)$_2$]) (Lai *et al.* 1994). Some proteins are also used to detect ˙NO for the same reason, particularly Hb (Blumberg 1981) and Mb (Duprat *et al.* 1995). Other spin-traps include stable organic radicals like 2-phenyl-4,4,5,5-tetramethylimidazoline-1-oxyl 3-oxide (PTIO) (Akaike *et al.* 1996) and 3,5-dibromo-4-nitrosobenzenesulfonate (DBNBS) (Ichimori *et al.* 1996). ESR methods are cumulative (adducts are stable and long-lasting) and can provide adequate specificity in ˙NO detection, but they are limited by expensive and complex instrumentation, time-consuming sample preparation, and complicated operation and interpretation of data. The usage of transition

metals to form spin-trap complexes can also alter the cellular redox environment, causing unwanted physiological changes.

1.6.5 - Electrochemistry

The previous methodologies are suitable to detect ˙NO in a number of model systems, but are inadequate to monitor its real-time endogenous production in hippocampus. A reliable real-time investigation of ˙NO dynamics in slices is only achievable by means of a sensitive and fast-responding method. This can be obtained by means of electrochemical methods combined with microelectrodes. Due to their small size, sensitivity, minimal or no reagents requirements, and nondestructive properties, microelectrodes are versatile tools to investigate ˙NO production, as clearly demonstrated by the measurement of ˙NO release of a single cell *in situ* (Malinski *et al.* 1992).

The first electrochemical sensor for ˙NO in biological samples was published by Shibuki in 1989, and consisted of a Clark-type oxygen sensor with reversed polarity to detect not oxygen but ˙NO at +0.9 V (Shibuki 1990). The second widely publicized electrochemical sensor was published by Malinski and Taha and was termed the porphyrinic sensor because it was composed of a carbon fiber modified by electropolymerized nickel(II) tetrakis(3-methoxy-4-hydroxyphenyl) porphyrin (NiTMHPP) (Malinski *et al.* 1992). This modification of the carbon surface was intended to lower the oxidation potential and enhance the oxidation current of ˙NO by electrocatalyzing his oxidation. The surface was also coated with another film made of Nafion®, a sulfonated tetrafluorethylene polymer with sulfonic acid side chains that forms a negatively-charged membrane and improves selectivity against nitrite, nitrate and other biological anions (Brazell *et al.* 1987). When hydrated the sulfonic acid side chains are neutralized by solvent

cations, which further diminishes the film permeability to anionic species (Sakai *et al.* 1986).

A number of electrochemical techniques can be used with microsensors to detect $^\bullet$NO in biological samples. Electrochemical assays are based on the electrochemical oxidation of $^\bullet$NO on solid electrodes. If the current generated during $^\bullet$NO oxidation is linearly proportional to the concentration, the oxidation current can be used as the analytical signal (Malinski *et al.* 1996). Amongst the most widely used techniques amperometry occupies the central stage and consists in polarizing microsensors at a certain potential while recording the analyte oxidation current. When measuring $^\bullet$NO, an oxidizing potential of +0.9 V is typically used, but care must be taken as other species might contribute to the analytical signal (including ascorbic acid and nitrite). The use of selective films provides protection up to a certain concentration level of the interfering substance, and appropriate controls are required to ensure $^\bullet$NO detection. The major advantages of amperometry are its short response time and the ability to detect $^\bullet$NO before its reaction with other species. Other techniques such as differential pulse voltammetry (DPV) have been employed by some researchers (Meulemans 2002), but the low concentrations and short life of $^\bullet$NO result in considerable difficulties in evaluating these voltammograms.

Others sensors are commercially available that display very good analytical characteristics. These are integrated sensors made of gas permeable membranes, which confers them a very high level of selectivity and isolate all sensing elements from the sample solution, making them immune to changes in ionic strength or conductivity. The fact that all components (reference, auxiliary and working electrodes) are placed in the same structure enables its use with no special handling care. However, the fragility of the protective membranes and the high cost of each sensor and components are major disadvantages, along with tedious calibration procedures and severe

temperature dependence. Most importantly, their macroscopic dimensions prevent their usage in reduced biological samples.

Given the above mentioned scenario and in order to investigate the rate and pattern of ˙NO dynamics in hippocampus via stimulation of glutamate ionotropic receptors, we have used a porphyrin/Nafion carbon fiber selective microsensor and amperometry as the analytical tool.

1.7 - Objectives

˙NO production in hippocampus is mediated by glutamatergic receptors. These are implicated in physiological events but also in oxidative/nitrosative stress, particularly after excessive activation of the NMDA subtype. However, and despite reports demonstrating its increase following non-NMDA receptors activation, little is known about the role of other receptors on ˙NO production and, most importantly, the concentration dynamics of ˙NO in the extracellular space. Furthermore, cells are expected to counteract any pathway leading to excessive ˙NO production, setting in motion protective mechanism to prevent cellular degeneration. These are expected to be linked to glutamate homeostasis, as excitotoxicity is closely related to its extracellular concentrations and release from synaptic elements.

Considering the previous notion, we have implemented an experimental strategy consisting of electrochemical ˙NO microsensors inserted into acute hippocampal brain slices and primary cultures of astrocytes to meet the following objectives:

1) To investigate ˙NO concentration dynamics in hippocampus following glutamate receptors activation, determining the extent and pattern of

endogenous ˙NO production following brief and toxic stimulations of NMDA receptors (Chapter 3);

2) To determine the role of non-NMDA receptors, namely the AMPA subtype, in NOS activation in hippocampus, and its relation with NMDA-elicited ˙NO production (Chapter 4);

3) To investigate the contribution of astrocytes to GSH extracellular pool under conditions of high glutamate concentrations, as an experimental model for excitotoxic (Chapter 5).

CHAPTER **2**

MATERIALS AND METHODS

2.1 - Nitric Oxide Microsensors

2.1.1 - Reagents and Solutions

N-methyl-D-aspartate (NMDA), α-amino-3-hydroxy-5-methylisoxazole-4-propionate (AMPA), NG-Nitro-L-arginine methyl ester (L-NAME), D(–)-2-amino-5-phosphonopentanoic acid (AP5), and 2,3-Dioxo-6-nitro-1,2,3,4-tetrahydrobenzo[f]quinoxaline-7-sulfonamide (NBQX) were purchased from Tocris Cookson (Avonmouth, U.K.); Nafion® from Aldrich; L-glutamate from Biochemical; ascorbic acid and dopamine from Fluka Chimica; $NaNO_2$ from Merck; diethylenetriaminepentacetic acid (DTPA), diethylenetriamine/NO (DETA/NO), serotonin (5-HT), glutathione (GSH) and L-arginine (L-arg) from Sigma. All other reagents were purchased from Merck.

Buffer solutions used for microsensor testing and calibrations were prepared in ultra pure water with resistivity higher than 18 $M\Omega$.cm (milli-Q, Milipore). Buffer was phosphate buffer saline (PBS), with the following composition: 140 mM NaCl, 2.7 mM KCl, 8.1 mM $NaHPO_4$, 1.8 mM KH_2PO_4, pH 7.4. To remove traces of metal ions the ion chelator DTPA was added at a concentration of 0.1 mM.

10 mM DETA/NO stock solutions were prepared in 10 mM NaOH and kept at -18 ºC. Additional solutions used for microsensors calibration referred in text were prepared in PBS degassed with argon (AirLiquid) for at least 15 minutes.

The active surface of microsensors was modified with the following solutions:

a) 0.5 mM metal porphyrin (NiTMHPP) solution - nickel(II) tetrakis (3-methoxy-4-hydroxyphenyl)-porphyrin, prepared in 0.1 M NaOH (Interchim, France).

b) Nafion® - 5% aliphatic alcohols solution (Aldrich, Germany).

2.1.2 - Fabrication

Microsensors were prepared as previously described (Millar 1992; Barbosa *et al.* 1998; Ledo *et al.* 2002; Ferreira *et al.* 2005). Briefly, a single carbon fiber (8 μm i.d.; Courtaulds, London, UK) was inserted into one borosilicate glass capillary (1.16 mm i.d. X 2.0 mm o.d.; Harvard Apparatus, UK) previously filled with acetone. This solvent was used to facilitate fiber insertion and remove any surface impurities resulting from the manufacturing process. After solvent evaporation at room temperature the capillary was placed on a vertical puller (single barrel model, Harvard Apparatus, UK) and both extremities were subjected to a traction force while heating the middle section, in order to obtain a glass seal on the surface of the carbon fiber while leaving a small exposed active surface. The micropipette containing the protruding carbon fiber obtained was cut 1 cm away from the glass sealing and the remaining micropipette discarded. A portion of conductive silver paint (RS, Northants, U.K.) was inserted into the micropipette with the help of a teflon tube and a syringe. To ensure the electrical contact between the carbon fiber and the recording device a cooper wire was introduced into the micropipette and immersed into the conductive paint, after which the topmost part of the wire was glued to the capillary with standard cianoacrylate glue. The protruding carbon fiber was finally cut to desired tip length, typically 100-150 μm, under a microscope (Nikon, Japan) using small forceps. Figure 2.1 and Figure 2.2 show a complete microsensor and an Electron Scan Microscopy details of the active surface, respectively.
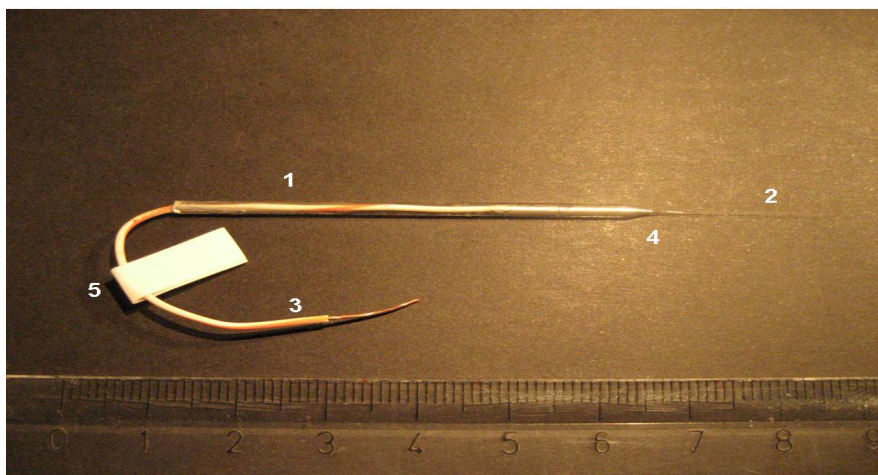
Figure 2.1: Fully assembled ˙NO microsensor. A borosilicate glass capillary (1) containing a carbon fiber was placed in a puller to obtain a micropipette with a glass-encased protruding carbon surface (2), later modified with NiTMHPP and Nafion®. To ensure connectivity between the sensor and the recording device a copper wire (3) was immersed into previously inserted conductive paint (4) and glued in place to prevent unwanted displacement of parts under usage. A small tag was used to label each sensor (5). Bottom scale in centimeters.

Once completed, the microsensor was tested for general recording characteristics in PBS by fast cyclic voltammetry (FCV), using a triangular wave between -0.4 and +1.6 V at a scan rate of 200 V/s. FCV was carried out on an EI-400 potentiostat (Ensman Instruments, Bloomington, USA), and signals were monitored on a digital storage oscilloscope (Tektronix TDS 220, USA). This testing was performed to evaluate microsensor's response and to ensure that sensors selected for surface modification had the appropriate characteristics for subsequent usage in experiments. In electric terms, an electrode exhibits both capacitive and resistive characteristics. However, a suitable microsensor exhibits a more capacitive behavior (Stamford *et al.* 1992), as a result of an adequate sealing between the glass and the carbon fiber and a good electric contact between components. A stable background current and sharp transients at reversal potentials indicated suitable recording properties of the microsensor, as displayed in Figure 2.3, A. Several
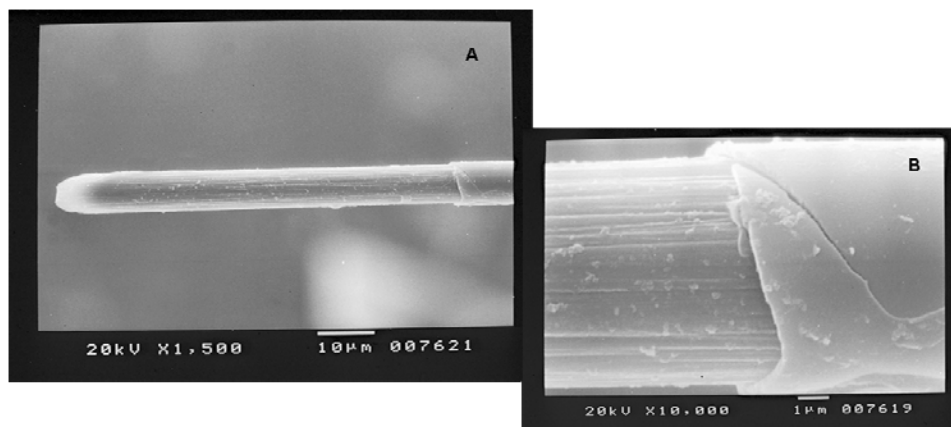
Figure 2.2: Electron Scan Microscopy images of a 75 µm microsensor. A) The active surface, modified previously with NiTMHPP and six layers of Nafion® (films not visible). B) Detail of the glass seal area, separating the active surface from the glass body. Magnification and scale as indicated in images.

manufactured microsensors exhibited different profiles (Figure 2.3, B) and were therefore considered inappropriate for experiments and discarded. Microsensors considered adequate for future experiments were labeled and keep at room temperature in storage racks until experiments on slices.
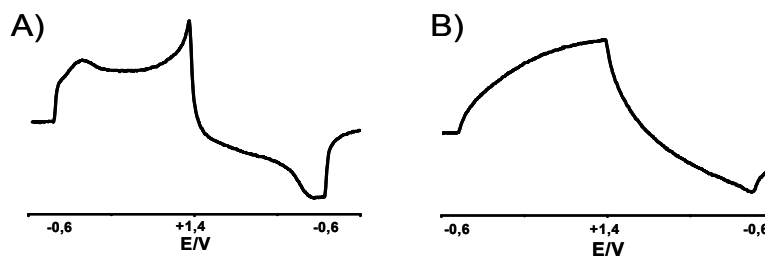
Figure 2.3: FCV voltammograms of microsensors in PBS. A) A good microsensor exhibits stable background current and sharp transients at reversal potentials. B) A bad electrode with resistive characteristics, discarded for further experiments.

2.1.3 - Chemical Modification of Surface

The detection of a molecule using sensors requires the use of a device that exhibits good sensitivity and linearity towards it with minimal interference from possible environmental contaminants. It was therefore necessary to modify the active surface of microsensors to ensure with good analytical characteristics towards ˙NO (Malinski *et al.* 1996). Based on previous reports (Malinski *et al.* 1992), the active carbon surface was therefore modified in a two-step protocol designed to increase the microsensor's sensitivity and selectivity to ˙NO produced in slices.

The first modification step intended to cover the microsensor's active surface with a polymer shown to catalyze the oxidation of ˙NO, and thus increase the microsensor's sensitivity towards ˙NO (Figure 2.4) (Malinski *et al.*
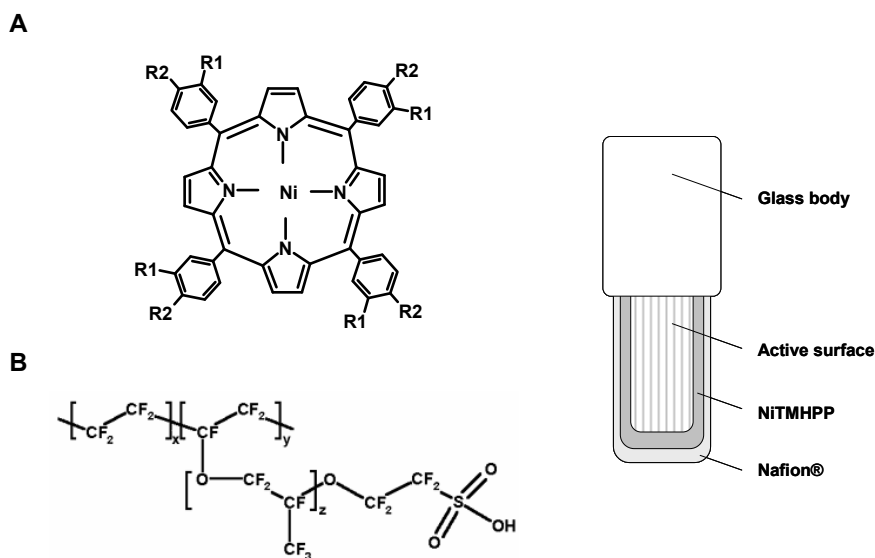
Figure 2.4: Chemical structure of molecules used to modify the active surface of ˙NO microsensors. A) NiTMHPP, used as a catalytic film to facilitate ˙NO oxidation and improve sensitivity. B) Nafion®, used to increase sensitivity towards ˙NO after NiTMHPP polymerization. C) Schematic representation of modifications with NiTMHPP and Nafion® on the active surface of a microsensor.

1996). It consisted in the electrochemical polymerization of a metal porphyrin (Ni-TMHPP), prepared in 0.1 M NaOH at a concentration of 0.5 mM, by continuous-scan cyclic voltammetry. This was performed in 40 voltage sweeps at 0.1 V/s from 0.0 to +1.2 V *vs* Ag/AgCl with platinum wire as an auxiliary electrode, and using the Autolab PGSTAT12 Potentiostat in conjunction with the General Purpose Electrochemical Software (GPES) from Eco Chemie (Utrecht, The Netherlands). Coverage was monitored by observing the growth of Ni(II)/Ni(III) redox couple, as depicted in Figure 2.5.

The second modification step was designed to increase the microsensor's selectivity towards ˙NO, in order to ensure that the oxidation current observed was due to the oxidation of the analyte under investigation and not a contaminant (Malinski *et al.* 1996). This consisted in coating the NiTMHPP-modified active surface with Nafion® (Figure 2.4), which forms an anionic barrier capable of preventing the oxidation of endogenous anionic compounds like DA or nitrite (Brazell *et al.* 1987). Each layer was obtained by dipping the sensor in a Nafion® solution at room temperature for 30 seconds, followed by drying at 80-85ºC for 10 minutes. Total time required for microsensors modification with Nafion® was 1 hour, as six layers were
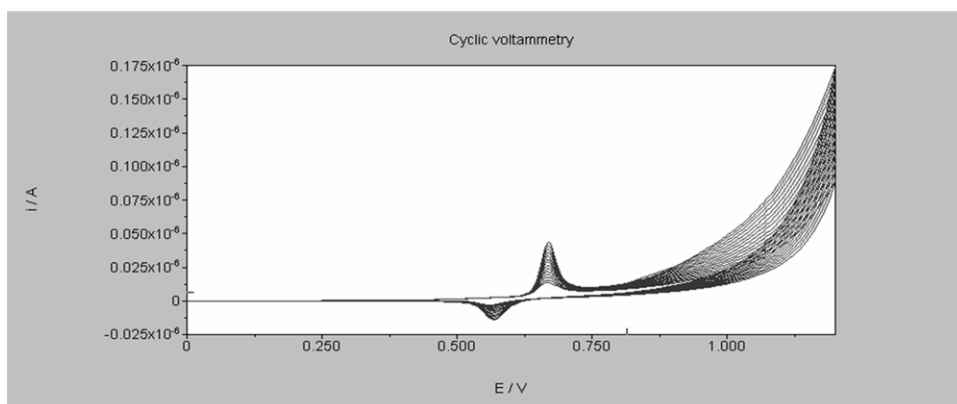
Figure 2.5: Cyclic voltammetric polymerization of NiTMHPP on the surface of a microsensor using GPES software. Electropolymerization of NiTMHPP was monitored by following the growth of the Ni(II)/Ni(III) redox couple peaks between 0 and +1.4 V, as depicted above after 24 scans.

consider ideal for experiments in hippocampal slices after comparative analysis between microsensors modified with one or six layers of Nafion®. Once completed ˙NO microsensors (Figure 2.1) were stored dry at room temperature prior to experiments and in PBS at 4.0 ºC after insertion on hippocampal brain slices.

2.1.4 - Analytical Parameters

Microsensors were tested for a number of key features to ensure good analytical properties before experiments. Protocols and instrumental apparatus used in sensitivity, detection limit, response time and selectivity studies are detailed in the following sections.

2.1.4.1 - Nitric Oxide Oxidation Potential

The oxidation potential for detecting ˙NO was determined by square wave voltammetry (SWV), an electrochemical technique that retains a good resolution and sensitivity while allowing a high scan rate. A typical
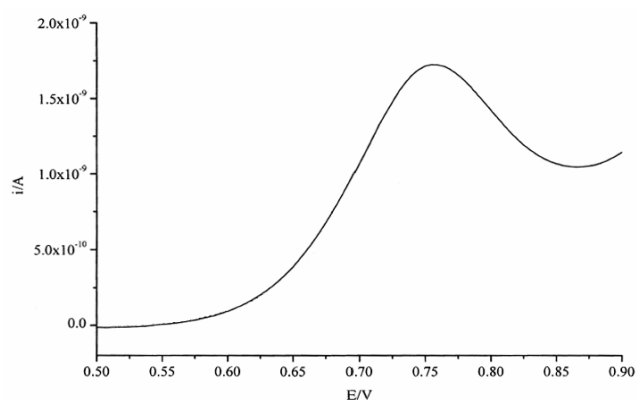
Figure 2.6: Background-subtracted voltammogram obtained by square wave voltammetry of 10 μM ˙NO in deaerated PBS. Peak potential is 740 mV *vs* Ag/AgCl. Experimental conditions: pulse amplitude 25 mV, frequency 25 Hz, step potential 2 mV and scan rate 50 mV/s.

voltammogram of 10 μM ˙NO prepared in PBS is presented in Figure 2.6. ˙NO exhibited an oxidation potential of +0.75 V *vs* Ag/AgCl, in agreement with the value reported by Friedemann *et al.* for NiTMHPP coated electrodes (+0.74 V *vs* Ag/AgCl) (Friedemann *et al.* 1996) and higher than the obtained by Malinsky and Taha (+0.64 V *vs* saturated calomel reference electrode) (Malinski *et al.* 1992). Following this result we used an oxidizing potential of +0.9 V to detect ˙NO by amperometry, a value 150 mV above the peak oxidizing potential. No current changes were observed when the oxidizing potential was set at +0.55 V. Since interferents like ascorbic acid, dopamine and 5-HT exhibit lower peak oxidation potentials than ˙NO (below +0.5 V) (Stamford *et al.* 1992), +0.55 V was selected for future electrochemical control experiments to determine their contribution in recorded currents.

2.1.4.2 - Sensitivity

Microsensors were calibrated with ˙NO standard solutions prepared from DETA/NO. DETA/NO is a ˙NO donor stable at alkaline pH that releases ˙NO at room temperature and low pH with a half-life of 52 hours (Keefer *et al.* 1996). It was used as a ˙NO source to calibrate microsensors at pH 7.4. The release profile of DETA/NO solutions was studied with the commercial sensor ISO-NOP 2 mm Pt connected to an ISO-NO Mark II amperometer (World Precision Instruments, USA). This sensor contains a gas-permeable Teflon membrane that allows its calibration with chemically generated ˙NO at an oxidizing potential of +865 mV (*vs* Ag/AgCl), according to reaction 14. The 1:1 stoichiometry between added NO_2^- and ˙NO at low pH allows for a robust calibration protocol, that could not be used with microsensors due to the potentially harmful effect of low pH on NiTMHPP and Nafion® films. This sensor demonstrated a good linearity and sensitivity between 0 and 2 μM ˙NO after calibration.

$$2KNO_2 + 2KI + 2H_2SO_4 \quad \rightarrow \quad 2^{\bullet}NO + I_2 + H_2O + 2K_2SO_4 \qquad (14)$$

$^{\bullet}$NO release profiles from DETA/NO in deaerated PBS were obtained by following the decomposition of 10 μM, 50 μM and 100 μM solutions DETA/NO over time, as depicted in Figure 2.7. A plateau phase was reached after 60 minutes and remained stable throughout the rest of experiment, indicating that $^{\bullet}$NO release was maximal after 1 hour at room temperature and pH 7.4. The relationship between added DETA/NO and released $^{\bullet}$NO was calculated to be 100:1 from the calibration plot (R=0.999, n=3 for all concentrations). Hence, DETA/NO solutions used to calibrate microsensors were prepared in deaerated PBS at least one hour before experiments, at a
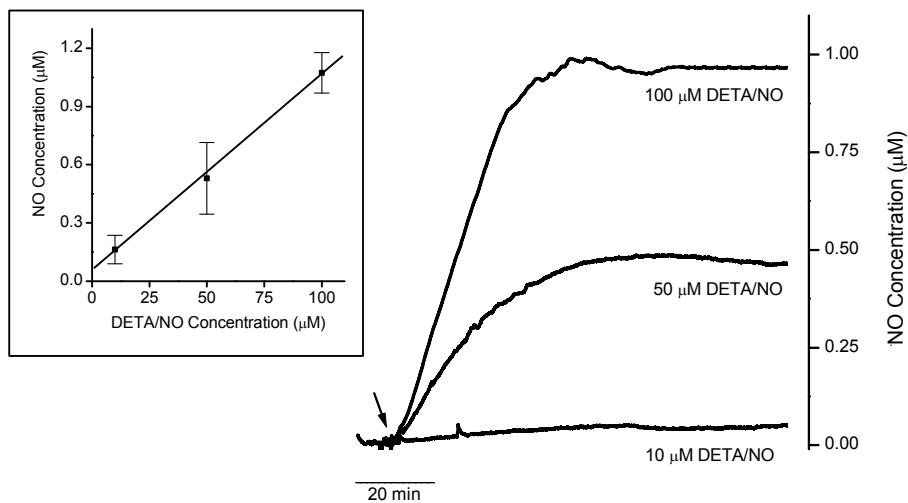
Figure 2.7: DETA/NO decomposition profiles. Typical amperometric recordings of DETA/NO solutions in deaerated PBS using ISO-NOP reveal a steady-state release of $^{\bullet}$NO after 60 minutes at pH 7.4 and room temperature. Arrow indicates beginning of experiments. Insert: From linear regression analysis the relationship between DETA/NO and $^{\bullet}$NO concentrations was calculated to be 100:1. Data obtained from n=3 for 10, 50 and 100 μM DETA/NO, with Y = 0,0101 (X) + 0,06 and R=0.999. Adapted from (Ledo 2007).

concentration 100 times higher than required. When using DETA/NO solutions, data is presented as $^{\bullet}$NO concentration.

Calibrations were performed in a single-stream Flow Injection Analysis (FIA) system. This apparatus consisted of a peristaltic pump connected to a homemade flow cell, where PBS was used to deliver a plug of 500 µl of different $^{\bullet}$NO standards to the microsensor. Quadruplicates of 0.125, 0.25, 0.50 and 1.00 µM $^{\bullet}$NO solutions were injected one minute apart with a four-valve port at a flow rate of 2.0 ml/min and room temperature. Transient oxidation currents at +0.9 V *vs* Ag/AgCl were recorded using the PGSTAT12 Potentiostat in conjunction with GPES (Eco Chemie, Utrecht, The Netherlands). Figure 2.8 illustrates a typical calibration of one microsensor
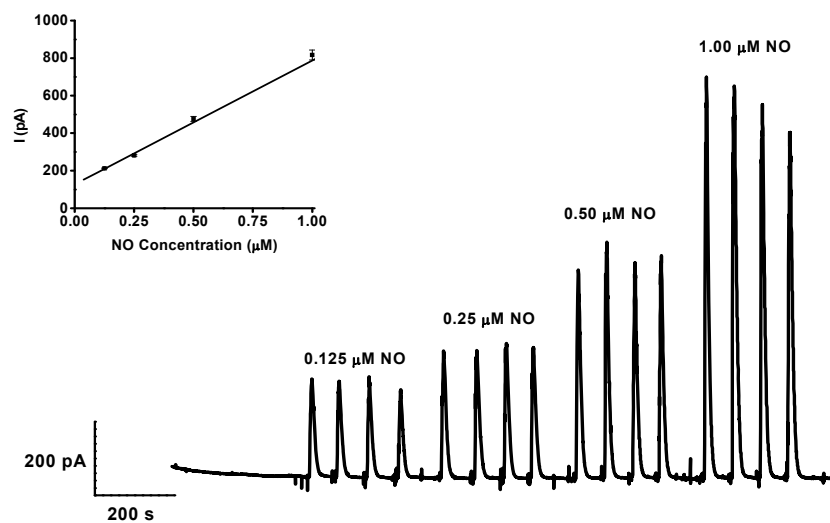
Figure 2.8: Typical amperometric recording for the calibration of one microsensor with DETA/NO-derived $^{\bullet}$NO. Each $^{\bullet}$NO concentration (top label) was minute-by-minute injected and changes in baseline current (in pA) related to the corresponding concentration to determine sensitivity. Insert: representative linear regression analysis of mean of 4 injections for 4 different concentrations, with Y = 659.28 X + 127.75 (R=0.994).

modified with NiTMHPP and six layers of Nafion®, with a linear response between 0 and 1 μM ˙NO. Current mean values were plotted against the corresponding concentration to determine sensitivity by means of linear regression, calculated to be 679 ± 55 pA/μM ˙NO (n=55).

2.1.4.3 - Detection Limit

Linear regression analysis of calibration plots can be used along with equation *1*, where m stands for slope and S.D. represents standard deviation of regression line, to determine the limit of detection (L.O.D.) of microsensors.

$$L.O.D. = 3 \times (S.D./m) \qquad\qquad (1)$$

Microsensors were calibrated with ˙NO solutions 10 times less concentrated than previously used, ranging from 12.5 nM to 100 nM ˙NO. As observed for higher concentrations, currents peaks changed linearly with concentration at +0,9 V *vs* Ag/AgCl, with a good signal to noise ratio. Values obtained indicate that, after modifying the active surface with NiTMHPP and six layers of Nafion®, the detection limit was 6 ± 3 nM ˙NO (n=10 microsensors).

2.1.4.4 - Selectivity

Microsensors were used to determine the selectivity against endogenous interferents when compared to 1 µM ˙NO (prepared from DETA/NO). Figure 2.9 displays a typical amperometric recording of a selectivity assay against endogenous molecules: nitrite (100 µM), ascorbic
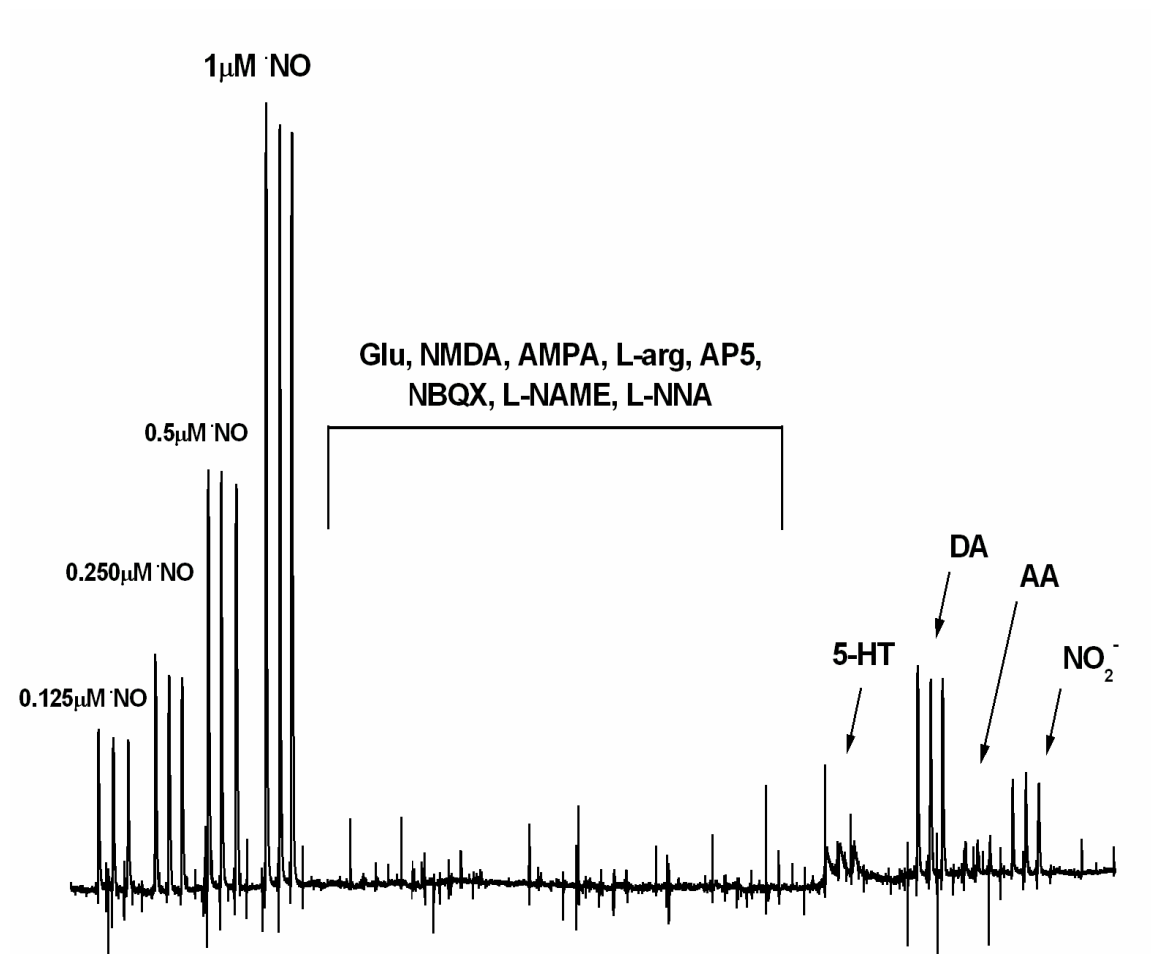
Figure 2.9: Representative amperometric recording of a selectivity assay. Microsensor was calibrated and used to determine the interference caused by indicated molecules. Middle interferents (from Glu to L-NNA) caused negligible modifications in baseline current.

acid (100 µM), dopamine (10 µM), 5-HT (10 µM) and glutamate (1 mM); Glutamate receptor modulators: NMDA (100 µM), AMPA (100 µM), AP5 (50 µM), NBQX (50 µM); and NOS substrate and inhibitors: L-arg (1 mM), L-NAME (500 µM) and L-NNA (500 µM).

2.1.4.5 - Response time

The response time of microsensors to $^{\cdot}$NO at +0.9 V *vs* Ag/AgCl was calculated as the time required to obtain 50 % of maximal current change ($T_{50\%}$) after flow injection of 250 µM $^{\cdot}$NO (prepared from DETA/NO). Results from 8 different microsensors indicate that, after the abovementioned modifications, $T_{50\%}$ was 0.38 ± 0.04 s (n=8).

2.2 - Hippocampal Slices

2.2.1 - Reagents and Solutions

NMDA, AMPA, AP5 and NBQX were purchased from Tocris Cookson (Avonmouth, U.K.); Philantotoxin-4,3,3 (PhTx-4,3,3) and glutathione (GSH) from Sigma. All other reagents, including Methylene Blue (MB), were from Merck. All solutions were prepared in ultra pure water (milli-Q, Milipore).

Media for hippocampal slice experiments was normal artificial cerebrospinal fluid (aCSF) composed of 120 mM NaCl, 3 mM KCl, 26 mM NaHCO$_3$, 1.5 mM NaH$_2$PO$_4$, 1.4 mM MgCl$_2$, 1.5 mM CaCl$_2$, and 10 mM D-glucose. Experiments with NMDA were conducted in the absence of MgCl$_2$, whereas stimulations with AMPA were performed with normal aCSF supplemented with 25 µM AP5. Modified aCSF was used to increase cellular viability during dissection and recovery, with the following composition: 120

mM NaCl, 3 mM KCl, 26 mM NaHCO$_3$, 1.5 mM NaH$_2$PO$_4$, 10 mM MgCl$_2$, 0.5 mM CaCl$_2$, 10 mM D-glucose, 0.2 mM ascorbic acid and 3 mM GSH. Increased MgCl$_2$ and decrease CaCl$_2$ concentrations were used to reduce NMDA receptors activation during recovery, while ascorbic acid and GSH were used as antioxidants. In both cases aCSF was continuously bubbled with humidified Carbox (95%O2/5%CO2, Air Liquide, Portugal) for oxygenation and pH buffering (pH 7.4).

2.2.2 - Acute Hippocampal Brain Slice Preparation

Adult male Wistar rats (100-150 g) were purchased from Charles River Laboratories (Barcelona, Spain) and maintained in quarantine for at least 3 days before experiments, with standard light/dark cycles and food *ad libitum*. Animals were killed by cervical displacement according to approved guidelines and the brain was rapidly removed and placed in a large Petri dish containing ice-cold modified aCSF, previously bubbled with Carbox for at least 20 minutes. The hippocampi were dissected with the help of small forceps and subsequently placed on the stage of a McIlwain Tissue Chopper (Campden Instruments, London, UK), on top of a small circle of transparency film. 400 µm thick slices were obtained, and gently transferred with the help of the film to a small Petri dish containing ice-cold modified aCSF previously bubbled with Carbox. Slices were then separated using bottom-sealed Pasteur pipettes and transferred to a pre-incubation chamber (BSC-PC, Harvard Apparatus, USA) containing modified aCSF at room temperature, also continuously bubbled with Carbox. Slices were allowed to recover for at least one hour under these conditions before any recordings.

2.2.3 - Signal Recordings

Experiments with hippocampal slices were conducted in the recording chamber BSC-BU with BSC-ZT top (Harvard Apparatus, USA). Amperometric currents were recorded with the inNO model T Electrochemical Detection System coupled to a computer equipped with inNO v3.1 software (Innovative Instruments, Tampa, FL, USA). The PSSAT 12 potentiostat (Eco Chimie, The Netherlands) was used to perform experiments at low oxidation potentials. A two-electrode circuit was used, with an Ag/AgCl pellet as a reference electrode and one microsensor held at a constant potential of +0.9 V (unless otherwise stated) as a working electrode. Recordings were conducted inside a grounded Faraday cage, on top of a metallic plaque that allowed the fixation of hardware *e.g.* micromanipulators' bars and magnifying lens (Olympus, Japan). Once recovered, individual slices were placed in the chamber and perfused with normal aCSF, continuously bubbled with humidified Carbox, at a flow rate of 2 ml/min. All experiments were conducted at controlled temperature maintained by a water bath (GFL, EUA) located outside the cage that pre-heated all solutions to 36 ºC and a temperature controller (model TC-202A, Harvard Apparatus, USA), used to ensure an optimal recording temperature on the perfusing chamber of 32 °C. Figure 2.10 depicts this setup.

After recovery, one hippocampal slice was placed in the recording chamber and attached to a nylon mesh to avoid flow-induced displacement (Figure 2.11). The microsensor was inserted under visual guidance in the CA1 subregion, 200-300 μm into the tissue at the level of the pyramidal cell layer. This site is known to be concentrated in nNOS (Wendland *et al.* 1994; Burette *et al.* 2002) and was easy to identify, allowing precise reproduction of microsensor's insertion. Moreover, we have previously shown that at this depth the cell layers enjoy a physiological O_2 tension. This is an important

Pre-heated aCSF

Water bath

Magnifying lens

Recording chamber

Tissue Chopper   Pre-incubation chamber   Light source

Faraday cage

Magnifying lens

Recording chamber

Metallic base   Temperature controller   Computer with inNO v1.3 software
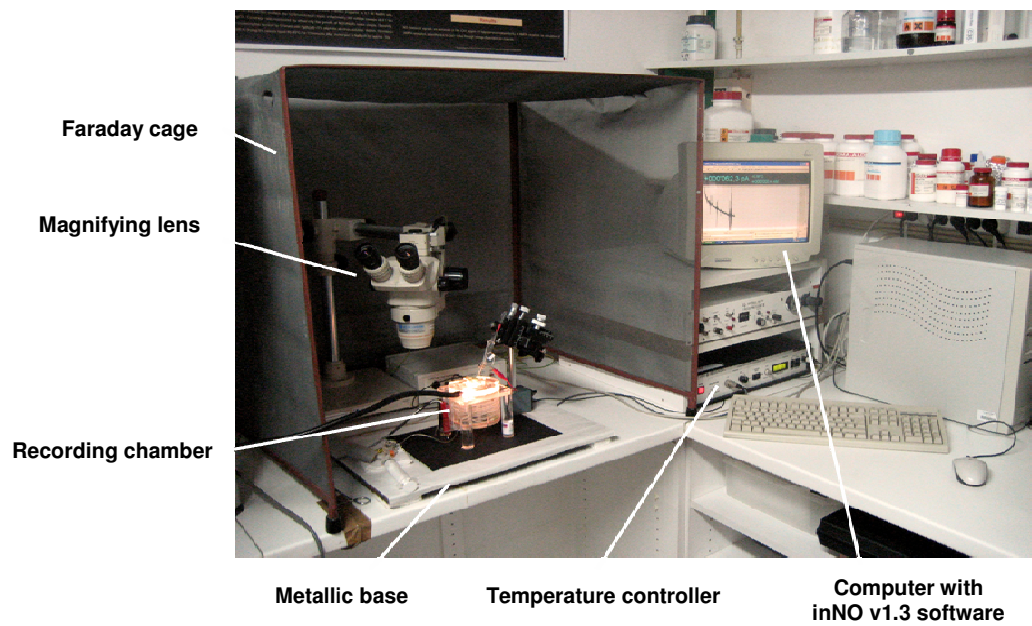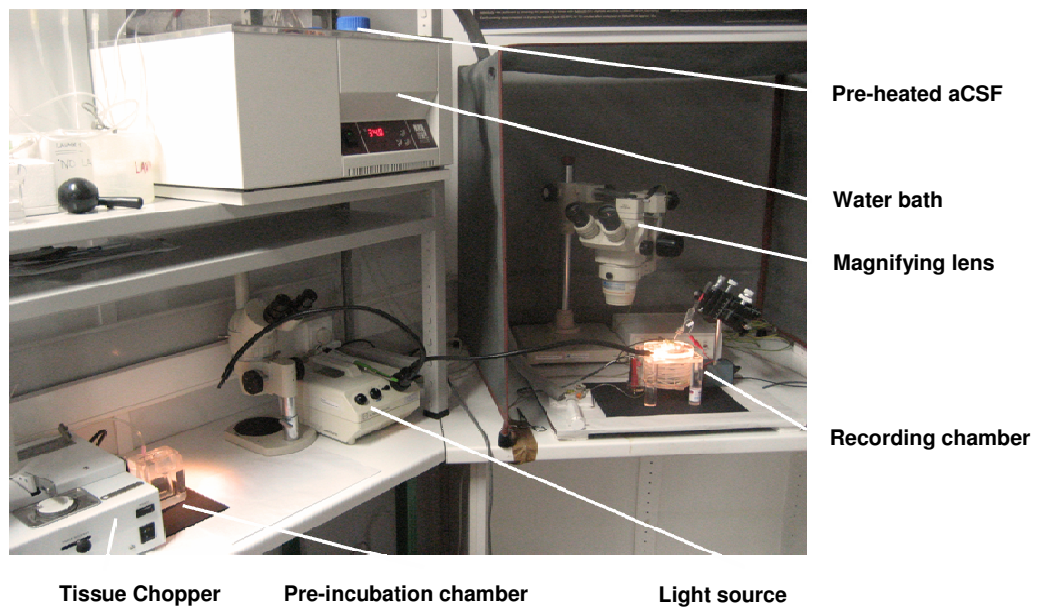
Figure 2.10: Hippocampal slices setup and apparatus used to record endogenous $^{\bullet}$NO production.

Magnifying lens

Micromanipulator

inNO Electrochemical Detection System

˙NO microsensor

Recording chamber

two-valve port with tubings

˙NO microsensor

Reference electrode

Hippocampal slice

aCSF flow

Temperature sensor

Reference electrode

nylon mesh

˙NO microsensor
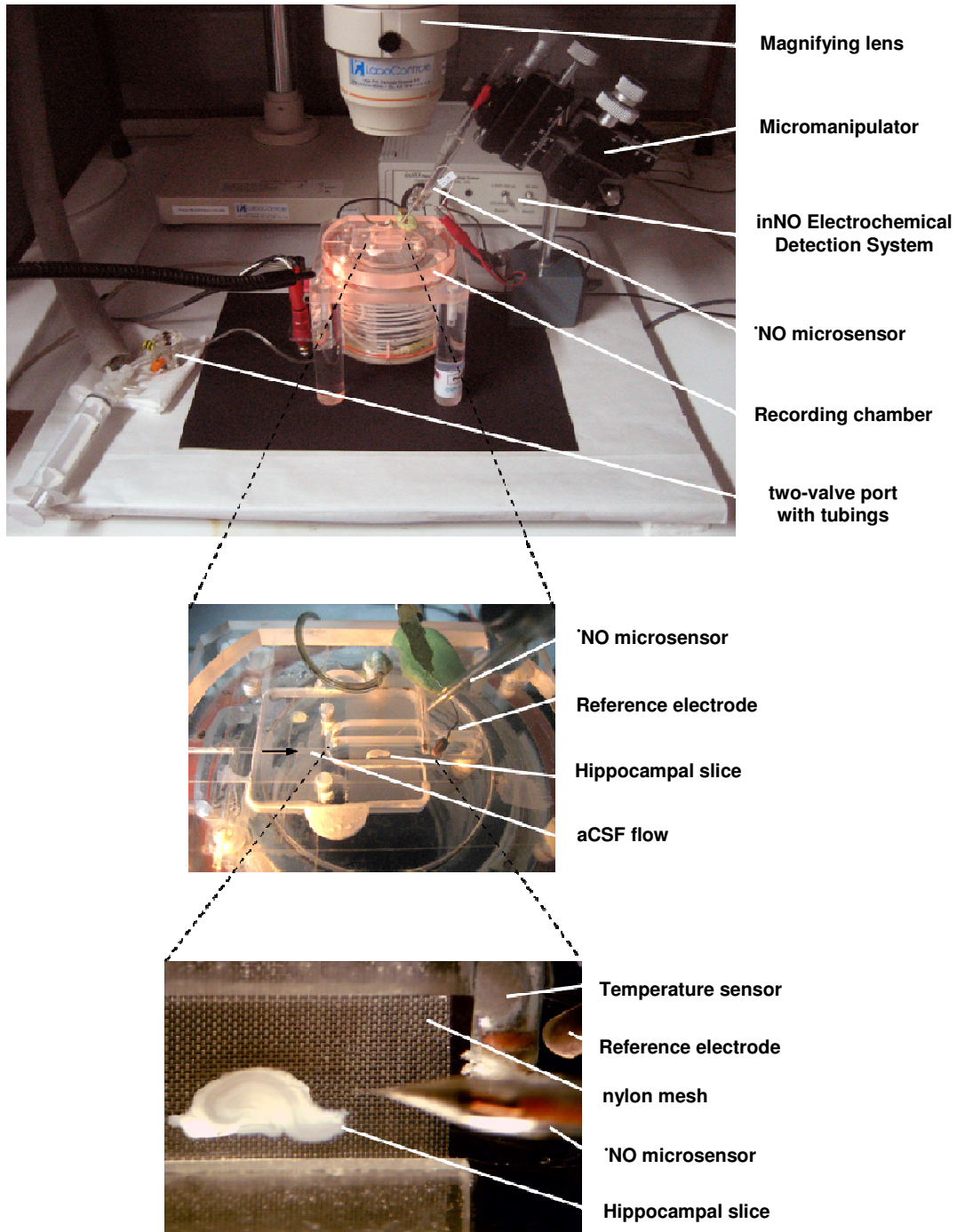
Hippocampal slice

Figure 2.11: Recording chamber used to monitor endogenous ˙NO production in hippocampal slices. Bottom figure depicts a microsensor inserted in the CA1 region of an hippocampal slice (tip not visible).

feature when considering that the reaction of $^{\bullet}NO$ with O_2 occurs slowly over time but may interfere with $^{\bullet}NO$ dynamics for high tensions of both gases (Ledo *et al.* 2005). This observation demonstrates that reported results were not biased by using Carbox to maintain pH and media oxygenation. Media was removed from the perfusion chamber by means of a vacuum pump for latter disposal. Figure 2.11 details the perfusion chamber with a hippocampal slice setup, together with main required parts and components.

2.2.4 - Stimulation Protocol

Stimulation and/or administration of inhibitors in slices was conducted by a two-valve port located upstream of the perfusion chamber, that allowed modifications of perfusing media by switching between two tubing sets. Whenever necessary, the appropriate tubing was filled with the solution containing the drug using the disposal exit of the valve. Time was set to two minutes (or as otherwise stated) and the selector quickly changed from aCSF to drug-containing solution. This setup design allowed an effective and reproducible stimulation of slices with minimal interference on flow rate. To ensure that flow rate was the same between the 2 sets both tubing had equal length and inner diameter, and were periodically cleaned with 1 M HCl and 1 % acetic acid solutions to remove bacteria and Ca^{2+} precipitates (respectively). All solutions were prepared by supplementing normal aCSF with the desired compound, and maintained in the water bath at 36 ºC under Carbox before perfusion. A vertical marker was used in inNO v3.1 software to indicate stimulation, as presented in figures.

2.3 - Astrocytes Cultures

2.3.1 - Reagents and Solutions

Experiments with astrocytes were performed in collaboration with groups from London (UK) and Bremen (Germany). For experiments performed in London, the following reagents were used. Tripsin/EDTA, L-glutamine, antibiotic/antimycotic solution (10 units/ml penicillin, 1 μg/ml streptomycin, 2.5 ng/ml amphotericin), poly-D-lysine, DNAse, BSA, Earle's Balanced Salt Solution (EBSS) and Hank's Balanced Salt Solution (HBSS) were purchased from Sigma (Poole, UK). Minimum essential medium (MEM, L-valine based) and fetal bovine serum (FBS) were purchased from Gibco-Invitrogen (Paisley, UK). Cell culture flasks were purchased from Nalgene Nunc International (Naperville, IL, USA). Six-well plates were purchased from Corning Costar (High Wycombe, UK).

Solution A was composed of EBSS containing 2 mg DNAse, 300 mg BSA and 1% (v/v) antibiotic/antimycotic solution. Solution B was composed of 20 ml of Solution A supplemented 3 mg DNAse and 5 mg trypsin. Astrocyte Medium was composed of MEM supplemented with 2mM L-glutamine, 10 % FBS and 1% (v/v) antibiotic/antimycotic solution.

For the experiments performed in Bremen, the following reagents were used. Dulbecco´s modified Eagle´s medium (DMEM) was from Gibco-Invitrogen (Karlsruhe, Germany). Fetal calf serum and penicillin/streptomycin stock solution were from Biochrom (Berlin, Germany). Sulfosalycilic acid (SSA) and NADPH were from AppliChem (Darmstadt, Germany). Glutathione reductase and GSSG were obtained from Roche Diagnostics (Mannheim, Germany). All other chemicals were obtained from Sigma (Steinheim, Germany), Fluka (Neu-Ulm, Germany) or Merck (Darmstadt, Germany). Sterile 24-well dishes were from Sarstedt (Nümbrecht, Germany).

2.3.2 - Primary Astrocyte Culture

2.3.2.1 - Isolation of Astrocytes

Astrocytes were isolated from neonatal (0-2 days) Wistar rats as previously described (Griffin *et al.* 2005). These were decapitated, and small scissors were used to cut skin and scull along midline and sides. Once brain was exposed, cerebellum was discarded and both hemispheres were removed to an ice-cold HBSS-containing Petri dish with the help of a small spatula. Under dissecting microscope meninges and midbrain were removed and both cortex and hippocampus were dissected and placed in a small Petri dish containing Solution A. The following steps were performed separately for cortex and hippocampus, to obtain separate cultures of cortical and hippocampal astrocytes. Curved edge scissors and a Gilson pipette were used to break down tissue to small pieces in Solution A. This triturated brain solution was centrifuged at 500 g and 4 ºC for 5 minutes and the supernatant discarded. The pellet was then trypsin-digested with Solution B for 10-15 minutes at 37 ºC. Digestion was terminated by adding 1 ml FBS and astrocytes were pelleted by centrifugation at 500 g and 4 ºC for 5 minutes. Pellet was resuspended in Solution A and passed through nylon gauze (40 μm pore size) to remove cell debris. Astrocytes were plated in 80-cm^2 flasks (1 head per flask) and cultured in Astrocyte Medium in an incubator (95 % air/5 % CO_2) at 37 ºC for 7 days. Medium was changed no later than 24 hours and then every 3 days. Figure 2.12, A refers to a one-day old astrocyte culture, characterized by small rounded bodies.

2.3.2.2 - Passage of Astrocytes

Astrocytes were passaged on day 7 when they reached confluence (Figure 2.12, B). Media was removed from flasks, the cells washed with warmed HBSS to remove serum, and incubated with 10 ml trypsin/EDTA solution for 5 minutes at 37 ºC. Trypsinisation was terminated by the addition of 1 ml FBS, and astrocytes were pelleted by centrifugation at 500 g and 4 ºC for 5 minutes. Pellet was resuspended in Astrocyte Medium and astrocytes cultured in twice the number of flasks for further 6 days in the conditions described above. Figure 2.12, C shows a detail of astrocyte culture at Day 8 after medium change.

2.3.2.3 - Plating on 6-well plates

On day 13 astrocytes (Figure 2.12, D) were removed from the flasks with trypsin, as mentioned in the previous section, and carefully resuspended in Astrocyte Medium. Cells were counted and seeded onto poly-lysine coated 6-well plates (in 1 ml Astrocyte Medium) at a density of 1×10^6 cells/well. These were incubated for another 24 hours and experiments conducted at Day 14.

For experiments shown in Chapter 5, Figure 5.1, B and Table 5.1 were performed on primary astrocyte cultures that were prepared according to the method described by Hamprecht and Loeffler (Hamprecht *et al.* 1985) by seeding 3×10^5 cells/well of 24 well dishes. These cultures were used at day 15 -23.
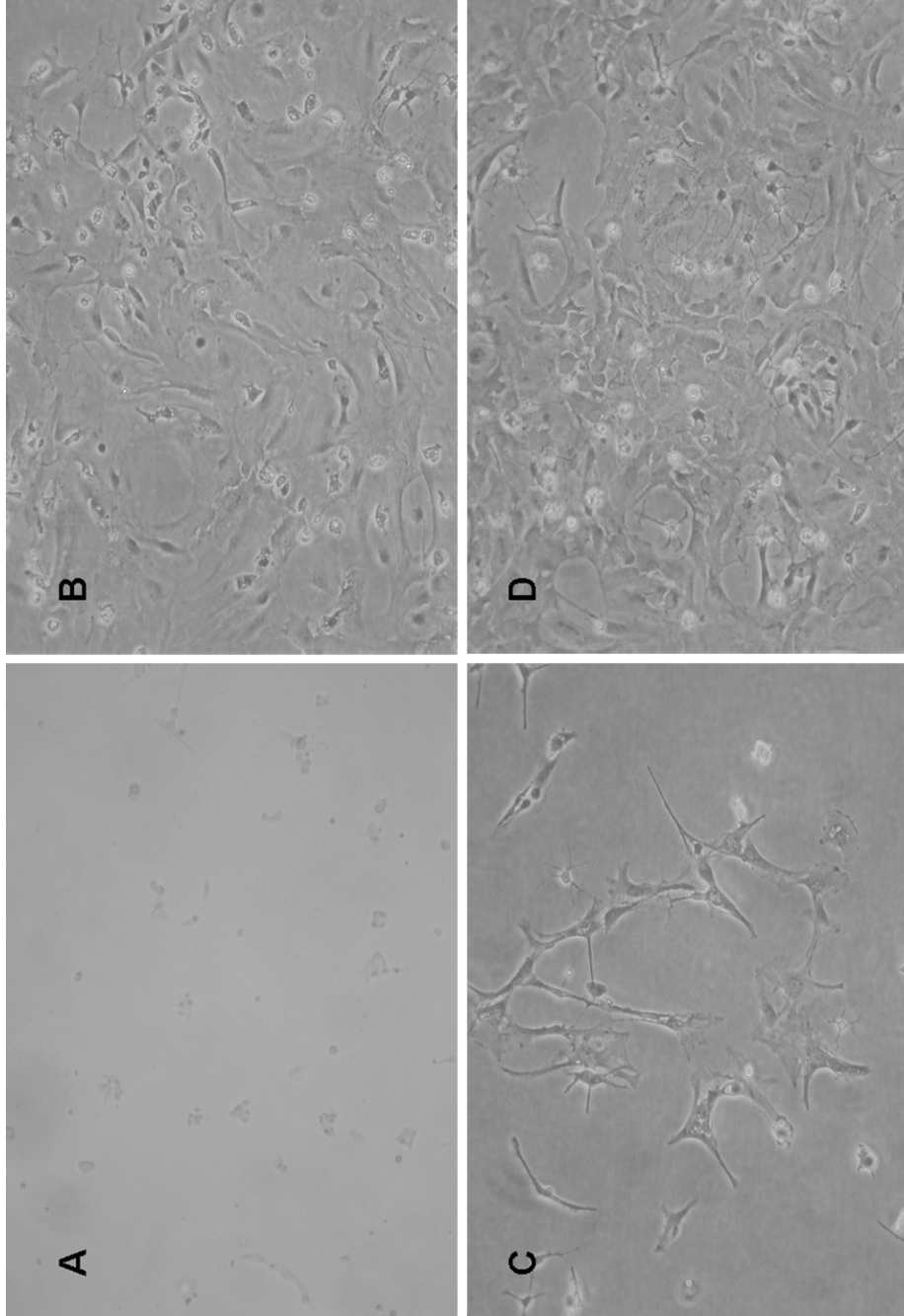
Fig 2.12: Optical Microscopy photographs of astrocyte cultures. A) Day 1, after medium change. B) Day 7, confluent flask before passage of astrocytes. C) Day 8, after cell passage and medium change. D) Day 13, confluent flask before astrocytes plating on 6-well plates.

2.3.3 - Glutathione Release from Astrocytes

At day 14 the media of six-well plates was removed and the cells were washed twice in 1 ml HBSS. 1 ml Minimal Medium (44 mM $NaHCO_3$, 110 mM NaCl, 1.8 mM $CaCl_2$, 5.4 mM $MgSO_4$, 0.92 mM NaH_2PO_4, 5 mM glucose, adjusted with CO_2 to pH 7.4) was added to each well, supplemented with 5 mM sodium glutamate, 5 mM buthionine sulphoxime (BSO) or both. For BSO experiments, cells were incubated in minimal medium containing 5 mM BSO for two hours before and during supplementation with glutamate. After

 stimulation for 15, 45, 120 and 240 minutes, 500 μl of medium was removed and centrifuged to remove cell debris (different wells were used for each timepoint). 250 μl of supernatant was added to the same volume of 30 mM ortho-phosphoric acid, centrifuged at room temperature for 5 minutes at 14000 g to pellet protein and kept at -80 °C for up to three weeks until high performance liquid chromatography (HPLC) determination of GSH. The stability of GSH extracted with 15 mM ortho-phosphoric acid was unaffected by freezing and storage at -80 °C for at least one year.

For experiments on primary cultures on 24 well dishes, cells were washed with 0.5 ml of pre-warmed (37 °C) Minimal Medium, pre-incubated for 2 h in 0.5 ml MM with 100 μM of the γ-glutamyl transpeptidase (γGT)-inhibitor acivicin (Dringen *et al.* 1997) in the absence or the presence of BSO (5 mM), and incubated in the cell incubator with 0.5 ml incubation medium (Minimal Medium with 100 μM acivicin) in the absence or presence of glutamate (5 mM) and/or BSO (5 mM). Extracts of cells and media in 1% (w/v) of sulfosalicylic acid were used to determined the total glutathione content (GSx = amount of GSH plus twice the amount of GSSG). For determination of the content of GSSG in lysates or media the GSH present was derivatised with 2-vinylpyridine as described previously (Minich *et al.* 2006). For all conditions investigated the GSSG values were in the range of the detection limit of the

assay used (<5 % of GSx). Therefore, the GSx amounts determined are considered and addressed as GSH amounts.

2.3.4 - Glutathione Quantification by HPLC

Cellular GSH quantification was determined by reverse-phase HPLC coupled to a dual electrode electrochemical detector as previously described by Riederer *et al.* (Riederer *et al.* 1989). Sample was injected by a Kontron HPLC 360 autosampler (Watford, UK) through a guard column (octadecasilyl; 3 mm x 10 mm) to remove debris, and resolved using a reverse-phase Techsphere octadecasilyl column (particle size 5 μm, 4.6 mm x 250 mm) maintained at 30 ºC by a column heater (Jones Chromatography, Glamorgan, UK). The mobile phase was 15 mM ortho-phosphoric acid prepared in ultra pure water (milli-Q, Milipore) and degassed by a DEG-1033 degasser (Kontron Instruments). The flow rate was maintained at 0.5 ml/min by a Jasco PU-1580 pump (Great Dunmow, UK). Following separation by the column, GSH was electrochemically detected by an ESA 5010 analytical cell containing an upstream and downstream electrode (ESA Analytical, Aylesbury, UK). The upstream electrode screens out molecules with a lower oxidation potential than GSH, while the downstream electrode oxidizes GSH. Current generated by the oxidation of GSH at the downstream electrode was proportional to the amount of GSH and was recorded as a chromatogram on a Thermoseparation Products Chromejet integrator (Anachem, Luton, UK) at a chart speed of 0.25 cm/min. Prior to detection of samples mobile phase was circulated through the column and electrode for 18 hours to allow the electrochemical detector to settle and yield a low baseline current. Electrochemical detection of GSH standards (prepared in 15 mM ortho-phosphoric acid and stored at -70 ºC) at + 0.85 V was linear between 0 and 10 μM. These were injected at regular intervals between samples to monitor

analysis. Figure 2.13 shows a typical chromatogram for a GSH standard (5μM) (A) and a cortical astrocyte sample (B).

2.3.4 - Lactate Dehydrogenase Release

LDH activity was determined by measurement of NADH oxidation at 340 nm in the presence of pyruvate. The assay was performed in 96 well plates as described (Dringen *et al.* 1998). The percentage of LDH released
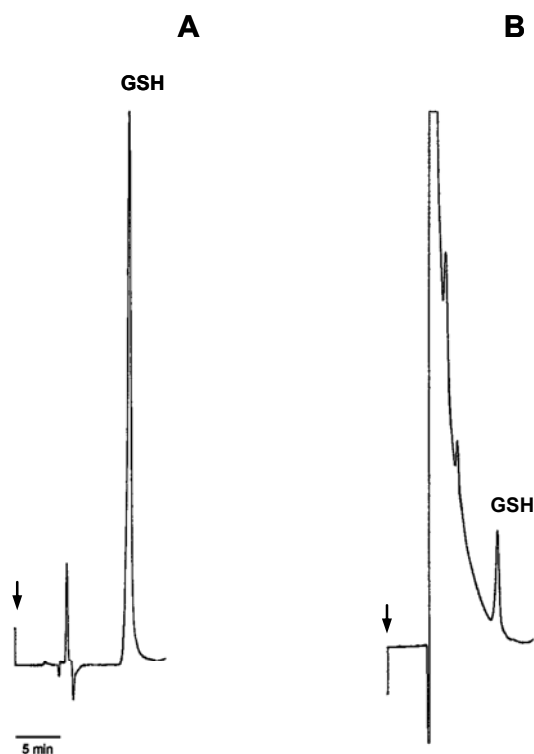
Figure 2.13: Typical GSH chromatograms. A) A 5 μM GSH standard prepared in 15 mM ortho-phosphoric acid and separated by reverse-phase HPLC. GSH was detected electrochemically at +0.85 V. Retention time was 12.9 minutes. B) GSH released from astrocytes. Following incubation with 5 mM Glu for 240 minutes an aliquot of supernatant was added to the same volume of 30 mM ortho-phosphoric acid and GSH quantified by HPLC. Arrows indicate point of injection.

into medium was calculated for three separate preparations (mean ± SEM) by the following: (LDH activity in medium/Total LDH in medium after cell lysis with Triton X-100) x 100.

2.4 - Statistical Analysis

Results are expressed as mean ± SEM values, with n as indicated. As depicted in Figure 2.14, T_{Rise} is the time necessary to reach maximum current amplitude after signal onset from basal current levels. Peak [˙NO] corresponds to maximum current amplitude converted to ˙NO concentration using sensitivity of microsensors. Signal charge values correspond to current integer. Statistical significance for the comparison of two groups was assessed using Student's t-test. Multiple comparisons were made by one-way ANOVA followed by the Bonferroni test unless otherwise stated. Values considered significant were indicated by *, $p < 0.05$ and **, $p < 0.01$. For astrocytes, data expressed as ratios were transformed as previously described (Gegg *et al.* 2003) prior to statistical analysis.
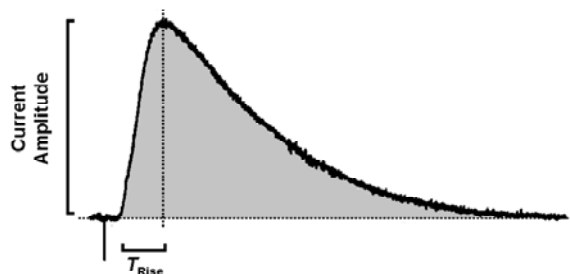
Figure 2.14: Signal parameters. Signals were analyzed to determine T_{Rise} (s), Peak [˙NO] (nM) and signal charge (nC) (grey area) as indicated in text.

CHAPTER 3

REAL-TIME MEASUREMENT OF NITRIC OXIDE IN HIPPOCAMPAL SLICES USING MICROSENSORS

3.1 - Introduction

A number of techniques can be used to measure ˙NO in biological samples, including gas and liquid phase chemiluminescence, electron spin resonance spectroscopy, UV/visible spectroscopy, fluorescence and electrochemistry. Owing to their analytical properties the latter are suitable to measure ˙NO in biological samples due to small electrode size, minimal damage to tissue, sensitivity, selectivity and low manufacturing cost (Ciszewski *et al.* 2003; Taha 2003). This led us to fabricate microsensors to measure ˙NO in rat hippocampal slices by means of electrochemical methods associated with microsensors, particularly amperometry. In this technique a constant potential is applied to the working electrode against a reference electrode, while recording the oxidizing or reducing current arising reaction at the electrode's surface. Amperometry is widely used to investigate changes in concentration of an interest molecule with time because of its response time and sensitivity, and was thus appropriate to investigate the dynamics of ˙NO production in hippocampus. However, because other species can contribute to the analytical signal at the applied potential (+0.9 V) protective films were used to exclude interfering molecules from the microsensor's active surface. As these films provide a limited protection care must be taken in determining the contribution of interferents to the measured signal, and particularly their effect at physiological concentrations.

Glutamate is the principal excitatory neurotransmitter in hippocampus, a brain structure involved in learning and memory formation (Scoville *et al.* 1957; Squire *et al.* 1991), where it mediates a great number of physiological pathways (Kullmann *et al.* 2007). Glutamate receptors, particularly NMDAR, were initially implicated in ˙NO production by Garthwaite and collaborators using cerebellar cells as a model system (Garthwaite *et al.* 1988). Wendland

and co-workers demonstrated that neuronal NOS was expressed in both dendrites and cell bodies of CA1 pyramidal cells (Wendland *et al.* 1994), and ˙NO was latter considered as a retrograde messenger involved in pre- and postsynaptic cells changes (Holscher 1997; Haley 1998; Prast *et al.* 2001) necessary for the maintenance of LTP (Lynch *et al.* 1985; Malinow *et al.* 1990). Given the previous, microsensors were used to measure the rate and pattern of ˙NO change in hippocampus connected with the stimulation of ionotropic glutamate receptors.

3.2 - Calibration and Response Time

Microsensors were modified in a two-step protocol to optimize ˙NO detection. This included the use of NiTMHPP to enhance oxidation currents by electrocatalyzing the oxidation of ˙NO (Malinski *et al.* 1992; Friedemann *et al.* 1996; Pontié *et al.* 1996; Taha 2003), and Nafion® to increase the selectivity towards ˙NO by preventing diffusion of anions like nitrite to the porphyrinic surface (Malinski *et al.* 1992; Friedemann *et al.* 1996). The use of DETA-NO to prepare ˙NO standards provided an easy-to-use calibration protocol, allowing each microsensor to be screened for sensitivity before experiments. This was also used to determine other key analytical properties. From data presented in Chapter 2, recorded oxidation currents were linear up to 1 μM ˙NO (prepared from DETA/NO), at a sensitivity of 679 ± 55 pA/μM ˙NO (n=55) for microsensors with six layers of Nafion®. Sensitivity loss was not statistically significant (p>0.05) from that obtained with microsensors modified with one layer of Nafion®. Detection limit was calculated to be 6 ± 3 nM ˙NO (n=10), while the response time, defined as the time required to obtain 50 % of maximal current change ($T_{50\%}$), was 0.38 ± 0.04 s (n=8). These properties are summarized in Table 3.1.

Table 3.1: Calibration parameters for NiTMHPP- and 1x or 6x Nafion®-modified microsensors.

	1x Nafion®	n	6x Nafion®	n
Sensitivity (pA/µM ˙NO)	855 ± 56	8	679 ± 55 pA/µM ˙NO	55
Detection Limit (nM ˙NO)	-	-	6 ± 3	10
Response Time (s)	-	-	0.38 ± 0.04	8

Values are mean ± SEM, n as indicated.

3.3 - Selectivity Ratios

The use of Nafion® affords a gain of selectivity towards ˙NO, but a major drawback of increasing Nafion® layers is that improving selectivity with additional coatings is usually at the expense of sensitivity, as observed for microsensors coated with one or six layers (Table 3.1) (Friedemann *et al.* 1996). Microsensors were coated with one and six layers of Nafion® and studied for selectivity against major interferents, as presented in Table 3.2. A

Table 3.2: Selectivity ratios for 1x and 6x Nafion®-coated microsensors. Numbers indicate the concentration of interferent (in µM) necessary to reach the same oxidation current as 1µM ˙NO.

Categories	Interferent	Selectivity Ratios			
		1 x Nafion®	n	6 x Nafion®	n
Endogenous molecules	NO_2^-	858:1 ± 88	10	2177:1 ± 319 **	11
	Ascorbic acid	2400:1 ± 354	10	2833:1 ± 683	11
	Dopamine	32:1 ± 3	9	43:1 ± 4 *	11
	5-HT	-	-	140:1 ± 19	10
GluR modulators	Glu	-		>10000	6
	NMDA	-	-	>10000	6
	AMPA	-	-	>10000	6
	AP5	-	-	>10000	6
	NBQX	-	-	>10000	6
NOS substrate and inhibitors	L-arg	-	-	>10000	6
	L-NAME	-	-	>10000	6

Values are mean ± SEM, n as indicated. *, p<0.05; **, p<0.01.

statistically significant 2.5-fold and 1.3-fold increase in selectivity was observed for both nitrite and dopamine, respectively, for microsensors coated with six layers of Nafion®. Selectivity against ascorbic acid also increased, although not significantly. On basis of these experimental results demonstrating a good compromise between gain of selectivity and sensitivity, microsensors used in hippocampal ˙NO monitoring were fabricated with six layers of Nafion®.

3.4 - Measuring Nitric Oxide in Hippocampal Slices

3.4.1 - Glutamate *vs* NMDA

˙NO production dynamics in the CA1 region of hippocampal slices was investigated using distinct glutamatergic agonists (Figure 3.1). Slices were
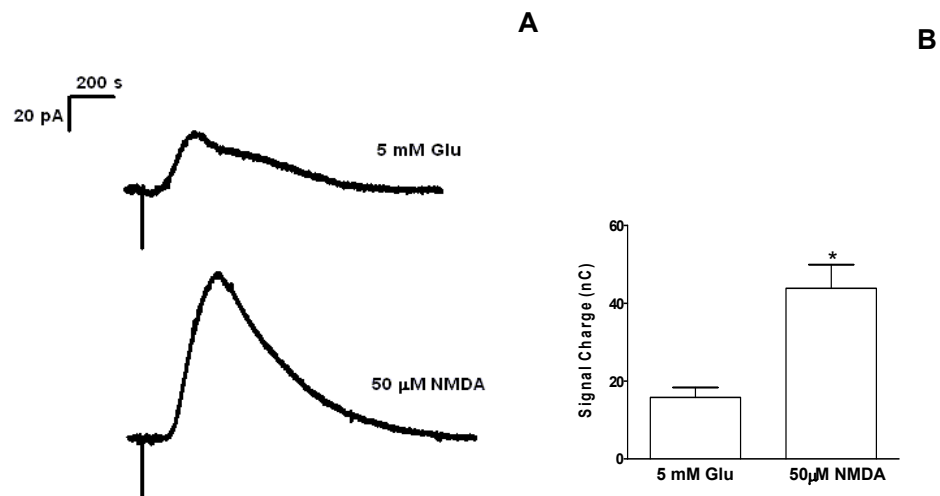
Figure 3.1: Glutamate- *vs* NMDA-mediated ˙NO production. A) Representative amperometric recordings of endogenously-produced ˙NO after perfusion of 5 mM glutamate (upper trace) or 50 μM NMDA (lower trace) for two minutes. B) Statistically significant increase in ˙NO production elicited by 100-times less concentrated NMDA solutions when compared to glutamate (p<0.05). Values obtained were 15.7 ± 2.5 nC for glutamate (n=8) and 43.8 ± 6.1 nC for NMDA (n=20). *, p<0.05.

perfusion-stimulated with 5 mM Glutamate or 50 µM NMDA for two minutes, and changes in ˙NO oxidation current were monitored. Typical signals obtained at +0.9 V reached a maximum oxidation current within minutes and decreased to baseline values typically after 30 minutes, thus reflecting a transient production of ˙NO (Figure 3.1, A). Comparative analysis demonstrated that NMDA induces a significantly higher ˙NO oxidation signal in hippocampal slices when compared to those obtained at a 100-fold higher concentration of glutamate (Figure 3.1, B). Mean results presented in Figure 3.1, B suggest that NMDA is 250 times more potent than glutamate in eliciting a similar change in ˙NO oxidation current, probably due to the absence of an efficient removal mechanism (Gadea *et al.* 2001).

3.4.2 - NMDA Receptor-Mediated Nitric Oxide Production

Despite the good analytical properties of our microsensors towards ˙NO detection (Ledo *et al.* 2002; Ferreira *et al.* 2005), a number of control experiments were also devised to verify that the recorded signals were a result of ˙NO oxidation and not of another endogenous molecule. These included electrochemical and pharmacological controls, as detailed below.

The first control addressed the activation of NMDAR. When perfusing slices with 50 µM NMDA in the presence of 50 µM AP5, a competitive NMDAR, inhibitor, ˙NO oxidation currents were abolished (Figure 3.2, A). AP5 removal followed by a second stimulation elicited a marked ˙NO oxidation current, demonstrating that NMDAR activation was the pathway by which NO was being produced. Polarizing microsensors at +0.55 V was shown to prevent the detection of ˙NO (Chapter 2) while still enabling the oxidation of interferents with lower oxidation potentials. As expected, no signal current was observed in slices at +0.55 V after 50 µM NMDA stimulation (Figure 3.2, B),
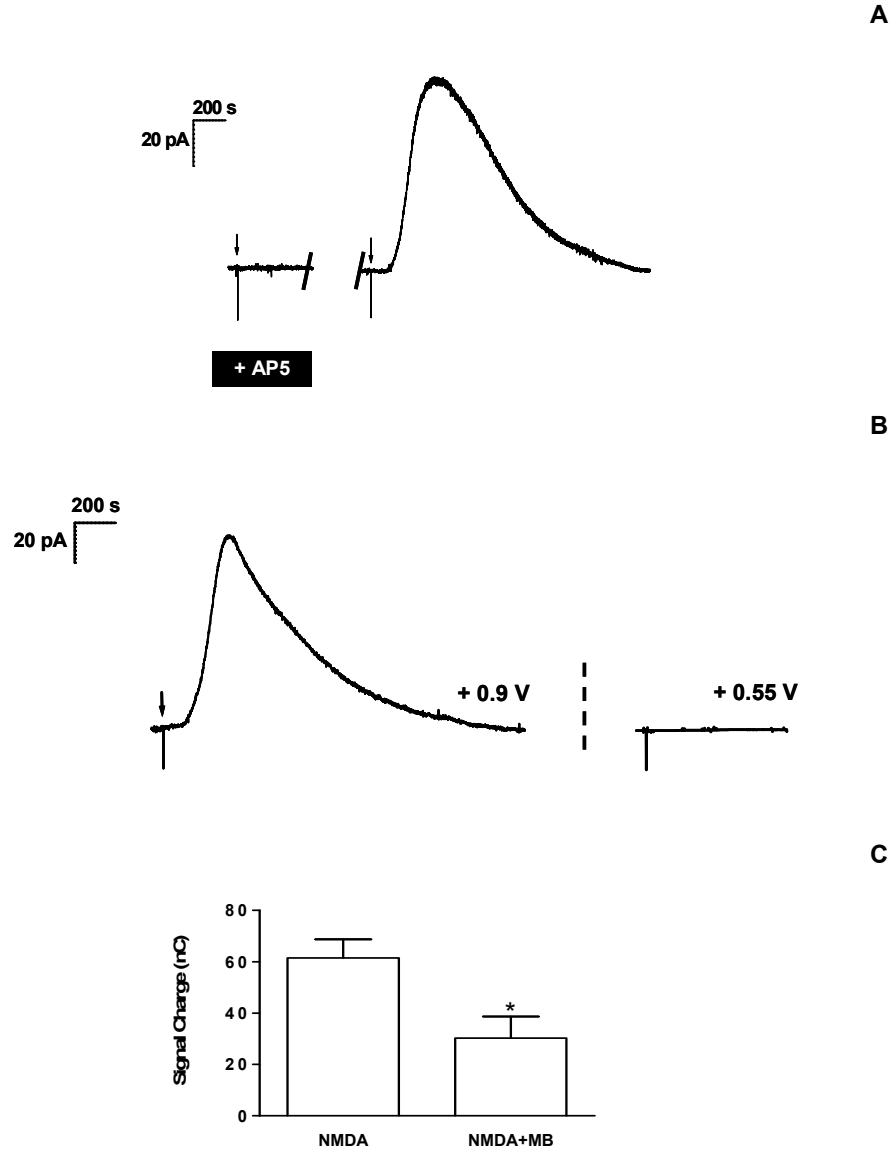
Figure 3.2: Electrochemical and pharmacological controls for 50 μM NMDA-induced production of $^{\bullet}$NO. A) NMDA-induced signal abolishment and recovery (53.3 nC) in the presence and absence of 50 μM AP5, respectively. B) Polarizing microsensors at +0.55 V results in loss of oxidation current, previously detected at +0.9 V. C) Methylene blue inhibits NMDA-induced $^{\bullet}$NO production. Stimulation of hippocampal slices with 50 M NMDA after a 15 minutes incubation with 100 μM MB (NMDA+MB) leads to less intense signals when compared to control slices (NMDA). Values were 61. 4 nC (NMDA, n=5) and 30.2 nC (NMDA+MB, n=4). *, p<0.05.

confirming that the previous signals were not due to the oxidation of endogenously-produced interferents but instead $^\bullet$NO. Additionally, a pharmacological strategy was devised to inhibit nNOS with MB, an heme-oxidant agent known to inhibit nNOS (Griscavage *et al.* 1994) and used in humans to counteract sepsis-related widespread vasodilation and hypotension (Kwok *et al.* 2006). Also, this inhibitor was shown to decrease hippocampal nNOS activity *in vivo* (Volke *et al.* 1999). Incubation of slices with 100 μM MB for 15 minutes resulted in a 50.8% decrease in $^\bullet$NO production following 50 μM NMDA stimulation (n=4) (Figure 3.2, C), when compared to control slices not incubated with MB, further confirming its endogenous production.

NMDA stimulation consisted in perfusing hippocampal slices for two minutes at the required concentration, using aCSF as a carrier. This was modified to address the role of extracellular Ca^{2+} on recorded signals, as nNOS activity is critically dependent on intracellular Ca^{2+} concentration increases. Hence, hippocampal slices were perfused with 50 μM NMDA in the presence and absence of Ca^{2+}. As illustrated in Figure 3.3, the signal evoked by 50 μM NMDA obtained with one slice perfused with aCSF containing 1.5 mM Ca^{2+} (left) was abolished upon perfusion with aCSF without Ca^{2+} (right).
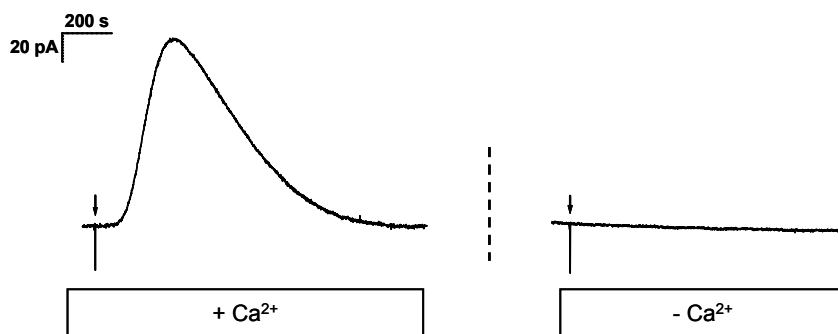
Figure 3.3: Extracellular Ca^{2+} is necessary for $^\bullet$NO production in hippocampal slices. The amperometric $^\bullet$NO signal recorded after 50 μM NMDA stimulation in the presence of Ca^{2+} (left) is abolished after Ca^{2+} removal from the perfusion media (right).

This result demonstrated that measured currents were dependent on extracellular Ca^{2+}, further supporting the detection of endogenously-produced $^{\bullet}$NO in hippocampal slices following NMDA stimulation.

To further investigate $^{\bullet}$NO production elicited by NMDAR we investigated whether hippocampal slices could sustain repeated stimulations with NMDA. Results obtained by perfusing hippocampal slices twice with 50 μM NMDA are depicted in Figure 3.4 (filled bars). A 92.2 % drop in mean signal charge values between first (1st) and second (2nd) stimulation was observed. As this decrease could result from excessive NMDAR activation leading to a high level of endogenous $^{\bullet}$NO, the same experiment was repeated
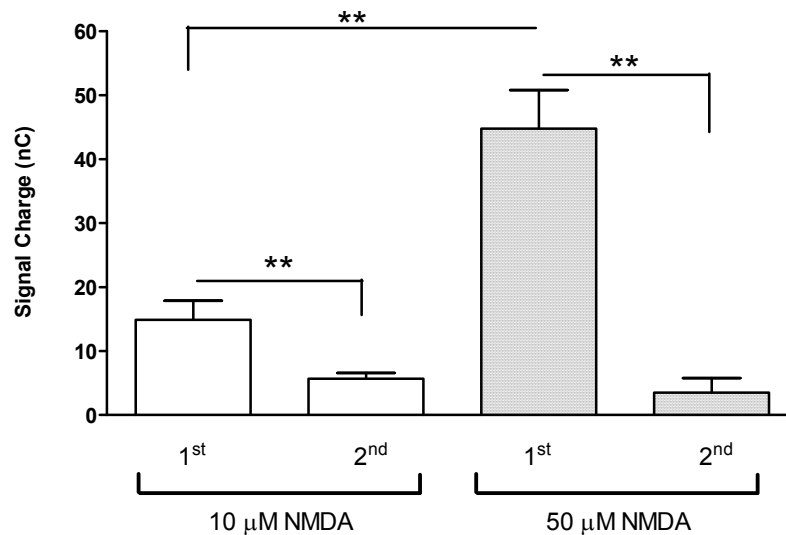
Figure 3.4: $^{\bullet}$NO production upon two consecutive stimulations with NMDA. $^{\bullet}$NO signal charge significantly decreases after a second perfusion of hippocampal slices with 10 μM NMDA (empty bars; from 14.9 ± 2.9, n=15 to 5.6 ± 0.9, n=15) or 50 μM NMDA (filled bars; from 44.7 ± 6.0, n=22 to 3.4 ± 2.2, n=4). A concentration-dependent increase in $^{\bullet}$NO signal charge is observed after stimulation of slices for the first time with 10 or 50 μM NMDA (14.9 ± 2.9 *vs* 41.7 ± 4.8, respectively), but not upon a second stimulation. **, $p < 0.01$

with 10 μM NMDA. Under these conditions, a significant smaller ˙NO production was observed after the first stimulation, and this was accompanied by a 61.9 % drop in signal charge between first and second NMDA stimulations (Figure 3.4, empty bars). Interestingly, second signals were similar to the ones obtained with 50 μM NMDA, suggesting that ˙NO production in slices was only dependent on NMDA concentration for the first stimulation. Accordingly, statistically significant differences occurred between first and second stimulations with the same NMDA concentration and between first stimulations with either 10 or 50 μM NMDA, but not between second ones. Hence, an increase in endogenous ˙NO concentration did not account for signal loss after the second stimulation, suggesting that other mechanisms were responsible for its reduced production.

When perfusing slices five consecutive times with 10 μM NMDA it was observed that, following the abovementioned drop from the first to the second stimulus, current remain approximately constant for the remaining stimulations (Figure 3.5). To ensure that signals were due to ˙NO oxidation an electrochemical control was performed by decreasing the oxidation potential to +0.55 V after the third stimulation. As expected a significant signal loss was observed (fourth stimulation), which was subsequently recovered by re-setting the oxidation potential to +0.9 V (fifth stimulation). Although difficult to reproduce, as a complete loss in ˙NO production was sometimes observed after third or fourth perfusion with NMDA, the ability to sustain up to five consecutive stimulations suggested that slices retained the ability to produce ˙NO via NMDAR stimulation, thus imparting biological relevance to the investigations using a single or double stimulation protocol used along the work.

To further investigate how slices respond to NMDA stimulations in terms of ˙NO production we addressed the question of whether increasing the
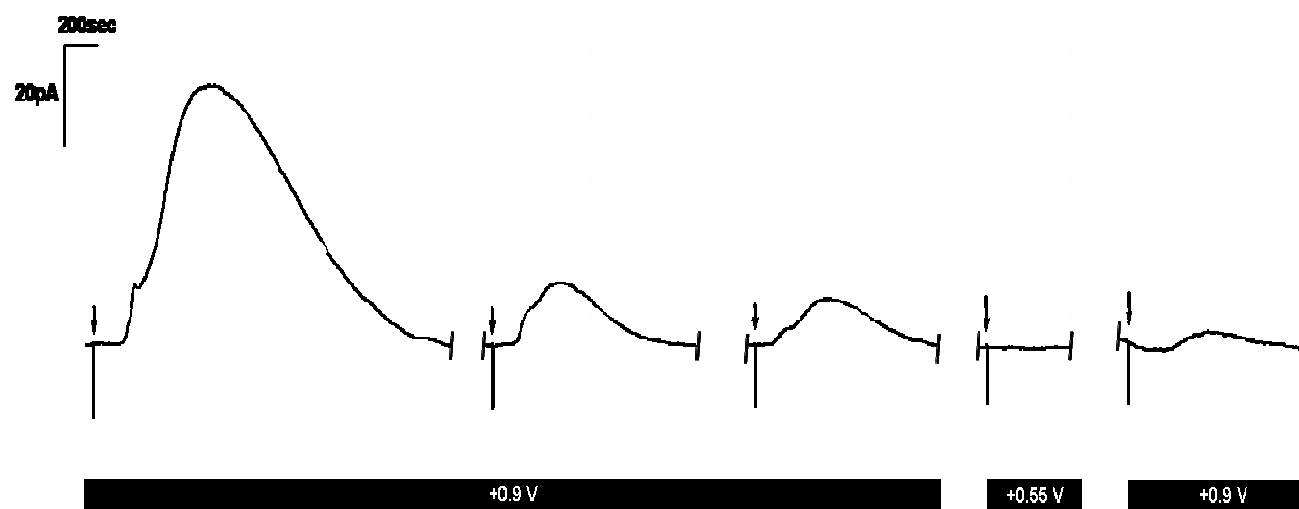
Figure 3.5: Representative amperograms of five consecutive stimulations of hippocampal slices with 10 μM NMDA. A marked decrease in ˙NO oxidation signal is observed between the first and second stimulations. Oxidation at +0.55 V resulted in signal loss, recovered after repolarization at +0.9 V. Signal charge values obtained for signals, from left to right: 49.6, 6.3, 4.9, 0.1 (at +0.55 V) and 1.4 nC.

time period between stimulations could prevent the observed decay in ˙NO signals, as a result of more pronounced tissue recovery under continuous aCSF flow. Slices were stimulated with 10 μM NMDA for two minutes and allowed to rest in the recording chamber for 1 hour, after which a second stimulation with NMDA was performed. As illustrated in Figure 3.6, amperometric signals were similar to the ones previously obtained, and a 75.9 % decay in ˙NO signal charge was observed between 1st and 2nd stimulations, indicating that, after the first stimulation, ˙NO production could not be maintained even after prolonged recovery periods.

Figure 3.6: Decay of ˙NO signal amplitude for long periods of recovery between NMDA stimulations. Slices were stimulated with 10 µM NMDA for two minutes and allowed to recover for one hour before the second stimulation. A second NMDA stimulation did not elicit the same production of endogenous ˙NO, with signal charge decreasing 75.9 % from 16.2 nC to 3.9 nC.

To address the issue of whether ˙NO production was occurring at maximum rate we extended the stimulation period beyond two minutes to compare brief and continuous stimulations. Figure 3.7 details the observed results. When compared to the first two-minute stimulation (Figure 3.7, A), a second stimulation by continuously perfusing slices with 10 μM NMDA

resulted in a more robust signal that decayed linearly over time. A pharmacological control experiment with the NMDAR inhibitor AP5 was performed under conditions of continuous stimulation. The use of 20 μM AP5 on-top of NMDA-induced signal resulted in a faster decay rate (Figure 3.7 B, right), suggesting that NMDAR where still active during current recovery and that a mechanism other than NMDAR inactivation was responsible for complete ˙NO production and decay. The data afforded by AP5 was also used in conjunction with that obtained by differential pulse amperometry (DPA) (Figure 3.7 B, left). This amperometric technique uses several potential steps to eliminate the current due to oxidation of undesired molecules, thus allowing increased selectivity towards the analyte. Experiments were conducted using a three-step protocol, by applying +0.5 V for 1.6 s, +0.7 V for 0.37 s and +0.9 V for 0.03 s, with recordings at every 2 seconds. The signal detected was a result of current subtraction between +0.7 and +0.9 V and therefore only due to ˙NO oxidation, since at +0.7 V the most frequent contaminants in slices were already oxidized. As depicted (Figure 3.7 B, left), after continuous perfusion with 10 μM NMDA a robust signal was observed, which decayed to baseline levels when 100 μM AP5 was perfused on-top, suggesting that NMDAR were still active and mediating nNOS activity. A statistically significant 3-fold increase in signal charge was observed after continuous stimulation of slices with 10 μM NMDA (Figure 3.7, C), indicating that previous two minutes stimulations did not induce ˙NO production at maximal capacity.

3.4.3 - KCl

To extent the results obtained with NMDA and AMPA stimulations we investigated the endogenous ˙NO production following KCl perfusion. KCl induces a strong depolarization of postsynaptic cells and consequently a large
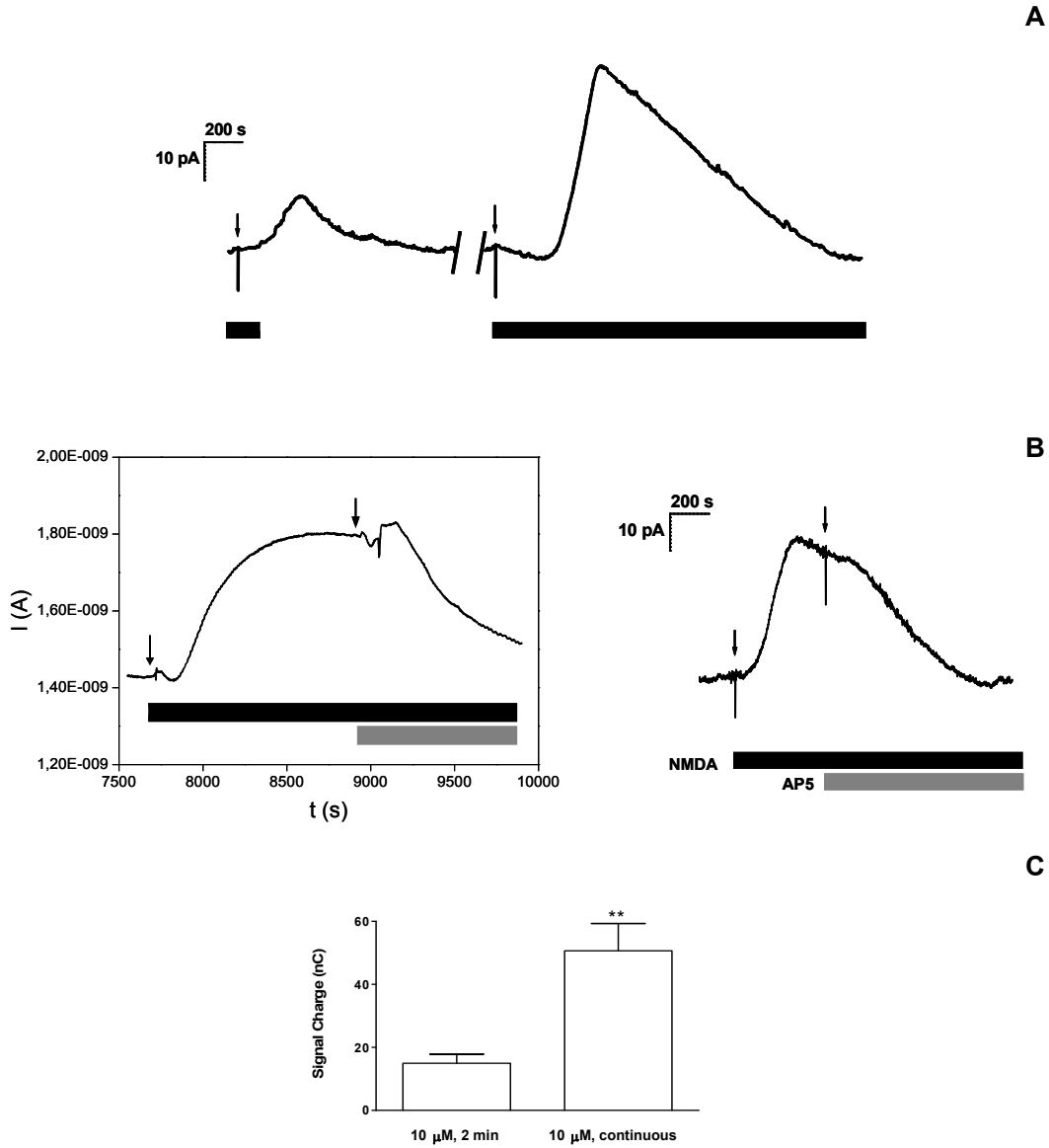
Figure 3.7: Transient *vs* continuous stimulation of hippocampal slices with NMDA. (A) Perfusion of slices with 10 μM NMDA for two minutes results in nNOS activation and ˙NO production. However, a continuous stimulation results in a stronger oxidation signal. (B) When stimulating slices continuously with 10 μM NMDA, on-top perfusion with AP5 (100 μM, left and 20 μM, right) induces an increase in current decay rate. Result were obtained using DPA (left) and amperometry (right). C) Signal charge values obtained after brief stimulations with 10 μM NMDA (14.9 ± 2.9, n=15) are significantly different from the ones observed after continuous perfusion (50.6 ± 8.7, n=6). DPA settings as in text. Dark bars represent NMDA perfusion, while grey correspond to AP5. **, p<0.01.

intracellular Ca^{2+} increase, being largely used to non-specifically stimulate excitable cells. As with NMDA, slices were perfused for two minutes with 100 mM KCl in aCSF without Mg^{2+} while recording ˙NO oxidation currents at +0.9 V. As illustrated in Figure 3.8 (left panel), and as observed after NMDA stimulations, ˙NO production was pronounced after the first perfusion with KCl (Figure 3.8, A) but decayed markedly (85.5 %) upon a second one (Figure 3.8, B and right panel). As our reference electrode was an Ag/AgCl pellet, high KCl solutions could interfere with the electrochemical cell, leading to a false positive result. However, placing the microsensor in the recording chamber in the absence of slice resulted in signal loss in the presence of KCl (Figure 3.8, C), thus indicating that the observed current was a consequence of ˙NO produced endogenously. Surprisingly, KCl perfusion also caused a change in signal profile as compared with previously used agonists. Following an initial
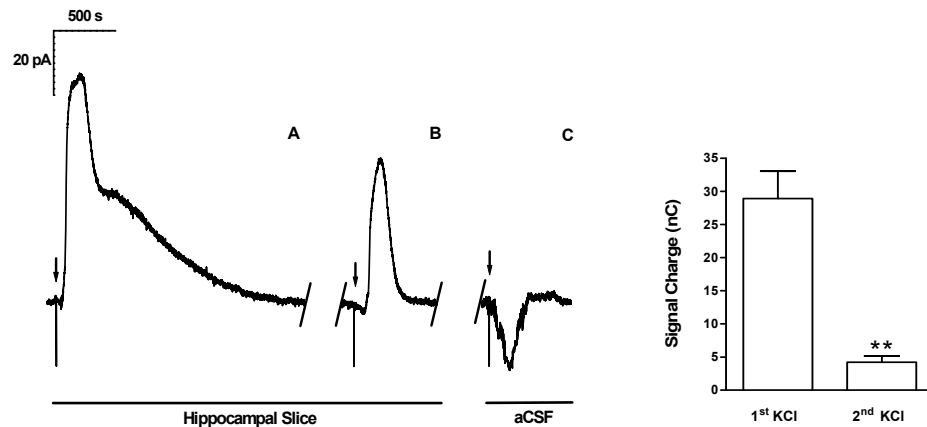
Figure 3.8: KCl perfusion induces depolarization and ˙NO production in hippocampal slices with distinct signal profiles. Left) ˙NO oxidation signal after a first KCl perfusion exhibited a two-phase signal, characterized by a sharp increase but slow decaying profile, with an apparent plateau in between (A). A subsequent stimulation resulted in a sharp increasing and sharp decaying profile, with loss of plateau (B). KCl did not interfere with the electrochemical cell, as signals were lost when perfusing the microsensor in the absence of slice (C). Right) As observed for NMDA, KCl-induced ˙NO production dropped between first (28.9 ± 4.1, n=4) and second (4.2 ± 0.9, n=4) stimulations. ** , p<0.01.

sharp current rise a plateau phase became apparent, after which a slow decay phase was observed (Figure 3.8, A). Furthermore, a second ˙NO oxidation signal was significantly different, and displayed an almost symmetric profile due to a similar increase and decaying phases (Figure 3.8, B). This suggests the occurrence of winding routes for ˙NO production and decay. In this regard, a similar profile was observed for glutamate (Figure 3.1), and further suggested the existence of an endogenous modulatory mechanism regulating ˙NO production.

3.4.4 - L-arginine and L-NAME

L-NAME is a derivative of the NOS substrate L-arg that inhibits NOS activity. Both the substrate and the derivative inhibitor are convenient tools to investigate the production of ˙NO from NOS. After insertion of microsensors in the CA1 region, hippocampal slices were continuously perfused with 500 μM L-arg (Figure 3.9). The expected increase in ˙NO oxidation current reached a plateau shortly after L-arg perfusion (Figure 3.9, I), and simultaneous perfusion with 500 μM L-NAME induced an approximately 50 % drop in signal current (Figure 3.9, II). L-arg was then removed from aCSF while keeping L-NAME perfusion. This induced an additional drop of ˙NO oxidation current to baseline levels (Figure 3.9, III) that remained unchanged when aCSF supplemented with L-NAME was replaced by normal aCSF (Figure 3.9, IV). Although inducing considerable smaller signals when compared to those obtained with glutamate receptors agonists, L-arg perfusion led to ˙NO production after nNOS activation, in turn inhibited by L-NAME. This set of experiments represented a demonstration of the selectivity of ˙NO measurements and the applicability of the methodology to study ˙NO concentration dynamics in slices.
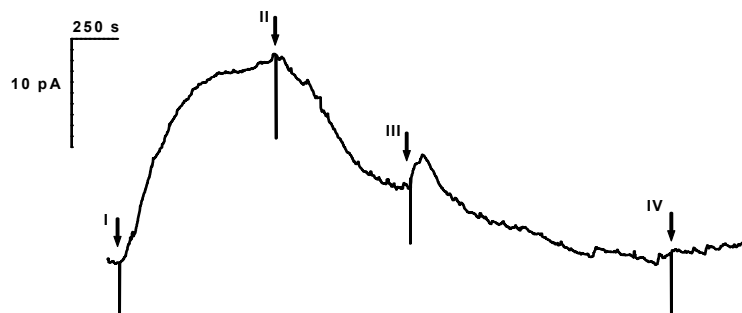
Figure 3.9: Substrate-induced ˙NO production in hippocampal slices. Perfusion of slices with 500 μM L-arg leads to ˙NO production (I), which decreases with the co-administration of 500 μM of the competitive substrate inhibitor L-NAME (II). Removal of L-arg while keeping L-NAME induces a slow but continuous decrease in signal current to baseline levels (III). Removal of L-NAME and perfusion with normal aCSF had no effect on baseline current values (IV).

3.5 - Discussion and Conclusions

3.5.1 - Microsensors

A recent work by Hrbac and co-workers address the attempt to lower the detection limit of porphyrin microsensors while keeping selectivity towards ˙NO (Hrbac *et al.* 2007). Interest in improving this analytical tool arises as this is a suitable methodology to measure the endogenous production of ˙NO in different biological systems (Taha 2003). The fabrication of NiTMHPP-based microsensors and the subsequent evaluation of their analytical properties allowed the use of this technology to follow ˙NO dynamics in hippocampal slices. Microsensors were initially screened by FCV to exclude those

exhibiting resistive characteristics, and therefore considered inadequate for hippocampal experiments. This led us to identify and exclude bad microsensors, a procedure that clearly highlighted the advantage of using this strategy to avoid the use of malfunctioning sensors.

The electroanalytical properties of microsensors supported their use in the real-time measurement of ˙NO. In fact, as shown in Tables 3.1, 3.2 and 3.3 (see below) and as reviewed by others for a great number of porphyrinic as well as other polymer-modified ˙NO sensors (Ciszewski *et al.* 2003), they exhibited (1) high selectivity towards ˙NO; (2) elevated selectivity against major endogenous interferents (Stamford *et al.* 1992), resulting from the choice of a six layers of Nafion® coating; (3) high sensitivity and low detection limit; and finally (4) reduced dimensions, affording their use in neuronal tissue sections with minimal physical damage (Stamford *et al.* 1992). These and other features are summarized in Table 3.3 and agree with reports where NiTMHPP and Nafion® were employed to modify the active surface of

Table 3.3: Comparison of microsensors fabricated in our lab and literature reports.

	Malinski and Taha (1992)[1]	Friedemann *et al.* (1996)[2]		Lab made		Hrbac *et al* (2007)[3]
NiTMHPP	0.5 mM	0.05 mM		0.5 mM		0.4 mM
Nafion Layers	1x	1x, 85 ºC	6x, 200 ºC	1x, 85 ºC	6x, 85 ºC	1x, 45 ºC
Detection Limit (nM)	10	-	76 ± 12	-	5.7 ± 3.1	2-3
Response Time (ms)	< 10	-	350 ± 24	-	380 ± 40	-
Dopamine	3:1	1.3:1	4:1 ± 1	32:1 ± 3	43:1 ± 4	550:1
Ascorbic acid	-	139:1	986:1 ± 13	2400:1 ± 354	2833:1 ± 683	18000:1
Nitrite	20:1	43:1	181:1 ± 28	858:1 ± 88	2177:1 ± 319	600:1

[1]: *(Malinski et al. 1992). Selectivity values are estimates from text.* [2]: *(Friedemann et al. 1996). Selectivity for 1x Nafion® estimated from text; 6x Nafion® as reported by authors.* [3]: *(Hrbac et al. 2007).*

microsensors, particularly those presented by Malinski and Taha (Malinski *et al.* 1992) for NiTMHPP modified with 1 layer of Nafion® and Friedmann *et al.* for NiTMHPP with one and six layers of Nafion® (Friedemann *et al.* 1996).

Differences can be partially explained by distinct surface modification strategies. Friedman and co-workers used a temperature of 200 °C to heat dry a single Nafion®-layered microsensor and suggest that this can increase selectivity (Friedemann *et al.* 1996), an observation supported by others (Brown *et al.* 2003). In turn, we obtained a Nafion® film by drying at a temperature of 80 °C, a fact that could account for the reduced performance in terms of selectivity. However, the concentration of NiTMHPP solution used to modify the active carbon surface seems to be a key aspect, as Hrbac and colleagues demonstrated recently that analytical characteristics are dependent on NiTMHPP monomer concentration (Hrbac *et al.* 2007). In agreement to this, the fact that we used a 10 times more concentrated NiTMHPP solution to coat microsensors when compared to that used by Friedman *et al.*, with a considerable gain in selectivity, suggests this to be a critical aspect in determining microsensors analytical properties. Still, an additional gain in selectivity was observed by Hrbac *et al.* when going from 0.5 mM to 0.4 mM NiTMHPP solutions, suggesting that film formation could be favored at a slightly lower monomer concentration (Hrbac *et al.* 2007). Finally, different manufacturing procedures like cyclic voltammetry settings, number of voltage sweeps and selected reversal potentials may also determine analytical properties and explain observed differences.

3.5.2 - Nitric Oxide Production Dynamics

Microsensors were used to investigate ˙NO dynamics in the CA1 region of hippocampal slices using glutamate as agonist. However, it became clear that glutamate stimulations elicited less intense signals, particularly when

compared to those following slice perfusion with the non-physiological agonist NMDA (Figure 3.1, A). Rapid glutamate clearance from the synaptic cleft is a result of specific glutamate transporter expressed in glial cells (Gadea *et al.* 2001). Since synaptic glutamate concentration is within milimolar range after release of synaptic vesicles, and astrocytes in the CA1 region of hippocampal slices are capable of clearing extracellular glutamate within 1 ms after release (Diamond 2005), this could account for the fact that, despite the use of higher glutamate solutions, ˙NO oxidation signals were significantly lower than the ones elicited by NMDA. Incubation of slices with the nNOS inhibitor MB signals resulted in a decrease in signal charge, confirming the NMDA-induced production of ˙NO (Figure 3.2).

Subsequent studies were set to investigate hippocampal ˙NO production via NMDAR activation. The dependency of nNOS on intracellular Ca^{2+} became apparent after Ca^{2+} removal from the perfusion media (Figure 3.3). The distinctive ˙NO oxidation current observed after stimulation with 50 μM NMDA with 1.5 mM extracellular Ca^{2+} was abolished in the absence of the latter in aCSF. This clearly highlighted the interplay between nNOS and Ca^{2+}, a very effective regulatory mechanism to control the production of ˙NO (Garthwaite *et al.* 1995; Alderton *et al.* 2001). A number of different types of channels are responsible for intracellular Ca^{2+} increases, namely voltage-sensitive Ca^{2+} channels, store-operated channels, and receptor-operated channels such as the NMDAR. Ca^{2+} can mediate a number of cell death pathways and is therefore tightly regulated, being sequestered in organelles, particularly mitochondria and the endoplasmic reticulum (ER), or via one of numerous Ca^{2+}- binding proteins (Hara *et al.* 2007). In this regard, a consequence of Ca^{2+} deregulation in excitotoxic events (Sattler *et al.* 2000; Arundine *et al.* 2003; Weiergraber *et al.* 2007) is the NMDAR-mediated ˙NO production, as it is implicated in neuronal damage (Dawson *et al.* 1991).

As different agonists elicited different ˙NO dynamics, the extent at which ˙NO could be produced in hippocampal slices after stimulation with NMDA was of obvious relevance. This was investigated by perfusing slices with NMDA and allowing ˙NO oxidation current to develop and return to baseline values; once this was achieved, slices were again perfused with NMDA at the same concentration. Results obtained after 10 μM or 50 μM NMDA displayed in Figure 3.4 demonstrate a close relation between ˙NO oxidation currents and NMDA concentration. Saturation of NMDAR is dependent on the conditions by which vesicular glutamate is released, namely the number of vesicles that fuse within the presynaptic membrane and the amount of glutamate molecules per vesicle (Holmes 1995). Obtained results suggest that, for the concentration range under study, receptors within the CA1 region could be activated only to a certain extent. They also demonstrate that ˙NO production could not be maintained in slices after the first stimulation, regardless of stimulus concentration and amount of ˙NO produced. A dependency on NMDA concentration was only apparent for the first stimulation, as a subsequent one elicited ˙NO signals with similar charge values, regardless of agonist concentration. This was further confirmed by increasing the number of stimulations. After consecutive challenges of hippocampal slices with low NMDA concentration (Figure 3.5), only the first signal was shown to be robust: in fact, a pronounced decrease in total signal charge was obtained between the first and second stimulations but not between subsequent ones, that in turn remained within the same range of signal charge. Selectivity studies with microsensors indicate that recorded signals were due to ˙NO oxidation, as lowering the oxidizing potential to values below ˙NO peak oxidation potential abolished signals (Figure 3.5). One possible explanation to the decreased ˙NO production after a first signal could be an insufficient recovery time between NMDA stimuli, despite the use of non toxic NMDA concentrations (Alano *et al.* 2002). This hypothesis was

addressed by increasing the time between NMDA perfusions to one hour after first signal recovery. Representative results, as displayed in Figure 3.6, demonstrated that this was not the case. Hippocampal slices nourished and perfused with normal aCSF for one hour were still incapable of restoring previous ˙NO production peak levels, as diminished ˙NO signals were still recorded one hour after the first NMDA perfusion under conditions of standard glucose, Ca^{2+} concentration and physiological pH. Hence, insufficient recovery after NMDA perfusion was ruled out to explain decreased ˙NO signals. Hence, evidences suggest the activation of regulatory mechanisms within slices that critically determine ˙NO dynamics following activation of NMDAR.

A relevant issue was whether ˙NO was being produced at maximal rate in hippocampal slices. If this was the case, a reduced ˙NO production after an initial stimulation could be explained, amongst others, by nNOS inhibition and/or substrate depletion. This was addressed by perfusing slices continuously with NMDA. Results depicted in Figure 3.7 with 10 µM NMDA clearly suggest that hippocampal slices do not produce ˙NO at maximal capacity after a brief (two minutes) stimulation with NMDA, as a subsequent continuous perfusion resulted in a more pronounced ˙NO production (as observed in A and B). ˙NO levels were significantly higher when NMDA was perfused continuously and notably appeared to decay linearly over time, a feature not observed after previous brief stimulations (Figure 3.1 and Figure 3.7). The same results were obtained by DPA, a different electrochemical technique (Figure 3.8), suggesting further that NMDAR were still active. Altogether, results indicated that nNOS activity could be modulated in hippocampal slices, and suggested a mechanism rather than nNOS inhibition or L-arg depletion to explain decreased ˙NO levels with repeated NMDA stimulations.

NMDAR desensitization could result in a diminished Ca^{2+} influx and reduced nNOS activation in slices (Nakamichi *et al.* 2005). NMDAR

desensitization and nNOS inactivation were further discarded as the mechanism(s) responsible for decreased ˙NO production after a second stimulation because AP5, a NMDAR inhibitor, was able to increase ˙NO decay when perfused on-top of ˙NO signals elicited by continuous NMDA perfusion (Figure 3.7). Both NMDAR and nNOS were shown to be active and responsive to perfused antagonist by means of distinct electrochemical techniques, suggesting that they would not account for the previous decay in ˙NO production. This stimulation protocol also excluded nNOS substrate depletion as the reason why second stimulations result in diminished ˙NO levels: if this was the case, continuous NMDA perfusions would not elicit such robust signals, as cells would run out of L-arg (Figure 3.7). It could be argued that neuronal cells would increase L-arg uptake only during continuous NMDA perfusion but not after two-minute stimulations, thus diminishing intracellular L-arg and ˙NO production upon a second NMDA perfusion. However, this possibility is difficult to accept, as 1 h in between stimulations (Figure 3.6) would allow neurons to restore L-arg levels (Cossenza *et al.* 2000). Cells that express eNOS were shown to have an intracellular L-arg available to L-arg-requiring enzymes that is not freely exchangeable with extracellular L-arg (Closs *et al.* 2000), and this was also reported in the neuronal cell line CAD cells (Bae *et al.* 2005). Neuronal ˙NO production was shown to depend largely on extracellular L-arg on these cells, but their restrict intracellular L-arg pool supplies the substrate for ˙NO production in the absence of extracellular L-arg (Bae *et al.* 2005). Further supporting the notion that substrate depletion is not responsible for ˙NO decayed production, K_M values for L-arg calculated *in vitro* for purified NOS were between 1 and 10 μM, one to two orders of magnitude below the intracellular concentrations of the amino acid measured in macrophages and endothelial cells (100-800 μM) (Forstermann *et al.* 1994; McDonald *et al.* 1997). L-arg is supplied to neurons by astrocytes (Kharazia *et al.* 1997) and hippocampal neurons in slices would rely on these cells to

maintain nNOS-saturating L-arg levels (Grima *et al.* 1997), possibly after NMDAR activation (Cossenza *et al.* 2006). As a final note, experiments with 500 μM L-arg demonstrated that nNOS could be activated by its substrate (as verified with 500 μM L-NAME) (Figure 3.9) but that L-arg supplementation had a small (although detectable) effect on ˙NO production when compared to NMDA or glutamate, as indicated by amplitude of signals (Figure 3.1).

˙NO regulates a number of events in neuronal cells that may underlie the pattern of stimulation observed. Mitochondria respiratory chain can be inhibited by ˙NO leading to the formation of ROS (Brown *et al.* 1994; Cleeter *et al.* 1994; Stewart *et al.* 2002), and nNOS itself can become uncoupled and produce $O_2^{˙-}$ when L-arg levels are low (Pou *et al.* 1992). Both events can lead to increased levels of $ONOO^-$ following the reaction of ˙NO with $O_2^{˙-}$ (Beckman *et al.* 1996), and this could result in the reported decrease in ˙NO oxidation signals. That is, following the first stimulation a more oxidized cellular environment, encompassing the production of $O_2^{˙-}$, would prevent ˙NO from diffusing extracellularly and rise to the initially observed concentration. Glutamatergic ionotropic receptors can also regulate nNOS activity by means of NMDAR, as demonstrated in cerebellar granule cells, being Ca^{2+} an important signal transduction molecule involved in this regulatory process (Baader *et al.* 1996). In this regard, nNOS is constitutively phosphorylated and NMDA receptor activation decreases this level of phosphorylation (enhancing NOS activity) by a mechanism that is blocked specifically by NMDAR antagonists in rat cortical neurons (Rameau *et al.* 2003). However, protein kinase C and Ca^{2+}-dependent enzymes like Ca^{2+}/calmodulin (CaM)-dependent protein kinases I an II (CaMKI and CaMKII) can counteract this NMDAR-mediated nNOS activation by increasing phosphorylation nNOS on several serine residues, consequently decreasing ˙NO production (Nakane *et al.* 1991; Komeima *et al.* 2000; Song *et al.* 2004). ˙NO itself can feedback-regulate

NOS, decreasing its activity (Assreuy *et al.* 1993; Vickroy *et al.* 1995), and downregulate NMDAR activity by means of S-nitrosation of thiol group(s) located on the receptor's redox modulatory site (Lipton *et al.* 1993). ˙NO-related species like nitroxyl anion (NO⁻) also bind to the NR2A subunit of the NMDAR to limit excessive Ca^{2+} influx, in what can be regard as a neuroprotective mechanism against excitotoxic insults. (Kim *et al.* 1999). More recently Tiso *et al.* demonstrated that the C-terminal tail of nNOS exerts multifaceted effects on the enzyme's catalytic activity (Tiso *et al.* 2007), providing new insights into novel mechanisms that regulate nNOS catalysis. Therefore, a number of mechanism can account to the observed decrease in ˙NO production.

Continuous NMDA stimulation of hippocampal slices can be considered as a model for studying the excitotoxic production of ˙NO following excessive NMDAR activation (Stewart *et al.* 2002) that leads to oxidative stress and cellular degeneration in a number of pathologies (Coyle *et al.* 1993). In fact, the elevated ˙NO oxidation currents recorded suggest that a number of cellular pathways can become impaired, particularly mitochondria (Brown *et al.* 1994; Cleeter *et al.* 1994). Rameau demonstrated that treatment of neurons with 5 µM glutamate stimulated CaMKII phosphorylation of nNOS at serine 847 (thus decreasing its activity), whereas excitotoxic concentrations of glutamate (100-500 µM) induced serine 847 dephosphorylation by protein phosphatase 1 (presumably increasing ˙NO levels) (Rameau *et al.* 2004). The observation that a distinct decay in ˙NO signals occurred after continuous stimulation with NMDA supports the possibility that cellular impairment (but not physiological mechanisms) lead to ˙NO decay to baseline levels. This could be assessed by determining ROS formation in hippocampal slices and the extent of necrotic or apoptotic cell death following prolonged NMDA stimulations, thus providing relevant insights on ˙NO effects during these events.

Subsequent experiments using KCl as a general depolarizing agent in hippocampal slices (Youssef *et al.* 2006) provided an additional tool in addressing $^\bullet$NO dynamics. Results obtained after perfusion of 100 mM KCl for two minutes were similar to NMDA ones, as a marked drop in $^\bullet$NO oxidation currents was observed upon a second stimulation, but signal kinetics were clearly distinct (Figure 3.8). The fact that a plateau phase could be identified when using KCl (Youssef *et al.* 2006), and that this profile was lost upon a second stimulation, suggests the activation of different cellular pathways by KCl. Remarkably, this dynamic could be a result of Ca^{2+} accumulation by mitochondria, due to its ability to sequester and regulate intracellular Ca^{2+} concentration, as suggested by Baron and Thayer (Baron *et al.* 1997). In this report, intracellular free Ca^{2+} concentration ($[Ca^{2+}]_i$) was monitored by indo-1-based microfluorimetry in single dorsal root ganglion neurons after 50 mM KCl perfusion. $[Ca^{2+}]_i$ increased transiently upon depolarization with KCl, but a plateau phase was observed during recovery to basal values due to mitochondria-mediated $[Ca^{2+}]_i$ buffering. Using an inhibitor of mitochondrial Na^+/Ca^{2+} exchange the authors demonstrated that Ca^{2+} accumulates in mitochondria during depolarization and is latter released to the cytoplasm slowly. This afforded an equilibrium between mitochondrial Ca^{2+} release and Ca^{2+} extrusion from the cytoplasm, which lasted while mitochondrial Ca^{2+} was not depleted. The kinetics of our KCl-induced $^\bullet$NO amperogram followed a similar profile (Figure 3.8), suggesting that mitochondria could be implicated in Ca^{2+} regulation and modulation of $^\bullet$NO production in hippocampal slices. Simultaneous recordings of $[Ca^{2+}]i$ changes and $^\bullet$NO production could help clarify this issue, and provide relevant clues on the role of mitochondria regulation of hippocampal $^\bullet$NO production.

In summary, ˙NO production in hippocampal slices assessed in real-time by ˙NO selective microsensors was shown to be transient and dependent on a number of factors. While the use of the physiological agonist glutamate required the use of elevated concentrations, the efficacy of NMDA perfusions in eliciting ˙NO production reflected the NMDAR-nNOS coupling in hippocampus. Consecutive and prolonged NMDA stimulations suggested that ˙NO dynamics is determined by effective regulatory pathways. Additionally, agents such KCl can lead to ˙NO increases in hippocampal slices and provide insights on pathways that condition ˙NO production, owing to the observed differences in ˙NO signal profiles. Last, the prolonged stimulation protocol with NMDA might constitute an adequate model to investigate ˙NO production during excitotoxic events, mimicking the overactivation of NMDAR.

CHAPTER **4**

GLUTAMATE IONOTROPIC RECEPTORS - MEDIATED PRODUCTION OF NITRIC OXIDE

4.1 - Introduction

In the hippocampus, $\cdot$NO has been implicated in the pathways leading to spatial memory formation and LTP by means of glutamatergic receptors activation (Morris *et al.* 1982; O'Dell *et al.* 1991; Schuman *et al.* 1991; Bliss *et al.* 1993). The NMDAR has been in the center of most studies (Garthwaite *et al.* 1995; Christopherson *et al.* 1999; Rameau *et al.* 2003), due to its permeability to Ca^{2+} and its role in $\cdot$NO production (Sattler *et al.* 1999). However, it has been claimed that glutamate-dependent $\cdot$NO production and ensued cellular events can be mediated by pathways other than NMDAR activation, while still requiring a rise in postsynaptic intracellular Ca^{2+} concentrations (Grover *et al.* 1990). The activation of voltage-gated calcium channels (VGCC) is one candidate pathway to explain Ca^{2+} rise (Grover *et al.* 1990; Freir *et al.* 2003); alternatively, this can occur after AMPAR activation (Zamanillo *et al.* 1999). AMPAR have been implicated in both NMDA-mediated neuronal plasticity and LTP (Shi *et al.* 1999) as well as in NMDA-independent events. Concerning the later, a number of studies indicated that Ca^{2+}-dependent synaptic plasticity could be critically dependent on the entrance mechanism of Ca^{2+} in the postsynaptic cell (*e.g.* VGCC) and/or on AMPAR subunit composition (Chen *et al.* 1998; Chittajallu *et al.* 1998; Zamanillo *et al.* 1999). GluR2-lacking Ca^{2+}-permeable AMPAR have long been described as occurring throughout the hippocampus (Isa *et al.* 1996; Gryder *et al.* 2005), and in recent years an increasing number of reports have implicated these receptors in plasticity events in rat hippocampal slices (Ge *et al.* 2006; Plant *et al.* 2006). The expression of Ca^{2+}-permeable AMPAR might change dramatically in non-physiological circumstances, as demonstrated after global ischemia, where pronounced and cell-specific reduction occurred in GluR2 in

CA1 vulnerable neurons, strikingly with no significant changes in AMPAR subunit GluR1 at CA1, CA3 or dentate gyrus (Opitz *et al.* 2000).

Considering the abovementioned controversial scenario on the role of NMDAR and AMPAR in connection with ˙NO-dependent pathways the contribution of AMPAR in endogenous ˙NO production in hippocampal slices was investigated.

4.2 - AMPA-Receptor Dependent Nitric Oxide Production

To investigate the effect of AMPAR activation on endogenous ˙NO levels we perfused hippocampal slices with 50 μM AMPA in Mg^{2+}-supplemented aCSF. As AMPA perfusion was expected to lead to cellular depolarization, recorded signals could arise via release of vesicular glutamate and activation of pos-synaptic NMDAR. Hence, and despite the fact that glutamate clearance from the synaptic cleft is a highly efficient mechanism (Diamond 2005), experiments were performed in the presence of the 25 μM AP5 to rule out their possible contribution in the recorded signals, as this concentration was shown to inhibit NMDAR in slices (Ledo *et al.* 2005).

Perfusion of slices with 50 μM AMPA for two minutes in AP5-supplemented aCSF afforded a marked production of ˙NO, as depicted in Figure 4.1 (panel A, left). As for NMDA, a number of experiments were conducted to ensure that recorded signals resulted from ˙NO production and ensuing oxidation at +0.9 V. In order to further determine that NMDAR were not contributing to AMPA-elicited ˙NO signals, slices were perfused with a higher concentration of AMPA with either 25 or 100 μM AP5. As depicted in Figure 4.1 (panel A, right), no significant differences were observed in ˙NO production when slices were stimulated with 175 μM AMPA in the presence of

A
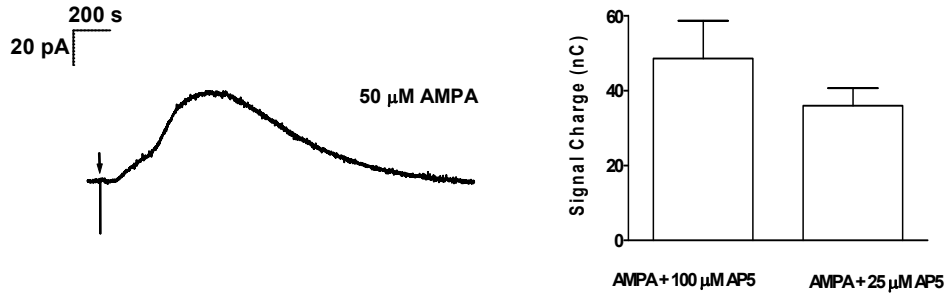
B
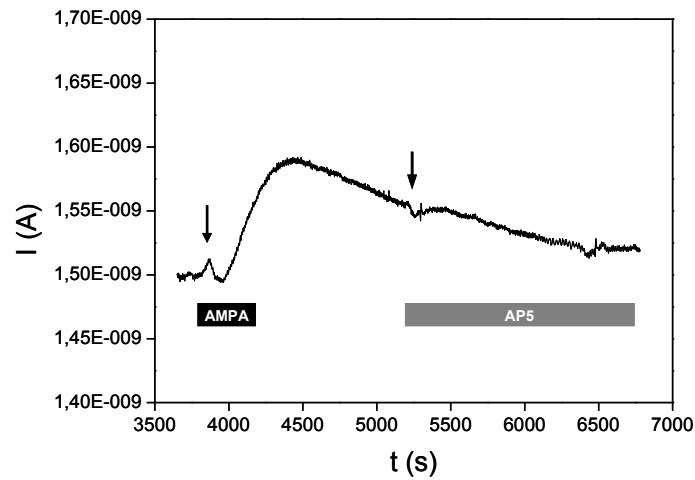
Figure 4.1: AMPA elicits ·NO production in hippocampal slices independently of NMDAR activation. A) In the presence of 25 μM AP5, 50 μM AMPA elicits a marked production of ·NO (left). No differences were observed in AMPA-elicited ·NO production by increasing the concentration of the NMDAR inhibitor AP5 to 100 μM, even with 175 μM AMPA stimulations (right, p>0.05). B) DPA amperogram was after a two minutes stimulation with 10 μM AMPA. Signal decay rate remained unchanged with 100 μM AP5 perfusion (↓). Black bar represents AMPA perfusion, while grey corresponds to AP5. DPA settings as in text.

either 25 or 100 μM AP5. Still, AP5 was used in conjunction with DPA to further clarify the role of NMDAR on AMPA-induced ˙NO production. As depicted in Figure 4.1 (B), a distinctive signal was obtained after a two-minutes perfusion of slices with 10 μM AMPA. No change in ˙NO oxidation current elicited by 10 μM AMPA was observed after on-top perfusion of 100 μM AP5, demonstrating that NMDAR activation does not account for the recorded signal, and supporting the notion that AMPAR activation can lead to a marked production of ˙NO in hippocampal slices.

Similarly to what was previously observed for NMDA and AP5, a pharmacological control with the selective AMPAR antagonist NBQX demonstrated that activation of this subtype of glutamatergic receptors, and not another pathway, was responsible for recorded signals with AMPA. Figure 4.2 highlights the results obtained using a two-stimulation protocol. No oxidation current was observed when slices were perfused with 50 μM NBQX for 15 minutes and stimulated with 10 μM AMPA for two minutes (Figure 4.2, A). However, ˙NO oxidation signal was again observed after NBQX removal and an additional stimulation with AMPA. In order to confirm that signals were a result of ˙NO production and oxidation after AMPAR activation, experiments were conducted at +0.55 V. Recordings at low potential resulted in the abolishment of oxidation current following slices stimulation with 50 μM AMPA (Figure 4.2, B), suggesting that ˙NO and not other endogenous molecules were responsible for recorded signals. A pharmacological control designed to inhibit nNOS activity was performed, using MB as an inhibitor (similarly to what was previously presented for NMDAR in Chapter 3). Incubation of hippocampal slices for 15 minutes with 100 μM MB afforded a 55.7 % reduction (n=4) in ˙NO oxidation current (Figure 4.2, C), confirming its production by nNOS as a result of AMPAR activation.

A

B

C
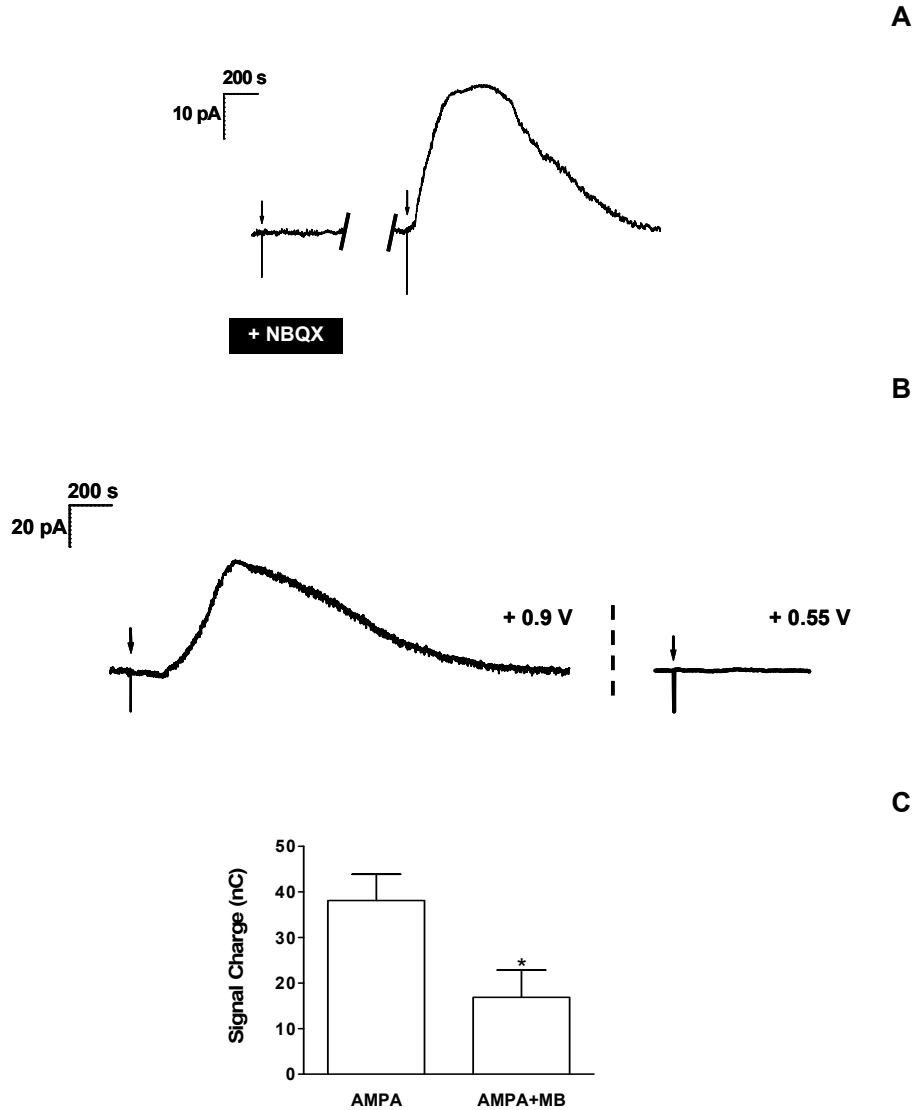
Figure 4.2: Control experiments for AMPA-dependent production of ˙NO. A) Perfusion of slices with 10 μM AMPA for two minutes in the presence of 50 μM of the AMPAR antagonist NBQX abolishes oxidation current. Antagonist removal restores ˙NO signals upon a second stimulation (25.2 nC). B) Perfusion of hippocampal slices with 50 μM AMPA for two minutes results in a robust ˙NO signal at +0.9 V, lost when the oxidizing potential is decrease to +0.55 V. C) MB inhibits ˙NO production elicited by AMPA. After incubation of slices with 100 μM MB for 15 minutes, perfusion of 50 μM AMPA for two minutes (AMPA+MB, 16.9 ±5.9, n=4) results in a 55.7 % reduction in ˙NO signal charge when compared to control (AMPA, 38.1 ± 5.7, n= 6). *, $p < 0.05$

4.3 - Nitric Oxide Production and Stimulus Strength

Following initial reports linking the production of ˙NO with NMDA-receptor activation (Garthwaite *et al.* 1995) a quantitative analysis in terms of ˙NO concentration dynamics along the trisynaptic loop in hippocampus has only recently been achieved (Ledo *et al.* 2005). Here, and in order to compare with AMPAR-derived ˙NO production, we established a quantitative relationship between NMDA stimulus strength and endogenous ˙NO profiles measured in a selective and real-time fashion by means of microsensors inserted in the CA1 region of hippocampal slices. Results obtained after slice perfusion with 5, 10, 25, 50, 100 and 175 μM NMDA showed a concentration-dependent production of ˙NO, that reached a plateau phase at 50 μM NMDA (Figure 4.3, closed circles). ˙NO peak concentrations (Peak [˙NO], Figure 4.2, B) remained in the nM range and reached a maximum of 150 nM ˙NO (Figure 4.3, closed circles). Signal charge values obtained for individual NMDA concentrations were also calculated and are displayed in Table 4.1. The half maximal effective concentration (EC50) value for NMDA stimulation was calculated to be 17.66 μM (R^2=0.999) in our slice model, following Boltzmann sigmoidal fitting of values presented in Table 4.1 and Figure 4.3 (closed circles).

In order to further study ˙NO production via AMPAR, hippocampal slices were stimulated with increasing concentrations of AMPA. This production was evident after 10, 50 and 175 μM AMPA perfusion, as previously mentioned, and even when slices were stimulated with concentrations as low as 5 μM AMPA (Figure 4.3, open circles). As presented in Table 4.1 and Figure 4.3, AMPA stimulation reached a plateau for

concentrations higher than 50 μM, with an EC50 value of 23.12μM (R^2=0.977) after Boltzmann sigmoidal fit of data.

Contrary to what was observed with NMDA, 5 and 10 µM AMPA elicited a similar extracellular ˙NO increase. Interestingly, not only the EC50 calculated for AMPA was higher than the one obtained for NMDA, but also a lower ˙NO peak concentration was obtained with AMPA when compared to the same concentration of NMDA (Figure 4.3). ˙NO increase in the extracellular medium is also a distinctive aspect between NMDA- and AMPA-dependent
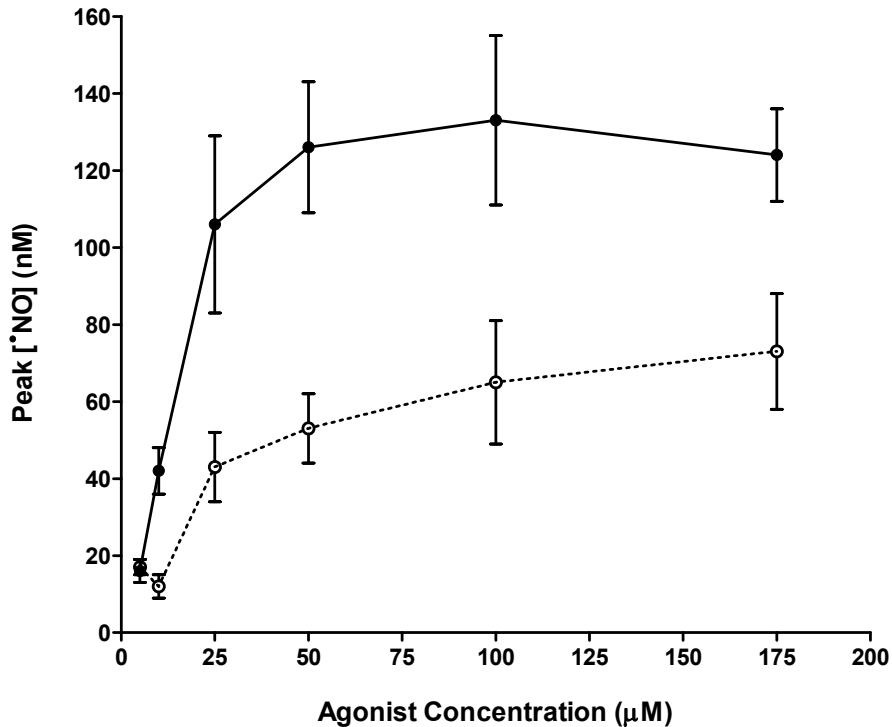
Figure 4.3: Dose-response curve for NMDA- and AMPA-induced ˙NO production. Slices were perfused with NMDA (●) or AMPA (○) at indicated concentrations for two minutes. ˙NO concentration was calculated as indicated in Figure 4.1 and Table 4.1. ˙NO production reaches a plateau with either NMDA or AMPA with EC50 values of 17.66 µM and 23.12 µM after Boltzmann Sigmoidal fitting, respectively.

˙NO production. When calculating the time necessary to reach maximum ˙NO oxidation current after signal onset (T_{Rise}, as presented in Figure 2.14) for both AMPA and NMDA (above 25 µM), it became evident that AMPA-dependent ˙NO production was 1.5-2.5 slower when compared with that dependent on NMDA (Table 4.1). This suggests that ˙NO production after AMPAR activation is slower and less effective, suggesting distinct contribution and involvement of these receptors in ˙NO production.

4.4 - Selective Inhibition of Glutamate Receptors

The activation of NMDA and AMPA receptors by the physiological agonist glutamate is an interrelated process and ˙NO plays a regulatory role in the pathways downstream the activation of these glutamate ionotropic receptors (Rameau *et al.* 2007; Sossa *et al.* 2007). We therefore investigated

Table 4.1: Signal charge, T_{Rise} and Peak [˙NO] values obtained after hippocampal slices stimulation with NMDA and AMPA.

Agonist	Concentration (µM)	Signal Charge (nC, mean ± SEM)	T_{Rise} (s, mean ± SEM)	Peak [˙NO] (nM)	n
NMDA					
	5	5.7 ± 1.2	257.3 ± 30.1	15.8 ± 2.8	8
	10	13.7 ± 1.9	279.4 ± 17.5	42.5 ± 6.2	19
	25	33.8 ± 6.1	225.6 ± 12.3	106.4 ± 23.3	10
	50	44.8 ± 6.0	252.4 ± 7.6	126.2 ± 16.9	22
	100	48.2 ± 6.3	211.8 ± 14.5	133.3 ± 21.5	9
	175	48.9 ± 5.1	193.8 ± 13.0	124.1 ± 12.1	7
AMPA					
	5	5.1 ± 1.1	305.1 ± 38.3	16.6 ± 2.4	7
	10	4.0 ± 1.1	269.6 ± 34.6	12.3 ± 3.3 **	6
	25	19.7 ± 4.8	320.1 ± 44.6 *	43.3 ± 8.7 **	5
	50	33.1 ± 4.4	438.0 ± 43.6 **	53.4 ± 9.2 **	9
	100	29.4 ± 5.9	309.2 ± 40.3 **	64.6 ± 15.8 **	5
	175	35.9 ± 4.7	446.1 ± 39.8 **	73.1 ± 14.6 **	5

*AMPA T_{Rise} and Peak [˙NO] values significantly different at *, p<0.05 and **, p<0.01 when compared with corresponding NMDA concentrations.*

if AMPA-dependent $^{\bullet}$NO production could be observed in the presence of glutamate by selectively inhibiting glutamate receptors, as a mean of determining the role of NMDAR and AMPAR on $^{\bullet}$NO production following glutamate stimulation. As depicted in Figure 4.4, hippocampal slices were perfused for 15 minutes with aCSF supplemented with 25 μM AP5 (an inhibitor of NMDAR), 25 μM NBQX (an inhibitor of AMPA/Kainate receptors) and a combination of both. 5 mM glutamate prepared in the perfusion media was applied for two minutes, and signals recorded as previously. As expected, glutamate induced the production of $^{\bullet}$NO, with an average $^{\bullet}$NO peak concentration of 69.5 ± 7.3 nM (n=4) (Figure 4.4, A and Glu). Repeating the stimulation in the presence of AP5 resulted in a decrease in peak concentration to 48.6 ± 3.0 nM (n=4), demonstrating a contribution of NMDAR to glutamate-induced $^{\bullet}$NO production, as expected (Figure 4.4, B and Glu+AP5). Interestingly, when an identical stimulation was conducted in the presence of 25 μM AP5 and 25 μM NBQX signals dropped even further, reaching 22.1 ± 0.9 nM $^{\bullet}$NO (n=3) (Figure 4.4, C and Glu+AP5+NBQX). Despite the absence of a complete inhibition, this suggests that AMPAR were activated by glutamate and induced NOS activation during NMDAR inhibition (*i.e.* in the presence of AP5). Therefore, we next tried to determine the mechanism responsible for this effect, as presented in the following sections.

4.5 - AMPA Receptors and Extracellular Calcium

Considering that a rise in cytosolic Ca^{2+} levels is essential for nNOS activation and that AMPAR are largely Ca^{2+} impermeable, we sought to determine the origin of Ca^{2+} in AMPA-mediated $^{\bullet}$NO production. Hippocampal slices were perfused for 5 minutes with aCSF without Ca^{2+} and subsequently stimulated with AMPA for two minutes. As shown in Figure 4.5 (right), Ca^{2+}
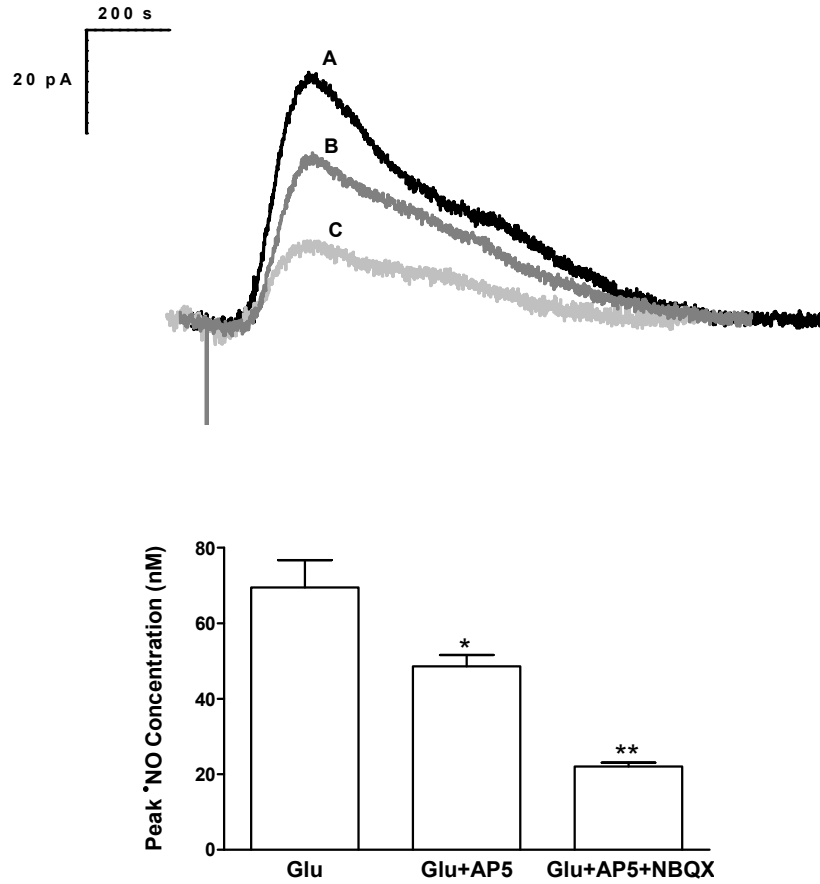
Figure 4.4: AMPA and NMDA receptors contribution to ˙NO oxidation signals following stimulation with glutamate. A / Glu) Slices stimulated with 5 mM glutamate for two minutes (69.5 ± 7.3 nM, n=4). B / Glu+AP5) Stimulation in the presence of AP5 (25 μM) results in a decrease in peak ˙NO concentration to 48.6 ± 3.0 nM (n=4, * p<0.05). C / Glu+AP5+NBQX) The AMPA inhibitor NBQX (25 μM) induces an additional drop in endogenous ˙NO levels to 22.1 ± 0.9 nM ˙NO (n=3, ** p<0.01).

 removal from aCSF prevented ˙NO production, as no signal was observed after 50 μM AMPA perfusion, and strongly suggested that ˙NO production was critically dependent on extracellular Ca^{2+} in our model. Accordingly, slices stimulated subsequently with 50 μM AMPA for two minutes in aCSF
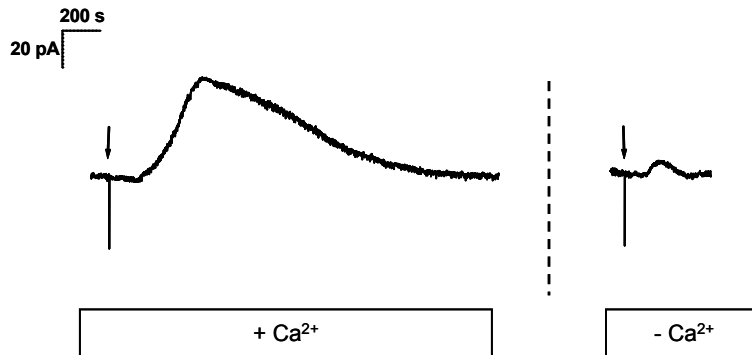
Figure 4.5: AMPAR-dependent ˙NO production in hippocampal slices is dependent of extracellular Ca^{2+}. Representative traces of ˙NO oxidation current observed after 50μM AMPA stimulation in the presence of Ca^{2+} (left), abolished when Ca^{2+} is absent from the perfusion media (right).

supplemented with 1.5 mM Ca^{2+} showed a small but evident production of ˙NO (Figure 4.5, left). This observation led us to investigate possible pathways of Ca^{2+} entry that could be activated by AMPA.

4.6 - Calcium-Permeable AMPA Receptors

Literature reports recently highlighted the role played by Ca^{2+}-permeable AMPA receptors in LTP, and we investigated their role, if any, in AMPA-mediated ˙NO production using specific inhibitors. The naturally occurring wasp venom toxin philanthotoxin-4,3,3 (PhTx-4,3,3) is an uncompetitive antagonist of Ca^{2+}-permeable AMPAR, and was shown to inhibit both homomeric GluR1 and GluR3 AMPA receptors (Toth *et al.* 1998; Terashima *et al.* 2004). Slices were placed in the recording chamber and perfused simultaneously with 50 μM AMPA and 10 μM PhTx-4,3,3 for two minutes. As depicted in Figure 4.6 (grey line), a statistically significant 20.7 %
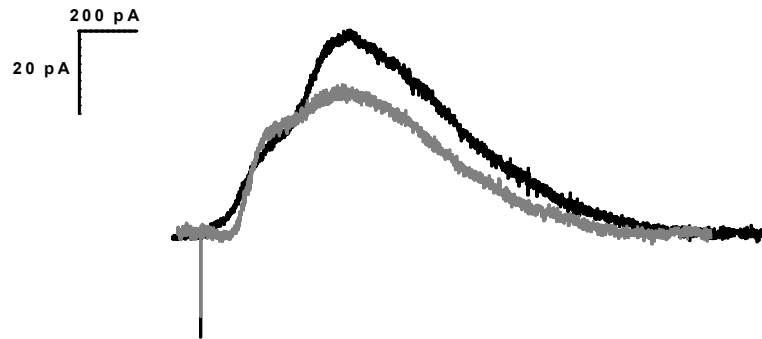
Figure 4.6: Inhibition of Ca^{2+}-permeable AMPAR results in a decreased ˙NO production. Representative traces of co-administration of 50 μM AMPA and 10 μM PhTx-4,3,3 (grey line), an uncompetitive inhibitor of Ca^{2+}-permeable AMPAR, highlighting a decreased ˙NO production in hippocampal slices when compared to those stimulated with AMPA alone (black line, n=3, p<0.05).

decrease in ˙NO oxidation currents recorded in the presence of PhTx-4,3,3 (34.8 ± 0.3 nC, n=3) was observed when compared to slices stimulated with AMPA alone (27.6 ±1.8 nC, n=3) (Figure 4.6, black line). This observation supports the expression of Ca^{2+}-permeable AMPAR receptors in adult hippocampal CA1 region, and suggests their participation in intracellular Ca^{2+} changes following AMPA stimulation.

4.7 - Discussion

It is widely accepted that ˙NO plays a relevant role in hippocampal physiology, and we investigated the production of ˙NO in integral hippocampal slices mediated by different subtypes of ionotropic glutamate receptors. The physical and functional coupling of NMDAR to nNOS is a major and well-

established pathway for $^\bullet$NO production: NMDAR interacts via PSD-95 with nNOS, enabling the enzyme to sense Ca^{2+} and leading to $^\bullet$NO diffusion to the extracellular media, which concentration dynamics has been demonstrated by the real time measurement of $^\bullet$NO (Ledo *et al.* 2005). Here, also on basis of direct and real-time measurement of endogenous $^\bullet$NO, we report that not only NMDA but also AMPA receptors are involved in $^\bullet$NO production in hippocampus, and suggest a role for Ca^{2+}-permeable AMPAR in intracellular Ca^{2+} changes following slices stimulation with AMPA.

Considering that AMPAR, despite their low conductance to Ca^{2+} (Hollmann et al. 1991), have been implicated in Ca^{2+}-dependent plasticity (Chittajallu et al. 1998; Zamanillo et al. 1999) we investigated if and how endogenous $^\bullet$NO could be produced upon stimulation of this type of ionotropic glutamate receptor. Slice stimulation with 50 μM AMPA resulted in a marked production of $^\bullet$NO (Figure 4.1), confirmed by control experiments with the AMPAR inhibitor NBQX, following stimulation of slices below $^\bullet$NO oxidation potential, that resulted in complete signal loss, and by inhibiting nNOS activity with MB, which in turn led to a 55.7 % decrease in signal intensity (Figure 4.2).

It is known that AMPA perfusion can cause depolarization of presynaptic cells and release of vesicular glutamate (Sattler et al. 2001), ultimately leading to activation of synaptic or extrasynaptic NMDAR. This event could account for the signal observed after perfusion with AMPA. However, the clearance rate of synaptic glutamate was shown to increase during development and to be higher in adult cells, with astrocytes in the CA1 region of hippocampal slices being capable of clearing extracellular glutamate within 1 ms, thus preventing any extrasynaptic NMDAR activation (Diamond 2005). AMPA-induced release of vesicular glutamate was therefore expected to be actively removed from the synaptic cleft and this is in agreement with previous experiments in this model system presented in Chapter 3, where

glutamate was shown to induce ˙NO production only at concentrations several-fold higher (mM range) than the ones used (μM range). To further rule out any contribution of synaptic NMDAR in AMPA-stimulated slices all experiments were conducted in the presence of 25 μM AP5, a concentration shown to inhibit NMDAR (Ledo et al. 2005). Furthermore, stimulation of slices with 175 μM AMPA in the presence of higher AP5 concentration (100 μM AP5) resulted in robust signals, without significant changes in ˙NO signal charge when compared to the ones obtained with 175 AMPA in the presence of 25 μM AP5 (Figure 4.1). DPA experiments were AP5 was perfused on-top of AMPA-elicited NO oxidation currents further excluded a contribution of NMDAR, as signal decay profile remained unchanged (Figure 4.1).

Experiments using AMPA clearly demonstrate that other glutamate receptor agonists can induce ˙NO production. Considering that nNOS is long known to be coupled to NMDAR activation (Christopherson *et al.* 1999; Sattler *et al.* 1999) we addressed the relationship between ˙NO production and ionotropic glutamate receptor activation, particularly NMDAR and AMPAR. As observed in Chapter 3, perfusion of hippocampal slices with NMDA led to a transient ˙NO oxidation current, characterized by a rapid rising phase and a slow decreasing period with basal current values recovered approximately 30 minutes after stimulation, as previously reported (Ledo *et al.* 2005). Perfusion of slices with 5 to 175 μM NMDA resulted in a concentration-dependent production of ˙NO (Figure 4.3, closed circles) that reached a plateau for 50 μM NMDA, with an EC50 for NMDA of 17.66 μM. This suggests that nNOS activity and ˙NO levels in hippocampus can be modulated within certain boundaries. Single synapses located in individual dendritic spines of CA1 pyramidal neurons are known to release variable amounts of glutamate per action potential and increase NMDAR activation (Oertner *et al.* 2002), supporting the notion that NOS activity can be modulated as a result of stimulus strength

(Figure 4.3, closed circles). Previously, East and Garthwaite found, in a similar model system, a concentration-dependent elevation in hippocampal cyclic GMP levels upon a two minute stimulation with NMDA, with an EC50 of approximately 30 μM for NMDA (East *et al.* 1991). Our results clearly agree with these, but provide key information about the kinetics of production and decay of ˙NO, the cellular messenger linking NMDAR activation and cGMP production (Chetkovich *et al.* 1993; Monfort *et al.* 2002). The fact that T_{Rise} values were lower after NMDA stimulation of slices (Table 4.1) agrees with the notion that nNOS is physically linked to NMDAR. Furthermore, ˙NO is produced transiently and decays within a prolonged period of time, with peak concentrations remaining within nanomolar range. This demonstrated that, even at high NMDA concentrations, ˙NO concentration in slices remained below values considered to be toxic (micromolar). The fact that recorded signals took prolonged periods of time to drop to baseline levels conflicts with reports suggesting rapid inactivation mechanisms for ˙NO in cerebellum slices (Hall *et al.* 2006) and, moreover, raises intriguing questions as to the effects of prolonged elevated ˙NO levels in hippocampus.

AMPA-mediated ˙NO production was observed over the concentration range used with NMDA (5 to 175 μM) and a similar plateau was reached at 50 μM, but lower levels of ˙NO peak concentration were obtained (Figure 4.3, open circles). Signal analysis showed that, for concentrations higher than 25 μM, not only the T_{Rise} following AMPA perfusion increased but it was also 1.5 to 2.5 times higher in slices stimulated with AMPA than in those treated with NMDA (Table 4.1). This observation might be related to differences in nNOS activation following receptor activation. In fact, conversely to AMPAR, NMDAR where shown to bind nNOS by means of PDZ domains and protein-protein interactions with a number of proteins such as PSD-95 (Sattler *et al.* 1999), which would allow a close relationship between NMDAR opening, Ca^{2+} influx and nNOS activation. In which concerns AMPAR, PSD95 and a number of

other synaptic proteins are also involved in the regulation and control of synaptic AMPAR activity in different brain structures (Beique *et al.* 2003; Bredt *et al.* 2003), including the hippocampus (Stein *et al.* 2003). Boehm *et al* concluded recently that, in organotypic hippocampal slice cultures, destroying or introducing a point mutation on the PDZ-ligand domain of the C-terminal of the AMPA receptor subunit GluR1 leads to different effects on synaptic plasticity (Boehm *et al.* 2006). However, although the AMPA GluR2/3 subunits also contain a PDZ domain on their C-terminal, the receptor binds proteins other than the PSD-95, including PICK1 (protein interacting with C kinase), GRIP1 (glutamate receptor interacting protein) and ABP (AMPA binding protein) (Dong *et al.* 1997). As such, activation of this type of glutamate receptor is not physically linked to nNOS activation, although its participation in the pathways of ˙NO production was reported years ago in cerebellar slices prepared from adult rats (Okada 1992). The lack of interaction of the AMPAR with nNOS may imply that the activation of this receptor is more appropriate for a fine tuning of ˙NO signaling. Thus, conversely to activation of NMDAR, the activation of AMPAR may lead only to a partial activation of nNOS. The Ca^{2+} required for nNOS activation may enter, for instance, through either Ca^{2+}-permeable AMPAR or voltage sensitive Ca^{2+} channels.

In vivo glutamatergic synapses require the combined action of AMPA and NMDA receptors to induce membrane depolarization and Ca^{2+} entry. According to the classical mechanism, AMPAR activation allows Na^+ entry into the post-synaptic cell, which results in membrane depolarization; this event subsequently allows for Mg^{2+} removal from the NMDAR pore, resulting in massive Ca^{2+} entry and activation of nNOS (among other enzymes and/or pathways). Therefore, it was pertinent to investigate if stimulating slices with the physiological agonist would result in the same pattern of ˙NO production observed with AMPA. Perfusion of 5 mM glutamate for two minutes originated

a signal similar to the ones previously observed, although less intense. In this regard, ˙NO peak concentration was almost half the one obtained with NMDA (69 *vs* 126 nM), despite the use of higher glutamate concentrations (5 mM glutamate *vs* 50 µM NMDA). This was considered a consequence of glutamate removal from the extracellular media by cells in the slice, that in physiological conditions maintain a tight regulation over extracellular glutamate activation (Diamond 2005). In the presence of 25 µM of the NMDAR inhibitor AP5 a decreased production of ˙NO was observed when compared to control experiments, highlighting the contribution of NMDAR following glutamate perfusion (Figure 4.4). Interestingly, when the stimulation was conducted with co-administration of 25 µM AP5 and 25 µM NBQX, to inhibit both NMDAR and AMPAR, ˙NO production dropped further, strongly suggesting that, even when NMDAR are inhibited, AMPAR activation can elicit a marked production of ˙NO (Figure 4.4). A basal ˙NO production was always observed in the presence of both inhibitors, probably as a result of the competitive nature of NMDAR and AMPAR inhibitors and/or incomplete inhibition of receptors. Nevertheless, this is in agreement with previous reports demonstrating *in vivo* changes in basal ˙NO in hippocampus following AMPA and NMDA receptors inactivation (Bhardwaj *et al.* 1997), as well increases of cGMP levels in cultured rat cerebellar astroglia after glutamate, AMPA or Kainate stimulation (Baltrons *et al.* 1997). Interestingly, the abovementioned AMPA-induced production was shown to be dependent on extracellular Ca^{2+} (Figure 4.5), as no current was observed due to ˙NO oxidation after slice stimulation in Ca^{2+}-free aCSF, suggesting that Ca^{2+} was originating from the extracellular media and not intracellular stores. Following this result, we then addressed the issue of what AMPA-mediated pathway was responsible for intracellular Ca^{2+} increases.

Several reports recently demonstrated the role of Ca^{2+}-permeable AMPAR in ischemic events (Noh *et al.* 2005) and plasticity (Plant *et al.* 2006)

in hippocampus. We therefore conducted experiments with the uncompetitive inhibitor PhTx-4,3,3 in order to clarify the role of these receptors in $^{\bullet}$NO production. Co-administration of 10 μM PhTx-4,3,3 with 50 M AMPA for two minutes led to a 20.7 % decrease in AMPA-induced $^{\bullet}$NO signals (Figure 4.6). This striking result might prove relevant in light of events known to be mediated by Ca^{2+}-permeable AMPAR (Noh *et al.* 2005) and by $^{\bullet}$NO (Jiang *et al.* 2007), such as ischemia. The observation that AMPAR in CA1 and CA3 pyramidal neurons are mainly hetero-oligomers containing the GluR2 subunit (Jonas *et al.* 1992) could rise questions as to the contribution of GluR2-lacking Ca^{2+}-permeable AMPAR towards $^{\bullet}$NO production after stimulation of slices with AMPA, as this was observed with micro sensors inserted in pyramidal cell layer of CA1 region. This contradiction might be resolved considering that a fraction of hippocampal AMPAR (approximately 25%) could not be labeled after immunocytochemical localization of GluR2-containing AMPA receptors (Gryder *et al.* 2005). Furthermore, the small size of our microsensors affords a spatial discrimination between regions, but not so much between layers of the same region. In fact, we have recently demonstrated that $^{\bullet}$NO is able to diffuse as far as 400 μm away from the point of production, as verified by stimulating hippocampal slices with NMDA injected at increasing distances from the inserted micro sensor (Ledo *et al.* 2005). Hence, recorded oxidation currents might be attributed to $^{\bullet}$NO produced by cells located in the vicinity of the pyramidal cell layer (Isa *et al.* 1996). In this regard, Takata *et al.* have recently used the $^{\bullet}$NO-reactive fluorescent dye diaminorhodamine-4M (DAR-4M) to investigate time-dependent $^{\bullet}$NO production in hippocampal slices upon NMDA, and demonstrated an heterogeneous production between subregions of the CA1 region, with fluorescence being significantly greater in stratum radiatum when compared to stratum oriens or the pyramidal cell layer (Takata *et al.* 2005). Thus, the marked decrease in $^{\bullet}$NO oxidation current detected after PhTx incubation cannot rule out the contribution of non-pyramidal cells like

interneurons located in other layers, proven by others to be involved in excitatory synaptic transmission in the hippocampus (Isa *et al.* 1996).

In summary, results suggest that ionotropic glutamate receptors independently mediate the production of $^{\bullet}$NO although with distinctive features. Signals obtained with AMPA elicited smaller increases in $^{\bullet}$NO extracellular concentration and took longer to reach maximum intensity. This probably reflects a less effective coupling between nNOS and membrane receptors. The same result was observed with glutamate, with selective inhibition of ionotropic receptors with AP5, NBQX or both supporting the role of AMPAR in $^{\bullet}$NO increases. Signals were also showed to be dependent on extracellular Ca^{2+}, and Ca^{2+}-permeable AMPAR are suggested to mediate (to a certain extent) the increase in intracellular Ca^{2+}. To fully account the importance of these results further experiments are required, in order to clarify the relevance of this pathway to the overall hippocampus physiological and/or pathological events.

CHAPTER 5

**GLUTAMATE-INDUCED RELEASE OF
ASTROCYTIC GLUTATHIONE**

5.1 - Introduction

In conditions where release and/or uptake of glutamate are altered, extracellular glutamate can accumulate and cause a persistent or excessive activation of glutamate-gated ion channels, a condition known as excitotoxicity (Coyle *et al.* 1993; Mark *et al.* 2001). The extracellular levels of glutamate have been measured in various *in vivo* disease models by microdialysis and have been shown to reach concentrations of >500 μM following spinal cord injury (McAdoo *et al.* 1999) and be maintained at concentrations of >50 μM for 1-2 hours during and following ischemic insults (Orwar *et al.* 1994; Ritz *et al.* 2004; Homola *et al.* 2006). Astrocytes have a fundamental role in the regulation of extracellular glutamate levels and in the protection of neurones in ways such as through metabolic and antioxidant support (Hertz *et al.* 2004). One of the most important molecules in this respect is GSH (Schulz *et al.* 2000), and the trafficking of GSH between astrocytes and neurons is particularly important in conditions of oxidative stress (Dringen 2000). Previous studies have shown that astrocytes increase GSH release in response to increases in reactive nitrogen and oxygen species (RNOS), such as ˙NO (Gegg *et al.* 2003) and H_2O_2 (Sagara *et al.* 1996). This increase in GSH release is hypothesized to be a neuroprotective mechanism which maintains and/or increases neuronal GSH levels to counteract the damaging effects of RNOS. Since oxidative stress is considered to be a key component of glutamate toxicity it was the aim of this study to investigate whether high concentrations of extracellular glutamate also had an effect on GSH release from astrocytes.

5.2 - Glutamate-Induced Increase in Extracellular Glutathione

To assess the effect of extracellular glutamate on GSH release, rat cortical astrocytes were treated with glutamate and extracellular GSH was measured at various time points by HPLC (Figure 5.1, A). In these initial experiments 5 mM glutamate was used. Although this could be thought of as a comparatively high glutamate concentration, similar glutamate concentrations are thought to be reached in the synaptic cleft following release of a single synaptic vesicle (hypothesized to be between 0.24 - 11 mM) (Harris *et al.* 1995) and milimolar glutamate has been used before to model glutamate excitotoxicity in astrocytes (Chen *et al.* 2000).

In the absence of glutamate, extracellular GSH increased to 0.5 ± 0.1 µM after 120 minutes and 1.2 ± 0.2 µM after 240 minutes (Figure 5.1, A ■). In the presence of 5 mM glutamate, the concentration of extracellular GSH was significantly higher after 120 and 240 minutes when compared to control astrocytes, reaching 1.2 ± 0.1 and 2.3 ± 0.2 µM, respectively (Figure 5.1, A □, $p<0.05$). Similar results were obtained for primary astrocyte cultures on 24-well dishes (Figure 5.1 B). These results indicate that glutamate, at this concentration, induces an increase in extracellular GSH in rat astrocyte cultures. However, this increase in extracellular GSH could be the result of increased GSH synthesis following incubation with glutamate, increased leakage of intracellular contents due to glutamate toxicity or due to inhibition of extracellular GSH breakdown. The following sections address these hypotheses.

A

B
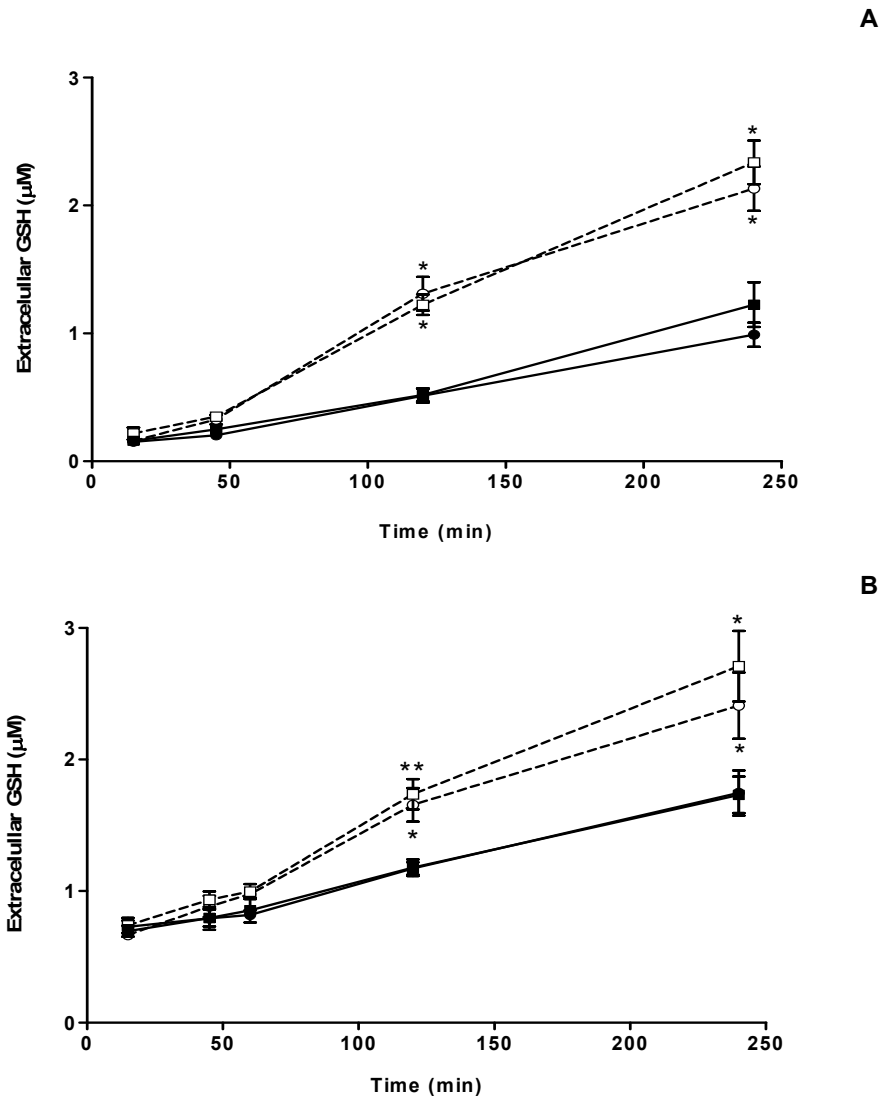
Figure 5.1: Glutamate induces an increase in extracellular GSH in astrocyte cultures. Cortical astrocytes on 6-well plates (A) and primary astrocytes on 24-well plates (B) were incubated with (□, dashed line) or without (■, full line) 5 mM glutamate in Minimal Media and extracellular GSH quantified at the indicated time points. Glutamate induced a marked increase in extracellular GSH when compared to control astrocytes. Astrocytes were also incubated with 5 mM of the GSH synthesis inhibitor BSO for 2 hours prior to and throughout experiments with (○, dashed line) or without (●, full line) 5 mM glutamate. No significant differences were observed in extracellular GSH between BSO treated and untreated cells. (n=4-6 different cell preparations; *, p<0.05 and **, p<0.01 control *vs* glutamate conditions).

5.2.1 - *de novo* Synthesis of Glutathione

Glutamate can be used by cells for GSH synthesis, provided other precursors are not limited (Dringen *et al.* 1998), and constitutive GSH release from astrocytes correlates with intracellular GSH concentration (Sagara *et al.* 1993). The increase in extracellular GSH observed in the presence of high extracellular glutamate could therefore result from increased GSH synthesis. To determine whether this was the case, glutamate-induced GSH release was measured in the presence and absence of the GSH synthesis inhibitor BSO (Figure 5.1). Astrocytes were incubated with or without 5 mM BSO (a concentration that has previously been shown to inhibit *de novo* GSH synthesis) (Gegg *et al.* 2002) in minimal media (MM) for 2 hours prior to and throughout experiments. In the absence of glutamate, extracellular GSH levels for BSO-treated astrocytes were not significantly different from control astrocytes, reaching 0.9 ± 0.1 μM after 240 minutes (Figure 5.1, A ●). When glutamate was added to BSO-treated astrocytes a significant increase in extracellular GSH was detected, reaching 2.3 ± 0.2 μM after 240 minutes (Cont+BSO *vs.* Glu+BSO, $p<0.05$) (Figure 5.1, A ○), similar to what was observed in glutamate-treated astrocytes in the absence of BSO. These results were confirmed for primary astrocyte cultures on 24-well dishes (Figure 5.1, B).

5.2.2 - Lacate Dehydrogenase Release

In order to determine if the increase in extracellular GSH was due to glutamate-induced cellular damage, LDH levels were measured in media and cells as an indicator of membrane disruption. As determined for the 240 minute time point, LDH levels were not significantly different between control (1.6 ± 0.3 %,) and glutamate-treated cortical astrocytes (2.0 ± 1.2 %, $p>0.05$),

suggesting that the increase in extracellular GSH was not a consequence of leakage of intracellular content. LDH release levels were also not significantly different between glutamate-treated and control astrocytes in the presence of BSO (2.2 ± 0.3 % *vs.* 2.4 ± 0.6 %, p>0.05, respectively).

5.2.3 - Extracellular Glutathione and γGT Inhibition

Expressed on the surface of astrocytes, γGT breaks down extracellular GSH by catalyzing the transfer of the glutamyl residue of GSH to a number of amino acid and dipeptide acceptors (Dringen *et al.* 1997). Inhibition of γGT by acivicin has been shown to result in an increase in extracellular GSH (Dringen *et al.* 1997). To investigate the possibility that glutamate was increasing extracellular GSH levels by inhibiting γGT, the effect of acivicin with or without glutamate on the release of extracellular GSH by primary rat astrocytes was tested (Figure 5.2).

Treatment with 100 µM acivicin resulted in a slight but not significant increase in extracellular GSH in control astrocytes after 240 minutes (1.4 ± 0.1 µM for Cont *vs.* 1.7 ± 0.1 µM for Cont+Aciv), suggesting that γGT was not particularly active in our cultures to metabolize the GSH released from the cells. However, a combination of acivicin and glutamate did result in a significant increase in extracellular GSH after 240 minutes compared to astrocytes treated with glutamate alone (3.2 ± 0.1 µM for Glu alone *vs* 3.8 ± 0.1 µM for Glu+Aciv, p<0.05). As acivicin was used at a concentration which has previously been reported to maximally inhibit γGT (Dringen *et al.* 1997) and glutamate increased extracellular GSH even in the presence of acivicin, this data suggests that glutamate does not act by inhibiting γGT.
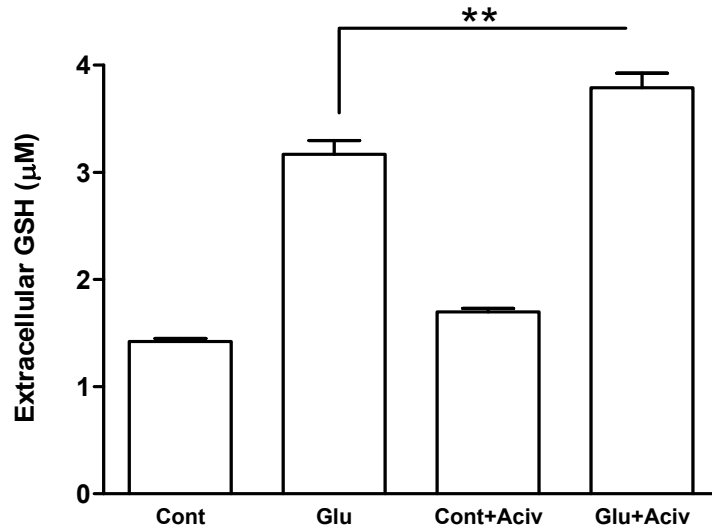
Figure 5.2: Effect of acivicin on glutamate-induced GSH release from rat astrocytes. Cortical astrocytes were incubated with (Glu) or without (Cont) 5 mM glutamate for 240 minutes and extracellular GSH levels were determined. The same experiment was repeated in the presence of 100 µM acivicin (Glu+Aciv and Cont+Aciv columns). Acivicin did not have a significant effect on extracellular GSH in control astrocytes (Cont *vs*. Cont+Aciv; 1.4 ± 0.1 µM *vs*. 1.7 ± 0.1 µM; p>0.05) but significantly increased extracellular GSH in the presence of glutamate (Glu *vs*. Glu+Aciv; 3.2 ± 0.1 µM *vs* 3.8 ± 0.1µM; **, p< 0.01) (n=3 separate wells from the same astrocyte preparation).

5.3 - Determination of Cellular Glutathione

In order to further investigate the effects of glutamate and BSO on GSH metabolism and GSH release in astrocytes, intra- and extracellular GSH was measured before and after glutamate stimulation of primary astrocytes on 24-well dishes (Table 5.1). Primary astrocyte cultures in wells of 24-well dishes were pre-incubated for two hours in MM with or without BSO (5 mM) before they were incubated for 4 h in 0.5 ml MM in the presence or absence of glutamate (5 mM) and/or BSO (5 mM). In the absence of glutamate, approximately 50 % of the initial cellular GSH was found in the medium after 240 minutes incubation. This amount was increased to approximately 70 %, if

Table 5.1: Intra- and extracellular GSH contents (nmol/well) of primary astrocyte cultures treated with glutamate and/or BSO.

	0 min Cells	240 min Cells	240 min Media	240 min Cells + Media
Cont	1.9 ± 0.2	1.0 ± 0.1 (53 ± 5%)	0.9 ± 0.1 (45 ± 4%)	1.9 ± 0.1 (98 ± 3%)
Glu	1.9 ± 0.2	1.1 ± 0.1 (57 ± 5%)	1.4 ± 0.1 * (70 ± 7%) *	2.5 ± 0.2 (127 ± 10%)
Cont + BSO	1.7 ± 0.2	0.7 ± 0.0 * (41 ± 3%)	0.9 ± 0.1 (51 ± 5%)	1.6 ± 0.1 (92 ± 7%)
Glu + BSO	1.7 ± 0.2	0.8 ± 0.1 (48 ± 5%)	1.2 ± 0.1 (70 ± 7%) *	2.0 ± 0.2 (118 ± 11%)

The basal cellular GSH content of untreated primary astrocyte cultures was 23.0 ± 1.8 nmol/mg protein. The two hour pre-incubation of these cultures without and with BSO (5 mM) lowered the GSH content to 19.7 ± 1.0 nmol/mg and 17.5 ± 0.5 nmol/mg, respectively. Data presented is from experiments performed on 4 independently prepared cultures. The significance of differences to the data obtained for the control condition (no glutamate, no BSO) are indicated as *p<0.05.

glutamate was present during the incubation. In contrast, the presence of BSO did not alter the extracellular GSH content compared to the respective controls without BSO. The differences found for the sum of cellular plus extracellular GSH after 240 minutes of incubation were not significant ($p > 0.05$). For all conditions shown in Table 5.1, GSSG accounted for less than 5 % of the GSx contents in cells or media, indicating that GSH and not GSSG was released from astrocytes and that the presence of glutamate did not significantly affect the extracellular GSH/GSSG ratio. GSH release rates from cultured astrocytes have previously been reported to be between 2 and 4 nmol / mg / h (Gegg et al., 2003; Hirrlinger, Schulz and Dringen, 2002; Sagara, Makino and Bannai, 1996). In the current study, the GSH release rate was calculated to be 2.25 nmol / mg / h under control conditions and 3.5 nmol / mg / h after addition of glutamate. As previously observed, for all conditions the extracellular activity of LDH was less than 10 % of initial cellular LDH and the values did not differ

significantly between the individual groups, further ruling out membrane damage as the mechanism by which GSH was being released.

5.4 - Ionotropic Glutamate Receptors and Glutathione Release

To study whether GSH release was dependent on the activation of glutamate receptors, agonists to the NMDA or non-NMDA ionotropic glutamate receptors were added to astrocyte cultures (50 μM NMDA and 50 μM AMPA, respectively). No significant effect on GSH release at the 240 minute time point was observed when compared to control astrocytes, and only glutamate had a significant effect on extracellular GSH when compared to control cells ($p<0.01$) (Table 5.2). The same result was obtained with agonists for metabotropic glutamate receptors.

5.5 - Glutathione Release From Hippocampal Astrocytes

In order to investigate whether glutamate-induced increase in extracellular GSH could be observed in hippocampus, hippocampal astrocytes

Table 5.2: Effect of glutamate receptor agonists on GSH release from astrocytes.

	Ex GSH	% control	n
Control	1.4 ± 0.2	100 ± 13.9	6
5 mM Glutamate	2.8 ± 0.3 **	208.8 ± 24.1 **	6
50 µM NMDA	1.3 ± 0.3	104.1 ± 14.8	3
50 µM AMPA	1.2 ± 0.2	93.0 ± 7.1	3

*% control is the extracellular GSH concentration after 4 hours compared to the control for that experiment. n numbers are as indicated. **, $p<0.01$.*

at DIV 14 were compared with cortical astrocytes (Figure 5.3). In the absence of glutamate, extracellular GSH increased to 1.1 ± 0.2 μM after 240 minutes in hippocampal cultures (Figure 5.3, ▲) compared to 1.2 ± 0.1 µM for cortical cultures (Figure 5.3, ■). As observed for cortical cultures (Figure 5.3, □), in the presence of 5 mM glutamate (Figure 5.3, Δ) the concentration of extracellular GSH in hippocampal cultures was significantly increased when compared to controls (2.7 ± 0.4 μM *vs* 1.1 ± 0.2 μM, respectively at 240 minutes; $p < 0.05$). This increase in extracellular GSH is of the same order of magnitude to that observed in cortical astrocyte cultures. As observed for cortical astrocytes, no significant difference could be observed between control and glutamate-treated hippocampal cells in terms of LDH release (1.7 ± 0.5 % *vs* 1.5 ± 0.3 %, respectively,).
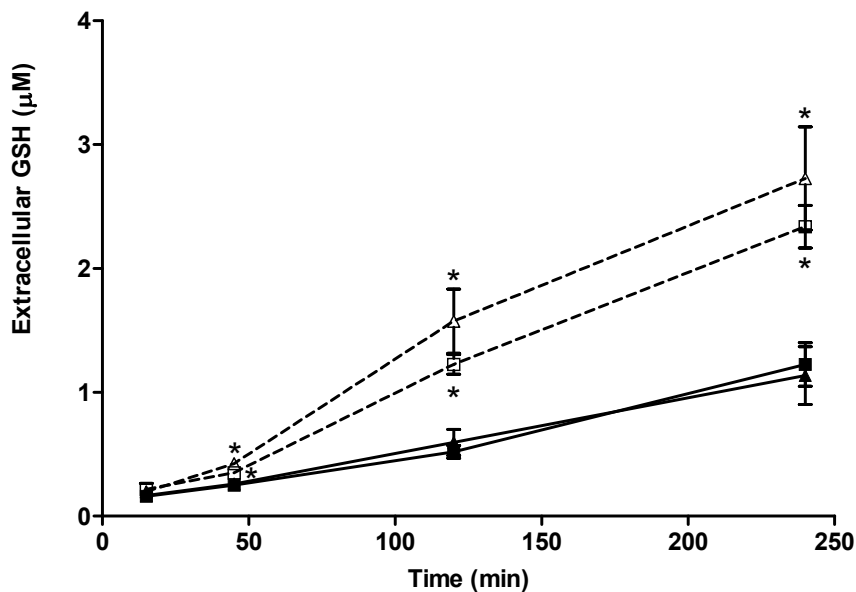
Figure 5.3: Glutamate induces release of GSH in hippocampal and cortical astrocytes. Incubation with 5 mM glutamate for 15, 45, 120 and 240 minutes induced a significant increase in extracellular GSH in hippocampal astrocytes (Δ) when compared to control without glutamate (▲, n=3 separate cell preparations, * $p < 0.05$ control *vs* glutamate conditions), similar to the increase observed for glutamate-treated cortical astrocytes (■, control; □, with 5 mM glutamate).

5.6 - Dose-Response Curve

The above experiments were all performed using 5 mM glutamate, a relatively high concentration that is only likely to be present transiently under physiological conditions. Therefore the above GSH release experiments were repeated using lower concentrations of glutamate. The dose response curves generated for both cortical and hippocampal astrocytes indicate that GSH release is increased after 240 minutes even at relatively low glutamate concentrations (0.1 mM) and maximal GSH release is already achieved with 0.5 mM glutamate (Figure 5.4). Half-maximal GSH release was achieved at approximately 250 µM glutamate for both hippocampal and cortical cultures.
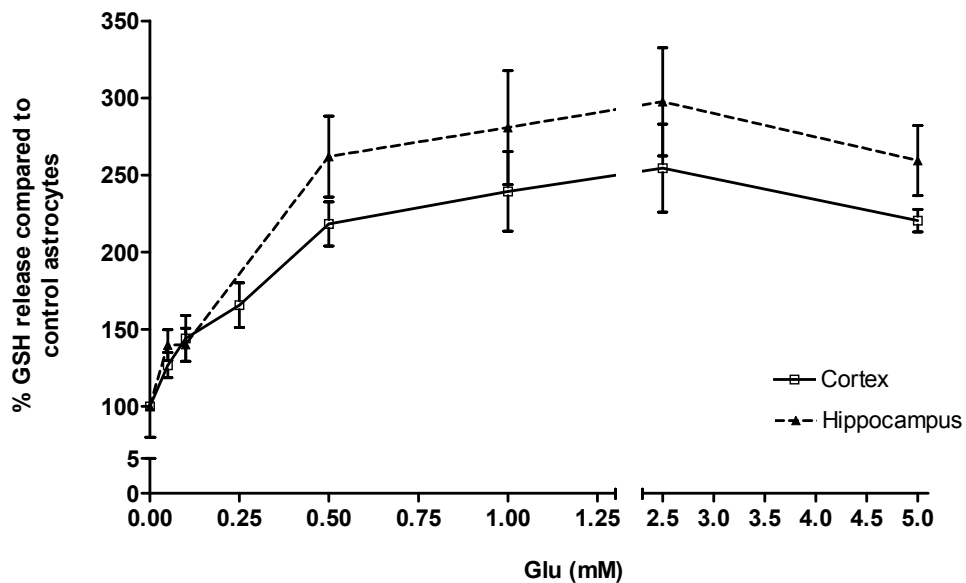
Figure 5.4: Glutamate dose response curves, showing the effect of glutamate concentration on GSH release from primary cultures of cortical (□) and hippocampal (Δ) rat astrocytes after 240 minutes incubation (n=3 separate cell preparations). For each cell preparation GSH release from control astrocytes with no glutamate added was considered 100%.

5.7 - Discussion

In the present Chapter it was demonstrated that prolonged exposure to glutamate induces an increase in the concentration of extracellular GSH in three different types of cultured astrocytes. These cells are known to release GSH (Sagara *et al.* 1996), and when cultured with 5 mM glutamate we observed a significant increase in the amount of extracellular GSH over 240 minutes (Figure 5.1), without evidence of cellular damage. At least a 2-fold increase in extracellular GSH was observed in both cortical and hippocampal astrocytes after 240 minutes treatment with glutamate, suggesting this to be a feature common to astrocytes from different brain regions. Dose response curves also indicated that glutamate induces GSH release from astrocytes at concentrations as low as 0.1 mM (Figure 5.4). A number of possible causes for this increase in extracellular GSH have been investigated in this study and are discussed in more detail below.

Glutamate is one of the precursors of GSH (Kranich *et al.* 1996), and an increase in the synthesis of GSH could result in its increased release into the media. However, under our experimental conditions, glutamate did not cause a significant increase in intracellular GSH (Table 5.1). This is not surprising as it has been shown previously that addition of 1 mM glutamate to astrocytes only results in an increase in intracellular GSH concentration if cystine/cysteine and glycine are also added (Dringen *et al.* 1996). The absence of these substrates in our media suggests that *de novo* GSH synthesis does not explain the increase in extracellular levels. Support for this argument also come from our experiments with BSO, a potent and specific inhibitor of glutamate-cysteine ligase (the rate limiting step in GSH synthesis) (Griffith *et al.* 1979). Presence of BSO had no significant effect on GSH release in the time frame of the experiment (Figure 5.1). A longer BSO

incubation would be expected to lower intracellular GSH to a larger extent, and possibly have an effect on glutamate-induced release if critical intracellular GSH levels were reached. Altogether, these results are in agreement with reports showing that astrocytes rely on stored GSH to resist otherwise harmful conditions, failing to survive only when these pools are depleted (Chen *et al.* 2000), and emphasize the capacity of astrocytes to release GSH when exposed to glutamate.

High concentrations of glutamate can be toxic to some cell types, leading to necrotic cell death with membrane rupture and leakage of intracellular content (Coyle *et al.* 1993). Since intracellular GSH concentrations are about 1000-times extracellular concentrations (mM *vs.* μM, respectively) (Dringen 2000), an increase in membrane leakage could explain the significant increase in extracellular GSH in the current study. However, no significant differences could be detected between control and glutamate-treated cells in terms of LDH release, suggesting that increased extracellular GSH detection was not a result of membrane rupture induced by glutamate. Our results are consistent with those of others in terms of the gliotoxic action of glutamate. Chen *et al* demonstrated that 10 mM L-glutamate leads to LDH release only after a very prolonged incubation period (16 h), during which changes in cell morphology and oxidative stress occurs (Chen *et al.* 2000). These changes could be terminated by removal of glutamate before the onset of cell damage (estimated to occur at 4h-6h), indicating that the glutamate effect was reversible and that continuous exposure was required for astrocyte death. Since glutamate did not appear to cause release of GSH through non-specific cell leakage other mechanisms were investigated.

The data in Table 5.1 show that glutamate increases the proportion of GSH that is extracellular in astrocyte cultures. Two possible explanations for this rise in extracellular GSH have been ruled out in this study - namely

glutamate inhibition of extracellular processing of GSH by γGT (Figure. 5.2) and glutamate affecting the extracellular GSH/GSSG ratio. Therefore the most likely explanation for the increase in extracellular GSH in astrocyte cultures upon exposure to glutamate is stimulation of GSH release (Figure 5.5). This increased release of GSH from rat astrocytes could result from the activation
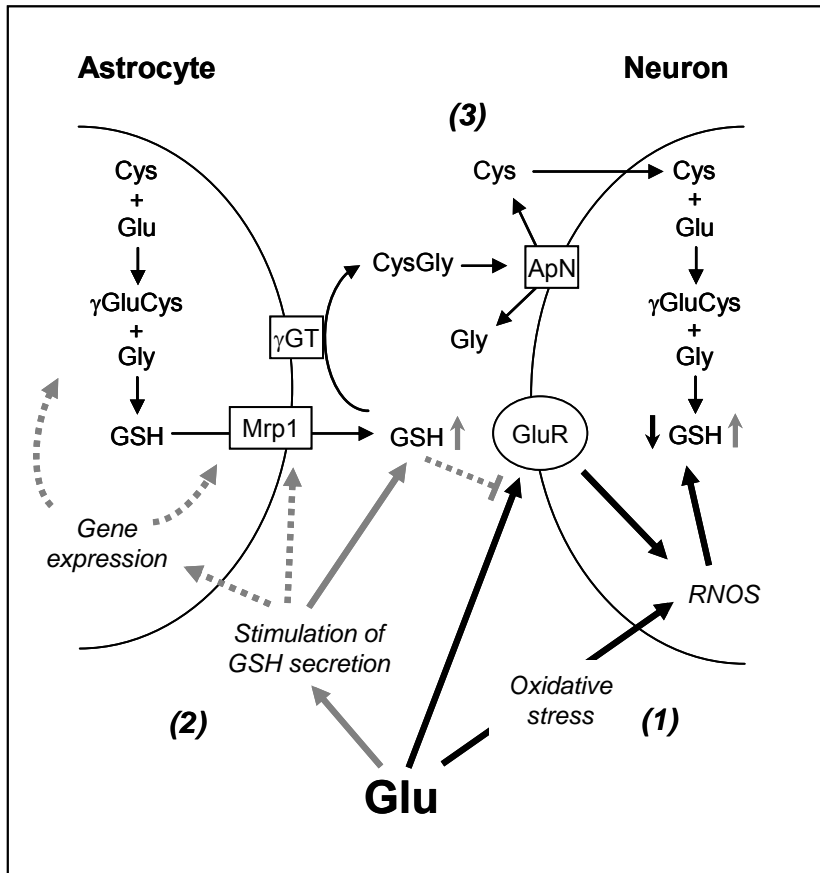
Figure 5.5: Proposed neuroprotective role of glutamate-induced upregulation of GSH release from astrocytes. (1) Extracellular glutamate is toxic to neurones via excessive stimulation of glutamate receptors (GluR) (Coyle *et al.* 1993), which may result in increased oxidative stress and an increase in GSH consumption (black full arrows). (2) In the present study we have demonstrated that extracellular glutamate also increases the release of GSH from astrocytes (grey full arrows) by an unknown mechanism(s), possibly via the transporter Mrp1 (Minich *et al.* 2006) and/or modifications at gene level (Shih *et al.* 2003) (grey dashed arrows). (3) This extracellular GSH can be used by neurones to increase their intracellular GSH levels (Dringen 2000), making them more resistant to glutamate-induced oxidative stress (Gegg *et al.* 2005). Increased extracellular GSH may also counteract glutamate toxicity by competing with glutamate for binding sites on glutamate receptors (Oja *et al.* 2000).

of glutamate receptors and/or activation of downstream signaling pathways by glutamate. Glutamate receptors are considered to be expressed mainly on neurons but are also present on astrocytes (Porter *et al.* 1996; Porter *et al.* 1997), where they have been increasingly implicated in a number of important pathways, including e.g. regulation of intracellular Ca^{2+} levels, stimulation of protein kinase C and inhibition of adenylate cyclase (Porter *et al.* 1996; Winder *et al.* 1996; Porter *et al.* 1997). Neurotransmitter(s) released from pre-synaptic terminals could therefore activate receptors located on astrocytes, leading to GSH release. However, data from experiments using agonists for ionotropic glutamate receptors suggests that neither NMDA nor AMPA/Kainate receptors are involved in GSH release, since we were unable to detect elevated extracellular levels of GSH after incubation with NMDA or AMPA. Experiments have also failed to show a role of metabotropic receptors in GSH release. Glutamate is also able to induce various changes in astrocytes which are not mediated via glutamate receptors. These changes include a switch of astrocytic metabolism from glycolytic to oxidative, via decreased glucose utilization and increased mitochondrial activity (Liao *et al.* 2003). Such changes to astrocyte energy metabolism may also affect GSH metabolism and export, although this remains to be elucidated.

RNOS such as H_2O_2 and ˙NO have also been implicated in the increase of GSH in cultured astrocytes (Sagara *et al.* 1996; Gegg *et al.* 2003), and oxidative stress was shown to result in the overexpression of Nrf2, a transcription factor implicated in GSH use, production and efflux pathways in astrocytes, via antioxidant-response element (ARE) activation (Shih *et al.* 2003). Hypothetically, such transcription factor regulated changes could also be induced by glutamate and increase GSH efflux. However, significant changes to gene expression are likely to take hours rather than minutes and are therefore unlikely to contribute to the initial glutamate-induced GSH

release observed in this study. Several of the transporters reported to transport GSH are expressed in cultured astrocytes (Minich *et al.* 2006). However, so far only multidrug resistance protein 1 (Mrp1) has been identified in astrocytes to participate in GSH transport under basal conditions (Minich *et al.* 2006). Whether this transporter, other Mrps, organic anion transporters or the CFTR protein contribute to the elevated GSH release from astrocytes in the presence of glutamate remains to
be elucidated.

This increased release of GSH in response to high extracellular glutamate can be regarded as a candidate antioxidant defense mechanism preventing neuronal damage (Drukarch *et al.* 1997; Drukarch *et al.* 1998; Gegg *et al.* 2005), but GSH may also be implicated in other regulatory events. GSH has been described as candidate modulator of central nervous system excitability, through binding to the NMDA receptor complex as either an agonist or antagonist in particular circumstances (Ogita *et al.* 1995; Oja *et al.* 2000); has been shown to limit cell sensitivity to NO-mediated mitochondrial injury (Bolanos *et al.* 1996; Gegg *et al.* 2005); and GSH and other reductants have also been demonstrated to increase the glutamate uptake current of glutamate transporters, an event that could be reversed by the oxidative agent 5,5'-dithio-bis(2-nitrobenzoic) acid (DTNB) (Trotti *et al.* 1997). In light of this, the ability of astrocytes to release GSH may prove to be important in protecting neurons from glutamate toxicity in distinct brain structures by means other than its role as an antioxidant.

In conclusion, our experimental strategy mimics conditions where extracellular glutamate levels are raised for prolonged periods such as during ischemia. Considering the range of glutamate-mediated mechanisms leading to neuronal death, including nitrosative and oxidative stress, the increased availability of GSH, an endogenous low-molecular weight antioxidant, may

constitute an important protective mechanism in response to excitotoxic insults.

CHAPTER 6

FINAL DISCUSSION AND CONCLUSIONS

Since its discovery as the EDRF in 1987, ˙NO activity in biological systems has been the matter of intense research. This has led researchers to identify and characterize a number of effects of this gaseous free radical in a growing number of biological actions. A comprehensive review of these is an overwhelming task, as it has been investigated in such different model systems as mammals, bacteria and plants. However, striking examples in humans are its role in vasorelaxation, where it regulates blood flow by determining vessel diameter at the smooth muscle level after being produced by endothelial cells; its participation in host defense, following reaction with radical superoxide anion to form the oxidizing agent peroxynitrite by activated macrophage; and its role in brain physiology and particularly memory formation, where it has been suggested to act as a retrograde messenger, being capable of integrating the activity of a number of neurons in the vicinity of its production, regardless of whether the neurons are connected directly by synapses.

The bioactivity of ˙NO is afforded by its unusual chemical properties. Composed by only two atoms, it cannot convey information as other classical neurotransmitters and hormones, which make use of particular chemical structural features to activate specific receptors. Being highly diffusible, ˙NO cannot be stored in vesicles, and therefore the regulation of its production by nitric oxide synthases and the chemistry in the vicinity of its production are the relevant factors in determining its bioactivity. Finally, its free radical nature affords distinctive chemical properties in redox regulatory and pathological events. These chemical properties become apparent when considering the range of direct and indirect reactions mediated by ˙NO. By reacting with metal centers, protein residues, other free radicals or even with its own derivatives, the pathways modulated by ˙NO may be affected by the redox cellular environment and its local concentration. Hence, the real-time measurement of

the local concentration of ˙NO in a particular tissue, as well as its pattern of change, is of obvious relevance to gain critical insights of its role in physiological and pathological processes. In this regard, indirect measures prevent a significant understanding of its activity *in vivo*, by missing the notion that ˙NO conveys information associated to its concentration dynamics.

Given this scenario, hippocampal slice preparations exhibit a number of merits pertinent for measuring ˙NO dynamics, for functionally-induced changes with impact in extracellular ˙NO changes may be investigated. Particularly relevant is the production of ˙NO via glutamate-dependent receptors because these have been strongly implicated in learning and development processes, and ˙NO has been shown to play an essential role in the induction of LTP in the hippocampus, the most widely studied neuronal equivalent of learning.

In order to accurately follow ˙NO production in the hippocampus the present work was initiated by the fabrication of sensitive and selective ˙NO microsensors. These were of reduced dimensions, allowing ˙NO measurements with minimal tissue damage. In combination with electrochemical techniques, the modifications introduced (particularly the increase in Nafion® layers) allowed a gain of selectivity against endogenous interferents while maintaining suitable electrochemical characteristics such as low detection limit and good sensitivity. Its usefulness to monitor ˙NO production in hippocampus was demonstrated by the selective activation of glutamatergic receptors. Both NMDA and glutamate stimulations were shown to elicit ˙NO production, but with distinct features: while the former resulted in marked increases at even low concentrations, the later originated smaller signals, likely due to the activation of glutamate uptake pathways in the slice. Thus, the preferential use of NMDA allowed the targeting of a particularly effective pathway in ˙NO production, namely the NMDAR receptor-nNOS

coupling. The use of NMDA also demonstrated that hippocampal ˙NO production was dependent on regulatory pathways, as consecutive stimulations consistently resulted in signal intensity decay. Additional results where hippocampal slices were continuously stimulated with NMDA, a condition resembling excitotoxicity, proved that ˙NO production increased to a higher but limited extent, suggesting the existence of still unidentified cellular mechanisms for ˙NO removal. Finally, the induction of ˙NO production by the general depolarizing molecule KCl and the NOS substrate L-arg demonstrated the possible occurrence of distinct NOS activation mechanisms, by eliciting distinct ˙NO profiles when compared to the previous ones.

Glutamatergic receptors and ˙NO production have long been related in hippocampus, particularly those afforded by NMDAR. However, AMPAR have also been implicated in mechanisms known to be ˙NO related, and several reports highlighted the requirement of both pathways in synaptic alterations. When addressing the role of AMPAR receptors in ˙NO production it was found that, as for NMDAR, AMPA stimulation resulted in a lower but marked ˙NO production. To our knowledge, this was the first direct identification of ˙NO following AMPA stimulation in hippocampus. This was dependent on extracellular Ca^{2+} and exhibited distinctive characteristics as compared with NMDA-dependent production, particularly a slower rate of ˙NO appearance in the extracellular medium. The role of AMPAR in ˙NO production was further demonstrated by stimulating hippocampal slices with glutamate while inhibiting both NMDA and AMPA receptors. As nNOS is dependent on intracellular Ca^{2+} changes and AMPAR are known to be Ca^{2+}-impermeable, a major issue was the Ca^{2+} source. Following reports where Ca^{2+}-permeable AMPAR where identified in hippocampus, experiments with selective inhibitors for these receptors proved their involvement (at least partially) in AMPA-mediated ˙NO production.

Excitotoxic conditions like the one mimicked by stimulating slices continuously with NMDA presumably lead to the activation of protective mechanisms, not only in neurons but also in other cell types. In this regard, astrocytes are major players in supporting and protecting neurons in harmful conditions. GSH is long known to be a major endogenous antioxidant, participating in a number of ROS detoxification pathways, and astrocytes are known maintain neuronal GSH levels by releasing GSH. When investigating the response of astrocytes in the presence of high glutamate it was observed the increase in extracellular GSH over time. A number of detailed results, namely absence of LDH release, no *de novo* GSH synthesis and lack of significant extracellular GSH degradation pointed to intracellular GSH release to be the mechanism responsible for the observed increase. Glutamate receptors where not responsible for this effect, observed in both cortical and hippocampal astrocytes, considered to be a possible protective mechanism against glutamate toxicity.

Owing the previous, the following conclusions are supported by the results:

1. Porphyrin microsensors are suitable to follow in real-time conditions the endogenous production of the labile free radical ˙NO in hippocampal slices, following stimulation with both selective and non-selective agonists of glutamatergic receptors and nNOS substrate;

2. Hippocampal slices produce ˙NO transiently, and the signal amplitude decreases upon consecutive stimulations. Such decrease occurs for the whole range of stimuli concentration and is independent of initial stimulation strength and endogenous ˙NO produced. This suggests the existence of an inhibitory mechanism at the level of NMDAR or NOS.

Additionally, the transient *vs* prolonged stimulation of slices with NMDA affords distinct profiles in terms of ˙NO production, the later being stronger and decaying linearly, but under conditions in which NMDAR was still functional. The prolonged stimulation protocol might constitute an adequate model to investigate ˙NO production during excitotoxic events, in circumstances where the NMDAR is not (at least completely) inhibited via a feed-back mechanism by ˙NO;

3. Similarly to NMDAR, the stimulation of AMPAR in hippocampus evokes the production of ˙NO. AMPAR-dependent signals are transitory but exhibit distinctive features as compared with those dependent on NMDAR, namely a slower rate of ˙NO production and lower ˙NO levels, despite similar recovery periods to baseline levels. These characteristics point to a less efficient coupling between AMPAR and nNOS as compared with that of NMDAR and nNOS. Overall, this is compatible with the notion of a fine tuning of ˙NO production via AMPAR;

4. Both NMDA and AMPA receptors elicit a concentration-dependent production of ˙NO, and both are dependent on extracellular Ca^{2+}. Pharmacological modulation of receptors suggest that NMDAR and constitutively expressed Ca^{2+}-permeable AMPAR are responsible for Ca^{2+} influx required to elicit the ˙NO signals upon stimulation wit NMDA and AMPA, respectively, although other mechanisms cannot be ruled out after AMPAR stimulation;

5. In conditions related to excitotoxicity, glutamate induces the release of GSH from intracellular pools in cultured astrocytes, in cells derived from cortex and hippocampus. Glutamate effect on astrocytic GSH is

not a consequence of astrocytes damage and subsequent GSH release, *de novo* synthesis, inhibition of extracellular degradation, or activation of membrane receptors, suggesting the participation of transmembrane transport pathway(s) in GSH release in what might be a protective mechanism to neurons.

Two major issues could be considered in future experiments. The first relates to the ˙NO production and the signal profiles obtained after KCl and glutamate stimulations. These differ from the signals obtained with NMDA and, to a lesser extent, AMPA, and suggest the occurrence of decay mechanisms that determine ˙NO profiles and rates of change. In this regard, Ca^{2+} recycling across the cellular membrane or intracellular stores could critically influence cytosolic levels and consequently nNOS activity. This would contribute to the knowledge of ˙NO production downstream of membrane receptor activation, a theme detailed scarcely in literature. A second question addresses GSH release from astrocytes in slices, where two major questions arise: first, are Mrp proteins involved in the glutamate-induced GSH release as already reported by others and, if not, what could be the mechanism involved; and two, could GSH and/or GSNO determine the activity of glutamatergic receptors in slices, and influence ˙NO production *ex vivo*. This second line of research would clarify the possible protective role of GSH, and contribute to the field of the modulatory role of astrocytes on neuronal activity.

CHAPTER 7

BIBLIOGRAPHY

Abu-Soud, H. M., K. Ichimori, A. Presta and D. J. Stuehr (2000). "Electron transfer, oxygen binding, and nitric oxide feedback inhibition in endothelial nitric-oxide synthase." *J Biol Chem* **275**(23): 17349-57.

Abu-Soud, H. M., D. L. Rousseau and D. J. Stuehr (1996). "Nitric oxide binding to the heme of neuronal nitric-oxide synthase links its activity to changes in oxygen tension." *J Biol Chem* **271**(51): 32515-8.

Abu-Soud, H. M., J. Wang, D. L. Rousseau, J. M. Fukuto, L. J. Ignarro and D. J. Stuehr (1995). "Neuronal nitric oxide synthase self-inactivates by forming a ferrous-nitrosyl complex during aerobic catalysis." *J Biol Chem* **270**(39): 22997-23006.

Adak, S., C. Crooks, Q. Wang, B. R. Crane, J. A. Tainer, E. D. Getzoff and D. J. Stuehr (1999). "Tryptophan 409 controls the activity of neuronal nitric-oxide synthase by regulating nitric oxide feedback inhibition." *J Biol Chem* **274**(38): 26907-11.

Akaike, T. and H. Maeda (1996). "Quantitation of nitric oxide using 2-phenyl-4,4,5,5-tetramethylimidazoline-1-oxyl 3-oxide (PTIO)." *Methods Enzymol* **268**: 211-21.

Alano, C. C., G. Beutner, R. T. Dirksen, R. A. Gross and S. S. Sheu (2002). "Mitochondrial permeability transition and calcium dynamics in striatal neurons upon intense NMDA receptor activation." *J Neurochem* **80**(3): 531-8.

Alderton, W. K., C. E. Cooper and R. G. Knowles (2001). "Nitric oxide synthases: structure, function and inhibition." *Biochem J* **357**(Pt 3): 593-615.

Almeida, A., S. Moncada and J. P. Bolanos (2004). "Nitric oxide switches on glycolysis through the AMP protein kinase and 6-phosphofructo-2-kinase pathway." *Nat Cell Biol* **6**(1): 45-51.

Amaral, D. G. and M. P. Witter (1989). "The three-dimensional organization of the hippocampal formation: a review of anatomical data." *Neuroscience* **31**(3): 571-91.

Andersen, P., T. V. Bliss, T. Lomo, L. I. Olsen and K. K. Skrede (1969). "Lamellar organization of hippocampal excitatory pathways." *Acta Physiol Scand* **76**(1): 4A-5A.

Andersen, P., A. F. Soleng and M. Raastad (2000). "The hippocampal lamella hypothesis revisited." *Brain Res* **886**(1-2): 165-171.

Anderson, C. M. and R. A. Swanson (2000). "Astrocyte glutamate transport: review of properties, regulation, and physiological functions." *Glia* **32**(1): 1-14.

Arancio, O., I. Antonova, S. Gambaryan, S. M. Lohmann, J. S. Wood, D. S. Lawrence and R. D. Hawkins (2001). "Presynaptic role of cGMP-dependent protein kinase during long-lasting potentiation." *J Neurosci* **21**(1): 143-9.

Arancio, O., M. Kiebler, C. J. Lee, V. Lev-Ram, R. Y. Tsien, E. R. Kandel and R. D. Hawkins (1996). "Nitric oxide acts directly in the presynaptic neuron to produce long-term potentiation in cultured hippocampal neurons." *Cell* **87**(6): 1025-35.

Araque, A., G. Carmignoto and P. G. Haydon (2001). "Dynamic signaling between astrocytes and neurons." *Annu Rev Physiol* **63**: 795-813.

Arnold, W. P., C. K. Mittal, S. Katsuki and F. Murad (1977). "Nitric oxide activates guanylate cyclase and increases guanosine 3':5'-cyclic monophosphate levels in various tissue preparations." *Proc Natl Acad Sci U S A* **74**(8): 3203-7.

Arundine, M. and M. Tymianski (2003). "Molecular mechanisms of calcium-dependent neurodegeneration in excitotoxicity." *Cell Calcium* **34**(4-5): 325-37.

Assreuy, J., F. Q. Cunha, F. Y. Liew and S. Moncada (1993). "Feedback inhibition of nitric oxide synthase activity by nitric oxide." *Br J Pharmacol* **108**(3): 833-7.

Auger, C. and D. Attwell (2000). "Fast removal of synaptic glutamate by postsynaptic transporters." *Neuron* **28**(2): 547-58.

Baader, S. L. and K. Schilling (1996). "Glutamate receptors mediate dynamic regulation of nitric oxide synthase expression in cerebellar granule cells." *J Neurosci* **16**(4): 1440-9.

Bae, S. Y., Q. Xu, D. Hutchinson and C. A. Colton (2005). "Y+ and y+ L arginine transporters in neuronal cells expressing tyrosine hydroxylase." *Biochim Biophys Acta* **1745**(1): 65-73.

Baltrons, M. A. and A. Garcia (1997). "AMPA receptors are coupled to the nitric oxide/cyclic GMP pathway in cerebellar astroglial cells." *Eur J Neurosci* **9**(11): 2497-501.

Barbosa, R. M., A. M. Silva, A. R. Tome, J. A. Stamford, R. M. Santos and L. M. Rosario (1998). "Control of pulsatile 5-HT/insulin secretion from single mouse pancreatic islets by intracellular calcium dynamics." *J Physiol* **510**: 135-43.

Baron, K. T. and S. A. Thayer (1997). "CGP37157 modulates mitochondrial Ca2+ homeostasis in cultured rat dorsal root ganglion neurons." *Eur J Pharmacol* **340**(2-3): 295-300.

Bates, T. E., A. Loesch, G. Burnstock and J. B. Clark (1995). "Immunocytochemical evidence for a mitochondrially located nitric oxide synthase in brain and liver." *Biochem Biophys Res Commun* **213**(3): 896-900.

Bazan, N. G., M. G. Packard, L. Teather and G. Allan (1997). "Bioactive lipids in excitatory neurotransmission and neuronal plasticity." *Neurochem Int* **30**(2): 225-31.

Bear, M. F. and R. C. Malenka (1994). "Synaptic plasticity: LTP and LTD." *Curr Opin Neurobiol* **4**(3): 389-99.

Beckman, J. S. and W. H. Koppenol (1996). "Nitric oxide, superoxide, and peroxynitrite: the good, the bad, and ugly." *Am J Physiol* **271**(5 Pt 1): C1424-37.

Beique, J. C. and R. Andrade (2003). "PSD-95 regulates synaptic transmission and plasticity in rat cerebral cortex." *J Physiol* **546**(Pt 3): 859-67.

Bender, A. T., A. M. Silverstein, D. R. Demady, K. C. Kanelakis, S. Noguchi, W. B. Pratt and Y. Osawa (1999). "Neuronal nitric-oxide synthase is regulated by the Hsp90-based chaperone system in vivo." *J Biol Chem* **274**(3): 1472-8.

Benveniste, H., J. Drejer, A. Schousboe and N. H. Diemer (1984). "Elevation of the extracellular concentrations of glutamate and aspartate in rat hippocampus during transient cerebral ischemia monitored by intracerebral microdialysis." *J Neurochem* **43**(5): 1369-74.

Berliner, L. J., V. Khramtsov, H. Fujii and T. L. Clanton (2001). "Unique in vivo applications of spin traps." *Free Radic Biol Med* **30**(5): 489-99.

Bettler, B., J. Egebjerg, G. Sharma, G. Pecht, I. Hermans-Borgmeyer, C. Moll, C. F. Stevens and S. Heinemann (1992). "Cloning of a putative glutamate receptor: a low affinity kainate-binding subunit." *Neuron* **8**(2): 257-65.

Bhardwaj, A., F. J. Northington, R. N. Ichord, D. F. Hanley, R. J. Traystman and R. C. Koehler (1997). "Characterization of ionotropic glutamate receptor-mediated nitric oxide production in vivo in rats." *Stroke* **28**(4): 850-6; discussion 856-7.

Blackmore, R. S., C. Greenwood and Q. H. Gibson (1991). "Studies of the primary oxygen intermediate in the reaction of fully reduced cytochrome oxidase." *J Biol Chem* **266**(29): 19245-9.

Blackshaw, S., M. J. Eliasson, A. Sawa, C. C. Watkins, D. Krug, A. Gupta, T. Arai, R. J. Ferrante and S. H. Snyder (2003). "Species, strain and developmental variations in hippocampal neuronal and endothelial nitric oxide synthase clarify discrepancies in nitric oxide-dependent synaptic plasticity." *Neuroscience* **119**(4): 979-90.

Bliss, T. V. and G. L. Collingridge (1993). "A synaptic model of memory: long-term potentiation in the hippocampus." *Nature* **361**(6407): 31-9.

Blumberg, W. E. (1981). "The study of hemoglobin by electron paramagnetic resonance spectroscopy." *Methods Enzymol* **76**: 312-29.

Boehm, J., I. Ehrlich, H. Hsieh and R. Malinow (2006). "Two mutations preventing PDZ-protein interactions of GluR1 have opposite effects on synaptic plasticity." *Learn Mem* **13**(5): 562-5.

Bolanos, J. P., S. J. Heales, J. M. Land and J. B. Clark (1995). "Effect of peroxynitrite on the mitochondrial respiratory chain: differential susceptibility of neurones and astrocytes in primary culture." *J Neurochem* **64**(5): 1965-72.

Bolanos, J. P., S. J. Heales, S. Peuchen, J. E. Barker, J. M. Land and J. B. Clark (1996). "Nitric oxide-mediated mitochondrial damage: a potential neuroprotective role for glutathione." *Free Radic Biol Med* **21**(7): 995-1001.

Borst, P., R. Evers, M. Kool and J. Wijnholds (1999). "The multidrug resistance protein family." *Biochim Biophys Acta* **1461**(2): 347-57.

Braughler, J. M., C. K. Mittal and F. Murad (1979). "Effects of thiols, sugars, and proteins on nitric oxide activation of guanylate cyclase." *J Biol Chem* **254**(24): 12450-4.

Brazell, M. P., R. J. Kasser, K. J. Renner, J. Feng, B. Moghaddam and R. N. Adams (1987). "Electrocoating carbon fiber microelectrodes with Nafion improves selectivity for electroactive neurotransmitters." *J Neurosci Methods* **22**(2): 167-72.

Bredt, D. S., C. E. Glatt, P. M. Hwang, M. Fotuhi, T. M. Dawson and S. H. Snyder (1991). "Nitric oxide synthase protein and mRNA are discretely localized in neuronal populations of the mammalian CNS together with NADPH diaphorase." *Neuron* **7**(4): 615-24.

Bredt, D. S., P. M. Hwang and S. H. Snyder (1990). "Localization of nitric oxide synthase indicating a neural role for nitric oxide." *Nature* **347**(6295): 768-70.

Bredt, D. S. and R. A. Nicoll (2003). "AMPA receptor trafficking at excitatory synapses." *Neuron* **40**(2): 361-79.

Bredt, D. S. and S. H. Snyder (1990). "Isolation of nitric oxide synthetase, a calmodulin-requiring enzyme." *Proc Natl Acad Sci U S A* **87**(2): 682-5.

Bredt, D. S. and S. H. Snyder (1994). "Nitric oxide: a physiologic messenger molecule." *Annu Rev Biochem* **63**: 175-95.

Brenman, J. E., D. S. Chao, S. H. Gee, A. W. McGee, S. E. Craven, D. R. Santillano, Z. Wu, F. Huang, H. Xia, M. F. Peters, S. C. Froehner and D. S. Bredt (1996). "Interaction of nitric oxide synthase with the postsynaptic density protein PSD-95 and alpha1-syntrophin mediated by PDZ domains." *Cell* **84**(5): 757-67.

Brigelius-Flohe, R. (1999). "Tissue-specific functions of individual glutathione peroxidases." *Free Radic Biol Med* **27**(9-10): 951-65.

Brigelius-Flohe, R. and M. G. Traber (1999). "Vitamin E: function and metabolism." *Faseb J* **13**(10): 1145-55.

Briviba, K., L. O. Klotz and H. Sies (1999). "Defenses against peroxynitrite." *Methods Enzymol* **301**: 301-11.

Brown, F. O. and J. P. Lowry (2003). "Microelectrochemical sensors for in vivo brain analysis: an investigation of procedures for modifying Pt electrodes using Nafion." *Analyst* **128**(6): 700-5.

Brown, G. C. (2001). "Regulation of mitochondrial respiration by nitric oxide inhibition of cytochrome c oxidase." *Biochim Biophys Acta* **1504**(1): 46-57.

Brown, G. C. (2007). "Nitric oxide and mitochondria." *Front Biosci* **12**: 1024-33.

Brown, G. C. and C. E. Cooper (1994). "Nanomolar concentrations of nitric oxide reversibly inhibit synaptosomal respiration by competing with oxygen at cytochrome oxidase." *FEBS Lett* **356**(2-3): 295-8.

Bruckdorfer, R. (2005). "The basics about nitric oxide." *Mol Aspects Med* **26**(1-2): 3-31.

Burette, A., U. Zabel, R. J. Weinberg, H. H. Schmidt and J. G. Valtschanoff (2002). "Synaptic localization of nitric oxide synthase and soluble guanylyl cyclase in the hippocampus." *J Neurosci* **22**(20): 8961-70.

Busse, R. and A. Mulsch (1990). "Induction of nitric oxide synthase by cytokines in vascular smooth muscle cells." *FEBS Lett* **275**(1-2): 87-90.

Calabrese, V., C. Mancuso, M. Calvani, E. Rizzarelli, D. A. Butterfield and A. M. Stella (2007). "Nitric oxide in the central nervous system: neuroprotection versus neurotoxicity." *Nat Rev Neurosci* **8**(10): 766-75.

Carlile, G. W., R. M. Chalmers-Redman, N. A. Tatton, A. Pong, K. E. Borden and W. G. Tatton (2000). "Reduced apoptosis after nerve growth factor and serum withdrawal: conversion of tetrameric glyceraldehyde-3-phosphate dehydrogenase to a dimer." *Mol Pharmacol* **57**(1): 2-12.

Cassina, A. and R. Radi (1996). "Differential inhibitory action of nitric oxide and peroxynitrite on mitochondrial electron transport." *Arch Biochem Biophys* **328**(2): 309-16.

Chen, C. J., S. L. Liao and J. S. Kuo (2000). "Gliotoxic action of glutamate on cultured astrocytes." *J Neurochem* **75**(4): 1557-65.

Chen, H. S. and S. A. Lipton (2006). "The chemical biology of clinically tolerated NMDA receptor antagonists." *J Neurochem* **97**(6): 1611-26.

Chen, H. X., E. Hanse, M. Pananceau and B. Gustafsson (1998). "Distinct expressions for synaptic potentiation induced by calcium through voltage-gated

calcium and N-methyl-D-aspartate receptor channels in the hippocampal CA1 region." *Neuroscience* **86**(2): 415-22.

Chetkovich, D. M., E. Klann and J. D. Sweatt (1993). "Nitric oxide synthase-independent long-term potentiation in area CA1 of hippocampus." *Neuroreport* **4**(7): 919-22.

Chittajallu, R., S. Alford and G. L. Collingridge (1998). "Ca2+ and synaptic plasticity." *Cell Calcium* **24**(5-6): 377-85.

Cho, H. J., Q. W. Xie, J. Calaycay, R. A. Mumford, K. M. Swiderek, T. D. Lee and C. Nathan (1992). "Calmodulin is a subunit of nitric oxide synthase from macrophages." *J Exp Med* **176**(2): 599-604.

Choi, Y. B., L. Tenneti, D. A. Le, J. Ortiz, G. Bai, H. S. Chen and S. A. Lipton (2000). "Molecular basis of NMDA receptor-coupled ion channel modulation by S-nitrosylation." *Nat Neurosci* **3**(1): 15-21.

Christopherson, K. S., B. J. Hillier, W. A. Lim and D. S. Bredt (1999). "PSD-95 assembles a ternary complex with the N-methyl-D-aspartic acid receptor and a bivalent neuronal NO synthase PDZ domain." *J Biol Chem* **274**(39): 27467-73.

Ciabarra, A. M., J. M. Sullivan, L. G. Gahn, G. Pecht, S. Heinemann and K. A. Sevarino (1995). "Cloning and characterization of chi-1: a developmentally regulated member of a novel class of the ionotropic glutamate receptor family." *J Neurosci* **15**(10): 6498-508.

Ciszewski, A. and G. Milczarek (2003). "Electrochemical detection of nitric oxide using polymer modified electrodes." *Talanta* **61**: 11-26.

Cleeter, M. W., J. M. Cooper, V. M. Darley-Usmar, S. Moncada and A. H. Schapira (1994). "Reversible inhibition of cytochrome c oxidase, the terminal enzyme of the mitochondrial respiratory chain, by nitric oxide. Implications for neurodegenerative diseases." *FEBS Lett* **345**(1): 50-4.

Clementi, E., G. C. Brown, M. Feelisch and S. Moncada (1998). "Persistent inhibition of cell respiration by nitric oxide: crucial role of S-nitrosylation of mitochondrial complex I and protective action of glutathione." *Proc Natl Acad Sci U S A* **95**(13): 7631-6.

Closs, E. I., J. S. Scheld, M. Sharafi and U. Forstermann (2000). "Substrate supply for nitric-oxide synthase in macrophages and endothelial cells: role of cationic amino acid transporters." *Mol Pharmacol* **57**(1): 68-74.

Collingridge, G. L., J. T. Isaac and Y. T. Wang (2004). "Receptor trafficking and synaptic plasticity." *Nat Rev Neurosci* **5**(12): 952-62.

Collingridge, G. L. and R. A. Lester (1989). "Excitatory amino acid receptors in the vertebrate central nervous system." *Pharmacol Rev* **41**(2): 143-210.

Conrad, L. C., C. M. Leonard and D. W. Pfaff (1974). "Connections of the median and dorsal raphe nuclei in the rat: an autoradiographic and degeneration study." *J Comp Neurol* **156**(2): 179-205.

Cossenza, M., D. V. Cadilhe, R. N. Coutinho and R. Paes-de-Carvalho (2006). "Inhibition of protein synthesis by activation of NMDA receptors in cultured retinal cells: a new mechanism for the regulation of nitric oxide production." *J Neurochem* **97**(5): 1481-93.

Cossenza, M. and R. Paes de Carvalho (2000). "L-arginine uptake and release by cultured avian retinal cells: differential cellular localization in relation to nitric oxide synthase." *J Neurochem* **74**(5): 1885-94.

Coyle, J. T. and P. Puttfarcken (1993). "Oxidative stress, glutamate, and neurodegenerative disorders." *Science* **262**(5134): 689-95.

Crane, B. R., R. J. Rosenfeld, A. S. Arvai, D. K. Ghosh, S. Ghosh, J. A. Tainer, D. J. Stuehr and E. D. Getzoff (1999). "N-terminal domain swapping and metal ion binding in nitric oxide synthase dimerization." *Embo J* **18**(22): 6271-81.

Czapski, G. A., M. Cakala, M. Chalimoniuk, B. Gajkowska and J. B. Strosznajder (2007). "Role of nitric oxide in the brain during lipopolysaccharide-evoked systemic inflammation." *J Neurosci Res* **85**(8): 1694-703.

Danbolt, N. C. (2001). "Glutamate uptake." *Prog Neurobiol* **65**(1): 1-105.

Davis, K. L., E. Martin, I. V. Turko and F. Murad (2001). "Novel effects of nitric oxide." *Annu Rev Pharmacol Toxicol* **41**: 203-36.

Dawson, V. L. and T. M. Dawson (1998). "Nitric oxide in neurodegeneration." *Prog Brain Res* **118**: 215-29.

Dawson, V. L., T. M. Dawson, E. D. London, D. S. Bredt and S. H. Snyder (1991). "Nitric oxide mediates glutamate neurotoxicity in primary cortical cultures." *Proc Natl Acad Sci U S A* **88**(14): 6368-71.

Demas, G. E., L. J. Kriegsfeld, S. Blackshaw, P. Huang, S. C. Gammie, R. J. Nelson and S. H. Snyder (1999). "Elimination of aggressive behavior in male mice lacking endothelial nitric oxide synthase." *J Neurosci* **19**(19): RC30.

Denninger, J. W. and M. A. Marletta (1999). "Guanylate cyclase and the.NO/cGMP signaling pathway." *Biochim Biophys Acta* **1411**(2-3): 334-50.

Dev, K. K. and B. J. Morris (1994). "Modulation of alpha-amino-3-hydroxy-5-methylisoxazole-4-propionic acid (AMPA) binding sites by nitric oxide." *J Neurochem* **63**(3): 946-52.

Diamond, J. S. (2005). "Deriving the glutamate clearance time course from transporter currents in CA1 hippocampal astrocytes: transmitter uptake gets faster during development." *J Neurosci* **25**(11): 2906-16.

Dinerman, J. L., T. M. Dawson, M. J. Schell, A. Snowman and S. H. Snyder (1994). "Endothelial nitric oxide synthase localized to hippocampal pyramidal cells: implications for synaptic plasticity." *Proc Natl Acad Sci U S A* **91**(10): 4214-8.

Dong, H., R. J. O'Brien, E. T. Fung, A. A. Lanahan, P. F. Worley and R. L. Huganir (1997). "GRIP: a synaptic PDZ domain-containing protein that interacts with AMPA receptors." *Nature* **386**(6622): 279-84.

Doyle, M. P. and J. W. Hoekstra (1981). "Oxidation of nitrogen oxides by bound dioxygen in hemoproteins." *J Inorg Biochem* **14**(4): 351-8.

Dringen, R. (2000). "Glutathione metabolism and oxidative stress in neurodegeneration." *Eur J Biochem* **267**(16): 4903.

Dringen, R. (2000). "Metabolism and functions of glutathione in brain." *Prog Neurobiol* **62**(6): 649-71.

Dringen, R., J. M. Gutterer, C. Gros and J. Hirrlinger (2001). "Aminopeptidase N mediates the utilization of the GSH precursor CysGly by cultured neurons." *J Neurosci Res* **66**(5): 1003-8.

Dringen, R. and B. Hamprecht (1996). "Glutathione content as an indicator for the presence of metabolic pathways of amino acids in astroglial cultures." *J Neurochem* **67**(4): 1375-82.

Dringen, R. and B. Hamprecht (1997). "Involvement of glutathione peroxidase and catalase in the disposal of exogenous hydrogen peroxide by cultured astroglial cells." *Brain Res* **759**(1): 67-75.

Dringen, R. and B. Hamprecht (1998). "Glutathione restoration as indicator for cellular metabolism of astroglial cells." *Dev Neurosci* **20**(4-5): 401-7.

Dringen, R., O. Kranich and B. Hamprecht (1997). "The gamma-glutamyl transpeptidase inhibitor acivicin preserves glutathione released by astroglial cells in culture." *Neurochem Res* **22**(6): 727-33.

Dringen, R., L. Kussmaul and B. Hamprecht (1998). "Detoxification of exogenous hydrogen peroxide and organic hydroperoxides by cultured astroglial cells assessed by microtiter plate assay." *Brain Res Brain Res Protoc* **2**(3): 223-8.

Dringen, R., B. Pfeiffer and B. Hamprecht (1999). "Synthesis of the antioxidant glutathione in neurons: supply by astrocytes of CysGly as precursor for neuronal glutathione." *J Neurosci* **19**(2): 562-9.

Drukarch, B., E. Schepens, C. A. Jongenelen, J. C. Stoof and C. H. Langeveld (1997). "Astrocyte-mediated enhancement of neuronal survival is abolished by glutathione deficiency." *Brain Res* **770**(1-2): 123-30.

Drukarch, B., E. Schepens, J. C. Stoof, C. H. Langeveld and F. L. Van Muiswinkel (1998). "Astrocyte-enhanced neuronal survival is mediated by scavenging of extracellular reactive oxygen species." *Free Radic Biol Med* **25**(2): 217-20.

Duncan, A. J. and S. J. Heales (2005). "Nitric oxide and neurological disorders." *Mol Aspects Med* **26**(1-2): 67-96.

Duport, S. and J. Garthwaite (2005). "Pathological consequences of inducible nitric oxide synthase expression in hippocampal slice cultures." *Neuroscience* **135**(4): 1155-66.

Duprat, A. F., T. G. Traylor, G. Z. Wu, M. Coletta, V. S. Sharma, K. N. Walda and D. Magde (1995). "Myoglobin-NO at low pH: free four-coordinated heme in the protein pocket." *Biochemistry* **34**(8): 2634-44.

East, S. J. and J. Garthwaite (1991). "NMDA receptor activation in rat hippocampus induces cyclic GMP formation through the L-arginine-nitric oxide pathway." *Neurosci Lett* **123**(1): 17-9.

Egebjerg, J., B. Bettler, I. Hermans-Borgmeyer and S. Heinemann (1991). "Cloning of a cDNA for a glutamate receptor subunit activated by kainate but not AMPA." *Nature* **351**(6329): 745-8.

Ehrhart, J. and G. D. Zeevalk (2001). "Hydrogen peroxide removal and glutathione mixed disulfide formation during metabolic inhibition in mesencephalic cultures." *J Neurochem* **77**(6): 1496-507.

Elfering, S. L., T. M. Sarkela and C. Giulivi (2002). "Biochemistry of mitochondrial nitric-oxide synthase." *J Biol Chem* **277**(41): 38079-86.

Ferreira, N. R., A. Ledo, J. G. Frade, G. A. Gerhardt, J. Laranjinha and R. M. Barbosa (2005). "Electrochemical measurement of endogenously produced nitric oxide in brain slices using Nafion/o-phenylenediamine modified carbon fiber microelectrodes." *Anal. Chim. Acta* **535**: 1-7.

Fielden, E. M., P. B. Roberts, R. C. Bray, D. J. Lowe, G. N. Mautner, G. Rotilio and L. Calabrese (1974). "Mechanism of action of superoxide dismutase from pulse radiolysis and electron paramagnetic resonance. Evidence that only half the active sites function in catalysis." *Biochem J* **139**(1): 49-60.

Ford, P. C., D. A. Wink and D. M. Stanbury (1993). "Autoxidation kinetics of aqueous nitric oxide." *FEBS Lett* **326**(1-3): 1-3.

Forfia, P. R., T. H. Hintze, M. S. Wolin and G. Kaley (1999). "Role of nitric oxide in the control of mitochondrial function." *Adv Exp Med Biol* **471**: 381-8.

Forstermann, U., E. I. Closs, J. S. Pollock, M. Nakane, P. Schwarz, I. Gath and H. Kleinert (1994). "Nitric oxide synthase isozymes. Characterization, purification, molecular cloning, and functions." *Hypertension* **23**(6 Pt 2): 1121-31.

Forstermann, U. and K. Ishii (1996). Measurement of cyclic GMP as an indicator of nitric oxide production. *Methods in nitric oxide research*. M. Feelisch and J. Stamler. New York, Wiley**:** 555-566.

Freir, D. B. and C. E. Herron (2003). "Inhibition of L-type voltage dependent calcium channels causes impairment of long-term potentiation in the hippocampal CA1 region in vivo." *Brain Res* **967**(1-2): 27-36.

Freund, T. F. and G. Buzsaki (1996). "Interneurons of the hippocampus." *Hippocampus* **6**(4): 347-470.

Fridovich, I. (1995). "Superoxide radical and superoxide dismutases." *Annu Rev Biochem* **64**: 97-112.

Friedemann, M. N., S. W. Robinson and G. A. Gerhardt (1996). "o-Phenylenediamine-modified carbon fiber electrodes for the detection of nitric oxide." *Anal Chem* **68**(15): 2621-8.

Furchgott, R. F. and J. V. Zawadzki (1980). "The obligatory role of endothelial cells in the relaxation of arterial smooth muscle by acetylcholine." *Nature* **288**(5789): 373-6.

Gachhui, R., H. M. Abu-Soud, D. K. Ghosha, A. Presta, M. A. Blazing, B. Mayer, S. E. George and D. J. Stuehr (1998). "Neuronal nitric-oxide synthase interaction with calmodulin-troponin C chimeras." *J Biol Chem* **273**(10): 5451-4.

Gadea, A. and A. M. Lopez-Colome (2001). "Glial transporters for glutamate, glycine and GABA I. Glutamate transporters." *J Neurosci Res* **63**(6): 453-60.

Garcia-Cardena, G., R. Fan, V. Shah, R. Sorrentino, G. Cirino, A. Papapetropoulos and W. C. Sessa (1998). "Dynamic activation of endothelial nitric oxide synthase by Hsp90." *Nature* **392**(6678): 821-4.

Garcia-Cardena, G., P. Oh, J. Liu, J. E. Schnitzer and W. C. Sessa (1996). "Targeting of nitric oxide synthase to endothelial cell caveolae via palmitoylation: implications for nitric oxide signaling." *Proc Natl Acad Sci U S A* **93**(13): 6448-53.

Gardner, S. M., K. Takamiya, J. Xia, J. G. Suh, R. Johnson, S. Yu and R. L. Huganir (2005). "Calcium-permeable AMPA receptor plasticity is mediated by subunit-specific interactions with PICK1 and NSF." *Neuron* **45**(6): 903-15.

Gardoni, F., A. Caputi, M. Cimino, L. Pastorino, F. Cattabeni and M. Di Luca (1998). "Calcium/calmodulin-dependent protein kinase II is associated with NR2A/B subunits of NMDA receptor in postsynaptic densities." *J Neurochem* **71**(4): 1733-41.

Garthwaite, J. and C. L. Boulton (1995). "Nitric oxide signaling in the central nervous system." *Annu Rev Physiol* **57**: 683-706.

Garthwaite, J., S. L. Charles and R. Chess-Williams (1988). "Endothelium-derived relaxing factor release on activation of NMDA receptors suggests role as intercellular messenger in the brain." *Nature* **336**(6197): 385-8.

Garthwaite, J., G. Garthwaite, R. M. Palmer and S. Moncada (1989). "NMDA receptor activation induces nitric oxide synthesis from arginine in rat brain slices." *Eur J Pharmacol* **172**(4-5): 413-6.

Gaston, B. (1999). "Nitric oxide and thiol groups." *Biochim Biophys Acta* **1411**(2-3): 323-33.

Ge, W. P., X. J. Yang, Z. Zhang, H. K. Wang, W. Shen, Q. D. Deng and S. Duan (2006). "Long-term potentiation of neuron-glia synapses mediated by Ca2+-permeable AMPA receptors." *Science* **312**(5779): 1533-7.

Gegg, M. E., B. Beltran, S. Salas-Pino, J. P. Bolanos, J. B. Clark, S. Moncada and S. J. Heales (2003). "Differential effect of nitric oxide on glutathione metabolism and mitochondrial function in astrocytes and neurones: implications for neuroprotection/neurodegeneration?" *J Neurochem* **86**(1): 228-37.

Gegg, M. E., J. B. Clark and S. J. Heales (2002). "Determination of glutamate-cysteine ligase (gamma-glutamylcysteine synthetase) activity by high-performance liquid chromatography and electrochemical detection." *Anal Biochem* **304**(1): 26-32.

Gegg, M. E., J. B. Clark and S. J. Heales (2005). "Co-culture of neurones with glutathione deficient astrocytes leads to increased neuronal susceptibility to nitric oxide and increased glutamate-cysteine ligase activity." *Brain Res* **1036**(1-2): 1-6.

Ghafourifar, P. and C. Richter (1997). "Nitric oxide synthase activity in mitochondria." *FEBS Lett* **418**(3): 291-6.

Giap, B. T., C. N. Jong, J. H. Ricker, N. K. Cullen and R. D. Zafonte (2000). "The hippocampus: anatomy, pathophysiology, and regenerative capacity." *J Head Trauma Rehabil* **15**(3): 875-94.

Giocomo, L. M. and M. E. Hasselmo (2006). "Difference in time course of modulation of synaptic transmission by group II versus group III metabotropic glutamate receptors in region CA1 of the hippocampus." *Hippocampus* **16**(11): 1004-16.

Giuffre, A., P. Sarti, E. D'Itri, G. Buse, T. Soulimane and M. Brunori (1996). "On the mechanism of inhibition of cytochrome c oxidase by nitric oxide." *J Biol Chem* **271**(52): 33404-8.

Giulivi, C. (2003). "Characterization and function of mitochondrial nitric-oxide synthase." *Free Radic Biol Med* **34**(4): 397-408.

Giulivi, C., J. J. Poderoso and A. Boveris (1998). "Production of nitric oxide by mitochondria." *J Biol Chem* **273**(18): 11038-43.

Gogas, K. R. (2006). "Glutamate-based therapeutic approaches: NR2B receptor antagonists." *Curr Opin Pharmacol* **6**(1): 68-74.

Greenstein, B. and A. Greenstein (2000). *Color Atlas of Neuroscience.* New York, Thieme.

Griffin, S., J. B. Clark and L. Canevari (2005). "Astrocyte-neurone communication following oxygen-glucose deprivation." *J Neurochem* **95**(4): 1015-22.

Griffith, O. W. (1999). "Biologic and pharmacologic regulation of mammalian glutathione synthesis." *Free Radic Biol Med* **27**(9-10): 922-35.

Griffith, O. W. and A. Meister (1979). "Glutathione: interorgan translocation, turnover, and metabolism." *Proc Natl Acad Sci U S A* **76**(11): 5606-10.

Grima, G., B. Benz and K. Q. Do (1997). "Glutamate-induced release of the nitric oxide precursor, arginine, from glial cells." *Eur J Neurosci* **9**(11): 2248-58.

Griscavage, J. M., J. M. Fukuto, Y. Komori and L. J. Ignarro (1994). "Nitric oxide inhibits neuronal nitric oxide synthase by interacting with the heme prosthetic group. Role of tetrahydrobiopterin in modulating the inhibitory action of nitric oxide." *J Biol Chem* **269**(34): 21644-9.

Grover, L. M. and T. J. Teyler (1990). "Two components of long-term potentiation induced by different patterns of afferent activation." *Nature* **347**(6292): 477-9.

Grover, L. M. and C. Yan (1999). "Evidence for involvement of group II/III metabotropic glutamate receptors in NMDA receptor-independent long-term potentiation in area CA1 of rat hippocampus." *J Neurophysiol* **82**(6): 2956-69.

Gruer, M. J., P. J. Artymiuk and J. R. Guest (1997). "The aconitase family: three structural variations on a common theme." *Trends Biochem Sci* **22**(1): 3-6.

Gryder, D. S., D. C. Castaneda and M. A. Rogawski (2005). "Evidence for low GluR2 AMPA receptor subunit expression at synapses in the rat basolateral amygdala." *J Neurochem* **94**(6): 1728-38.

Gryglewski, R. J., R. M. Palmer and S. Moncada (1986). "Superoxide anion is involved in the breakdown of endothelium-derived vascular relaxing factor." *Nature* **320**(6061): 454-6.

Hadjikoumi, I., A. Hassan and A. D. Milner (2002). "Exhaled nitric oxide measurements in childhood asthma: comparison of two sampling techniques." *Pediatr Res* **52**(5): 745-9.

Haley, J. E. (1998). "Gases as neurotransmitters." *Essays Biochem* **33**: 79-91.

Hall, C. N. and J. Garthwaite (2006). "Inactivation of nitric oxide by rat cerebellar slices." *J Physiol* **577**(Pt 2): 549-67.

Hamberger, A. and B. Nystrom (1984). "Extra- and intracellular amino acids in the hippocampus during development of hepatic encephalopathy." *Neurochem Res* **9**(9): 1181-92.

Hamprecht, B. and F. Loffler (1985). "Primary glial cultures as a model for studying hormone action." *Methods Enzymol* **109**: 341-5.

Han, D., R. Canali, J. Garcia, R. Aguilera, T. K. Gallaher and E. Cadenas (2005). "Sites and mechanisms of aconitase inactivation by peroxynitrite: modulation by citrate and glutathione." *Biochemistry* **44**(36): 11986-96.

Han, J., F. C. Cheng, Z. Yang and G. Dryhurst (1999). "Inhibitors of mitochondrial respiration, iron (II), and hydroxyl radical evoke release and extracellular hydrolysis of glutathione in rat striatum and substantia nigra: potential implications to Parkinson's disease." *J Neurochem* **73**(4): 1683-95.

Hara, M. R. and S. H. Snyder (2007). "Cell signaling and neuronal death." *Annu Rev Pharmacol Toxicol* **47**: 117-41.

Hardingham, G. E., Y. Fukunaga and H. Bading (2002). "Extrasynaptic NMDARs oppose synaptic NMDARs by triggering CREB shut-off and cell death pathways." *Nat Neurosci* **5**(5): 405-14.

Harris, K. M. and P. Sultan (1995). "Variation in the number, location and size of synaptic vesicles provides an anatomical basis for the nonuniform probability of release at hippocampal CA1 synapses." *Neuropharmacology* **34**(11): 1387-95.

Hayashi, Y., M. Nishio, Y. Naito, H. Yokokura, Y. Nimura, H. Hidaka and Y. Watanabe (1999). "Regulation of neuronal nitric-oxide synthase by calmodulin kinases." *J Biol Chem* **274**(29): 20597-602.

Heales, S. J., A. A. Lam, A. J. Duncan and J. M. Land (2004). "Neurodegeneration or neuroprotection: the pivotal role of astrocytes." *Neurochem Res* **29**(3): 513-9.

Hemmens, B., S. Woschitz, E. Pitters, B. Klosch, C. Volker, K. Schmidt and B. Mayer (1998). "The protein inhibitor of neuronal nitric oxide synthase (PIN): characterization of its action on pure nitric oxide synthases." *FEBS Lett* **430**(3): 397-400.

Hemmings, S. J. and K. B. Storey (1999). "Brain gamma-glutamyltranspeptidase: characteristics, development and thyroid hormone dependency of the enzyme in isolated microvessels and neuronal/glial cell plasma membranes." *Mol Cell Biochem* **202**(1-2): 119-30.

Hermann, A., V. Varga, R. Janaky, R. Dohovics, P. Saransaari and S. S. Oja (2000). "Interference of S-nitrosoglutathione with the binding of ligands to ionotropic glutamate receptors in pig cerebral cortical synaptic membranes." *Neurochem Res* **25**(8): 1119-24.

Hertz, L., R. Dringen, A. Schousboe and S. R. Robinson (1999). "Astrocytes: glutamate producers for neurons." *J Neurosci Res* **57**(4): 417-28.

Hertz, L., A. Schousboe, N. Boechler, S. Mukerji and S. Fedoroff (1978). "Kinetic characteristics of the glutamate uptake into normal astrocytes in cultures." *Neurochem Res* **3**(1): 1-14.

Hertz, L. and H. R. Zielke (2004). "Astrocytic control of glutamatergic activity: astrocytes as stars of the show." *Trends Neurosci* **27**(12): 735-43.

Hevel, J. M., K. A. White and M. A. Marletta (1991). "Purification of the inducible murine macrophage nitric oxide synthase. Identification as a flavoprotein." *J Biol Chem* **266**(34): 22789-91.

Hogg, N., V. M. Darley-Usmar, M. T. Wilson and S. Moncada (1993). "The oxidation of alpha-tocopherol in human low-density lipoprotein by the simultaneous generation of superoxide and nitric oxide." *FEBS Lett* **326**(1-3): 199-203.

Hollmann, M., M. Hartley and S. Heinemann (1991). "Ca2+ permeability of KA-AMPA--gated glutamate receptor channels depends on subunit composition." *Science* **252**(5007): 851-3.

Hollmann, M., A. O'Shea-Greenfield, S. W. Rogers and S. Heinemann (1989). "Cloning by functional expression of a member of the glutamate receptor family." *Nature* **342**(6250): 643-8.

Holmes, W. R. (1995). "Modeling the effect of glutamate diffusion and uptake on NMDA and non-NMDA receptor saturation." *Biophys J* **69**(5): 1734-47.

Holscher, C. (1997). "Nitric oxide, the enigmatic neuronal messenger: its role in synaptic plasticity." *Trends Neurosci* **20**(7): 298-303.

Homola, A., N. Zoremba, K. Slais, R. Kuhlen and E. Sykova (2006). "Changes in diffusion parameters, energy-related metabolites and glutamate in the rat cortex after transient hypoxia/ischemia." *Neurosci Lett* **404**(1-2): 137-42.

Hong, S. J., T. M. Dawson and V. L. Dawson (2004). "Nuclear and mitochondrial conversations in cell death: PARP-1 and AIF signaling." *Trends Pharmacol Sci* **25**(5): 259-64.

Hopper, R. A. and J. Garthwaite (2006). "Tonic and phasic nitric oxide signals in hippocampal long-term potentiation." *J Neurosci* **26**(45): 11513-21.

Hrbac, J., C. Gregor, M. Machova, J. Kralova, T. Bystron, M. Ciz and A. Lojek (2007). "Nitric oxide sensor based on carbon fiber covered with nickel porphyrin layer deposited using optimized electropolymerization procedure." *Bioelectrochemistry* **71**(1): 46-53.

Huang, C. S., L. S. Chang, M. E. Anderson and A. Meister (1993). "Catalytic and regulatory properties of the heavy subunit of rat kidney gamma-glutamylcysteine synthetase." *J Biol Chem* **268**(26): 19675-80.

Huang, Y., H. Y. Man, Y. Sekine-Aizawa, Y. Han, K. Juluri, H. Luo, J. Cheah, C. Lowenstein, R. L. Huganir and S. H. Snyder (2005). "S-nitrosylation of N-ethylmaleimide sensitive factor mediates surface expression of AMPA receptors." *Neuron* **46**(4): 533-40.

Huang, Y. Y., E. R. Kandel, L. Varshavsky, E. P. Brandon, M. Qi, R. L. Idzerda, G. S. McKnight and R. Bourtchouladze (1995). "A genetic test of the effects of mutations in PKA on mossy fiber LTP and its relation to spatial and contextual learning." *Cell* **83**(7): 1211-22.

Huang, Y. Y., X. C. Li and E. R. Kandel (1994). "cAMP contributes to mossy fiber LTP by initiating both a covalently mediated early phase and macromolecular synthesis-dependent late phase." *Cell* **79**(1): 69-79.

Hughes, M. N. (1999). "Relationships between nitric oxide, nitroxyl ion, nitrosonium cation and peroxynitrite." *Biochim Biophys Acta* **1411**(2-3): 263-72.

Huie, R. E. and S. Padmaja (1993). "The reaction of no with superoxide." *Free Radic Res Commun* **18**(4): 195-9.

Hume, R. I., R. Dingledine and S. F. Heinemann (1991). "Identification of a site in glutamate receptor subunits that controls calcium permeability." *Science* **253**(5023): 1028-31.

Hurst, R. D., S. Azam, A. Hurst and J. B. Clark (2001). "Nitric-oxide-induced inhibition of glyceraldehyde-3-phosphate dehydrogenase may mediate reduced endothelial cell monolayer integrity in an in vitro model blood-brain barrier." *Brain Res* **894**(2): 181-8.

Ichimori, K., C. M. Arroyo and H. Nakazawa (1996). "Electron spin resonance for spin trapping of 3,5-dibromo-4-nitrosobenzene sulfonate." *Methods Enzymol* **268**: 203-11.

Ignarro, L. J. (1990). "Haem-dependent activation of guanylate cyclase and cyclic GMP formation by endogenous nitric oxide: a unique transduction mechanism for transcellular signaling." *Pharmacol Toxicol* **67**(1): 1-7.

Ignarro, L. J. (1998). "Nitric oxide: an unique endogenous signaling molecule in vascular biology." *Nobel Lecture*.

Ignarro, L. J., G. M. Buga, K. S. Wood, R. E. Byrns and G. Chaudhuri (1987). "Endothelium-derived relaxing factor produced and released from artery and vein is nitric oxide." *Proc Natl Acad Sci U S A* **84**(24): 9265-9.

Iida, S., H. Ohshima, S. Oguchi, T. Hata, H. Suzuki, H. Kawasaki and H. Esumi (1992). "Identification of inducible calmodulin-dependent nitric oxide synthase in the liver of rats." *J Biol Chem* **267**(35): 25385-8.

Isa, T., S. Itazawa, M. Iino, K. Tsuzuki and S. Ozawa (1996). "Distribution of neurones expressing inwardly rectifying and Ca(2+)-permeable AMPA receptors in rat hippocampal slices." *J Physiol* **491 (Pt 3)**: 719-33.

Ishii, H., K. Shibuya, Y. Ohta, H. Mukai, S. Uchino, N. Takata, J. A. Rose and S. Kawato (2006). "Enhancement of nitric oxide production by association of nitric oxide synthase with N-methyl-D-aspartate receptors via postsynaptic density 95 in genetically engineered Chinese hamster ovary cells: real-time fluorescence imaging using nitric oxide sensitive dye." *J Neurochem* **96**(6): 1531-9.

Ishii, T., K. Moriyoshi, H. Sugihara, K. Sakurada, H. Kadotani, M. Yokoi, C. Akazawa, R. Shigemoto, N. Mizuno, M. Masu and et al. (1993). "Molecular characterization of the family of the N-methyl-D-aspartate receptor subunits." *J Biol Chem* **268**(4): 2836-43.

Ivanovic, A., H. Reilander, B. Laube and J. Kuhse (1998). "Expression and initial characterization of a soluble glycine binding domain of the N-methyl-D-aspartate receptor NR1 subunit." *J Biol Chem* **273**(32): 19933-7.

Izumi, Y. and C. F. Zorumski (1993). "Nitric oxide and long-term synaptic depression in the rat hippocampus." *Neuroreport* **4**(9): 1131-4.

Jaffrey, S. R., F. Benfenati, A. M. Snowman, A. J. Czernik and S. H. Snyder (2002). "Neuronal nitric-oxide synthase localization mediated by a ternary complex with synapsin and CAPON." *Proc Natl Acad Sci U S A* **99**(5): 3199-204.

Jaffrey, S. R., H. Erdjument-Bromage, C. D. Ferris, P. Tempst and S. H. Snyder (2001). "Protein S-nitrosylation: a physiological signal for neuronal nitric oxide." *Nat Cell Biol* **3**(2): 193-7.

Jaffrey, S. R., A. M. Snowman, M. J. Eliasson, N. A. Cohen and S. H. Snyder (1998). "CAPON: a protein associated with neuronal nitric oxide synthase that regulates its interactions with PSD95." *Neuron* **20**(1): 115-24.

Jaffrey, S. R. and S. H. Snyder (1996). "PIN: an associated protein inhibitor of neuronal nitric oxide synthase." *Science* **274**(5288): 774-7.

Jiang, M. H. and J. Hada (2007). "Early and sharp nitric oxide production and anoxic depolarization in the rat hippocampus during transient forebrain ischemia." *Eur J Pharmacol* **567**(1-2): 83-8.

Jonas, P. and B. Sakmann (1992). "Glutamate receptor channels in isolated patches from CA1 and CA3 pyramidal cells of rat hippocampal slices." *J Physiol* **455**: 143-71.

Josch, C., H. Sies and T. P. Akerboom (1998). "Hepatic mercapturic acid formation: involvement of cytosolic cysteinylglycine S-conjugate dipeptidase activity." *Biochem Pharmacol* **56**(6): 763-71.

Jourd'heuil, D., F. S. Laroux, A. M. Miles, D. A. Wink and M. B. Grisham (1999). "Effect of superoxide dismutase on the stability of S-nitrosothiols." *Arch Biochem Biophys* **361**(2): 323-30.

Ju, W., W. Morishita, J. Tsui, G. Gaietta, T. J. Deerinck, S. R. Adams, C. C. Garner, R. Y. Tsien, M. H. Ellisman and R. C. Malenka (2004). "Activity-dependent regulation of dendritic synthesis and trafficking of AMPA receptors." *Nat Neurosci* **7**(3): 244-53.

Kalyanaraman, B., H. Karoui, R. J. Singh and C. C. Felix (1996). "Detection of thiyl radical adducts formed during hydroxyl radical- and peroxynitrite-mediated oxidation of thiols--a high resolution ESR spin-trapping study at Q-band (35 GHz)." *Anal Biochem* **241**(1): 75-81.

Kang, Y., V. Viswanath, N. Jha, X. Qiao, J. Q. Mo and J. K. Andersen (1999). "Brain gamma-glutamyl cysteine synthetase (GCS) mRNA expression patterns correlate with regional-specific enzyme activities and glutathione levels." *J Neurosci Res* **58**(3): 436-41.

Kanner, J., S. Harel and R. Granit (1991). "Nitric oxide as an antioxidant." *Arch Biochem Biophys* **289**(1): 130-6.

Kawahara, Y., S. Kwak, H. Sun, K. Ito, H. Hashida, H. Aizawa, S. Y. Jeong and I. Kanazawa (2003). "Human spinal motoneurons express low relative abundance of GluR2 mRNA: an implication for excitotoxicity in ALS." *J Neurochem* **85**(3): 680-9.

Keefer, L. K., R. W. Nims, K. M. Davies and D. A. Wink (1996). ""NONOates" (1-substituted diazen-1-ium-1,2-diolates) as nitric oxide donors: convenient nitric oxide dosage forms." *Methods Enzymol* **268**: 281-93.

Keinanen, K., W. Wisden, B. Sommer, P. Werner, A. Herb, T. A. Verdoorn, B. Sakmann and P. H. Seeburg (1990). "A family of AMPA-selective glutamate receptors." *Science* **249**(4968): 556-60.

Kelm, M., R. Dahmann, D. Wink and M. Feelisch (1997). "The nitric oxide/superoxide assay. Insights into the biological chemistry of the NO/O-2. interaction." *J Biol Chem* **272**(15): 9922-32.

Kemp, J. A. and R. M. McKernan (2002). "NMDA receptor pathways as drug targets." *Nat Neurosci* **5 Suppl**: 1039-42.

Kharazia, V. N., P. Petrusz, K. Usunoff, R. J. Weinberg and A. Rustioni (1997). "Arginine and NADPH diaphorase in the rat ventroposterior thalamic nucleus." *Brain Res* **744**(1): 151-5.

Kim, C. H., H. J. Chung, H. K. Lee and R. L. Huganir (2001). "Interaction of the AMPA receptor subunit GluR2/3 with PDZ domains regulates hippocampal long-term depression." *Proc Natl Acad Sci U S A* **98**(20): 11725-30.

Kim, D. Y., S. H. Kim, H. B. Choi, C. Min and B. J. Gwag (2001). "High abundance of GluR1 mRNA and reduced Q/R editing of GluR2 mRNA in individual NADPH-diaphorase neurons." *Mol Cell Neurosci* **17**(6): 1025-33.

Kim, W. K., Y. B. Choi, P. V. Rayudu, P. Das, W. Asaad, D. R. Arnelle, J. S. Stamler and S. A. Lipton (1999). "Attenuation of NMDA receptor activity and neurotoxicity by nitroxyl anion, NO." *Neuron* **24**(2): 461-9.

Kirlin, W. G., J. Cai, S. A. Thompson, D. Diaz, T. J. Kavanagh and D. P. Jones (1999). "Glutathione redox potential in response to differentiation and enzyme inducers." *Free Radic Biol Med* **27**(11-12): 1208-18.

Klatt, P. and S. Lamas (2000). "Regulation of protein function by S-glutathiolation in response to oxidative and nitrosative stress." *Eur J Biochem* **267**(16): 4928-44.

Kojima, H., M. Hirotani, N. Nakatsubo, K. Kikuchi, Y. Urano, T. Higuchi, Y. Hirata and T. Nagano (2001). "Bioimaging of nitric oxide with fluorescent indicators based on the rhodamine chromophore." *Anal Chem* **73**(9): 1967-73.

Kojima, H., K. Kikuchi, M. Hirobe and T. Nagano (1997). "Real-time measurement of nitric oxide production in rat brain by the combination of luminol-H2O2 chemiluminescence and microdialysis." *Neurosci Lett* **233**(2-3): 157-9.

Komeima, K., Y. Hayashi, Y. Naito and Y. Watanabe (2000). "Inhibition of neuronal nitric-oxide synthase by calcium/ calmodulin-dependent protein kinase IIalpha through Ser847 phosphorylation in NG108-15 neuronal cells." *J Biol Chem* **275**(36): 28139-43.

Kone, B. C. (2000). "Protein-protein interactions controlling nitric oxide synthases." *Acta Physiol Scand* **168**(1): 27-31.

Kone, B. C., T. Kuncewicz, W. Zhang and Z. Y. Yu (2003). "Protein interactions with nitric oxide synthases: controlling the right time, the right place, and the right amount of nitric oxide." *Am J Physiol Renal Physiol* **285**(2): F178-90.

Koppenol, W. H. (1998). "The basic chemistry of nitrogen monoxide and peroxynitrite." *Free Radic Biol Med* **25**(4-5): 385-91.

Koppenol, W. H., J. J. Moreno, W. A. Pryor, H. Ischiropoulos and J. S. Beckman (1992). "Peroxynitrite, a cloaked oxidant formed by nitric oxide and superoxide." *Chem Res Toxicol* **5**(6): 834-42.

Kornau, H. C., L. T. Schenker, M. B. Kennedy and P. H. Seeburg (1995). "Domain interaction between NMDA receptor subunits and the postsynaptic density protein PSD-95." *Science* **269**(5231): 1737-40.

Kranich, O., R. Dringen, M. Sandberg and B. Hamprecht (1998). "Utilization of cysteine and cysteine precursors for the synthesis of glutathione in astroglial cultures: preference for cystine." *Glia* **22**(1): 11-8.

Kranich, O., B. Hamprecht and R. Dringen (1996). "Different preferences in the utilization of amino acids for glutathione synthesis in cultured neurons and astroglial cells derived from rat brain." *Neurosci Lett* **219**(3): 211-4.

Kristensen, B. W., J. Noraberg and J. Zimmer (2001). "Comparison of excitotoxic profiles of ATPA, AMPA, KA and NMDA in organotypic hippocampal slice cultures." *Brain Res* **917**(1): 21-44.

Krumenacker, J. S., K. A. Hanafy and F. Murad (2004). "Regulation of nitric oxide and soluble guanylyl cyclase." *Brain Res Bull* **62**(6): 505-15.

Kullmann, D. M. and K. P. Lamsa (2007). "Long-term synaptic plasticity in hippocampal interneurons." *Nat Rev Neurosci* **8**(9): 687-99.

Kutsuwada, T., N. Kashiwabuchi, H. Mori, K. Sakimura, E. Kushiya, K. Araki, H. Meguro, H. Masaki, T. Kumanishi, M. Arakawa and et al. (1992). "Molecular diversity of the NMDA receptor channel." *Nature* **358**(6381): 36-41.

Kwak, S. and J. H. Weiss (2006). "Calcium-permeable AMPA channels in neurodegenerative disease and ischemia." *Curr Opin Neurobiol* **16**(3): 281-7.

Kwok, E. S. and D. Howes (2006). "Use of methylene blue in sepsis: a systematic review." *J Intensive Care Med* **21**(6): 359-63.

Lai, C. S. and A. M. Komarov (1994). "Spin trapping of nitric oxide produced in vivo in septic-shock mice." *FEBS Lett* **345**(2-3): 120-4.

Lancaster, J. R., Jr. (1994). "Simulation of the diffusion and reaction of endogenously produced nitric oxide." *Proc Natl Acad Sci U S A* **91**(17): 8137-41.

Lancaster Jr., J. (1996). Nitric Oxide: Principles and Actions. J. Lancaster Jr. San Diego, Academic Press.

Ledo, A. (2007). *Dinâmica de concentração do óxido nítrico produzido no hipocampo de rato por activação de receptores do glutamato*, Universidade de Coimbra.

Ledo, A., R. M. Barbosa, J. Frade and J. Laranjinha (2002). "Nitric oxide monitoring in hippocampal brain slices using electrochemical methods." *Methods Enzymol* **359**: 111-25.

Ledo, A., R. M. Barbosa, G. A. Gerhardt, E. Cadenas and J. Laranjinha (2005). "Concentration dynamics of nitric oxide in rat hippocampal subregions evoked by stimulation of the NMDA glutamate receptor." *Proc Natl Acad Sci U S A* **102**(48): 17483-8.

Lehmann, A., H. Isacsson and A. Hamberger (1983). "Effects of in vivo administration of kainic acid on the extracellular amino acid pool in the rabbit hippocampus." *J Neurochem* **40**(5): 1314-20.

Lepoivre, M., J. M. Flaman and Y. Henry (1992). "Early loss of the tyrosyl radical in ribonucleotide reductase of adenocarcinoma cells producing nitric oxide." *J Biol Chem* **267**(32): 22994-3000.

Lerma, J., A. V. Paternain, A. Rodriguez-Moreno and J. C. Lopez-Garcia (2001). "Molecular physiology of kainate receptors." *Physiol Rev* **81**(3): 971-98.

Li, H., C. S. Raman, C. B. Glaser, E. Blasko, T. A. Young, J. F. Parkinson, M. Whitlow and T. L. Poulos (1999). "Crystal structures of zinc-free and -bound heme domain of human inducible nitric-oxide synthase. Implications for dimer stability and comparison with endothelial nitric-oxide synthase." *J Biol Chem* **274**(30): 21276-84.

Liao, S. L. and C. J. Chen (2003). "L-glutamate decreases glucose utilization by rat cortical astrocytes." *Neurosci Lett* **348**(2): 81-4.

Lipton, S. A., Y. B. Choi, Z. H. Pan, S. Z. Lei, H. S. Chen, N. J. Sucher, J. Loscalzo, D. J. Singel and J. S. Stamler (1993). "A redox-based mechanism for the neuroprotective and neurodestructive effects of nitric oxide and related nitroso-compounds." *Nature* **364**(6438): 626-32.

Lipton, S. A. and P. A. Rosenberg (1994). "Excitatory amino acids as a final common pathway for neurologic disorders." *N Engl J Med* **330**(9): 613-22.

Liu, D., G. Y. Xu, E. Pan and D. J. McAdoo (1999). "Neurotoxicity of glutamate at the concentration released upon spinal cord injury." *Neuroscience* **93**(4): 1383-9.

Liu, L., A. Hausladen, M. Zeng, L. Que, J. Heitman and J. S. Stamler (2001). "A metabolic enzyme for S-nitrosothiol conserved from bacteria to humans." *Nature* **410**(6827): 490-4.

Liu, L., T. P. Wong, M. F. Pozza, K. Lingenhoehl, Y. Wang, M. Sheng, Y. P. Auberson and Y. T. Wang (2004). "Role of NMDA receptor subtypes in governing the direction of hippocampal synaptic plasticity." *Science* **304**(5673): 1021-4.

Liu, P., P. F. Smith, I. Appleton, C. L. Darlington and D. K. Bilkey (2003). "Regional variations and age-related changes in nitric oxide synthase and arginase in the sub-regions of the hippocampus." *Neuroscience* **119**(3): 679-87.

Liu, S. J. and R. S. Zukin (2007). "Ca2+-permeable AMPA receptors in synaptic plasticity and neuronal death." *Trends Neurosci* **30**(3): 126-34.

Loesch, A., A. Belai and G. Burnstock (1994). "An ultrastructural study of NADPH-diaphorase and nitric oxide synthase in the perivascular nerves and vascular endothelium of the rat basilar artery." *J Neurocytol* **23**(1): 49-59.

Lonart, G., J. Wang and K. M. Johnson (1992). "Nitric oxide induces neurotransmitter release from hippocampal slices." *Eur J Pharmacol* **220**(2-3): 271-2.

Lores-Arnaiz, S., J. C. Perazzo, J. P. Prestifilippo, N. Lago, G. D'Amico, A. Czerniczyniec, J. Bustamante, A. Boveris and A. Lemberg (2005). "Hippocampal mitochondrial dysfunction with decreased mtNOS activity in prehepatic portal hypertensive rats." *Neurochem Int* **47**(5): 362-8.

Loy, R., D. A. Koziell, J. D. Lindsey and R. Y. Moore (1980). "Noradrenergic innervation of the adult rat hippocampal formation." *J Comp Neurol* **189**(4): 699-710.

Lucas, K. A., G. M. Pitari, S. Kazerounian, I. Ruiz-Stewart, J. Park, S. Schulz, K. P. Chepenik and S. A. Waldman (2000). "Guanylyl cyclases and signaling by cyclic GMP." *Pharmacol Rev* **52**(3): 375-414.

Lucas, S. M., N. J. Rothwell and R. M. Gibson (2006). "The role of inflammation in CNS injury and disease." *Br J Pharmacol* **147 Suppl 1**: S232-40.

Luperchio, S., S. Tamir and S. R. Tannenbaum (1996). "NO-induced oxidative stress and glutathione metabolism in rodent and human cells." *Free Radic Biol Med* **21**(4): 513-9.

Lynch, M. A., M. L. Errington and T. V. Bliss (1985). "Long-term potentiation of synaptic transmission in the dentate gyrus: increased release of [14C]glutamate without increase in receptor binding." *Neurosci Lett* **62**(1): 123-9.

MacDonald, J. F., M. F. Jackson and M. A. Beazely (2006). "Hippocampal long-term synaptic plasticity and signal amplification of NMDA receptors." *Crit Rev Neurobiol* **18**(1-2): 71-84.

Malinow, R. and R. W. Tsien (1990). "Presynaptic enhancement shown by whole-cell recordings of long-term potentiation in hippocampal slices." *Nature* **346**(6280): 177-80.

Malinski, T., S. Mesaros and P. Tomboulian (1996). "Nitric oxide measurement using electrochemical methods." *Methods Enzymol* **268**: 58-69.

Malinski, T. and Z. Taha (1992). "Nitric oxide release from a single cell measured in situ by a porphyrinic-based microsensor." *Nature* **358**(6388): 676-8.

Malinski, T., Z. Taha, S. Grunfeld, S. Patton, M. Kapturczak and P. Tomboulian (1993). "Diffusion of nitric oxide in the aorta wall monitored in situ by porphyrinic microsensors." *Biochem Biophys Res Commun* **193**(3): 1076-82.

Manabe, T. (1997). "Two forms of hippocampal long-term depression, the counterpart of long-term potentiation." *Rev Neurosci* **8**(3-4): 179-93.

Mannick, J. B. and C. M. Schonhoff (2002). "Nitrosylation: the next phosphorylation?" *Arch Biochem Biophys* **408**(1): 1-6.

Manzoni, O. and J. Bockaert (1993). "Nitric oxide synthase activity endogenously modulates NMDA receptors." *J Neurochem* **61**(1): 368-70.

Mark F. Bear, Barry W. Connors and M. A. Paradiso (1996). *Neuroscience: Exploring the Brain*, Williams & Wilkins, USA.

Mark, L. P., R. W. Prost, J. L. Ulmer, M. M. Smith, D. L. Daniels, J. M. Strottmann, W. D. Brown and L. Hacein-Bey (2001). "Pictorial review of glutamate excitotoxicity: fundamental concepts for neuroimaging." *AJNR Am J Neuroradiol* **22**(10): 1813-24.

Marletta, M. A. (1993). "Nitric oxide synthase structure and mechanism." *J Biol Chem* **268**(17): 12231-4.

Marletta, M. A., A. R. Hurshman and K. M. Rusche (1998). "Catalysis by nitric oxide synthase." *Curr Opin Chem Biol* **2**(5): 656-63.

Marsh, N. and A. Marsh (2000). "A short history of nitroglycerine and nitric oxide in pharmacology and physiology." *Clin Exp Pharmacol Physiol* **27**(4): 313-9.

Martinez-Ruiz, A. and S. Lamas (2004). "S-nitrosylation: a potential new paradigm in signal transduction." *Cardiovasc Res* **62**(1): 43-52.

Masters, B. S., K. McMillan, E. A. Sheta, J. S. Nishimura, L. J. Roman and P. Martasek (1996). "Neuronal nitric oxide synthase, a modular enzyme formed by convergent evolution: structure studies of a cysteine thiolate-liganded heme protein that hydroxylates L-arginine to produce NO. as a cellular signal." *Faseb J* **10**(5): 552-8.

Matsuda, H. and T. Iyanagi (1999). "Calmodulin activates intramolecular electron transfer between the two flavins of neuronal nitric oxide synthase flavin domain." *Biochim Biophys Acta* **1473**(2-3): 345-55.

Maurer, T. S. and H. L. Fung (2000). "Evaluation of nitric oxide synthase activity and inhibition kinetics by chemiluminescence." *Nitric Oxide* **4**(4): 372-8.

McAdoo, D. J., G. Y. Xu, G. Robak and M. G. Hughes (1999). "Changes in amino acid concentrations over time and space around an impact injury and their diffusion through the rat spinal cord." *Exp Neurol* **159**(2): 538-44.

McBain, C. J. and M. L. Mayer (1994). "N-methyl-D-aspartic acid receptor structure and function." *Physiol Rev* **74**(3): 723-60.

McBain, C. J., S. F. Traynelis and R. Dingledine (1990). "Regional variation of extracellular space in the hippocampus." *Science* **249**(4969): 674-7.

McDonald, K. K., S. Zharikov, E. R. Block and M. S. Kilberg (1997). "A caveolar complex between the cationic amino acid transporter 1 and endothelial nitric-oxide synthase may explain the   arginine paradox   ." *J. Biol. Chem.* **272**: 31213-31216.

Meffert, M. K., N. C. Calakos, R. H. Scheller and H. Schulman (1996). "Nitric oxide modulates synaptic vesicle docking fusion reactions." *Neuron* **16**(6): 1229-36.

Meffert, M. K., B. A. Premack and H. Schulman (1994). "Nitric oxide stimulates Ca(2+)-independent synaptic vesicle release." *Neuron* **12**(6): 1235-44.

Meguro, H., H. Mori, K. Araki, E. Kushiya, T. Kutsuwada, M. Yamazaki, T. Kumanishi, M. Arakawa, K. Sakimura and M. Mishina (1992). "Functional characterization of a heteromeric NMDA receptor channel expressed from cloned cDNAs." *Nature* **357**(6373): 70-4.

Meister, A. and M. E. Anderson (1983). "Glutathione." *Annu Rev Biochem* **52**: 711-60.

Meulemans, A. (2002). "A brain nitric oxide synthase study in the rat: production of a nitroso-compound NA and absence of nitric oxide synthesis." *Neurosci Lett* **321**(1-2): 115-9.

Micheva, K. D., J. Buchanan, R. W. Holz and S. J. Smith (2003). "Retrograde regulation of synaptic vesicle endocytosis and recycling." *Nat Neurosci* **6**(9): 925-32.

Miles, A. M., D. A. Wink, J. C. Cook and M. B. Grisham (1996). "Determination of nitric oxide using fluorescence spectroscopy." *Methods Enzymol* **268**: 105-20.

Millar, J. (1992). 1 - Extracellular Single and Multiple Unit Recording With Microelectrodes. *Monitoring Neuronal Activity*. J. A. Stamford, Oxford University Press.

Milner, B., L. R. Squire and E. R. Kandel (1998). "Cognitive neuroscience and the study of memory." *Neuron* **20**(3): 445-68.

Minich, T., J. Riemer, J. B. Schulz, P. Wielinga, J. Wijnholds and R. Dringen (2006). "The multidrug resistance protein 1 (Mrp1), but not Mrp5, mediates export of glutathione and glutathione disulfide from brain astrocytes." *J Neurochem* **97**(2): 373-84.

Mitchell, J. B., J. A. Cook, M. C. Krishna, W. DeGraff, J. Gamson, J. Fisher, D. Christodoulou and D. A. Wink (1996). "Radiation sensitisation by nitric oxide releasing agents." *Br J Cancer Suppl* **27**: S181-4.

Mohr, S., J. S. Stamler and B. Brune (1996). "Posttranslational modification of glyceraldehyde-3-phosphate dehydrogenase by S-nitrosylation and subsequent NADH attachment." *J Biol Chem* **271**(8): 4209-14.

Moncada, S., R. M. Palmer and R. J. Gryglewski (1986). "Mechanism of action of some inhibitors of endothelium-derived relaxing factor." *Proc Natl Acad Sci U S A* **83**(23): 9164-8.

Monfort, P., M. D. Munoz, E. Kosenko and V. Felipo (2002). "Long-term potentiation in hippocampus involves sequential activation of soluble guanylate cyclase, cGMP-dependent protein kinase, and cGMP-degrading phosphodiesterase." *J Neurosci* **22**(23): 10116-22.

Moriyoshi, K., M. Masu, T. Ishii, R. Shigemoto, N. Mizuno and S. Nakanishi (1991). "Molecular cloning and characterization of the rat NMDA receptor." *Nature* **354**(6348): 31-7.

Morris, R. G., P. Garrud, J. N. Rawlins and J. O'Keefe (1982). "Place navigation impaired in rats with hippocampal lesions." *Nature* **297**(5868): 681-3.

Mothet, J. P., A. T. Parent, H. Wolosker, R. O. Brady, Jr., D. J. Linden, C. D. Ferris, M. A. Rogawski and S. H. Snyder (2000). "D-serine is an endogenous ligand for the glycine site of the N-methyl-D-aspartate receptor." *Proc Natl Acad Sci U S A* **97**(9): 4926-31.

Murad, F. (1994). "The nitric oxide-cyclic GMP signal transduction system for intracellular and intercellular communication." *Recent Prog Horm Res* **49**: 239-48.

Nakamichi, N. and Y. Yoneda (2005). "Functional proteins involved in regulation of intracellular Ca(2+) for drug development: desensitization of N-methyl-D-aspartate receptor channels." *J Pharmacol Sci* **97**(3): 348-50.

Nakane, M., J. Mitchell, U. Forstermann and F. Murad (1991). "Phosphorylation by calcium calmodulin-dependent protein kinase II and protein kinase C modulates the activity of nitric oxide synthase." *Biochem Biophys Res Commun* **180**(3): 1396-402.

Nakano, M., H. Kimura, M. Hara, M. Kuroiwa, M. Kato, K. Totsune and T. Yoshikawa (1990). "A highly sensitive method for determining both Mn- and Cu-Zn superoxide dismutase activities in tissues and blood cells." *Anal Biochem* **187**(2): 277-80.

Nathan, C. and Q. W. Xie (1994). "Nitric oxide synthases: roles, tolls, and controls." *Cell* **78**(6): 915-8.

Nicholson, C. and E. Sykova (1998). "Extracellular space structure revealed by diffusion analysis." *Trends Neurosci* **21**(5): 207-15.

Nicoll, R. A. and R. C. Malenka (1995). "Contrasting properties of two forms of long-term potentiation in the hippocampus." *Nature* **377**(6545): 115-8.

Niethammer, M., E. Kim and M. Sheng (1996). "Interaction between the C terminus of NMDA receptor subunits and multiple members of the PSD-95 family of membrane-associated guanylate kinases." *J Neurosci* **16**(7): 2157-63.

Nims, R. W., J. C. Cook, M. C. Krishna, D. Christodoulou, C. M. Poore, A. M. Miles, M. B. Grisham and D. A. Wink (1996). "Colorimetric assays for nitric oxide and nitrogen oxide species formed from nitric oxide stock solutions and donor compounds." *Methods Enzymol* **268**: 93-105.

Nishi, M., H. Hinds, H. P. Lu, M. Kawata and Y. Hayashi (2001). "Motoneuron-specific expression of NR3B, a novel NMDA-type glutamate receptor subunit that works in a dominant-negative manner." *J Neurosci* **21**(23): RC185.

Noel, J., G. S. Ralph, L. Pickard, J. Williams, E. Molnar, J. B. Uney, G. L. Collingridge and J. M. Henley (1999). "Surface expression of AMPA receptors in hippocampal neurons is regulated by an NSF-dependent mechanism." *Neuron* **23**(2): 365-76.

Noh, K. M., H. Yokota, T. Mashiko, P. E. Castillo, R. S. Zukin and M. V. Bennett (2005). "Blockade of calcium-permeable AMPA receptors protects hippocampal neurons against global ischemia-induced death." *Proc Natl Acad Sci U S A* **102**(34): 12230-5.

Northington, F. J., R. C. Koehler, R. J. Traystman and L. J. Martin (1996). "Nitric oxide synthase 1 and nitric oxide synthase 3 protein expression is regionally and temporally regulated in fetal brain." *Brain Res Dev Brain Res* **95**(1): 1-14.

Nottingham, W. C. and J. R. Sutter (1989). "Kinetics of the oxidation of nitric oxide by chlorine and oxygen in non aqueous media." *Int J Chem Kinet* **25**: 375-381.

O'Dell, T. J., R. D. Hawkins, E. R. Kandel and O. Arancio (1991). "Tests of the roles of two diffusible substances in long-term potentiation: evidence for nitric oxide as a possible early retrograde messenger." *Proc Natl Acad Sci U S A* **88**(24): 11285-9.

O'Dell, T. J., P. L. Huang, T. M. Dawson, J. L. Dinerman, S. H. Snyder, E. R. Kandel and M. C. Fishman (1994). "Endothelial NOS and the blockade of LTP by NOS inhibitors in mice lacking neuronal NOS." *Science* **265**(5171): 542-6.

O'Riordan, K. J., I. C. Huang, M. Pizzi, P. Spano, F. Boroni, R. Egli, P. Desai, O. Fitch, L. Malone, H. J. Ahn, H. C. Liou, J. D. Sweatt and J. M. Levenson (2006). "Regulation

of nuclear factor kappaB in the hippocampus by group I metabotropic glutamate receptors." *J Neurosci* **26**(18): 4870-9.

Obrenovitch, T. P. and J. Urenjak (1997). "Altered glutamatergic transmission in neurological disorders: from high extracellular glutamate to excessive synaptic efficacy." *Prog Neurobiol* **51**(1): 39-87.

Oertner, T. G., B. L. Sabatini, E. A. Nimchinsky and K. Svoboda (2002). "Facilitation at single synapses probed with optical quantal analysis." *Nat Neurosci* **5**(7): 657-64.

Ogita, K., R. Enomoto, F. Nakahara, N. Ishitsubo and Y. Yoneda (1995). "A possible role of glutathione as an endogenous agonist at the N-methyl-D-aspartate recognition domain in rat brain." *J Neurochem* **64**(3): 1088-96.

Oja, S. S., R. Janaky, V. Varga and P. Saransaari (2000). "Modulation of glutamate receptor functions by glutathione." *Neurochem Int* **37**(2-3): 299-306.

Okada, D. (1992). "Two pathways of cyclic GMP production through glutamate receptor-mediated nitric oxide synthesis." *J Neurochem* **59**(4): 1203-10.

Okada, D. (1998). "Tetrahydrobiopterin-dependent stabilization of neuronal nitric oxide synthase dimer reduces susceptibility to phosphorylation by protein kinase C in vitro." *FEBS Lett* **434**(3): 261-4.

Okada, D., C. C. Yap, H. Kojima, K. Kikuchi and T. Nagano (2004). "Distinct glutamate receptors govern differential levels of nitric oxide production in a layer-specific manner in the rat cerebellar cortex." *Neuroscience* **125**(2): 461-72.

Opitz, T., S. Y. Grooms, M. V. Bennett and R. S. Zukin (2000). "Remodeling of alpha-amino-3-hydroxy-5-methyl-4-isoxazole-propionic acid receptor subunit composition in hippocampal neurons after global ischemia." *Proc Natl Acad Sci U S A* **97**(24): 13360-5.

Oppenheimer, L., V. P. Wellner, O. W. Griffith and A. Meister (1979). "Glutathione synthetase. Purification from rat kidney and mapping of the substrate binding sites." *J Biol Chem* **254**(12): 5184-90.

Orwar, O., X. Li, P. Andine, C. M. Bergstrom, H. Hagberg, S. Folestad and M. Sandberg (1994). "Increased intra- and extracellular concentrations of gamma-glutamylglutamate and related dipeptides in the ischemic rat striatum: involvement of glutamyl transpeptidase." *J Neurochem* **63**(4): 1371-6.

Osen, K. K., J. Storm-Mathisen, O. P. Ottersen and B. Dihle (1995). "Glutamate is concentrated in and released from parallel fiber terminals in the dorsal cochlear nucleus: a quantitative immunocytochemical analysis in guinea pig." *J Comp Neurol* **357**(3): 482-500.

Pacher, P., J. S. Beckman and L. Liaudet (2007). "Nitric oxide and peroxynitrite in health and disease." *Physiol Rev* **87**(1): 315-424.

Padgett, C. M. and A. R. Whorton (1997). "Glutathione redox cycle regulates nitric oxide-mediated glyceraldehyde-3-phosphate dehydrogenase inhibition." *Am J Physiol* **272**(1 Pt 1): C99-108.

Padmaja, S. and R. E. Huie (1993). "The reaction of nitric oxide with organic peroxyl radicals." *Biochem Biophys Res Commun* **195**(2): 539-44.

Palmer, R. M., D. S. Ashton and S. Moncada (1988). "Vascular endothelial cells synthesize nitric oxide from L-arginine." *Nature* **333**(6174): 664-6.

Palmer, R. M., A. G. Ferrige and S. Moncada (1987). "Nitric oxide release accounts for the biological activity of endothelium-derived relaxing factor." *Nature* **327**(6122): 524-6.

Palmer, R. M., D. D. Rees, D. S. Ashton and S. Moncada (1988). "L-arginine is the physiological precursor for the formation of nitric oxide in endothelium-dependent relaxation." *Biochem Biophys Res Commun* **153**(3): 1251-6.

Panda, K., S. Ghosh and D. J. Stuehr (2001). "Calmodulin activates intersubunit electron transfer in the neuronal nitric-oxide synthase dimer." *J Biol Chem* **276**(26): 23349-56.

Panda, K., R. J. Rosenfeld, S. Ghosh, A. L. Meade, E. D. Getzoff and D. J. Stuehr (2002). "Distinct dimer interaction and regulation in nitric-oxide synthase types I, II, and III." *J Biol Chem* **277**(34): 31020-30.

Pellerin, L. (2005). "How astrocytes feed hungry neurons." *Mol Neurobiol* **32**(1): 59-72.

Pineda-Molina, E., P. Klatt, J. Vazquez, A. Marina, M. Garcia de Lacoba, D. Perez-Sala and S. Lamas (2001). "Glutathionylation of the p50 subunit of NF-kappaB: a mechanism for redox-induced inhibition of DNA binding." *Biochemistry* **40**(47): 14134-42.

Plant, K., K. A. Pelkey, Z. A. Bortolotto, D. Morita, A. Terashima, C. J. McBain, G. L. Collingridge and J. T. Isaac (2006). "Transient incorporation of native GluR2-lacking AMPA receptors during hippocampal long-term potentiation." *Nat Neurosci* **9**(5): 602-4.

Pollock, J. S., U. Forstermann, J. A. Mitchell, T. D. Warner, H. H. Schmidt, M. Nakane and F. Murad (1991). "Purification and characterization of particulate endothelium-derived relaxing factor synthase from cultured and native bovine aortic endothelial cells." *Proc Natl Acad Sci U S A* **88**(23): 10480-4.

Pontié, M., F. Bedioui and J. Devynck (1996). "New composite modified carbon microfibers for sensitive and selective determination of physiologically relevant concentrations of nitric oxide in solution." *Electroanalysis* **11**(12): 845-850.

Porter, J. T. and K. D. McCarthy (1996). "Hippocampal astrocytes in situ respond to glutamate released from synaptic terminals." *J Neurosci* **16**(16): 5073-81.

Porter, J. T. and K. D. McCarthy (1997). "Astrocytic neurotransmitter receptors in situ and in vivo." *Prog Neurobiol* **51**(4): 439-55.

Pou, S., W. S. Pou, D. S. Bredt, S. H. Snyder and G. M. Rosen (1992). "Generation of superoxide by purified brain nitric oxide synthase." *J Biol Chem* **267**(34): 24173-6.

Prast, H. and A. Philippu (2001). "Nitric oxide as modulator of neuronal function." *Prog Neurobiol* **64**(1): 51-68.

Puppo, A. and B. Halliwell (1988). "Formation of hydroxyl radicals from hydrogen peroxide in the presence of iron. Is haemoglobin a biological Fenton reagent?" *Biochem J* **249**(1): 185-90.

Qiu, W., D. A. Kass, Q. Hu and R. C. Ziegelstein (2001). "Determinants of shear stress-stimulated endothelial nitric oxide production assessed in real-time by 4,5-diaminofluorescein fluorescence." *Biochem Biophys Res Commun* **286**(2): 328-35.

Quijano, C., B. Alvarez, R. M. Gatti, O. Augusto and R. Radi (1997). "Pathways of peroxynitrite oxidation of thiol groups." *Biochem J* **322 (Pt 1)**: 167-73.

Radenovic, L. and V. Selakovic (2005). "Differential effects of NMDA and AMPA/kainate receptor antagonists on nitric oxide production in rat brain following intrahippocampal injection." *Brain Res Bull* **67**(1-2): 133-41.

Radi, R., J. S. Beckman, K. M. Bush and B. A. Freeman (1991). "Peroxynitrite oxidation of sulfhydryls. The cytotoxic potential of superoxide and nitric oxide." *J Biol Chem* **266**(7): 4244-50.

Radi, R., A. Cassina and R. Hodara (2002). "Nitric oxide and peroxynitrite interactions with mitochondria." *Biol Chem* **383**(3-4): 401-9.

Radomski, M. W., R. M. Palmer and S. Moncada (1990). "Glucocorticoids inhibit the expression of an inducible, but not the constitutive, nitric oxide synthase in vascular endothelial cells." *Proc Natl Acad Sci U S A* **87**(24): 10043-7.

Rameau, G. A., L. Y. Chiu and E. B. Ziff (2003). "NMDA receptor regulation of nNOS phosphorylation and induction of neuron death." *Neurobiol Aging* **24**(8): 1123-33.

Rameau, G. A., L. Y. Chiu and E. B. Ziff (2004). "Bidirectional regulation of neuronal nitric-oxide synthase phosphorylation at serine 847 by the N-methyl-D-aspartate receptor." *J Biol Chem* **279**(14): 14307-14.

Rameau, G. A., D. S. Tukey, E. D. Garcin-Hosfield, R. F. Titcombe, C. Misra, L. Khatri, E. D. Getzoff and E. B. Ziff (2007). "Biphasic coupling of neuronal nitric oxide synthase phosphorylation to the NMDA receptor regulates AMPA receptor trafficking and neuronal cell death." *J Neurosci* **27**(13): 3445-55.

Ransom, B., T. Behar and M. Nedergaard (2003). "New roles for astrocytes (stars at last)." *Trends Neurosci* **26**(10): 520-2.

Riederer, P., E. Sofic, W. D. Rausch, B. Schmidt, G. P. Reynolds, K. Jellinger and M. B. Youdim (1989). "Transition metals, ferritin, glutathione, and ascorbic acid in parkinsonian brains." *J Neurochem* **52**(2): 515-20.

Ritz, M. F., P. Schmidt and A. Mendelowitsch (2004). "Acute effects of 17beta-estradiol on the extracellular concentration of excitatory amino acids and energy metabolites during transient cerebral ischemia in male rats." *Brain Res* **1022**(1-2): 157-63.

Roman, L. J., R. T. Miller, M. A. de La Garza, J. J. Kim and B. S. Siler Masters (2000). "The C terminus of mouse macrophage inducible nitric-oxide synthase attenuates electron flow through the flavin domain." *J Biol Chem* **275**(29): 21914-9.

Rothwell, N. J. and G. N. Luheshi (2000). "Interleukin 1 in the brain: biology, pathology and therapeutic target." *Trends Neurosci* **23**(12): 618-25.

Roychowdhury, S., J. Noack, M. Engelmann, G. Wolf and T. F. Horn (2006). "AMPA receptor-induced intracellular calcium response in the paraventricular nucleus is modulated by nitric oxide: calcium imaging in a hypothalamic organotypic cell culture model." *Nitric Oxide* **14**(4): 290-9.

Rubbo, H., R. Radi, M. Trujillo, R. Telleri, B. Kalyanaraman, S. Barnes, M. Kirk and B. A. Freeman (1994). "Nitric oxide regulation of superoxide and peroxynitrite-dependent lipid peroxidation. Formation of novel nitrogen-containing oxidized lipid derivatives." *J Biol Chem* **269**(42): 26066-75.

Sagara, J., N. Makino and S. Bannai (1996). "Glutathione efflux from cultured astrocytes." *J Neurochem* **66**(5): 1876-81.

Sagara, J. I., K. Miura and S. Bannai (1993). "Maintenance of neuronal glutathione by glial cells." *J Neurochem* **61**(5): 1672-6.

Sakai, T., H. Takenaka and E. Torikai (1986). "Gas diffusion in the dried and hydrated Nafions." *J Electrochem Soc* **133**: 88-92.

Salerno, J. C., D. E. Harris, K. Irizarry, B. Patel, A. J. Morales, S. M. Smith, P. Martasek, L. J. Roman, B. S. Masters, C. L. Jones, B. A. Weissman, P. Lane, Q. Liu and S. S. Gross (1997). "An autoinhibitory control element defines calcium-regulated isoforms of nitric oxide synthase." *J Biol Chem* **272**(47): 29769-77.

Santolini, J., S. Adak, C. M. Curran and D. J. Stuehr (2001). "A kinetic simulation model that describes catalysis and regulation in nitric-oxide synthase." *J Biol Chem* **276**(2): 1233-43.

Santschi, L., M. Reyes-Harde and P. K. Stanton (1999). "Chemically induced, activity-independent LTD elicited by simultaneous activation of PKG and inhibition of PKA." *J Neurophysiol* **82**(3): 1577-89.

Sattler, R. and M. Tymianski (2000). "Molecular mechanisms of calcium-dependent excitotoxicity." *J Mol Med* **78**(1): 3-13.

Sattler, R. and M. Tymianski (2001). "Molecular mechanisms of glutamate receptor-mediated excitotoxic neuronal cell death." *Mol Neurobiol* **24**(1-3): 107-29.

Sattler, R., Z. Xiong, W. Y. Lu, M. Hafner, J. F. MacDonald and M. Tymianski (1999). "Specific coupling of NMDA receptor activation to nitric oxide neurotoxicity by PSD-95 protein." *Science* **284**(5421): 1845-8.

Schmidt, H. H., J. S. Pollock, M. Nakane, L. D. Gorsky, U. Forstermann and F. Murad (1991). "Purification of a soluble isoform of guanylyl cyclase-activating-factor synthase." *Proc Natl Acad Sci U S A* **88**(2): 365-9.

Schulz, J. B., J. Lindenau, J. Seyfried and J. Dichgans (2000). "Glutathione, oxidative stress and neurodegeneration." *Eur J Biochem* **267**(16): 4904-11.

Schuman, E. M. (1997). "Synapse specificity and long-term information storage." *Neuron* **18**(3): 339-42.

Schuman, E. M. and D. V. Madison (1991). "A requirement for the intercellular messenger nitric oxide in long-term potentiation." *Science* **254**(5037): 1503-6.

Schwartz, S. E. and W. H. White (1983). Kinetics of reactive dissolutions of nitrogen oxides into aqueous solutions. *Trace atmospheric constituents. Properties, transformation and fates.* New York, John Wiley and Sons**:** 1-117.

Scoville, W. B. and B. Milner (1957). "Loss of recent memory after bilateral hippocampal lesions." *J Neurol Neurosurg Psychiatry* **20**(1): 11-21.

Semmler, A., T. Okulla, M. Sastre, L. Dumitrescu-Ozimek and M. T. Heneka (2005). "Systemic inflammation induces apoptosis with variable vulnerability of different brain regions." *J Chem Neuroanat* **30**(2-3): 144-57.

Sen, N. P. and B. Donaldson (1978). "Improved colorimetric method for determining nitrate and nitrate in foods." *J Assoc Off Anal Chem* **61**(6): 1389-94.

Shi, S. H., Y. Hayashi, R. S. Petralia, S. H. Zaman, R. J. Wenthold, K. Svoboda and R. Malinow (1999). "Rapid spine delivery and redistribution of AMPA receptors after synaptic NMDA receptor activation." *Science* **284**(5421): 1811-6.

Shibuki, K. (1990). "An electrochemical microprobe for detecting nitric oxide release in brain tissue." *Neurosci Res* **9**(1): 69-76.

Shih, A. Y., D. A. Johnson, G. Wong, A. D. Kraft, L. Jiang, H. Erb, J. A. Johnson and T. H. Murphy (2003). "Coordinate regulation of glutathione biosynthesis and release by Nrf2-expressing glia potently protects neurons from oxidative stress." *J Neurosci* **23**(8): 3394-406.

Siddhanta, U., A. Presta, B. Fan, D. Wolan, D. L. Rousseau and D. J. Stuehr (1998). "Domain swapping in inducible nitric-oxide synthase. Electron transfer occurs between flavin and heme groups located on adjacent subunits in the dimer." *J Biol Chem* **273**(30): 18950-8.

Sies, H. (1999). "Glutathione and its role in cellular functions." *Free Radic Biol Med* **27**(9-10): 916-21.

Singh, S. P., J. S. Wishnok, M. Keshive, W. M. Deen and S. R. Tannenbaum (1996). "The chemistry of the S-nitrosoglutathione/glutathione system." *Proc Natl Acad Sci U S A* **93**(25): 14428-33.

Sirover, M. A. (1999). "New insights into an old protein: the functional diversity of mammalian glyceraldehyde-3-phosphate dehydrogenase." *Biochim Biophys Acta* **1432**(2): 159-84.

Sohn, J. W., D. Lee, H. Cho, W. Lim, H. S. Shin, S. H. Lee and W. K. Ho (2007). "Receptor-specific inhibition of GABAB-activated K+ currents by muscarinic and metabotropic glutamate receptors in immature rat hippocampus." *J Physiol* **580**(Pt. 2): 411-22.

Sommer, B., M. Kohler, R. Sprengel and P. H. Seeburg (1991). "RNA editing in brain controls a determinant of ion flow in glutamate-gated channels." *Cell* **67**(1): 11-9.

Son, H., R. D. Hawkins, K. Martin, M. Kiebler, P. L. Huang, M. C. Fishman and E. R. Kandel (1996). "Long-term potentiation is reduced in mice that are doubly mutant in endothelial and neuronal nitric oxide synthase." *Cell* **87**(6): 1015-23.

Son, H., Y. F. Lu, M. Zhuo, O. Arancio, E. R. Kandel and R. D. Hawkins (1998). "The specific role of cGMP in hippocampal LTP." *Learn Mem* **5**(3): 231-45.

Song, T., N. Hatano, M. Horii, H. Tokumitsu, F. Yamaguchi, M. Tokuda and Y. Watanabe (2004). "Calcium/calmodulin-dependent protein kinase I inhibits neuronal nitric-oxide synthase activity through serine 741 phosphorylation." *FEBS Lett* **570**(1-3): 133-7.

Sossa, K. G., J. B. Beattie and R. C. Carroll (2007). "AMPAR exocytosis through NO modulation of PICK1." *Neuropharmacology* **53**(1): 92-100.

Squire, L. R. and E. R. Kandel (1999). *Memory: from mind to molecules*. New York, Scientif American Library.

Squire, L. R. and S. Zola-Morgan (1991). "The medial temporal lobe memory system." *Science* **253**(5026): 1380-6.

Stamford, J. A., F. Crespi and C. A. Marsden (1992). 5 - In Vivo Voltammetric Methods for Monitoring Monoamine Release and Metabolism. *Monitoring Neuronal Activity*. J. A. Stamford, Oxford University Press**:** 113-45.

Stamler, J. S. (1994). "Redox signaling: nitrosylation and related target interactions of nitric oxide." *Cell* **78**(6): 931-6.

Stamler, J. S., S. Lamas and F. C. Fang (2001). "Nitrosylation. the prototypic redox-based signaling mechanism." *Cell* **106**(6): 675-83.

Stanton, P. K., J. Winterer, C. P. Bailey, A. Kyrozis, I. Raginov, G. Laube, R. W. Veh, C. Q. Nguyen and W. Muller (2003). "Long-term depression of presynaptic release from the readily releasable vesicle pool induced by NMDA receptor-dependent retrograde nitric oxide." *J Neurosci* **23**(13): 5936-44.

Stein, V., D. R. House, D. S. Bredt and R. A. Nicoll (2003). "Postsynaptic density-95 mimics and occludes hippocampal long-term potentiation and enhances long-term depression." *J Neurosci* **23**(13): 5503-6.

Stewart, V. C., A. J. Heslegrave, G. C. Brown, J. B. Clark and S. J. Heales (2002). "Nitric oxide-dependent damage to neuronal mitochondria involves the NMDA receptor." *Eur J Neurosci* **15**(3): 458-64.

Stewart, V. C., R. Stone, M. E. Gegg, M. A. Sharpe, R. D. Hurst, J. B. Clark and S. J. Heales (2002). "Preservation of extracellular glutathione by an astrocyte derived factor with properties comparable to extracellular superoxide dismutase." *J Neurochem* **83**(4): 984-91.

Stole, E., T. K. Smith, J. M. Manning and A. Meister (1994). "Interaction of gamma-glutamyl transpeptidase with acivicin." *J Biol Chem* **269**(34): 21435-9.

Stone, J. R. and M. A. Marletta (1994). "Soluble guanylate cyclase from bovine lung: activation with nitric oxide and carbon monoxide and spectral characterization of the ferrous and ferric states." *Biochemistry* **33**(18): 5636-40.

Storm-Mathisen, J., N. C. Danbolt, F. Rothe, R. Torp, N. Zhang, J. E. Aas, B. I. Kanner, I. Langmoen and O. P. Ottersen (1992). "Ultrastructural immunocytochemical observations on the localization, metabolism and transport of glutamate in normal and ischemic brain tissue." *Prog Brain Res* **94**: 225-41.

Streit, W. J., M. B. Graeber and G. W. Kreutzberg (1988). "Functional plasticity of microglia: a review." *Glia* **1**(5): 301-7.

Stuehr, D., S. Pou and G. M. Rosen (2001). "Oxygen reduction by nitric-oxide synthases." *J Biol Chem* **276**(18): 14533-6.

Stuehr, D. J. (1997). "Structure-function aspects in the nitric oxide synthases." *Annu Rev Pharmacol Toxicol* **37**: 339-59.

Stuehr, D. J., H. J. Cho, N. S. Kwon, M. F. Weise and C. F. Nathan (1991). "Purification and characterization of the cytokine-induced macrophage nitric oxide synthase: an FAD- and FMN-containing flavoprotein." *Proc Natl Acad Sci U S A* **88**(17): 7773-7.

Stuehr, D. J., N. S. Kwon, C. F. Nathan, O. W. Griffith, P. L. Feldman and J. Wiseman (1991). "N omega-hydroxy-L-arginine is an intermediate in the biosynthesis of nitric oxide from L-arginine." *J Biol Chem* **266**(10): 6259-63.

Sucher, N. J., S. Akbarian, C. L. Chi, C. L. Leclerc, M. Awobuluyi, D. L. Deitcher, M. K. Wu, J. P. Yuan, E. G. Jones and S. A. Lipton (1995). "Developmental and regional expression pattern of a novel NMDA receptor-like subunit (NMDAR-L) in the rodent brain." *J Neurosci* **15**(10): 6509-20.

Sudhof, T. C., A. J. Czernik, H. T. Kao, K. Takei, P. A. Johnston, A. Horiuchi, S. D. Kanazir, M. A. Wagner, M. S. Perin, P. De Camilli and et al. (1989). "Synapsins: mosaics of shared and individual domains in a family of synaptic vesicle phosphoproteins." *Science* **245**(4925): 1474-80.

Sun, H., Y. Kawahara, K. Ito, I. Kanazawa and S. Kwak (2005). "Expression profile of AMPA receptor subunit mRNA in single adult rat brain and spinal cord neurons in situ." *Neurosci Res* **52**(3): 228-34.

Sun, W. M., Z. Z. Huang and S. C. Lu (1996). "Regulation of gamma-glutamylcysteine synthetase by protein phosphorylation." *Biochem J* **320 (Pt 1)**: 321-8.

Swanson, C. J., M. Bures, M. P. Johnson, A. M. Linden, J. A. Monn and D. D. Schoepp (2005). "Metabotropic glutamate receptors as novel targets for anxiety and stress disorders." *Nat Rev Drug Discov* **4**(2): 131-44.

Taha, Z. H. (2003). "Nitric oxide measurements in biological samples." *Talanta* **61**: 3-10.

Takata, N., T. Harada, J. A. Rose and S. Kawato (2005). "Spatiotemporal analysis of NO production upon NMDA and tetanic stimulation of the hippocampus." *Hippocampus* **15**(4): 427-40.

Terashima, A., L. Cotton, K. K. Dev, G. Meyer, S. Zaman, F. Duprat, J. M. Henley, G. L. Collingridge and J. T. Isaac (2004). "Regulation of synaptic strength and AMPA receptor subunit composition by PICK1." *J Neurosci* **24**(23): 5381-90.

Tiso, M., J. Tejero, K. Panda, K. S. Aulak and D. J. Stuehr (2007). "Versatile regulation of neuronal nitric oxide synthase by specific regions of its C-terminal tail." *Biochemistry* **46**(50): 14418-28.

Tomita, S., R. A. Nicoll and D. S. Bredt (2001). "PDZ protein interactions regulating glutamate receptor function and plasticity." *J Cell Biol* **153**(5): F19-24.

Torres, J., V. Darley-Usmar and M. T. Wilson (1995). "Inhibition of cytochrome c oxidase in turnover by nitric oxide: mechanism and implications for control of respiration." *Biochem J* **312 (Pt 1)**: 169-73.

Torres, J., M. A. Sharpe, A. Rosquist, C. E. Cooper and M. T. Wilson (2000). "Cytochrome c oxidase rapidly metabolises nitric oxide to nitrite." *FEBS Lett* **475**(3): 263-6.

Tortora, V., C. Quijano, B. Freeman, R. Radi and L. Castro (2007). "Mitochondrial aconitase reaction with nitric oxide, S-nitrosoglutathione, and peroxynitrite: mechanisms and relative contributions to aconitase inactivation." *Free Radic Biol Med* **42**(7): 1075-88.

Toth, K. and C. J. McBain (1998). "Afferent-specific innervation of two distinct AMPA receptor subtypes on single hippocampal interneurons." *Nat Neurosci* **1**(7): 572-8.

Trotti, D., B. L. Rizzini, D. Rossi, O. Haugeto, G. Racagni, N. C. Danbolt and A. Volterra (1997). "Neuronal and glial glutamate transporters possess an SH-based redox regulatory mechanism." *Eur J Neurosci* **9**(6): 1236-43.

Tsuchiya, K., M. Takasugi, K. Minakuchi and K. Fukuzawa (1996). "Sensitive quantitation of nitric oxide by EPR spectroscopy." *Free Radic Biol Med* **21**(5): 733-7.

Tzounopoulos, T., R. Janz, T. C. Sudhof, R. A. Nicoll and R. C. Malenka (1998). "A role for cAMP in long-term depression at hippocampal mossy fiber synapses." *Neuron* **21**(4): 837-45.

Umbriaco, D., S. Garcia, C. Beaulieu and L. Descarries (1995). "Relational features of acetylcholine, noradrenaline, serotonin and GABA axon terminals in the stratum radiatum of adult rat hippocampus (CA1)." *Hippocampus* **5**(6): 605-20.

Vallance, P. and N. Chan (2001). "Endothelial function and nitric oxide: clinical relevance." *Heart* **85**(3): 342-50.

Valtschanoff, J. G., R. J. Weinberg, V. N. Kharazia, M. Nakane and H. H. Schmidt (1993). "Neurons in rat hippocampus that synthesize nitric oxide." *J Comp Neurol* **331**(1): 111-21.

van Eijk, H. M., Y. C. Luiking and N. E. Deutz (2007). "Methods using stable isotopes to measure nitric oxide (NO) synthesis in the L-arginine/NO pathway in health and disease." *J Chromatogr B Analyt Technol Biomed Life Sci* **851**(1-2): 172-85.

Van Hoesen, G. W. and B. T. Hyman (1990). "Hippocampal formation: anatomy and the patterns of pathology in Alzheimer's disease." *Prog Brain Res* **83**: 445-57.

Vickroy, T. W. and W. L. Malphurs (1995). "Inhibition of nitric oxide synthase activity in cerebral cortical synaptosomes by nitric oxide donors: evidence for feedback autoregulation." *Neurochem Res* **20**(3): 299-304.

Vodovotz, Y., C. Bogdan, J. Paik, Q. W. Xie and C. Nathan (1993). "Mechanisms of suppression of macrophage nitric oxide release by transforming growth factor beta." *J Exp Med* **178**: 605-613.

Volke, V., G. Wegener, E. Vasar and R. Rosenberg (1999). "Methylene blue inhibits hippocampal nitric oxide synthase activity in vivo." *Brain Res* **826**(2): 303-5.

Wada, M., C. Morinaka, T. Ikenaga, N. Kuroda and K. Nakashima (2002). "A simple HPLC-fluorescence detection of nitric oxide in cultivated plant cells by in situ derivatization with 2,3-diaminonaphthalene." *Anal Sci* **18**(6): 631-4.

Wardman, P. (2007). "Fluorescent and luminescent probes for measurement of oxidative and nitrosative species in cells and tissues: progress, pitfalls, and prospects." *Free Radic Biol Med* **43**(7): 995-1022.

Wegener, G., V. Volke and R. Rosenberg (2000). "Endogenous nitric oxide decreases hippocampal levels of serotonin and dopamine in vivo." *Br J Pharmacol* **130**(3): 575-80.

Weiergraber, M., M. Henry, K. Radhakrishnan, J. Hescheler and T. Schneider (2007). "Hippocampal seizure resistance and reduced neuronal excitotoxicity in mice lacking the Cav2.3 E/R-type voltage-gated calcium channel." *J Neurophysiol* **97**(5): 3660-9.

Weisskopf, M. G., P. E. Castillo, R. A. Zalutsky and R. A. Nicoll (1994). "Mediation of hippocampal mossy fiber long-term potentiation by cyclic AMP." *Science* **265**(5180): 1878-82.

Wendland, B., F. E. Schweizer, T. A. Ryan, M. Nakane, F. Murad, R. H. Scheller and R. W. Tsien (1994). "Existence of nitric oxide synthase in rat hippocampal pyramidal cells." *Proc Natl Acad Sci U S A* **91**(6): 2151-5.

Werner, P., M. Voigt, K. Keinanen, W. Wisden and P. H. Seeburg (1991). "Cloning of a putative high-affinity kainate receptor expressed predominantly in hippocampal CA3 cells." *Nature* **351**(6329): 742-4.

Wiklund, N. P., H. H. Iversen, A. M. Leone, S. Cellek, L. Brundin, L. E. Gustafsson and S. Moncada (1999). "Visualization of nitric oxide formation in cell cultures and living tissue." *Acta Physiol Scand* **167**(2): 161-6.

Wilhelm, E., R. Battino and R. J. Wilcock (1977). "Low-pressure solubility of gases in liquid water." *Chem Rev* **77**: 219–262.

Wilson, R. I., A. Godecke, R. E. Brown, J. Schrader and H. L. Haas (1999). "Mice deficient in endothelial nitric oxide synthase exhibit a selective deficit in hippocampal long-term potentiation." *Neuroscience* **90**(4): 1157-65.

Winder, D. G. and P. J. Conn (1996). "Roles of metabotropic glutamate receptors in glial function and glial-neuronal communication." *J Neurosci Res* **46**(2): 131-7.

Wink, D. A. and P. C. Ford (1995). "Nitric oxide reactions important to biological systems: A survey of some kinetics investigations." *Methods: A Companion to Methods Enzymol.* **7**: 14-20.

Wink, D. A., I. Hanbauer, F. Laval, J. A. Cook, M. C. Krishna and J. B. Mitchell (1994). "Nitric oxide protects against the cytotoxic effects of reactive oxygen species." *Ann N Y Acad Sci* **738**: 265-78.

Wink, D. A. and J. B. Mitchell (1998). "Chemical biology of nitric oxide: Insights into regulatory, cytotoxic, and cytoprotective mechanisms of nitric oxide." *Free Radic Biol Med* **25**(4-5): 434-56.

Wink, D. A., R. W. Nims, J. F. Darbyshire, D. Christodoulou, I. Hanbauer, G. W. Cox, F. Laval, J. Laval, J. A. Cook, M. C. Krishna and et al. (1994). "Reaction kinetics for nitrosation of cysteine and glutathione in aerobic nitric oxide solutions at neutral pH. Insights into the fate and physiological effects of intermediates generated in the NO/O2 reaction." *Chem Res Toxicol* **7**(4): 519-25.

Wise, D. L. and G. Houghton (1969). "Solubilities and diffusivities of oxygen in hemolyzed human blood solutions." *Biophys J* **9**(1): 36-53.

Woitzik, J., N. Abromeit and F. Schaefer (2001). "Measurement of nitric oxide metabolites in brain microdialysates by a sensitive fluorometric high-performance liquid chromatography assay." *Anal Biochem* **289**(1): 10-7.

Wullner, U., J. Seyfried, P. Groscurth, S. Beinroth, S. Winter, M. Gleichmann, M. Heneka, P. Loschmann, J. B. Schulz, M. Weller and T. Klockgether (1999). "Glutathione depletion and neuronal cell death: the role of reactive oxygen intermediates and mitochondrial function." *Brain Res* **826**(1): 53-62.

Xu, W., I. G. Charles, S. Moncada, P. Gorman, D. Sheer, L. Liu and P. Emson (1994). "Mapping of the genes encoding human inducible and endothelial nitric oxide synthase (NOS2 and NOS3) to the pericentric region of chromosome 17 and to chromosome 7, respectively." *Genomics* **21**(2): 419-22.

Yao, D., A. G. Vlessidis and N. P. Evmiridis (2004). "Determination of nitric oxide in biological samples." *Microchimica Acta* **147**: 1-20.

Youssef, F. F., J. I. Addae and T. W. Stone (2006). "NMDA-induced preconditioning attenuates synaptic plasticity in the rat hippocampus." *Brain Res* **1073-1074**: 183-9.

Zabel, U., M. Weeger, M. La and H. H. Schmidt (1998). "Human soluble guanylate cyclase: functional expression and revised isoenzyme family." *Biochem J* **335 (Pt 1)**: 51-7.

Zamanillo, D., R. Sprengel, O. Hvalby, V. Jensen, N. Burnashev, A. Rozov, K. M. Kaiser, H. J. Koster, T. Borchardt, P. Worley, J. Lubke, M. Frotscher, P. H. Kelly, B. Sommer, P. Andersen, P. H. Seeburg and B. Sakmann (1999). "Importance of AMPA receptors for hippocampal synaptic plasticity but not for spatial learning." *Science* **284**(5421): 1805-11.

Zhang, X., W. S. Kim, N. Hatcher, K. Potgieter, L. L. Moroz, R. Gillette and J. V. Sweedler (2002). "Interfering with nitric oxide measurements. 4,5-diaminofluorescein reacts with dehydroascorbic acid and ascorbic acid." *J Biol Chem* **277**(50): 48472-8.